ARO 24929.20-

RESEARCH IN INORGANIC FLUORINE CHEMISTRY

FINAL REPORT

RI/RD91-165

Period 1 April 1988 - 31 March 1991

Prepared for:

U. S. ARMY RESEARCH OFFICE
RESEARCH TRIANGLE PARK, NC 27709

A Report on Work Sponsored by the U. S. Army Research Office, under Contract DAAL03-88-C-0005

Approved for public release; distribution unlimited Reproduction in whole or in part is permitted for any purpose of the United States Government.

AUTHOR: K. O. Christe

Rockwell International Corporation
Rocketdyne Division
6633 Canoga Avenue, Canoga Park, CA 91303

Date of Report: 28 May 1991

ii and 12/A-V

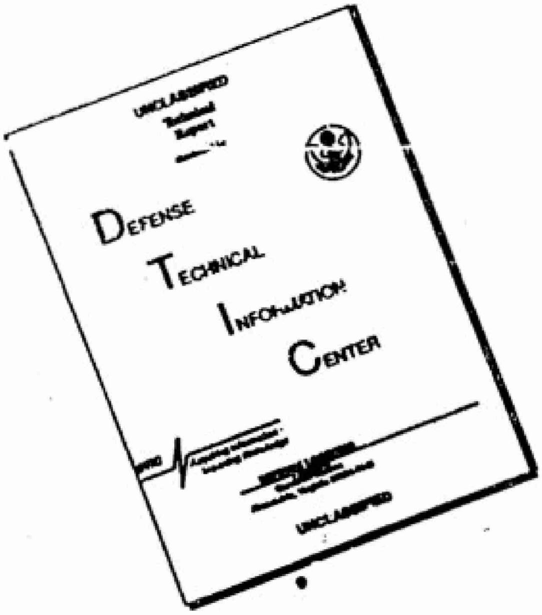

UNCLASSIFIED
Technical
Report

DEFENSE
TECHNICAL
INFORMATION
CENTER

UNCLASSIFIED

MASTER COPY KEEP THIS COPY FOR REPRODUCTION PURPOSES

REPORT DOCUMENTATION PAGE

Form Approved
OMB No. 0704-0188

1. AGENCY USE ONLY *(Leave blank)*

2. REPORT DATE
28 MAY 1991

3. REPORT TYPE AND DATES COVERED
FINAL: 1 APR 1988 - 31 MAR 1991

4. TITLE AND SUBTITLE
INORGANIC HALOGEN OXIDIZERS

5. FUNDING NUMBERS
DAAL03-88-C-0005

6. AUTHOR(S)
K.O. CHRISTE

7. PERFORMING ORGANIZATION NAME(S) AND ADDRESS(ES)
Rockwell International Corporation
ROCKETDYNE DIVISION
6633 Canoga Avenue
Canoga Park, CA 91303

8. PERFORMING ORGANIZATION REPORT NUMBER

9. SPONSORING/MONITORING AGENCY NAME(S) AND ADDRESS(ES)
U. S. Army Research Office
P. O. Box 12211
Research Triangle Park, NC 27709-2211

10. SPONSORING/MONITORING AGENCY REPORT NUMBER
ARO 24929.20-CH

11. SUPPLEMENTARY NOTES
The view, opinions and/or findings contained in this report are those of the author(s) and should not be construed as an official Department of the Army position, policy, or decision, unless so designated by other documentation.

12a. DISTRIBUTION/AVAILABILITY STATEMENT
Approved for public release; distribution unlimited.

12b. DISTRIBUTION CODE

13. ABSTRACT *(Maximum 200 words)*

A research program was carried out in inorganic halogen oxidizers. Major achievements include: the development of a quantitative oxidizer strength scale, the synthesis of anhydrous $N(CH_3)_4F$, the first successful combination of an organic cation with a chlorine fluoride anion in the form of the stable $N(CH_3)_4{}^+ClF_4{}^-$ salt, the first synthesis of the $ClF_6{}^-$ anion, the development of an improved process for the production of advanced $NF_4{}^+$ salts based on a novel acid and oxidizer resistant anion exchange medium, a systematic study of anions at their limits of oxidation and coordination with particular emphasis on the influence of lone valence electron pairs on their structures, the synthesis of $XeF_5{}^-$ which is the first known example of a pentagonal planar AX_5 species, the synthesis of the novel IF_6O^- and TeF_6O^{2-} anion,

(CONTINUED ON BACK)

14. SUBJECT TERMS
SYNTHESIS, NOVEL OXIDIZERS, QUANTITATIVE OXIDIZER STRENGTH SCALE, ANHYDROUS TETRAMETHYLAMMONIUM FLUORIDE, $N(CH_3)_4ClF_4$, $N(CH_3)_4XeF_5$, PENTAFLUOROXENATE(IV) ANION, HEXAFLUOROCHLORATE(V) ANION, (cont.)

15. NUMBER OF PAGES

16. PRICE CODE

17. SECURITY CLASSIFICATION OF REPORT	**18. SECURITY CLASSIFICATION OF THIS PAGE**	**19. SECURITY CLASSIFICATION OF ABSTRACT**	**20. LIMITATION OF ABSTRACT**
UNCLASSIFIED	UNCLASSIFIED	UNCLASSIFIED	UL

13. ABSTRACT

the improved synthesis of $NFCl_2$, a systematic study of fluorine-oxygen exchange reactions, the characterization of the N_2F^+ cation which has the shortest presently known N-F bond, the first crystal structure determination of an NF_4^+ salt, the preparation and characterization of $Ni(BiF_6)_2$, a structure determination of the Br_3^+ and Br_5^+ cations, and a solid propellant pure fluorine gas generator. A total of 22 papers, manuscripts and patents are included in the Appendices.

14. SUBJECT TERMS

TETRAFLUOROAMMONIUM CATION, GRAPHITE INTERCALATION SALTS, ANION EXCHANGE PROCESS, FLUORINE-OXYGEN EXCHANGE, CHLORINE FLUORIDES, IODINE FLUORIDES, XENON FLUORIDES, TRIBROMINE(1+) CATION, PENTABROMINE(1+) CATION, CABONYL FLUORIDE, CRYSTAL STRUCTURES, NICKEL(II) BISHEXAFLUOROBISMUTHATE(V), NITRATES, SULFATES, CHLORINE PENTAFLUORIDE, BROMINE PENTAFLUORIDE, AZIDES, IODINE HEPTAFLUORIDE, IODINE PENTAFLUORIDEOXIDE, FLUORIDE ANION, ACETONITRILE, CHLOROFORM, METHYLENE CHLORIDE, CHLOROFLUOROAMINES, OCTAFLUOROIODINE(VIII) ANION, OCTAFLUOROTELLURATE(VI) ANION, HEXAFLUOROOXOIODATE(VII) ANION, FLUORINE GAS GENERATORS, RADIATION AUGMENTED ENERGY STORAGE, SELECTIVE GAS SEPARATION.

MASTER COPY: PLEASE KEEP THIS "MEMORANDUM OF TRANSMITTAL" BLANK FOR REPRODUCTION PURPOSES. WHEN REPORTS GENERATE UNDER ARO SPONSORSHIP, FORWARD A COMPLETED COPY OF THIS FORM WITH EACH REPORT TO OUR OFFICE. THIS WILL ASSURE PROPER IDENTIFICATION.

MEMORANDUM OF TRANSMITTAL

U.S. Army Research Office
ATTN: SLCRO-IP-Library
P.O. Box 12211
Research Triangle Park, NC 27709-2211

Dear Library Technician:

☐ Reprint (15 copies) ☐ Technical Report (50 copies)

☐ Manuscript (1 copy) ☒ Final Report (50 copies)

☐ Thesis (1 copy)

☐ MS ☐ PhD ☐ Other________

TITLE: INORGANIC HALOGEN OXIDIZERS

is forwarded for your information.

SUBMITTED FOR PUBLICATION TO (applicable only if report is manuscript):

Sincerely,

Karl O. Christe

DO NOT REMOVE THE LABEL BELOW
THIS IS FOR IDENTIFICATION PURPOSES

Dr. Karl O. Christe 24929-CH
Rockwell International Corporation
Rocketdyne Division
6633 Canoga Avenue
Canoga Park, CA 91304

TABLE OF CONTENTS

FOREWORD

The research reported herein was supported by the U. S. Army Research Office with Dr. R. Husk as Scientific Officer. This report covers the period 1 April 1988 through 31 March 1991. The program has been directed by Dr. K. O. Christe. The scientific effort was carried out mainly by Drs. K. O. Christe, W. W. Wilson, C. J. Schack, E. C. Curtis and Mr. R. D. Wilson, and the program was administered by Dr. S. C. Hurlock.

Other contributors to these research efforts, at no cost to the contract were Dr. D. A. Dixon (Du Pont); Drs. R. Bougon, P. Charpin, J. Isabey, M. Lance, M. Nierlich, and J. Vigner (French Atomic Energy Commission); Drs. G. Schrobilgen, J. Sanders, R. Chirakal, and H. P. Mercier (McMaster University); Dr. R. Bau, J. Feng, S. Sukumar, and D. Zhao (University of Southern California); Dr. M. Lind (Science Center of Rockwell International); Dr. N. Thorup (University of Lingby, Denmark); Drs. D. Russell and J. Fawcett (University of Leicester, U. K.); and Drs. J. Gilbert and R. Conklin (University of Denver).

INTRODUCTION

This is the final report of a research program carried out at Rocketdyne between 1 April 1988 and 31 March 1991. The purpose of this program was to explore the synthesis and properties of energetic inorganic halogen oxidizers. Although the program was directed toward basic research, applications of the results were continuously considered.

Only completed items of research, which have been summarized in manuscript form, are included in this report. A total of 12 technical papers were published and 6 papers are in press in major scientific journals. In addition, 11 papers were presented at international and national conferences, and 6 invited lectures were given in the U.S. and abroad. A further testimony to the creativity of this program is the fact that it resulted in 4 U.S. patents. The technical papers and issued patents are given as Appendices A through V.

During this year, the author is serving on a Foreign Applied Sciences Assessment Center (FASAC) Panel on Soviet Chemical propellant R&D and is responsible for the liquid propellant area.

PUBLICATIONS AND PATENTS GENERATED UNDER THIS PROGRAM

Published Papers

1. "Formation of Chlorine-Fluorine and Nitrogen-Fluorine Bonds Using Carbonyl Difluoride as the Fluorinating Agent," by C.J. Schack and K.O. Christe, Inorg. Chem., 27, 4771 (1988).

2. "Crystal Structure of NF_4^+ Salts," by K.O. Christe, M.D. Lind, N. Thorup, D.R. Russell, J. Fawcett, and R. Bau, Inorg. Chem., 27, 2450 (1988).

3. "Preparation and Characterization of $Ni(BiF_6)_2$ and of the Ternary Adducts $[Ni(CH_3CN)_6](SbF_6)_2$," by R. Bougon, P. Charpin, K.O. Christe, J. Isabey, M. Lance, M. Nierlich, J. Vigner, and W.W. Wilson, Inorg. Chem., 27, 1389 (1988).

4. "Anion Exchange in NF_4^+ Salts Using Graphite Salts as an Oxidizer- and Acid-Resistant Anion Exchange Medium," by K.O. Christe and R.D. Wilson, Inorg. Chem., 28, 4175, (1989).

5. "Reactions of Chlorine Fluorides and Oxyfluorides with the Nitrate Anion and Alkali-Metal Fluoride Catalyzed Decomposition of ClF_5," by K.O. Christe, W.W. Wilson, R.D. Wilson, Inorg. Chem., 28, 675 (1989).

6. "Reactions of BrF_5 with the Azide, Nitrite and Sulfate Anions," by K.O. Christe, W.W. Wilson and C.J. Schack, J. Fluorine Chem., 43, 125 (1989).

7. "Fluorine-Oxygen Exchange Reactions in IF_5, IF_7, and IF_5O," by K.O. Christe, W.W. Wilson, and R.D.Wilson, Inorg. Chem., 28, 904 (1989).

8. "Reaction of the Fluoride Anion with Acetonitrile, Chloroform and Methylene Chloride," by K.O. Christe and W.W. Wilson, J. Fluorine Chem., 47, 117, (1990).

9. "Syntheses, Properties, and Structures of Anhydrous Tetramethylammonium Fluoride and its 1:1 Adduct with trans-3-Amino-2-Butene Nitrile," by K.O. Christe, W.W. Wilson, R.D. Wilson, R. Bau, J. Feng, J. Amer. Chem. Soc., 112, 7619 (1990).

10. "The Hexafluorochlorate (V) Anion, ClF_6^-," by K.O. Christe, W.W. Wilson, R.V. Chirakal, J. Sanders, G.J. Schrobilgen, Inorg. Chem., 29, 3506 (1990).

11. "New Synthesis of IF_5O," by C.J. Schack and K.O. Christe, J. Fluorine Chem., 49, 167 (1990).

12. Synthesis and Vibrational Spectra of Chlorofluoroamines," by J.V. Gilbert, R.A. Conklin, R.D. Wilson, and K.O. Christe, J. Fluorine Chem., 48, 361 (1990).

Submitted Papers

13. "The N_2F^+ Cation. An Unusual Ion Containing the Shortest Presently Known Nitrogen-Nitrogen and Nitrogen-Fluorine Bonds," by K.O. Christe, R.D. Wilson, W.W. Wilson, R. Bau, S. Sukumar, J. Amer. Chem. Soc.

14. "The Pentafluoroxenate (IV) Anion XeF_5^-; the First Example of a Pentagonal Planar AX_5 Species," by K.O. Christe, E.C. Curtis, D.A. Dixon, H.P. Mercier, J.P.C. Sanders, and G.J. Schrobilgen, J. Amer. Chem. Soc.

15. "X-ray Crystal Structure and Raman Spectrum of Tribromine (1+) Hexafluoroarsenate (V), $Br_3^+AsF_6^-$, and Raman Spectrum of Pentabromine (1+) Hexafluoroarsenate (V), $Br_5^+AsF_6^-$," by K.O. Christe, R. Bau, and D. Zhoa, Z. anorg. allg. Chem.

16. "Controlled Replacement of Fluorine by Oxygen in Fluorides and Oxyfluorides," by K.O. Christe, W.W. Wilson, and C.J. Schack, contributed chapter to a book on "Synthetic Fluorine Chemistry."

17. "High Coordination Number Fluoro- and Oxofluoro-Anions; IF_6O^- TeF_7^-, IF_8^- and TeF_8^{2-}," by K.O. Christe, J.C.P. Sanders, G.J. Schrobilgen, J. Chem. Soc. Chem. Commun.

18. "A Quantitative Scale for the Oxidizing Strength of Oxidative Fluorinators," by K.O. Christe and D.A. Dixon, J. Amer. Chem. Soc.

Papers Presented at Meetings

19. "Xenon Oxyfluoride Chemistry," by K.O. Christe and W. W. Wilson, Third Chemical Congress of North America, Toronto Canada, June 1988.

20. "Ion Exchange Process for the Production of Advanced NF_4^+ Salts," by K.O. Christe and R.D. Wilson, 12th International Symposium on Fluorine Chemistry, Santa Cruz, CA August 1988.

21. "Formation of Chlorine-Fluorine and Nitrogen-Fluorine Bonds Using Carbonyl Fluoride as the Fluorinating Agent," by C.J. Schack and K.O. Christe, 12th International Symposium on Fluorine Chemistry, Santa Cruz, CA, August 1988.

22. "The Nitrate Anion, A Useful Reagent for Fluorine-Oxygen Exchange," by W. W. Wilson and K.O. Christe, 12th International Symposium on Fluorine Chemistry, Santa Cruz, CA, August, 1988.

23. "Synthesis and Characterization of $[N(CH_3)_4]^+ClF_4^-$ and $[N(CH_3)_4]^+BrF_4^-$," by W.W. Wilson and K.O. Christe, 9th Winter Fluorine Conference, St. Petersburg, FL, February, 1989.

24. "Structural Studies at Rocketdyne and Their Relationship to VSEPR Rules," by K.O. Christe, Chemistry Symposium to Honor Ronald J. Gillespie, Hamilton, Ontario, June, 1989.

25. "Recent Advances in the Synthesis of New Energetic Materials," by K.O. Christe and W.W. Wilson, 9th European Symposium on Fluorine Chemistry, Leicester, U.K., September, 1989.

26. "Twenty-five Years of Excitement in Oxidizer Chemistry," by K.O. Christe, 24th Pauling Award Symposium, Portland, OR, November, 1989.

27. "Inorganic Halogen Oxidizers," by K.O. Christe, Loker Symposium on Synthetic Fluorine Chemistry, Los Angeles, CA, February, 1990.

28. "Synthesis and Characterization of Unusual, Highly Coordinated Anions," by K.O. Christe, W.W. Wilson and E.C. Curtis, 10th Winter Fluorine Conference, St. Petersburg, FL, February, 1991.

29. "Lewis Acid Behavior of Xenon(II) Cations and the Synthesis of the XeF_5^- Anion," by N.T. Arner, K.O. Christe, H.P. Mercier, M. Rokoss, J. Sanders, G. Schrobilgen, and J. Thrasher, 10th Winter Fluorine Conference, St. Petersburg, FL, February, 1991.

Invited Lectures

Invited lectures on work done under this contract were given at:

30. University of California, Berkeley

31. Free University of Berlin, Germany (series of four lectures)

Issued Patents

32. "Synthesis of R_fOTeF_5," by C.J. Schack and K.O. Christe, U.S. Pat. 4,675,088.

33. "Method for the Selective Separation of Gases," by K.O. Christe, U.S. Pat. 4,695,296.

34. "Pure Fluorine Gas Generator," by K.O. Christe, U.S. Pat. 4,711,680.

35. "Radiation Augmented Energy Storage System," by K.O. Christe, U.S. Pat. 4,903,479.

RESULTS AND DISCUSSION

Like under the previous program [Ref. 1], a vast amount of data was generated under the current program. Therefore, this discussion will be limited to a highlight of some of the major achievements. For more detail, the interested reader is referred to the Appendices.

Development of a Quantitative Oxidizer Strength Scale

Although a major effort of oxidizer chemistry is the development of new oxidizers of increased oxidizer strength, no quantitative methods existed until now to either define, measure or compute the strength of an oxidizer. the only data available were some isolated observations that some oxidizers were capable to fluorinate a given substrate while others were not. However, even these qualitative data were inconsistent because it was impossible to distinguish whether the failure of an attempted oxidative fluorination was due to an insufficient oxidizer strength or poorly chosen reaction conditions or excessively high activation energy barriers.

These problems were now overcome by the development of a quantitative oxidizer strength scale (see Appendix R). It was shown from Born-Haber cycles that the oxidizer strength of an oxidative fluorinator is exclusively a function of the F^+ detachment energies. Since the required F^+ detachment energy values are not directly available and are very difficult to compute, we have in collaboration with Dr. Dixon from Du Pont determined differences in F^+ detachment energies between given oxidizers by total energy computations using local density functional calculations. The resulting relative oxidizer strength scale was then converted to an absolute scale by defining a zero point for the scale and by anchoring the scale to the zero point by an experimental number. We have chosen F^+ as the zero point and an experimentally known KrF^+ value as the anchor point. The validity of the resulting quantitative scale was tested for XeF^+ and ArF^+ and gave excellent agreement with experimental values.

In this manner, the oxidizing strengths of 27 oxidizers were computed and summarized in Table 1 of Appendix R. This oxidizer strength table was also used to calculate the heats of formation of these oxidizers, thus providing yet another set of valuable information.

The development of a quantitative oxidizer strength scale is a significant advancement in oxidizer chemistry and will be invaluable for future experimental and theoretical work. The F^+ detachment energies (or their negative values which are the F^+ affinities) are the equivalents to the proton affinities in organic chemistry.

Nitrogen Fluoride Chemistry

Nitrogen fluorides are the most promising candidates for energetic halogen oxidizers. They offer the best compromise between a high energy content and chemical and thermal stability. During the current program, significant progress was made in the areas of NF_4^+ and $NFCl_2$ chemistry, unusually short N-F bonds, and the formation of N-F bonds.

In the area of NF_4^+ chemistry, a novel process was developed for the production of more energetic NF_4^+ salts (see Appendix D). The NF_4^+ cation is the most useful and stable highly energetic cationic oxidizer presently known. Its most accessible salt is NF_4SbF_6. The drawback of the latter is the high molecular weight and relatively low energy content of its anion. To obtain more useful NF_4^+ salts, NF_4SbF_6 must be converted to more energetic NF_4^+ salts such as NF_4BF_4. In the past, this had been achieved by low temperature metathesis [Ref. 2], but this approach involved a batch process with cumbersome low-temperature filtrations and recrystallizations and produced an impure (~10% impurities) product in about 80% yield. Our new process (Appendix D) is a continuous ion exchange process which can be operated at room temperature and produces pure NF_4^+ salts in quantitative yield. The major difficulty which had to be overcome was the finding of an anion exchanger which is stable towards the very strongly acidic HF solvent and the powerful NF_4^+ oxidizer. The anion exchangers which were found to work in our process were graphite salts and therefore, extensive efforts were made in the field of intercalation chemistry.

Also in the NF_4^+ area, in collaboration with four different groups located in the U.S., Denmark, France, and England, we have finally succeeded in solving the crystal structure of an NF_4^+ salt (Appendix B) after 20 years of futile efforts.

Another fascinating problem in nitrogen fluoride chemistry was the bonding in the N_2F^+ cation. Our previous spectroscopic studies [Ref. 3] had indicated that N_2F^+ either possesses an unusually short N-F bond [Ref. 4] or was a rare exception to Gordy's rule [Ref. 5] which correlates force constants with bond distances. A crystal structure determination of $N_2F^+AsF_6^-$, carried out in collaboration with Prof. Bau's group at USC, confirmed the extreme shortness of the N-F bond (1.217 Å) in N_2F^+ while also showing a very short (1.098 Å) N-N bond (Appendix M). A theoretical analysis of this problem using local density functional calculations revealed that the shortness of the N-F and the N-N bonds is due to the high s-character of the sigma bonds. This feature had previously been demonstrated only for carbon compounds.

Another surprising result in N-F chemistry was our discovery that an N-F bond can be formed from a fluorinating agent as mild as COF_2 (Appendix A).

In collaboration with Prof. Gilbert's group of the University of Denver we have worked out improved syntheses of $NFCl_2$ and NF_2Cl (Appendix L). These compounds are precursors for excited state nitrenes, such as $^1\Delta NF$ which are of importance for chemical lasers.

Oxygen-Fluorine Exchange Reactions

Our systematic study of oxygen-fluorine exchange reactions was completed. Whereas many methods are known for the replacement of oxygen by fluorine, very little work had been done on the opposite reaction, the controlled replacement of fluorine by oxygen. We have shown (Appendices E, F, G and Q) that oxoanions, such as NO_3^- or SO_4^{2-}, are effective, readily available, nontoxic, and low cost reagents for controlled, stepwise fluorine-oxygen exchange in highly fluorinated compounds of the more electronegative elements. Product separations can be facilitated greatly by appropriate choices of the oxoanion, the coutercations and the mole ratio of the reagents. These reactions appear to be quite general, controllable, safe, and scalable. It was also shown (Appendix K) that in IF_7 the PF_3O molecule readily replaces two fluorine ligands for a doubly bonded oxygen, thereby providing a new and convenient synthesis for IF_5O.

New Anions at the Limits of Oxidation and Coordination

Our discovery of a synthesis of pure and truly anhydrous tetramethylammonium fluoride (Appendix I) has led to significant advances in oxidizer chemistry. The $N(CH_3)_4F$ provides a fluoride ion source which, contrary to the alkali metal fluorides, is highly soluble in solvents such as CH_3CN, CHF_3, or alcohols. Furthermore, it was found that the $N(CH_3)_4^+$ cation and solvents such as CH_3CN or CHF_3 possess a high activation energy barrier towards strong oxidizers. These surprising properties were exploited. Thus, we have succeeded to combine for the first time an organic cation, i.e. $N(CH_3)_4^+$, with a chlorine fluoride anion, i.e. ClF_4^-. The resulting salt, $N(CH_3)_4^+ClF_4^-$ is stable up to 100°C and is not shock sensitive [Ref. 6]. This reaction chemistry was extended toward the synthesis of the previously unknown ClF_6^- anion (Appendix J). Although the isolation of a stable ClF_6^- salt was not possible due to consistent explosions, the existence and octahedral structure of the ClF_6^- anion has now been established by low-temperature Raman and NMR spectroscopy. The synthesis of ClF_6^- had been unsuccessfully pursued for more than 30 years.

Relatively little information had been available on fluoride structures with coordination numbers in excess of six and, in particular, on structures containing free valence electron pairs. Depending on the maximum coordination number of the central atom, the free valence electron pairs can be sterically either active or inactive. If these pairs are active, they can also induce fluxionality in these molecules. The availability of $N(CH_3)_4F$ as a highly soluble fluoride source, combined with the stabilizing effect of the large $N(CH_3)_4^+$ cations and the ease of growing single crystals of these salts for crystal structure studies, provided us with a unique opportunity to synthesize novel anions at the limits of oxidation and coordination and to study the structures of these new and also of other previously known anions.

As a typical example, we have discovered the novel XeF_5^- anion. To our great surprise, it was found that this anion is perfectly planar, i.e. all six atoms are in the same plane (Appendix N). This is the first known example of a pentagonal planar AX_5 species and as such is very unique.

Another novel anion discovered in the course of this study is the IF_6O^- anion (Appendix R). Its structure can be derived from a pentagonal bipyramid in which the axial positions are occupied by one fluorine and the oxygen ligand.

These structural studies are carried out in collaboration with the groups of Profs. Schrobilgen at McMaster University and Seppelt at the Free University of Berlin who have excellent x-ray diffraction and NMR facilities and with Dr. Dixon from DuPont who is a leading expert on ab initio and LDF computations. Other ions currently under investigation include IF_8^-, TeF_7^-, TeF_8^{2-}, TeF_6O^{2-}, XeF_5^-, XeF_7^-, and XeF_8^{2-}.

Miscellaneous

Other achievements include the inventions of solid propellant pure fluorine gas generators (Appendix U), a radiation augmented energy storage system (Appendix V), and a method for selectively removing unreactive gases from highly reactive gas streams consisting mainly of fluorine (Appendix T). The solid propellant pure fluorine gas generator is a direct spin off from the first chemical synthesis of elemental fluorine discovered by the author under the previous program [Ref. 1].

CONCLUSION

Our work during this contract period has again been extremely fruitful. The development of a quantitative oxidizer strength scale is of great significance. Furthermore, the discovery of a synthesis for anhydrous tetramethylammonium fluoride has led to the first successful combination of organic cations with chlorine fluoride anions and the first synthesis of the long sought ClF_6^- anion. It has also opened the door to a systematic study of novel and known anions at the limits of oxidation and coordination. So far, the new IF_6O^- and TeF_6O^{2-} and the spectacular XeF_5^- anions have been prepared and characterized. This study is expected to greatly contribute to our understanding of structures with coordination numbers in excess of six and of the influence of free valence electron pairs on the structure and fluxionality of these anions.

In spite of the basic nature of most of our studies, useful applications are always kept in mind as exemplified by the developments of an ion exchange process for the production of advanced NF_4^+ salts, of a solid propellant pure fluorine gas generator, or improved syntheses of precursors for chemical NF lasers. These and the other examples highlighted above demonstrate again the benefits which can be expected from well-planned, goal-oriented basic research and program continuity.

REFERENCES

[1] K.O. Christe, Rocketdyne, "Research in Inorganic Fluorine Chemistry," Final Report under Contract DAAG29-84-C-0001 (March 1, 1987).

[2] K.O. Christe; W.W. Wilson; C.J. Schack; and R.D. Wilson, Inorg. Synthesis, 24, 39 (1986).

[3] K.O. Christe; R.D. Wilson; and W. Sawodny, J. Mol. Structure, 8, 245 (1971) .

[4] K.O. Christe, Spectrochim. Acta, Part A, 42A, 939 (1986).

[5] W. Gordy, J. Chem. Phys., 14, 305 (1946).

[6] W.W. Wilson and K.O. Christe, Inorg. Chem., 28, 4172 (1989).

APPENDICES

N	The Pentafluoroxenate(IV) Anion XeF_5^-; the First Example of a Pentagonal Planar AX_5 Species
O	X-ray Crystal Structure and Raman Spectrum of Tribromine(1+) Hexafluoroarsenate(V), $Br_3^+AsF_6^-$, and Raman Spectrum of Pentabromine(1+) Hexafluoroarsenate(V), $Br_5^+AsF_6^-$
P	Controlled Replacement of Fluorine by Oxygen in Fluorides and Oxyfluorides
Q	High-Coordination Number Fluoro- and Oxofluoro-Anions; IF_6O^-, TeF_7^-, IF_8^- and TeF_8^{2-}
R	A Quantitative Scale for the Oxidizing Strength of Oxidative Fluorinators
S	United States Patent 4,675,088: Synthesis of R_fOTeF_5
T	United States Patent 4,695,296: Method for the Selective Separation of Gases
U	United States Patent 4,711,680: Pure Fluorine Gas Generator
V	United States Patent 4,903,479: Radiation Augmented Energy Storage System

APPENDIX A

Reprinted from Inorganic Chemistry, 1988, *27*, 4771

Contribution from Rocketdyne,
A Division of Rockwell International,
Canoga Park, California 91303

Formation of Chlorine–Fluorine and Nitrogen–Fluorine Bonds Using Carbonyl Difluoride as the Fluorinating Agent

Carl J. Schack and Karl O. Christe*

Received May 19, 1988

Previous studies by Shreeve and her co-workers have shown that carbonyl difluoride (COF_2) is a useful reagent for displacing either hydrogen by fluorine from P–H, N–H, and C–H bonds[1] or oxygen by fluorine from the oxides of V, Nb, Ta, Cr, Mo, W, B, Si, Ge, Sn, P, Se, Te, I, and U.[2] The latter study prompted us to examine whether COF_2 could also be used for the formation of Cl–F and N–F bonds from their oxides. The formation of Cl–F[3] and N–F[4] bonds usually requires relatively powerful fluorinating agents and previously has not been achieved with a fluorinating agent as mild as COF_2. Thermochemical calculations that were carried out by us revealed the feasibility of reaction 1 for M = Li and Na. It increases with decreasing atomic weight of M and

$$\begin{gathered} MNO_3 + COF_2 \rightarrow MF + FNO_2 + CO_2 \\ M = Li, Na, K, Rb, Cs \end{gathered} \tag{1}$$

for M = Li and Na results in ΔH values of −9.5 and −4.5 kcal mol^{-1}, respectively. Reaction 2 was found to be thermochemically feasible by comparable amounts with ΔH values of −20.6 and −11.2 kcal mol^{-1} for M = Li and Na, respectively.

$$\begin{gathered} MClO_3 + COF_2 \rightarrow MF + FClO_2 + CO_2 \\ M = Li, Na, K, Rb, Cs \end{gathered} \tag{2}$$

In view of the thermochemical results, reactions 1 and 2 were experimentally studied. It was found that $LiNO_3$, when heated with a slight excess of COF_2 in a steel cylinder at 45–90 °C, formed CO_2, N_2O_4, and O_2 in high yield. These products are best explained by reaction 3, followed by the attack of the steel cylinder by FNO_2.

$$LiNO_3 + COF_2 \rightarrow LiF + FNO_2 + CO_2 \tag{3}$$

Since HF generally promotes the attack of steel by oxidizers such as FNO_2, small amounts of CsF were added to the reaction as an HF getter (see reaction 4). In this manner, FNO_2

$$CsF + HF \rightarrow CsHF_2 \tag{4}$$

was isolable in essentially quantitative yield according to (3), with 12 mol % of CsF as an additive at 85 °C. For $NaNO_3$ with CsF addition, an 85% yield of FNO_2 was obtained under comparable conditions. For $CsNO_3$, either with or without CsF, no reaction was observed with COF_2, in agreement with the above thermochemical predictions.

The postulate that CsF serves only as an HF getter and not as a catalyst was confirmed by carrying out reaction 3 in an all-Teflon reactor. In such a reactor, high yields of FNO_2 were obtainable without CsF addition.

For the reaction of $NaClO_3$ with COF_2, reaction conditions similar to those used for $NaNO_3$, i.e. 85 °C and CsF catalysis, were required. The best yield obtained for $FClO_2$ was about 44% based on the limiting reagent $NaClO_3$, but no systematic effort was undertaken to maximize this yield.

Attempts failed to prepare $FClO_3$ from $LiClO_4$ and COF_2. Although this reaction is thermochemically favored by 14.8 kcal mol^{-1}, no reaction was observed up to 120 °C. At 160 °C, a 30% conversion of $LiClO_4$ to LiF was obtained, but even in the presence of CsF only chlorine and oxygen and no $FClO_3$ were isolated.

In summary, the successful formation of N–F and Cl–F bonds from the corresponding oxides by the very mild fluorinating agent COF_2 was quite unexpected and significantly expands the utility of this fluorinating agent.

Experimental Section

Materials and Apparatus. $LiNO_3$ (J. T. Baker, 99.7%) and $NaNO_3$ (J. T. Baker, 99.5%) were dried in a vacuum oven at 120 °C for 1 day prior to their use. The $CsNO_3$ was prepared from Cs_2CO_3 and HNO_3 and dried in the same manner. The CsF was dried by fusion in a platinum crucible, followed by immediate transfer of the hot clinker to the dry N_2 atmosphere of a glovebox. The $NaClO_3$ and $LiClO_4$ (Baker, Analyzed reagents) were used as received. The COF_2 (PCR Inc.) was used without further purification after removal of any volatile material at −196 °C.

Volatile materials were handled in a stainless steel–Teflon FEP vacuum line[5] and solids in the dry N_2 atmosphere of a glovebox.

Synthesis of FNO_2. In a typical experiment, $LiNO_3$ (2.10 mmol) and CsF (0.25 mmol) were loaded in the drybox into prepassivated (with ClF_3) 30-mL stainless steel cylinder, which was closed by a valve. On the vacuum line, COF_2 (2.38 mmol) was added to the cylinder at −196 °C. The cylinder was kept in an oven at 85 °C for 16 h and was then cooled again to −196 °C. It did not contain any significant amount of gas noncondensable at −196 °C. The material volatile at 25 °C was

---

[1] Gupta, O. D.; Shreeve, J. M. *J.* Chem. *Soc., Chem. Commun* 1984, 416 and references therein. Williamson, S. M.; Gupta, O. D.; Shreeve, J. M. *Inorg. Synth.* 1986, *24*, 62.

[2] Mallela, S. P., Gupta, O. D., Shreeve, J. M. *Inorg. Chem.* 1988, *27*, 208.

[3] Christe, K. O., Schack, C. J. *Adv. Inorg. Chem Radiochem.* 1976, *18*, 319.

[4] *Gmelin Handbook of Inorganic Chemistry*; Springer-Verlag Berlin, FRG, 1987, Fluorine Supplement Vol 5, Compounds with N

[5] Christe, K. O., Wilson, R. D., Schack, C. J. *Inorg. Synth.* 1986, *24*, 3

0020-1669/88/1327-4771$01.50/0

separated by fractional condensation, measured, and identified by infrared spectroscopy. It consisted of FNO_2 (2.09 mmol), CO_2 (2.1 mmol), and COF_2 (0.2 mmol). The white solid residue (91 mg, weight calculated for 2.10 mmol of LiF and 0.25 mmol of CsF 92.5 mg) consisted of LiF and CsF.

Synthesis of $FClO_2$. The reaction was carried out as described above for $LiNO_3$ and COF_2, with use of $NaClO_3$ (1.41 mmol), COF_2 (2.00 mmol), and CsF (0.3 mmol) at 85 °C for 46 h. The products consisted of $FClO_2$ (0.62 mmol, 44% of theory), CO_2 (0.64 mmol), unreacted COF_2, and smaller amounts of Cl_2 and material noncondensable at −196 °C.

Acknowledgment. We are grateful to R. D. Wilson for help with some of the experiments and to the U.S. Army Research Office for financial support of this work.

Registry No. COF_2, 353-50-4; CsF, 13400-13-0; FNO_2, 10022-50-1; $LiNO_3$, 7790-69-4; $FClO_2$, 13637-83-7; $NaClO_3$, 7775-09-9; $NaNO_3$, 7631-99-4; $CsNO_3$, 7789-18-6; $LiClO_4$, 7791-03-9.

Reprinted from Inorganic Chemistry, 1988, *27*, 2450

Contribution from Rocketdyne, A Division of Rockwell International, Canoga Park, California 91303,
the Science Center of Rockwell International, Thousand Oaks, California 91360,
and the Departments of Chemistry, Technical University of Denmark, Lyngby DK-2800, Denmark,
University of Southern California, Los Angeles, California 90007, and University of Leicester, Leicester LE1 7RH, U.K.

Crystal Structure of NF_4^+ Salts

Karl O. Christe,[*,1a] M. David Lind,[1b] Niels Thorup,[1c] David R. Russell,[1d] John Fawcett,[1d]
and Robert Bau[1e]

Received December 14, 1987

The room-temperature tetragonal structure of NF_4BF_4 has been determined by a combination of single-crystal X-ray diffraction analysis and vibrational spectroscopy. This compound crystallizes in the tetragonal space group $P\bar{4}2_1m$ with $Z = 4$ and unit cell dimensions $a = 9.92$ (1) and $c = 5.23$ (1) Å. The structure was refined to an R value of 0.071 by using 325 independent observed reflections. The structure is made up from an approximately tetrahedral NF_4^+ cation with a bond length of 1.30 Å and a BF_4^- anion that rotates or oscillates around a 3-fold axis along one of its bonds. This rotation of the BF_4^- ion provides a mechanism for averaging the anisotropic fluorine–fluorine repulsion effects caused by the packing requirements of two sets of tetrahedral ions in a primitive cubic type of arrangement. The use of a static X-ray model with nonrotating ions results in artifacts, such as an apparent lowering of the site symmetries of the ions and two sets of different NF_4^+ cations, which have no real physical meaning. Additional data, such as vibrational spectra or improved models incorporating dynamic effects, are required for an adequate description of structures exhibiting this type of ion rotation. Due to this ion rotation and/or disorder problems and the lack of a successful static model, only partial X-ray structures could be obtained for NF_4SbF_6 and $NF_4Sb_2F_{11}$. Although these partial structures yielded N–F bond lengths with apparently small estimated standard deviations, these values were either much too large or small, depending on the constraints employed for obtaining a structure solution.

Introduction

Although NF_4^+ salts have been known for 20 years, the exact structure of the NF_4^+ cation is still unknown. From ^{19}F NMR spectra it is known that in solution NF_4^+ is an ideal tetrahedron. Vibrational spectra of many NF_4^+ salts indicate that in the solid state the NF_4^+ cations are also essentially tetrahedral.[2] From the general valence force field, the bond length in NF_4^+ has been estimated as 1.31 Å.[3] This value is supported by ab initio calculations, which resulted in a value of 1.32 Å.[4] Numerous unsuccessful attempts were made, in both our and other laboratories, to determine a crystal structure for one of the NF_4^+ salts, and the only reported structure was incomplete, giving a range of 1.30–1.40 Å for the N–F bond length.[5] In this paper we report the crystal structure of $NF_4^+BF_4^-$ and partial structures of $NF_4^+SbF_6^-$ and $NF_4^+Sb_2F_{11}^-$ and address the problem of ion rotation and its effects on crystal structure determinations.

Experimental Section

Literature methods were used for the synthesis of $NF_4^+BF_4^-$,[6] $NF_4^+SbF_6^-$,[7] and $NF_4^+Sb_2F_{11}^-$.[8] The single crystals were grown from either anhydrous HF or BrF_5 solutions, with the latter generally giving better results. The crystals were handled in the dry nitrogen atmosphere of a glovebox that was equipped with a microscope and were sealed in quartz capillaries. Infrared spectra were recorded on a Perkin-Elmer Model 283 spectrophotometer using dry powders pressed between AgCl or AgBr windows in an Econo press (Barnes Engineering, Co.). The Raman spectra were obtained with a Spex Model 1403 spectrophotometer using the 647.1-nm exciting line of a Kr ion laser and sealed melting point capillaries as sample containers.

Results and Discussion

Single-Crystal Analysis of $NF_4^+BF_4^-$.[1b,c] The crystal data and details of the intensity data measurement and structure refinement are given in Table I. The lattice parameters and possible space groups were determined from Buerger precession photographs taken at 23 °C with Zr-filtered Mo Kα X-rays. Symmetry and systematic absences on those photographs indicated space group $P\bar{4}2_1m$ or $P42_12$, but no solution was found for the latter space group. X-ray diffraction intensities were measured with a Supper-Pace/Picker automatic diffractometer using Mo Kα X-rays and balanced Zr and Y filters. The rotation axis was the a axis. Continuous scans of each diffraction maximum were made with a scan rate of 1°/min (the scan widths were 2° or more), and background counts were made for one-sixth of the scan time at the beginning and end of the scan interval. All independent $I(hkl)$ with $(\sin\theta)/\lambda \leq 0.65$ Å^{-1} were measured. The crystal, sealed in a 0.5-mm capillary tube, was small enough to make absorption corrections negligible. The intensities were reduced to relative $|F_0(hkl)|^2$ values by application of the appropriate Lorentz–polarization factors.

The approximate structure was determined by a trial and error method using a ball-and-stick model, aided by the three-dimen-

Table I. Crystallographic Data for $NF_4^+BF_4^-$

fw	176.80
space group	$P\bar{4}2_1m$ (tetragonal: No. 113)
a, Å	9.92 (1)
c, Å	5.23 (1)
c/a	0.527
V, Å^3	514.7
Z	4
ρ(calcd), g/cm^3	2.281
radiation	Mo Kα
abs coeff (μ), cm^{-1}	3.75
no. of reflcns measd	388
no. of reflcns used in refinement	325
no. of params refined	55
function minimized	$\sum w(\lvert F_o\rvert - \lvert F_c\rvert)^2$
weighting scheme	$1/w = 1 + [(\lvert F_o\rvert - 50)/100]^2$
$R = \sum\lvert F_o\rvert - \lvert F_c\rvert\rvert/\sum\lvert F_o\rvert$	0.071
$R_w = [\sum w(\lvert F_o\rvert - \lvert F_c\rvert)^2/\sum w\lvert F_o\rvert^2]^{1/2}$	0.077
residual electron density, e/Å^3	−0.4 to +0.3

Table II. Fractional Atomic Coordinates with Estimated Standard Deviations for $NF_4^+BF_4^-$

atom	x	y	z
B	0.2460 (5)	0.7460	−0.3961 (14)
N(1)	0	0	0
N(2)	0	0.5	−0.0172 (21)
F(1)	−0.0641 (4)	0.0874 (4)	0.1401 (17)
F(2)	0.0737 (4)	0.5737	0.1221 (19)
F(3)	0.0759 (5)	0.4241	−0.1668 (19)
F(4)	0.2789 (8)	0.6205 (5)	−0.3101 (11)
F(5)	0.2460 (4)	0.7460	−0.6591 (8)
F(6)	0.3321 (5)	0.8321	−0.3039 (18)

---

(1) (a) Rocketdyne (b) Science Center of Rockwell (c) Technical University of Denmark (d) University of Leicester. (e) University of Southern California.

(2) For a review of NF_4^+ chemistry see. Nikitin, I. V., Rosolowskii, V. Ya. *Usp. Khim.* 1985, *54*, 722

(3) Christe, K O *Spectrochim. Acta, Part A* 1986, *42A*, 939

(4) Peters, N. J S Dissertation, Princeton University, 1982

(5) Charpin, P.; Lance, M.; Bui-Huy, T.; Bougon, R. *J. Fluorine Chem.* 1981, *17*, 484.

(6) Christe, K O., Schack, C J., Wilson, R D *Inorg Chem* 1976, *15*, 1275.

(7) Christe, K O.; Schack, C J.; Wilson, R D *J Fluorine Chem* 1976, *8*, 541

(8) Christe, K. O., Wilson, R. D., Schack, C J. *Inorg. Chem* 1977, *16*, 937

0020-1669/88/1327-2450$01.50/0 © 1988 American Chemical Society

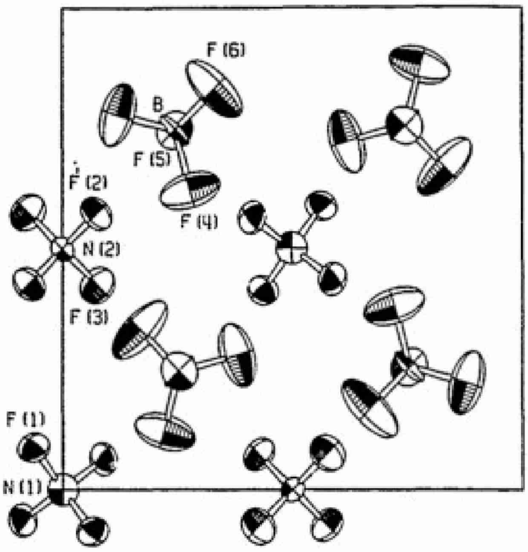

Figure 1. Crystal structure of $NF_4^+BF_4^-$ viewed along the *c* axis.

Table III. Bond Lengths (Å) and Bond Angles (deg) in NF_4^+ and BF_4^- with Esd's in Parentheses[a]

N(1)-F(1)	1.301 (6)	B-F(4)	1.363 (8)
N(2)-F(2)	1.265 (9)	B-F(5)	1.376 (9)
N(2)-F(3)	1.321 (10)	B-F(6)	1.301 (8)
F(1)-N(1)-F(1)	108.5 (3), 111.5 (5)	F(4)-B-F(4)	109.2 (6)
F(2)-N(2)-F(2)	109.7 (10)	F(4)-B-F(5)	109.3 (5)
F(2)-N(2)-F(3)	109.9 (4)	F(4)-B-F(6)	108.7 (6)
F(3)-N(2)-F(3)	107.4 (9)	F(5)-B-F(6)	111.8 (6)

[a] Interionic F···F distances: 2.66-2.78 Å.

sional Patterson function evaluated with a computer program written by M.D.L.

The trial model was refined by a least-squares technique using the program system SHELX-76.[9] Neutral-atom scattering factors were taken from ref 10. Reflections with $I < \sigma(I)$ were omitted from refinement. Two reflections (020 and 040) were discarded because of poor agreement with calculated values as well as film intensities. The resultant atomic coordinates are listed in Table II, while the anisotropic thermal parameters are given in the supplementary material. A projection of the structure is depicted in Figure 1, which also shows the atom numbering as well as thermal ellipsoids. The program ORTEP[11] was used to produce the crystal structure illustration, and geometry calculations were made with the program system X-ray.[12] Bond lengths and angles are given in Table III.

The structure consists of isolated tetrahedra of NF_4^+ cations and BF_4^- anions. The interionic F···F contact distances are in the range of 2.66-2.78 Å, which is normal for such interactions. There are two crystallographically independent NF_4^+ ions corresponding to N(1) and N(2) on $\bar{4}$ and *mm* sites, respectively. This leads to four identical N(1)-F distances of 1.301 Å and two pairs of N(2)-F distances that are 1.265 and 1.321 Å, giving an overall average distance of 1.30 Å. The BF_4^- tetrahedron also has an imposed symmetry of *mm* The B-F(6) distance appears significantly shorter than B-F(4) and B-F(5), even if esd's are underestimated.

Table IV. Correlation Table for the Internal Vibrations of NF_4^+ on the S_4 Sites of Space Group $P\bar{4}2_1m$ in NF_4BF_4

assignment	point group T_d	site group S_4	factor group D_{2d}
ν_{sym}	A_1(— RA)	A(— RA)	A_1(— RA)
			A_2(— —)
δ_{sym}	E(— RA)	A(— RA)	A_1(— RA)
			A_2(— —)
		B(IR, RA)	B_1(— RA)
			B_2(IR, RA)
ν_{asym}	F_2(IR, RA)	B(IR, RA)	B_1(— RA)
			B_2(IR, RA)
		E(IR, RA)	E (IR, RA)
δ_{asym}	F_2(IR, RA)	B(IR, RA)	B_1(— RA)
			B_2(IR, RA)
		E(IR, RA)	E(IR, RA)

Table V. Correlation Table for the Internal Vibrations of NF_4^+ on C_{2v} Sites of Space Group $P\bar{4}2_1m$ in NF_4BF_4

assignment	point group T_d	site group C_{2v}	factor group D_{2d}
ν_{sym}	A_1(— RA)	A_1(IR, RA)	A_1(— RA)
			B_2(IR, RA)
δ_{sym}	E(— RA)	A_1(IR, RA)	A_1(— RA)
			B_2(IR, RA)
		A_2(IR, RA)	A_2(— —)
			B_1(— RA)
ν_{asym}	F_2(IR, RA)	A_1(IR, RA)	A_1(— RA)
			B_2(IR, RA)
		B_1(IR, RA)	E (IR, RA)
		B_2(IR, RA)	E (IR, RA)
δ_{asym}	F_2(IR, RA)	A_1(IR, RA)	A_1(— RA)
			B_2(IR, RA)
		B_1(IR, RA)	E (IR, RA)
		B_2(IR, RA)	E (IR, RA)

To our knowledge, the NF_4BF_4 structure represents an original solution to the packing of two tetrahedral ions. The crystal packing can be considered as a superstructure of the primitive cubic CsCl structure, with the doubling of the cell in two directions being necessitated by the alternating orientations of identical ions. The NF_4^+ ions are stacked with their $\bar{4}$ or *mm*2 symmetry elements along the *c* axis, while the BF_4^- ions are packed with their pseudo-3-fold axis along the same axis. The stacks of $N(1)F_4^+$ and $N(2)F_4^+$ ions are rotated by 90° in relationship to each other in such a manner that room is made alternatively for either three or only one of the fluorine atoms of the BF_4^- anion. Therefore, the boron atoms are located either above or below the center of the small cubic cell depending on the up or down orientation of the BF_4^- ion in a given stack.

Analysis of the Vibrational Spectra of NF_4BF_4. On the basis of the X-ray crystal structure, solid $NF_4^+BF_4^-$ possesses a strongly distorted BF_4^- anion on a C_s site and two kinds of NF_4^+ cations, one of nearly tetrahedral symmetry on an S_4 site and one with two significantly different bond lengths on a C_{2v} site. These results, however, disagree with the previously reported infrared[6,13,14] and

---

(9) Sheldrick G. M. "SHELX-76", University of Cambridge. Cambridge, England, 1976.

(10) *International Tables for X-ray Crystallography*, Kynoch Birmingham, England, 1974; Vol IV, p 99.

(11) Johnson, C. K. "ORTEP"; Report ORNL-3794; Oak Ridge National Laboratory. Oak Ridge, TN, 1976

(12) Stewart, J. M.; Kruger, G. J.; Ammon, H. L.; Dickinson, C.; Hall, S. R. "The X-Ray System, Version 1972", Technical Report TR-192, Computer Science Center, University of Maryland College Park, MD, 1972.

(13) Sinel'nikov, S M , Rosolovskii, V Ya *Dokl Akad Nauk SSSR* 1970, *194*, 1341

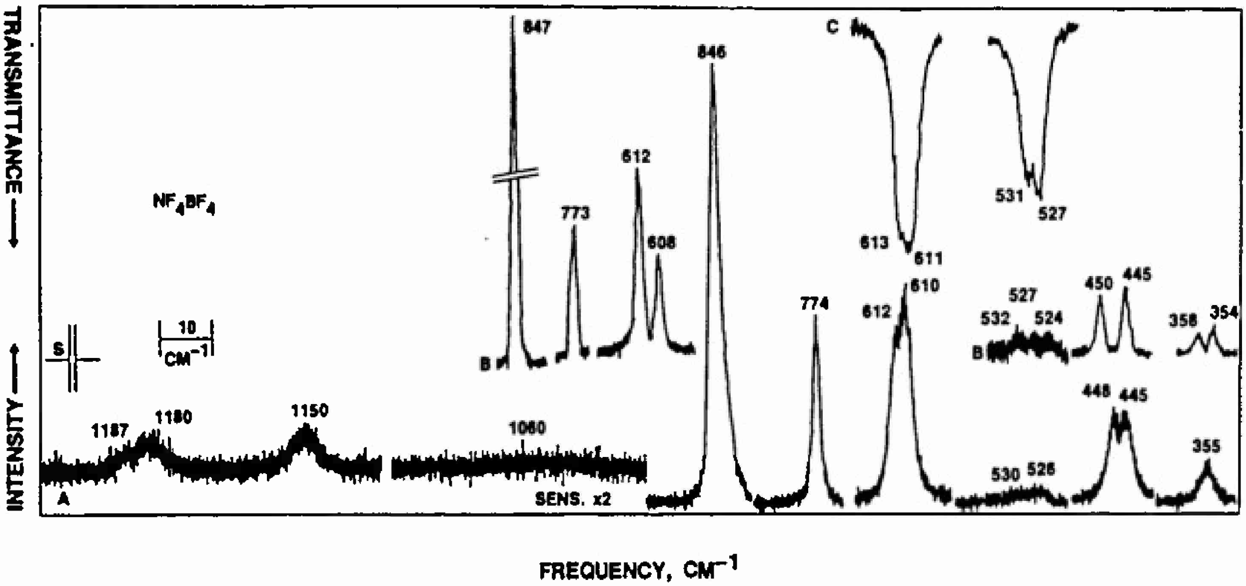

Figure 2. Vibrational spectra of NF_4BF_4: traces A and B, Raman spectra recorded at 25 and −140 °C, respectively; trace C, infrared spectrum recorded at 25 °C; S indicates spectral slit width.

Table VI. Correlation Table for the Interval Vibrations of BF_4^- on C_s Sites of Space Group $P\bar{4}2_1m$ in NF_4BF_4

assignment	point group T_d	site group C_s	factor group D_{2d}
ν_{sym}	A_1(— RA)	A'(IR, RA)	A_1(— RA)
			B_2(IR, RA)
			E (IR, RA)
δ_{sym}	E(— RA)	A'(IR, RA)	A_1(— RA)
			B_2(IR, RA)
			E (IR, RA)
		A''(IR, RA)	A_2(— —)
			B_1(— RA)
			E (IR, RA)
ν_{asym}	F_2(IR, RA)	A'(IR, RA)	A_1(— RA)
			B_2(IR, RA)
			E (IR, RA)
		A'(IR, RA)	A_1(— RA)
			B_2(IR, RA)
			E (IR, RA)
		A''(IR, RA)	A_2(— —)
			B_1(— RA)
			E (IR, RA)
δ_{asym}	F_2(IR, RA)	A'(IR, RA)	A_1(— RA)
			B_2(IR, RA)
			E (IR, RA)
		A'(IR, RA)	A_1(— RA)
			B_2(IR, RA)
			E (IR, RA)
		A''(IR, RA)	A_2(— —)
			B_1(— RA)
			E (IR, RA)

Table VII. Observed Infrared and Raman Spectra of NF_4BF_4

freq, rel intens			approx description of mode in point group T_d	
IR	RA		NF_4^+	BF_4^-
25°	25°	−140°		
	1187sh	1190w	$\nu_3(F_2)$, ν_{asym}	
1180s	1180w			
1159vs	1150w	1152w		
1130-1040vs,br	1060vw			$\nu_3(F_2)$, ν_{asym}
	846vs	847vs	$\nu_1(A_1)$, ν_{sym}	
775w	774s	773s		$\nu_1(A_1)$, ν_{sym}
613ms	612s	612s	$\nu_4(F_2)$, δ_{asym}	
611s	610s	608ms		
531m	530vw	532w		$\nu_4(F_2)$, δ_{asym}
527mw	526w	527vw		
		524w		
	448m	450m	$\nu_2(E)$, δ_{sym}	
	445m	445m		
	355mw	358mw		$\nu_2(E)$, δ_{sym}
		354mw		

Raman[6,14] spectra, which indicated nearly tetrahedral symmetry for both ions and only one kind of cation.[6] Therefore, we have rerecorded the individual hands of $NF_4^+BF_4^-$ under higher resolution conditions and carried out a site group and factor group analysis for NF_4BF_4 in space group $P\bar{4}2_1m$ using the correlation method.[15] The results are summarized in Tables IV–VII, , and the vihrational hands of interest are depicted in Figure 2. A comparison of the observed spectra with the predictions from the factor group analysis for NF_4BF_4 in space group $P\bar{4}2_1m$ allows the following conclusions: (i) There is no spectroscopic evidence for the presence of two distinct NF_4^+ cations. For example, no infrared band and only one symmetrical, narrow Raman line with a half-width of about 2 cm^{-1} at a spectral slit width of 1 cm^{-1} are observed for the symmetric NF_4^+ stretching vibration. For two distinct NF_4^+ cations, at least three strong Raman hands should be ohserved in this region. (ii) For NF_4^+, the number of bands and their infrared and Raman activities are incompatihle with a C_{2v} site symmetry. However, they are acceptable for either an S_4 symmetry, i.e. identical NF_4^+ bond lengths with a slight compression of the tetrahedral angle in one direction, or a tetrahedral symmetry, where the degeneracies of the E and F_2 modes

---

(14) Goetschel, C. T., Campanile, V. A., Curtis, R. M., Loos, K. R., Wagner, D. C.; Wilson, J. N. *Inorg. Chem.* 1972, *11*, 1696.

(15) Fateley, W. G.; Dollish, F. R.; McDevitt, N. T.; Bentley, F. F. In *Infrared and Raman Selection Rules for Molecular and Lattice Vibrations. The Correlation Method*, Wiley-Interscience New York, 1972.

Table VIII. Correlation Table for the Internal Vibrations of BF_4^- of Symmetry C_{3v}

T_d	C_{3v}	obsd freq, rel int IR	RA(25°)
A_1(— RA)	A_1(IR, RA)	775w	774s
E (— RA)	E (IR, RA)		355mw
F_2(IR, RA)	A_1(IR, RA) E (IR, RA)	1130–1040vw,br	1060vw,br
F_2(IR, RA)	A_1(IR, RA)	531m	530w
	E (IR, RA)	527mw	526mw

are partially lifted due to solid-state effects. This interpretation is supported by the fact that the infrared and Raman selection rules for T_d symmetry are retained. (iii) For BF_4^-, again the number of observed bands and their Raman and infrared activities are incompatible with a C_s site symmetry in space group $P\bar{4}2_1m$, and the actual symmetry must be higher. The observation of the symmetric BF_4^- stretching mode in the infrared spectrum eliminates both T_d and S_4 symmetries and also suggests that the symmetries of NF_4^+ and BF_4^- are different.

Reconciliation of the X-ray Data with the Vibrational Spectra. At first glance, the vibrational spectra and single-crystal X-ray data for NF_4BF_4 are incompatible. A closer inspection of the X-ray results, however, reveals the following facts. For the BF_4^- anion, three of the four fluorine atoms, F(6) and the two F(4) atoms, exhibit very large thermal parameters, and the orientations of their ellipsoids indicate rotation or oscillation around the B–F(5) axis.

If this rotating anion model is correct, the vibrational spectra of BF_4^- in NF_4BF_4 should exhibit approximately C_{3v} symmetry. The correlation for $T_d \rightarrow C_{3v}$ is given in Table VIII. As can be seen, the observed spectra are in excellent agreement with the predictions for C_{3v} symmetry. The only bands that, due to their very low intensities, have not been observed are the infrared component of the symmetric deformation and one of the two Raman components of the antisymmetric stretch.

The above model of a rotating BF_4^- anion can also nicely account for the discrepancies encountered with the NF_4^+ cations. With a static model, i.e. nonrotating BF_4^- anions, the fluorine–fluorine repulsions can be equalized within the tetrahedral packing requirements for only half of the NF_4^+ cations. The other half is then experiencing anisotropic repulsions, which lead to their distortion. If, however, the BF_4^- anion rotates or oscillates and thereby averages out the fluorine–fluorine repulsion effects, then all NF_4^+ cations become equivalent and should approximate ideal tetrahedra. This conclusion is in excellent agreement with the vibrational spectra, which show only one kind of NF_4^+ cation of tetrahedral or almost tetrahedral symmetry. From the small thermal parameters of the fluorines on nitrogen, it appears that in NF_4BF_4 the NF_4^+ cations do not appreciably rotate.

The discrepancy between the X-ray data and the vibrational spectroscopic results can therefore be attributed to the fact that a static model with nonrotating ions was used to solve a structure with rotating or oscillating ions. Therefore, the presence of two different sets of NF_4^+ cations, the strong C_{2v} distortion of one of them, and the strong C_s distortion of BF_4^- have no physical meaning and must be considered as artifacts of the method used.

The Raman spectrum of NF_4BF_4 was also recorded at −140 °C. The observed spectrum (see Table VII) was very similar to the room-temperature spectrum, except for the expected line sharpening, minor frequency shifts, and splittings of the 355-cm^{-1} band into two and of the 530- and 526-cm^{-1} bands into three components. Some of these bands are shown in Figure 2. These results suggest that cooling to −140 °C is insufficient to freeze out the rotational motion of the BF_4^- anions.

Most of the thermally more stable NF_4^+ salts undergo at elevated temperatures a phase change.[2] For NF_4AsF_6 and NF_4BF_4 this occurs at 145 ± 1 and 224 ± 2 °C, respectively. An X-ray powder pattern of the high-temperature phase of NF_4AsF_6 showed it to be cubic.[16] This transition from a tetragonal to a cubic phase suggests that at elevated temperature all ions rotate freely and act as spheres. Although no X-ray data are available for the high-temperature phase of NF_4BF_4, the cause for the phase transition is probably the same. A detailed study of the ion motions in NF_4^+ salts as a function of temperature, using methods such as second moment and relaxation time NMR measurements, would be most interesting but was beyond the scope of this study.

Table IX. Crystallographic Data for NF_4SbF_6 and $NF_4Sb_2F_{11}$

NF_4SbF_6

Room Temperature

tetragonal $a = 7.956$ (5) Å; $c = 5.840$ (4) Å
$V = 369.63$ Å^3, ρ(calcd) = 2.928 g cm^{-3}; $Z = 2$

Low Temperature (−120 °C)

tetragonal $a = 7.979$ (4) Å; $c = 11.428$ (4) Å
$V = 727.56$ Å^3; ρ(calcd) = 2.975 g cm^{-3}; $Z = 4$

$NF_4Sb_2F_{11}$

Room Temperature

tetragonal: $a = 18.326$ (9) Å; $c = 14.205$ (5) Å
$V = 4770.6$ Å^3; ρ(calcd) = 3.02 g cm^{-3}; $Z = 16$

Partial Crystal Structures of NF_4SbF_6 and $NF_4Sb_2F_{11}$. Attempts to solve the X-ray crystal structures of NF_4SbF_6 and $NF_4Sb_2F_{11}$ were carried out at the University of Leicester and the University of Southern California, respectively. Both compounds exhibited ion rotation and possibly disorder problems, and, therefore, their structures could only partially be solved.

For NF_4SbF_6, which appears to be isotypic with $PCl_4^+PCl_6^-$,[17] the structure could be refined to $R_w = 0.084$ for the antimony, nitrogen, and the four fluorines on nitrogen but did not result in reasonable positions for the fluorines on antimony. This is not surprising in view of the fact that in the closely related $PCl_4^+PCl_6^-$ structure the chlorines on the octahedral phosphorus exhibit very large thermal parameters and two longer axial bonds, indicative of anion rotation around 3-fold axes. Attempts were unsuccessful to overcome the problem of ion rotation by collecting a data set at low temperature (−120 °C). Although the c axis of the unit cell was doubled at −120 °C, the structure again could not be solved. Some of the crystallographic data for NF_4SbF_6 and $NF_4Sb_2F_{11}$ are summarized in Table IX.

It was hoped that the anion rotation problem could be solved by substituting the octahedral SbF_6^- anion by the less symmetrical $Sb_2F_{11}^-$ anion. With the positions of the $Sb_2F_{11}^-$ anions fixed first, the NF_4^+ cations appeared clearly visible, but problems arose during the least-squares refinement. By applying constraints on the distances and angles of the $Sb_2F_{11}^-$ anion, it was possible to refine the structure to an R factor of 0.126.

It should be emphasized that, although N–F bond lengths with reasonably small estimated standard deviation values were obtained in both cases, these N–F bond length values significantly deviated from the more reliable value obtained for NF_4BF_4. Furthermore, when the NF_4^+ geometry was fixed and the anion refined without constraints on symmetry, as for NF_4SbF_6, the resulting N–F bond length (1.25 (2) Å) was much too short. However, when the anion geometry was constrained, as for $NF_4Sb_2F_{11}$, the resulting N–F bond length (1.34 Å) was much too long. Thus, values obtained from incomplete structures of this type should not be trusted because errors induced by ion rotation and repulsion effects can cause apparent lengthening or shortening of bonds, depending on the constraints used for the refinement.

Conclusions. The bond length in NF_4^+ has been determined experimentally for the first time. The found value of 1.30 Å confirms the predictions of 1.31 and 1.32 Å, made from force field[3] and ab initio[4] calculations, and is the shortest known N–F bond. Its shortness is attributed to the high oxidation state (+V) of and the formal positive charge on nitrogen and a maximal number

---

(16) Bougon, R.; Bui Huy, T.; Burgess, J.; Christe, K. O.; Peacock, R. D. *J. Fluorine Chem.* 1982, *19*, 263.

(17) Preiss, H. *Z. Anorg. Allg. Chem.* 1971, *380*, 51.

of fluorine ligands. Partial double bonding, which can be invoked for the NF molecule

($r = 1.3173$ Å),[18] is unlikely for NF_4^+ because all of its atoms already possess an electron octet.

The problems previously encountered with solving a crystal structure of an NF_4^+ salt appear to be largely due to ion rotation and/or disorder in these salts. The main difficulty consisted of finding a static model with nonrotating ions that could describe a dynamic structure with rotating ions. The thermal parameters of the atoms from the X-ray data and vibrational spectroscopy coupled with a group factor analysis were found to be very useful for the detection and understanding of ion rotation. In the case of ion rotation, the X-ray analysis can result in an apparent lowering of the symmetry and in a nonequivalence of ions, which have no real physical meaning. Similarly, partial structure solutions or solutions in which the geometry of one set of ions has to be constrained can result in unreliable bond lengths with deceptively small estimated standard errors.

Acknowledgment. The work at Rocketdyne was sponsored by the Office of Naval Research and the U.S. Army Research Office. We thank Dr. M. Watkins and J. A. Feng for assistance during the structural analysis of $NF_4Sb_2F_{11}$ and Dr. P. Charpin for helpful comments.

Registry No. NF_4BF_4, 15640-93-4, NF_4SbF_6, 16871-76-4, $NF_4Sb_2F_{11}$, 58702-89-9.

Supplementary Material Available: A table of anisotropic thermal parameters for NF_4BF_4 (1 page); a listing of observed and calculated structure factors (2 pages). Ordering information is given on any current masthead page.

---

[18] Douglas, A. E.; Jones, W. E. *Can. J Phys.* **1966**, *44*, 2251.

APPENDIX C

Reprinted from Inorganic Chemistry, 1988, *27*, 1389

Contribution from the Departement de Physico-Chimie, Centre d'Etudes Nucléaires de Saclay,
IRDI/DESICP/DPC/SCM UA CNRS 331, 91191 Gif-sur-Yvette Cédex, France,
and Rocketdyne, A Division of Rockwell International, Canoga Park, California 91303

Preparation and Characterization of $Ni(BiF_6)_2$ and of the Ternary Adducts $[Ni(CH_3CN)_6](BiF_6)_2$ and $[Ni(CH_3CN)_6](SbF_6)_2$. Crystal Structure of $[Ni(CD_3CN)_6](SbF_6)_2$

Roland Bougon,*[1a] Pierrette Charpin,[1a] Karl O. Christe,[1b] Jacques Isabey,[1a] Monique Lance,[1a]
Martine Nierlich,[1a] Julien Vigner,[1a] and William W. Wilson[1b]

Received August 10, 1987

$Ni(BiF_6)_2$ was prepared from the reaction of NiF_2 with BiF_5 in anhydrous HF, followed by removal of the excess of BiF_5 by sublimation. The compound was characterized by elemental analysis, X-ray powder data, and vibrational spectroscopy. Both $Ni(BiF_6)_2$ and $Ni(SbF_6)_2$ react with acetonitrile to give ternary adducts of the formula $NiF_2 \cdot 2MF_5 \cdot 6CH_3CN$, with M = Bi or Sb. These isomorphous adducts are stable at room temperature and were characterized by elemental analyses, X-ray powder data, and infrared and electronic spectroscopy. In these ternary adducts the Ni^{2+} ion is octahedrally coordinated by six acetonitrile molecules via the nitrogen, and the counterions are MF_6^-. The $[Ni(CD_3CN)_6](SbF_6)_2$ complex was characterized by X-ray diffraction methods, crystallizing in the trigonal space group $R\bar{3}$ with $a = 11.346$ (2) Å, $c = 17.366$ (6) Å, $V = 1936$ Å^3, $Z = 3$, and $R = 0.034$. The Sb atoms lie on C_3 sites and are octahedrally coordinated by six F atoms with two nonequivalent Sb–F distances of 1.80 (1) and 1.83 (1) Å. The octahedrally coordinated Ni atoms lie on C_{3i} sites with Ni–N distances of 2.07 (1) Å. It is shown that coordination of the Ni^{2+} ions by six CH_3CN molecules lessens the strong polarizing effect of these ions on the MF_6^- counterions, which had been found for the $Ni(MF_6)_2$ salts, and reduces their distortion from octahedral symmetry.

Introduction

The preparation and characterization of $Ni(SbF_6)_2$ have been described in a recent paper,[2] and preliminary results concerning $Ni(BiF_6)_2$ and the acetonitrile adducts of both salts have been presented at a meeting.[3] This paper gives a full report on the preparation and characterization of $Ni(BiF_6)_2$ and the acetonitrile adducts. The previous formulation[2] of $NiF_2 \cdot 2SbF_5 \cdot 6CH_3CN$ as $[Ni(CH_3CN)_6]^{2+}(SbF_6^-)_2$ was confirmed by elemental analysis, vibrational and electronic spectroscopy, and a crystal structure determination. Furthermore, it was interesting to determine how coordination of the Ni^{2+} ion by CH_3CN influences its interaction with the MF_6^- counterions.

Experimental Section

Apparatus. Volatile materials were manipulated in an all-metal vacuum line equipped with Teflon or metal valves. Solid products were handled in a glovebox flushed with dry nitrogen. The high-pressure reactor used has previously been described.[4] Infrared spectra were recorded in the range 4000–200 cm^{-1} on a Perkin-Elmer Model 283 spectrophotometer. Spectra of solids were obtained by using dry powders pressed between AgCl or AgBr windows in an Econo press (Barnes Engineering Co.). The low-frequency parts of the spectra were also recorded as halocarbon (Voltalef) or Nujol mulls between silicon plates. Raman spectra were recorded on a Coderg Model T 800 spectrophotometer by using the 514.5-nm exciting line of an Ar ion Spectra Physics laser or the 647.1-nm exciting line of a Kr ion Spectra Physics laser. Sealed quartz capillaries were used as sample containers in the transverse-viewing–transverse-excitation mode. Low-temperature spectra were obtained with a Coderg liquid-nitrogen cryostat and a Coderg RC 200 regulator. The electronic absorption spectra were recorded on a Beckman UV 5240 spectrophotometer, the solution being contained in a 1 mm thick quartz cell fitted with a Teflon-TFE Rotaflo stopcock. X-ray diffraction powder patterns of the samples sealed in 0.3 mm o.d. quartz capillaries were obtained by using a Phillips camera (diameter 11.46 cm) using Ni-filtered Cu *Kα* radiation. Crystals suitable for structure determination were transferred into quartz capillaries in the drybox.

Materials. Anhydrous nickel difluoride[5] was obtained by the treatment of nickel acetate with HF at 270 °C followed by fluorination with F_2 at 200 °C. Bismuth and antimony trifluorides were from Ozark Mahoning Co., and their purities were checked by infrared spectroscopy and X-ray diffraction. Fluorine (Union Carbide Co.) was passed over NaF pellets to remove HF. Bismuth pentafluoride was prepaed by the reaction of BiF_3 with F_2 at 350 °C at a pressure of 20 atm. Acetonitrile (Prolabo) and acetonitrile-d_3 (CEA) were refluxed over P_2O_5 followed by treatment and storage on 5A molecular sieves. The adduct $Ni(SbF_6)_2$ was prepared as described previously[2] except that NiF_2 and SbF_5 were used instead of Ni and SbF_3, respectively. Microanalyses were by Analytische Laboratorien, Elbach, West Germany.

Preparation of $Ni(BiF_6)_2$. A mixture of NiF_2 (2.57 mmol) and BiF_5 (5.15 mmol) was loaded in the drybox into half of a prepassivated Teflon double-U metathesis apparatus.[6] Dry HF (≈10 mL) was added on the vacuum line to the half containing NiF_2–BiF_5, and the resulting mixture was stirred for 6 h at 25 °C. The metathesis apparatus was inverted, and the resulting solution, pressurized by 2 atm of dry nitrogen, was filtered into the other half of the apparatus. The HF solvent was pumped off for 12 h at 25 °C, leaving 1.4749 g of a pale yellow solid. The X-ray powder diffraction patterns indicated that this solid consisted of a mixture of $Ni(BiF_6)_2$ and BiF_5 and that the filter cake contained NiF_2 and $Ni(BiF_6)_2$. The solid residue obtained from the evaporation of the solution was ground and loaded in the drybox into a prepassivated 30 cm long sapphire tube, which was connected to an aluminum valve by a Swagelock compression fitting using Teflon ferrules. The lower part of the tube was

---

(1) (a) Centre d'Etudes Nucléaires de Saclay. (b) Rocketdyne.
(2) Christe, K. O.; Wilson, W. W.; Bougon, R.; Charpin, P. *J. Fluorine Chem.* **1987**, *34*, 287.
(3) Bougon, R.; Charpin, P.; Lance, M.; Isabey, J.; Christe, K. O.; Wilson, W. W. Presented at the 8th Winter Fluorine Conference of the American Chemical Society, St. Petersburg, Fl, Jan 25–30, 1987.
(4) Hagenmuller, P. *Preparative Methods in Solid State Chemistry*; Academic: New York and London, 1972; p 423.
(5) Sample kindly supplied to us by M. Berger, CEA/IRDI.
(6) Christe, K. O.; Schack, C. J.; Wilson, R. D. *Inorg. Chem.* **1977**, *16*, 849.

0020-1669/88/1327-1389$01.50/0 © 1988 American Chemical Society

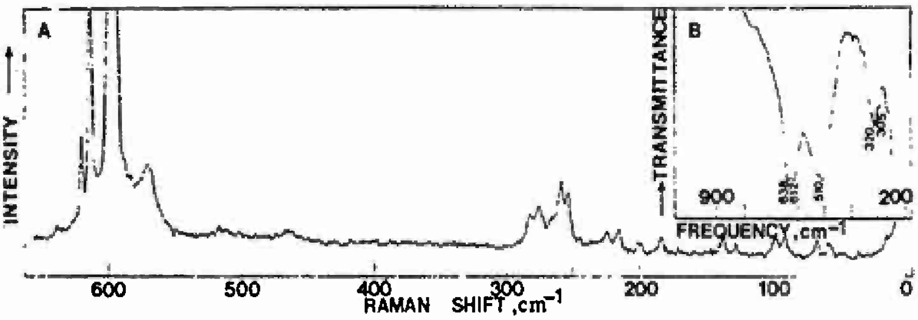

Figure 1. Vibrational spectra of $Ni(BiF_6)_2$.

Table I. X-ray Powder Data for $Ni(BiF_6)_2$

d, Å	intens	*d*, Å	intens
4.67	m	1.883	m
4.21	s	1.854	vw
		1.826	w
3.75	s		
3.68	m	1.742	w
		1.734	ms
2.77	w	1.717	vw
2.74	m		
		1.661	m
2.55	m	1.630	m
2.387	mw		
2.357	w	1.515	mw
		1.504	w
2.252	m	1.475	m
2.241	m	1.445	w
		1.411	w
2.189	mw	1.376	w
2.109	m	1.343	mw

heated for 17 h at 100 °C with pumping. The solid that had sublimed onto the wall of the tube was identified as BiF_5 whereas the X-ray pattern and the vibrational spectra showed that the solid residue in the bottom of the tube (0.757 g) contained only $Ni(BiF_6)_2$.

Anal. Calcd for $Ni(BiF_6)_2$: Ni, 8.33; Bi, 59.32; F, 32.35. Found: Ni, 8.27; Bi, 60.65; F, 30.41.

Preparation of $[Ni(CH_3CN)_6]^{2+}(MF_6^-)_2$ (M = Sb or Bi). The $Ni(MF_6)_2$ salts, typically on a 1–5 mmol scale, were loaded in the drybox into the Teflon double-U metathesis apparatus.[6] Approximately 10 mL of CH_3CN or CD_3CN was condensed at −196 °C onto the $Ni(MF_6)_2$; the mixture was warmed to 20 °C and stirred for 2 h. The blue solutions were filtered into the second half of the apparatus. Upon solvent removal in vacuo, the solutions yielded purple crystals of $[Ni(CH_3CN)_6](MF_6)_2$.

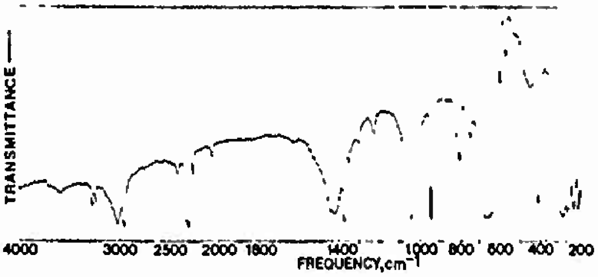

Figure 2. Infrared spectrum of $[Ni(CH_3CN)_6](SbF_6)_2$.

Single crystals of $[Ni(CD_3CN)_6](SbF_6)_2$ were grown from these solutions by slow evaporation of some of the solvent.

Anal. Calcd for $Ni(CH_3CN)_6(SbF_6)_2$: C, 18.56; H, 2.34; N, 10.82; F, 29.36; Sb, 31.36; Ni, 7.56. Found: C, 18.53; H, 2.32; N, 10.79; F, 29.31; Sb, 31.67; Ni, 7.59.

Anal. Calcd for $Ni(CH_3CN)_6(BiF_6)_2$: C, 15.16; H, 1.91; N, 8.84; F, 23.97; Bi, 43.95; Ni, 6.17. Found: C, 15.15; H, 1.86; N, 8.80; F, 22.85; Bi, 44.55; Ni, 6.20.

Results and Discussion

Synthesis of $Ni(BiF_6)_2$. The combination of NiF_2 with an excess of either BiF_5 at 160 °C in a Teflon FEP tube or $BiF_3 + F_2$ at 240 °C in an alumina crucible, contained in a Monel reactor, did not produce pure $Ni(BiF_6)_2$. The solid products were always contaminated with excess BiF_5 and to some extent NiF_2 and/or BiF_3. The NiF_2 impurity was removed by anhydrous HF in which NiF_2 is insoluble. Any excess of BiF_5 was removed by vacuum sublimation at 100 °C. In this manner pure $Ni(BiF_6)_2$ was obtained.

Table II. Vibrational Frequencies and Assignments for $Ni(BiF_6)_2$

obsd freq, cm⁻¹ (rel intens[a])				
	Raman			
IR	28 °C	−196 °C	assignment	
638 vs	639 (0+)	639 (2)	$\nu_{as}(BiF_3)$ out of phase	nonbridging BiF_3 stretching modes
	619 sh	621 (11)	$\nu_{as}(BiF_3)$ in phase	
612 vs	613 (33)	615 (33)	$\nu_{sym}(BiF_3)$ out of phase	
	596 (100)	596 (100)	$\nu_{sym}(BiF_3)$ in phase	
	569 sh	571 (10)	$\nu_{sym}(BiF_3)$ out of phase	bridging BiF_3 stretching modes
510 vs		517 (1)	$\nu_{as}(BiF_3)$ out of phase	
305 sh 320 ms			Ni···FBi stretching	
		283 (4)	Bi–F deformations	
	275 sh	276 (5)		
	261 (6)	259 (8)		
		254 (6)		
	225 (3)	225 (2)		
215 ms		216 (2)		
		201 (0+)		
	181 (0+)	184 (3)		
		138 (3)		
	123 (1)	128 (1)		
	95 (3)	99 (3)	Ni–F deformations or lattice modes	
		91 (3)		
	64 (3)	68 (2)		
	59 (3)	59 (2)		

[a] Uncorrected Raman intensities based on relative peak heights.

Table III. Electronic Absorption Data for $[Ni(CH_3CN)_6](SbF_6)_2$ in CH_3CN Solution

band max, cm^{-1}	ϵ_{max}, L mol^{-1} cm^{-1}	assignment
10430	40	$\Gamma_5(^3F) \leftarrow \Gamma_2(^3F)$
13910	9	$\Gamma_3(^1D) \leftarrow \Gamma_2(^3F)$
17120	35.4	$\Gamma_4(^3F) \leftarrow \Gamma_2(^3F)$
22990	weak sh	$\Gamma_5(^1D) \leftarrow \Gamma_2(^3F)$
27400	52.6	$\Gamma_4(^3P) \leftarrow \Gamma_2(^3F)$

X-ray Diffraction Data. The X-ray power diffraction data for $Ni(BiF_6)_2$, which are listed in Table I, indicate that the structure of this compound is very similar to that[2] of $Ni(SbF_6)_2$. Nevertheless, a splitting of some of the lines indicate that the symmetry is probably lowered, so that not all lines could be assigned in the hexagonal system proposed[2] for $Ni(SbF_6)_2$.

Vibrational Spectra. The observed infrared and Raman spectra of $Ni(BiF_6)_2$ are shown in Figure 1, and the frequencies are summarized in Table II. As discussed[2] for $Ni(SbF_6)_2$, the spectra clearly indicate that the MF_6^- anion is not octahedral but is strongly distorted, and that both bridging and nonbridging fluorines are present. The assignments given in Table II are based on those[2] previously proposed for $Ni(SbF_6)_2$.

Syntheses and Properties of the $[Ni(CH_3CN)_6](MF_6)_2$ Adducts. The $Ni(MF_6)_2$ salts, where M = Sb or Bi, are very soluble in CH_3CN and form bright blue solutions containing the $[Ni(CH_3CN)_6](MF_6)_2$ adducts. The electronic absorption spectra of these solutions are characteristic of an octahedrally coordinated Ni^{2+} ion and are quite comparable to those reported[7,8] for $[Ni(CH_3CN)_6]^{2+}(BF_4^-)_2$. The data obtained from the spectrum of $[Ni(CH_3CN)_6]^{2+}(SbF_6^-)_2$ are summarized in Table III. A strong

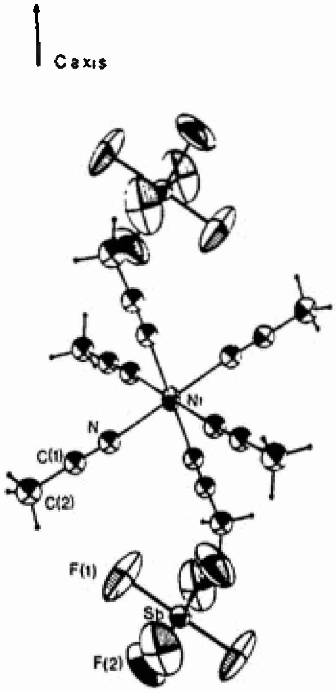

Figure 3. ORTEP[13] drawing of the molecular unit $[Ni(CD_3CN)_6](SbF_6)_2$.

Table IV. Infrared Data (cm^{-1}) for $[Ni(CH_3CN)_6]^{2+}(SbF_6^-)_2$, $[Ni(CH_3CN)_6]^{2+}(BiF_6^-)_2$, and $[Ni(CD_3CN)_6]^{2+}(SbF_6^-)_2$

Fundamental Modes of Free[a] and Coordinated CH_3CN (CD_3CN)

CH_3CN[a]	$[Ni(CH_3CN)_6]^{2+}$-$(SbF_6^-)_2$	$[Ni(CH_3CN)_6]^{2+}$-$(BiF_6^-)_2$	CD_3CN[a]	$[Ni(CD_3CN)_6]^{2+}$-$(SbF_6^-)_2$	assignment
2942	2946	2949	2115	2114	$\nu_1(A_1)$ sym $CH_3(D_3)$ str
2252	2299	2299	2259	2308	$\nu_2(A_1)$ C≡N str
1374	1373	1374	1102	1104	$\nu_3(A_1)$ sym $CH_3(D_3)$ def
919	942	945	832	858	$\nu_4(A_1)$ C—C str
3001	3012	3012	overlapped with ν_2	2257	$\nu_5(E)$ asym $CH_3(D_3)$ str
1415	1422	1429	1036	1034	$\nu_6(E)$ asym $CH_3(D_3)$ def
1039	1040	1039	848	overlapped with ν_4	$\nu_7(E)$ $CH_3(D_3)$ rock
378	412	412	347	382	$\nu_8(E)$ C—C≡N bend

Combination Modes of Coordinated $CH_3CN(CD_3CN)$

$[Ni(CH_3CN)_6]^{2+}$-$(SbF_6^-)_2$	$[Ni(CH_3CN)_6]^{2+}$-$(BiF_6^-)_2$	assignment	$[Ni(CD_3CN)_6]^{2+}$-$(SbF_6^-)_2$	assignment
3268	3267	$2\nu_4 + \nu_3$	3420	$\nu_2 + \nu_3$
3232	3239	$\nu_2 + \nu_4$	3282	$\nu_5 + \nu_6$
2740	2738	$2\nu_3$	3167	$\nu_1 + \nu_6$, $\nu_2 + \nu_4$, $\nu_2 + \nu_7$
			3120	$\nu_5 + \nu_7$, $\nu_4 + \nu_5$
			2957	$\nu_1 + \nu_4$, $\nu_1 + \nu_7$
2412	2420	$\nu_3 + \nu_7$, $\nu_6 + \nu_7$	2917	$2\nu_6 + \nu_4$
2320	2321	$\nu_3 + \nu_4$	1949	$\nu_3 + \nu_4$, $\nu_3 + \nu_7$
2252	2254	$2\nu_8 + \nu_6$	1880	$\nu_4 + \nu_6$, $\nu_6 + \nu_7$
2072	2070	$2\nu_7$	1725	$2\nu_4$, $2\nu_7$, $\nu_4 + \nu_7$
			1460	$\nu_3 + \nu_8$
819	820	$2\nu_8$		
800	799	?	743	$2\nu_8$

XF_6^- Modes (X = Sb, Bi)

$[Ni(CH_3CN)_6]^{2+}(SbF_6^-)_2$	$[Ni(CH_3CN)_6]^{2+}(BiF_6^-)_2$	$[Ni(CD_3CN)_6]^{2+}(SbF_6^-)_2$	assignment[b]
1306	1150	1304	$\nu_1 + \nu_3$
1228	1100	1226	$\nu_2 + \nu_3$
750	659		$\nu_2 + \nu_6$
			$\nu_1(A_{1g})$
665	570	668 sh 654	$\nu_3(F_{1u})$
570		568	$\nu_2(E_g)$
450			$\nu_5 + \nu_6$?
288	215	288	$\nu_4(F_{1u})$
270			$\nu_5(F_{2g})$

[a] Liquid at 35 °C.[10] [b] Assignment based on space group O_h. See text.

Table V. Crystal Data

formula	$C_{12}D_{18}F_{12}N_6NiSb_2$
fw	794.6
crystn solvent	acetonitrile-d_3
cryst syst	trigonal
space group	$R\bar{3}$
cryst dimens, mm	0.300 × 0.200 × 0.050
cryst color	purple
lattice params	
a, Å	11.346 (3)
c, Å	17.366 (6)
Z	3
V, Å^3	1936
d_{calcd}, g cm^{-3}	2.045
radiation	Mo Kα (λ = 0.7107 Å), graphite monochromator
μ(Mo Kα), cm^{-1}	29.1
temp, K	295
instrument	Enraf-Nonius CAD 4
ω range, deg	2–40
octants	h,k,l (0 to +10, 0 to +10, 0 to +16)
no. of collcd data	256
no. of data with $\sigma(I)/I < 0.33$	148
no. of params	45
data/variable ratio	5.7
resolution programs	SDP 80 program package, Enraf-Nonius, Delft, The Netherlands
scattering factor (f', f'') sources	a
structure soln	heavy-atom method
$R(F)$	(0.035)
$R_w(F)$	(0.042)
w	$4F_o^2/\sigma(I_o)^2 + (pF_o^2)$ with $p = 0.04$
function used in the least-squares refinement	$\sum w(\lvert F_o\rvert - \lvert F_c\rvert)^2$
deuterium atoms	in calcd positions, riding on their C atoms, with thermal param $B_H = 15B_c$

[a] *International Tables for X-ray Crystallography*; Kynoch: Birmingham, England, 1974; Vol. IV, Tables 2-2B and 2-3-1.

Table VI. Positional and Thermal Parameters for $[Ni(CD_3CN)_6](SbF_6)_2$

atom	x	y	z	B,[a] Å^2
Sb	0.000	0.000	0.3293 (1)	4.01 (3)*
F(1)	−0.131 (1)	−0.002 (2)	0.3891 (7)	14 1 (5)*
F(2)	−0.131 (1)	−0.129 (1)	0.2669 (7)	13.3 (5)*
Ni	0.000	0.000	0.000	2.38 (8)*
N	0.149 (1)	0.151 (1)	−0.0675 (6)	3.9 (3)
C(1)	0.241 (1)	0.243 (1)	−0.1012 (9)	4.1 (4)
C(2)	0.349 (1)	0.348 (1)	−0.1419 (9)	4.5 (4)
D(1)	0.317	0.387	−0.179	6.8
D(2)	0.407	0.416	−0.107	6.8
D(3)	0.398	0.311	−0.167	6.8

[a] Starred values denote anisotropically refined atoms for which $B_{equiv} = {}^4/_3\sum_{ij}\beta_{ij}a_ia_j$.

Table VII. Interatomic Distances (Å) and Angles (deg)

$[Ni(NCCD_3)_6]^{2+}$ Octahedron			
Ni–N	2.07 (1)	C(1)–C(2)	1.40 (2)
N–C(1)	1.20 (2)		
Ni–N–C(1)	175 (2)	N–C(1)–C(2)	179 (2)
SbF_6^- Octahedron			
Sb–F(1)	1.80 (1)	Sb–F(2)	1.83 (1)
F(1)–Sb–F(1)	90.2 (6)	F(1)–Sb–F(2)	91.7 (7)
F(1)–Sb–F(2)	89.7 (6)	F(1)–Sb–F(2)	178.2 (7)
F(2)–Sb–F(2)	88.5 (7)		

band at 46 510 cm^{-1}, which is not included in Table III, is assigned to a charge transfer. The value of the ligand field splitting (10Dq)[9] was found from the $\Gamma_5(^3F) \leftarrow \Gamma_2(^3F)$ transition to be equal to 10 430 cm^{-1}.

The acetonitrile adducts and their solutions are stable at room temperature. Owing to their absorption range, which includes the wavelengths of the laser exciting lines used for Raman spectroscopy, no Raman spectra of these adducts were obtained. However, information regarding the molecular arrangement could be obtained from the infrared spectra alone since they displayed sharp and well-defined bands (see Figure 2 and Table IV).

The positions of the ligand bands are as expected[7] for coordinated acetonitrile. Compared to those for free acetonitrile,[10] the bands assigned to the C—C≡N skeletal modes, ν_2, ν_4, and ν_8, show the expected[7,11] frequency increase while the remaining modes are essentially unshifted. The remaining bands in the infrared spectra can be assigned to the MF_6^- anions.[12] According to the crystal structure (see below), the site symmetry of the SbF_6^- anion is C_3, which implies that the modes corresponding to $\nu_3(F_{1u})$, $\nu_4(F_{1u})$, $\nu_5(F_{2g})$, and $\nu_6(F_{2u})$ of O_h symmetry each might be split into two components of symmetry A and E, which are active in both the Raman and infrared.[2] The number of infrared bands, their contours, and relative intensities indicate that the octahedral symmetry of the MF_6^- anions is indeed lower than O_h in these adducts but that the distortion is considerably less than that observed for the $Ni(MF_6)_2$ salts. This is not surprising in view of the fact that the polarizing strength and hardness of the Ni^{2+} acid is greatly diminished by surrounding it with six bulky CH_3CN ligands, which isolate the Ni^{2+} cations from the MF_6^- anions.

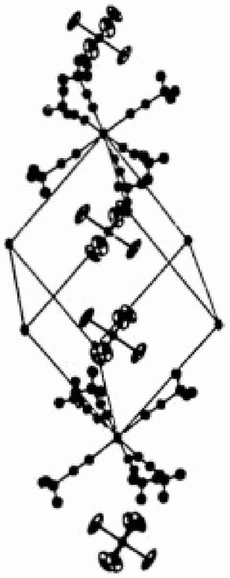

Figure 4. View of the molecular packing of $[Ni(CD_3CN)_6](SbF_6)_2$.

Crystal Structure. The molecular stereochemistry of the ternary adducts was established by a single-crystal study of the adduct $[Ni(CD_3CN)_6]^{2+}(SbF_6^-)_2$. Crystal data are given in Table V. Final positional and thermal parameters are given in Table VI with their estimated standard deviations. The relevant distances and angles are given in Table VII. Figure 3 shows the molecular unit and atomic labeling scheme, and Figure 4 gives a view of the molecular packing.[13] Both ions have octahedral geometry. In $[Ni(CD_3CN)_6]^{2+}$, the Ni atom lies on a C_{3i} symmetry and the six nitrogen atoms form a slightly compressed octahedron with

---

(7) Reedijk, J.; Groeneveld, W. L. *Recl. Trav. Chim. Pays-Bas* 1967, *86*, 1103.
(8) Hathaway, B. J.; Holah, D. G. *J. Chem. Soc.* 1964, 2400.
(9) Ballhausen, C. J. *Introduction to Ligand Field Theory*, McGraw-Hill New York, San Francisco, Toronto, London, 1962; p 261
(10) Shimanouchi, T *Natl. Stand Ref Data Ser. (U.S., Natl Bur. Stand) NSRDS-NBS 39*, 84. Pace, E. L.; Noe, L. W. *J. Chem. Phys.* 1968, *49*, 5317.
(11) Purcell, K. F. *J. Am. Chem. Soc.* 1967, *89*, 247.
(12) Reedijk, J., Zuur, A. P., Groeneveld, W. L. *Recl. Trav. Chim. Pays-Bas* 1967, *86*, 1127 and references therein.
(13) Johnson, C. K. "ORTEP II", Report ORNL 5138, Oak Ridge National Laboratory: Oak Ridge, TN, 1976.

the two N–N distances being significantly different: 2.95 (2) Å and 2.89 (2) Å. The SbF_6^- anion has only a C_3 symmetry and hence two independent F atoms: Sb–F(1) = 1.80 (1) Å; Sb–F(2) = 1.83 (1) Å. The F–F distances are equal: F(1)–F(1) = 2.55 (2) Å; F(2)–F(2) = 2.56 (2) Å; F(1)–F(2) = 2.57 (2) Å. Thus, in spite of the two nonequivalent F atoms, Sb lies in a nearly regular octahedron.

Conclusion. The results of this study show that the corrosion products formed in high-temperature fluorination reactions involving BiF_5 in nickel or Monel reactors are analogous to those[2] found for SbF_5. In the formed $Ni(MF_6)_2$ products the MF_6^- anions are strongly distorted by the strong polarizing effect of the small, doubly charged Ni^{2+} cations and the resulting strong fluorine bridging. Basic ligands with good donor properties, such as CH_3CN, can add to the Ni^{2+} cations and form ternary adducts of the composition $[Ni(CH_3CN)_6](MF_6)_2$. The increased size and softness of the new cations diminishes the strong polarizing effect of the Ni^{2+} cations on the MF_6^- anions in the $Ni(MF_6)_2$ type compounds.

Acknowledgment. The authors from Rocketdyne thank the U.S. Army Research Office and the Office of Naval Research for financial support.

Note Added in Proof. After submission of this paper, the results of an independent crystal structure determination of $[Ni(CH_3CN)_6](SbF_6)_2$ have been published by: Leban, Gantar, Frlec, Russell, and Holloway, *Acta Crystallogr., Sect. C: Cryst. Struct. Commun.* **1987**, *43*, 1888.

Registry No. $Ni(BiF_6)_2$, 112817-17-1; NiF_2, 10028-18-9; BiF_5, 7787-62-4; $[Ni(CH_3CN)_6]^{2+}(SbF_6^-)_2$, 69102-75-6; $[Ni(CH_3CN)_6]^{2+}\cdot(BiF_6^-)_2$, 112817-18-2; $[Ni(CD_3CN)_6](SbF_6)_2$, 112839-66-4.

Supplementary Material Available: Tables of bond distances, bond angles, atomic positional parameters, anisotropic thermal parameters, and lattice constants and space group (7 pages); a table of calculated and observed structure factors (2 pages). Ordering information is given on any current masthead page.

APPENDIX D

Reprinted from Inorganic Chemistry, 1989, *28*, 4175
Copyright © 1989 by the American Chemical Society and reprinted by permission of the copyright owner.

Contribution from Rocketdyne, A Division of Rockwell
International Corporation, Canoga Park, California 91303

Anion Exchange in NF_4^+ Salts Using Graphite Salts as an Oxidizer- and Acid-Resistant Anion-Exchange Medium

Karl O. Christe* and Richard D. Wilson

Received May 19, 1989

Although a large number of NF_4^+ salts are presently known,[1] only two of these salts, NF_4SbF_6[2] and NF_4BiF_6,[3] are readily accessible by direct synthesis from NF_3, F_2, and the corresponding Lewis acid at elevated temperatures and pressures. Since the SbF_6^- and BiF_6^- anions are heavy and do not significantly contribute to the performance of these salts in applications such as NF_3–F_2 gas generators[4] and energetic formulations,[5] it is necessary to replace the SbF_6^- anion in NF_4SbF_6 by lighter and/or more energetic anions.[4] In the past, this has been achieved mainly by a metathetical exchange of the anion at low temperature in anhydrous HF or BrF_5 as a solvent.[6]

$$NF_4SbF_6 + CsBF_4 \rightarrow CsSbF_6\downarrow + NF_4BF_4 \qquad (1)$$

The main drawbacks of reaction 1 include the following: the purity of the resulting NF_4BF_4 is only about 92%, unless repeated recrystallizations from HF and BrF_5 solutions are used;[2] the yields of NF_4BF_4 are less than quantitative (typically ~80%, due to losses during the recrystallizations and hold up of mother liquor on the filter cake); and the process is a batch process that requires troublesome low-temperature filtration steps involving anhydrous HF or BrF_5 solutions. It was, therefore, desirable to develop an improved process for exchanging the anion in NF_4SbF_6, which ideally would result in quantitative yields and high purities of the desired NF_4^+ salts in a simple, one-step process under ambient conditions. In this paper we describe such a process that had been discovered in our laboratory 8 years ago but could not be reported earlier due to the classification of a patent.[7]

Experimental Section

Starting Materials. Three different types of graphite were used in the course of this study. The first one consisted of spectrographic graphite (SG) electrodes, manufactured by the National Carbon Co., a Division of Union Carbide. The second one was a pyrolytic graphite (PG) slab for use in rocket nozzles, obtained from Hercules, and the third one was highly oriented pyrolytic graphite (HOPG) with a mirrorlike surface, obtained from Union Carbide by courtesy of Dr. A. Moore. All three types of graphite were ground in a mortar, classified according to particle size by the use of sieves, dried in a dynamic vacuum at 300 °C, and treated with 2 atm of F_2 pressure at room temperature for several hours prior to their use.

Hydrogen fluoride (Matheson) was dried by storage over BiF_5.[8] Arsenic pentafluoride (Ozark Mahoning), BF_3 and PF_5 (Matheson) were purified by fractional condensation prior to their use. The F_2 (Air Products) was passed through a NaF scrubber for removal of any HF. The preparations of NF_4SbF_6[6] and O_2AsF_6[9] have previously been described. The SO_2ClF (Ozark Mahoning) was pretreated at −78 °C with $O_2^+AsF_6^-$, followed by fractional condensation in a dynamic vacuum through a series of −78, −112, and −196 °C traps, with the material retained at −112 °C being used.

Caution! Anhydrous HF causes severe burns. Elemental fluorine and NF_4^+ salts are strong oxidizers and must be handled with the safety precautions previously described.[6]

Apparatus. Volatile materials were handled in stainless-steel–Teflon–FEP vacuum lines as previously described.[10] Nonvolatile materials

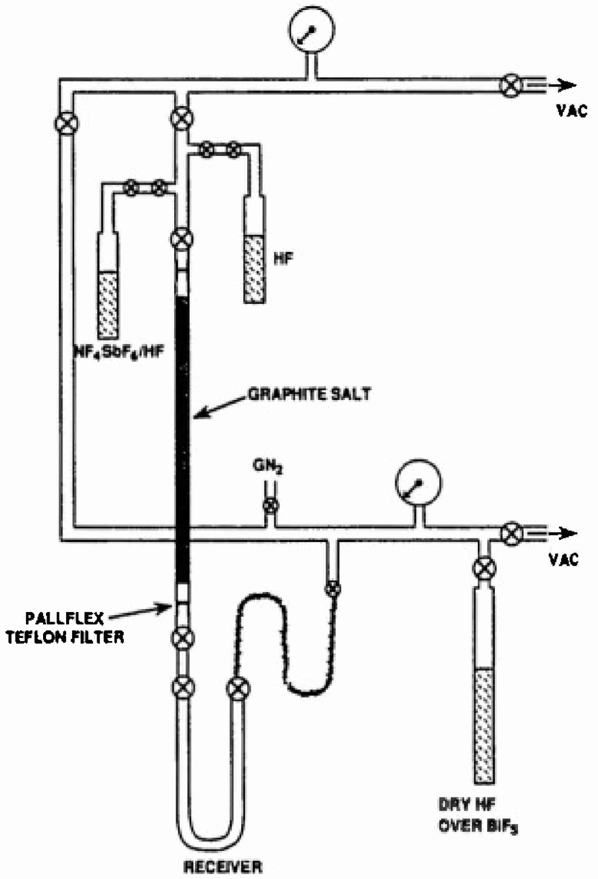

Figure 1. Apparatus used for the ion-exchange reactions between graphite salts and NF_4SbF_4.

---

(1) For a recent review on NF_4^+ chemistry see: Nikitin, I. V.; Rosolovskii, V. Ya. *Russ. Chem. Rev. (Engl. Transl.)* 1985, *54*, 426.
(2) Christe, K. O.; Schack, C. J.; Wilson, R. D. *J. Fluorine Chem.* 1976, *8*, 541 and references cited therein.
(3) Wilson, W. W., Christe, K. O. *J. Fluorine Chem.* 1988, *40*, 59 and references cited therein.
(4) Christe, K. O., Wilson, W. W. *Inorg. Chem.* 1982, *21*, 4113 and references cited therein.
(5) Christe, K. O. U.S. Pat. 4,207,124, 1980.
(6) Christe, K. O.; Wilson, W. W.; Schack, C. J.; Wilson, R. D. *Inorg. Synth.* 1986, *24*, 39.
(7) Christe, K. O. U.S. Pat. 4,683,129, 1987.
(8) Christe, K. O.; Wilson, W. W.; Schack, C. J. *J. Fluorine Chem.* 1978, *11*, 71.
(9) Shamir, J.; Binenboym, J. *Inorg. Chim. Acta* 1968, *2*, 37

were handled in the dry nitrogen atmosphere of a glovebox. The ion-exchange reactions were carried out in a specially built apparatus (see Figure 1), constructed from injection-molded Teflon–PFA tubes, valves, and fittings (Fluoroware). The exchange column consisted of a 40 cm long, $^3/_8$ in. o.d. heavy-wall Teflon–PFA tube and was packed with the graphite salt to a height of about 35 cm. The column packing was held in place at both ends by porous Teflon filter disks (Pallflex). Pure HF and an HF solution of NF_4SbF_6 were stored in two $^1/_2$ in. o.d. Teflon ampules attached at right angles to the Teflon manifold directly above the exchange column. These ampules could be rotated about their horizontal tube sections connecting them to the manifold, thereby allowing either neat HF or HF–NF_4SbF_6 solutions to be added to the top of the column. To overcome the resistance of the Teflon filters, the apparatus could be either pressurized with several atmospheres of dry gaseous N_2 or evacuated. The bottom of the exchange column was connected to a detachable $^3/_4$ in. o.d. Teflon U-trap receiver, equipped with two Teflon valves and attached with Teflon flex tubing (Penntube) to the vacuum manifold.

Infrared spectra were recorded on a Perkin-Elmer Model 283 spectrometer, and Raman spectra, on either a Spex Model 1403 instrument with 647.1-nm excitation or a Cary Model 83 instrument with 488-nm excitation. X-ray powder patterns were taken with a General Electric Model XRD-6 diffractometer, Ni-filtered Cu Kα radiation, and a 114.6 nm diameter Philips Norelco camera on powder samples in sealed 0.5-mm quartz capillaries.

Synthesis of Graphite Salts. C_nBF_4. All the graphite BF_4 salts were prepared by the method of Nikonorov[11] from graphite and a 2:1 molar mixture of BF_3 and F_2 at 2 atm pressure in a Monel cylinder at room temperature until no further weight uptake occurred. The initial BF_3–F_2 uptake by the graphite was rapid and exothermic for the pyrolytic graphite samples. After three 3-h exposures to BF_3–F_2 mixtures, followed each time by pumping on the sample for several hours at room temperature for the removal of loosely intercalated BF_3 and F_2, no further BF_3–F_2 uptake was observed. The value of *n* was determined from both the weight increase of the solids and the amounts of unreacted BF_3 and F_2 recovered, with both values generally being in excellent agreement. For the different types of graphite used in our study, the following compositions were obtained:

spectrographic graphite (SG)	$C_{11.12}{}^+BF_4{}^-$
pyrolytic graphite (PG)	$C_{8.10}{}^+BF_4{}^-$
highly oriented pyrolytic graphite (HOPG)	$C_{8.10}{}^+BF_4{}^-$

The PG and HOPG salts were shown by X-ray diffraction to be first-stage intercalates with a_0 = 2.46 Å and c_0 = 7.69 Å, in excellent agreement with previous literature values.[12,13]

C_nAsF_6. For the syntheses of graphite AsF_6 salts, two different methods were used. The first one was that of Nikonorov[11] and has been described above for C_nBF_4. With the different types of graphite, this method resulted in the following compositions:

spectrographic graphite (SG)	$C_{11.60}AsF_6$
pyrolytic graphite (GP)	$C_{9.83}AsF_6$
highly oriented pyrolytic graphite (HOPG)	$C_{9.70}AsF_6$

The second method was that of Bartlett and co-workers[14] which involved the oxidation of spectrographic graphite by O_2AsF_6 in SO_2ClF, first at −60 °C and then at room temperature. On the basis of the observed material balance, the final product had the composition $C_{8.72}AsF_6$.

All the C_nAsF_6 salts were first-stage intercalates with a_0 = 2.45 and c_0 = 7.87 Å, in excellent agreement with previous reports.[15,16]

C_nPF_6. For the synthesis of C_nPF_6, the method of Nikonorov[11] and the use of pyrolytic graphite resulted in a first-stage intercalate having the composition $C_{12.40}PF_6$ and repeat distances of a_0 = 2.45 Å and c_0 = 7.69 Å, in reasonable agreement with a previous report.[12]

Attempts to prepare C_nPF_6 by a displacement reaction at ambient temperature between (PG)$C_{8.1}BF_4$ and 4-fold excess of PF_5, in a stainless-steel cylinder of a small enough volume to result in a liquid PF_5 phase (vapor pressure of PF_5 at 21.1 °C = 28.2 atm) resulted in a product having the molar composition $0.493C_{8.1}BF_4 \cdot 0.507C_{12.5}PF_6$, as shown by the weight change of the solid and the amounts of PF_5 consumed and BF_3 liberated. A second treatment with PF_5 for more than 6 months under identical conditions, followed by removal of the volatile material at 50 °C, resulted in very little additional PF_5 uptake but an evolution of some BF_3, indicating that the $C_{8.1}BF_4$ may have contained, in addition to $BF_4{}^-$, some intercalated BF_3.

Preparation of NF_4BF_4 by Ion Exchange. In a typical experiment, 6.096 g (33.12 mmol) of (PG)$C_{8.10}BF_4$ having a particle size of 35 mesh was loaded inside the drybox into the Teflon exchange column. The column was attached to the Teflon manifold and wet with anhydrous HF. A Teflon ampule was loaded in the drybox with 1.094 g (3.357 mmol) of NF_4SbF_6 and attached to the Teflon manifold, and anhydrous HF (12 mL of liquid) was condensed into the ampule at −78 °C. The resulting HF solution of NF_4SbF_6 was slowly passed over a 1-h time period through the $C_{8.1}BF_4$ column, followed by a rinse with about 10 mL of anhydrous HF. The eluents were collected in the Teflon receiver U-tube and pumped to dryness at 50 °C. The white solid residue (573 mg: weight calculated for 3.357 mmol of NF_4BF_4 = 593 mg, 97% yield) was shown by infrared and Raman spectroscopy to be pure NF_4BF_4.[17]

Similarly, a sample of 4.91 mmol of NF_4SbF_6, when slowly passed through a column of 14.0 mmol of (SG)$C_{11.12}BF_4$, produced 3.78 mmol (77% yield) of pure NF_4BF_4.

Preparation of NF_4AsF_6 by Ion Exchange. In a typical experiment, 3.05 mmol of NF_4SbF_6, when passed through a column of 28.7 mmol of (PG)$C_{9.83}AsF_6$, produced 3.05 mmol (100% yield) of spectroscopically pure NF_4AsF_6.[17]

Similarly, a sample of 5.0 mmol of NF_4SbF_6, when passed through a column of 7.84 mmol of (SG)$C_{8.7}AsF_6$, resulted in 3.6 mmol of NF_4AsF_6 and 1.4 mmol of NF_4SbF_6.

Preparation of NF_4PF_6 by Ion Exchange. When a solution of 3.27 mmol of NF_4SbF_6 in anhydrous HF was passed through a column packed with 23.8 mmol of (PG)$C_{12.4}PF_6$, the eluted product consisted of 1.49 mmol of NF_4PF_6 and 0.49 mmol of NF_4SbF_6.

Results and Discussion

A metathetical reaction of the type

$$A^+B^- + C^+D \rightarrow AD\downarrow + C^+B^- \qquad (2)$$

is in principle a simple ion exchange in which the purity of the desired product is governed by the solubility products of the four salts involved. For this process to work efficiently, the solubility product of AD must be much smaller than those of the three remaining salts. Since this is not the case for reaction 1, low-temperature filtrations and multiple recrystallizations from anhydrous HF and BrF_5 are required that lower the yields. The solubility problem with AD might be overcome by making A^+ an insoluble, polymeric, stationary phase. This principle is well-known and is widely used in ion-exchange resins. Since the metathetical NF_4BF_4 process (1) is a simple anion exchange, it could be improved upon by replacing $CsBF_4$ with a $BF_4{}^-$ salt of a cationic resin that is stable toward both anhydrous HF and the strongly oxidizing $NF_4{}^+$ cation. Although acid- and oxidizer-resistant cation exchangers, such as Du Pont's Nafion, are well-known, no corresponding anion exchangers were available.

Attempts were made to utilize the cation exchanger Nafion (XR resin from Du Pont which is a copolymer of tetrafluoroethylene and perfluoro-4-methyl-3,6-dioxa-7-octenesulfonic acid) for the preparation of NF_4BF_4 according to (3) and (4). Although small

$$R_fSO_3{}^-Na^+ + NF_4{}^+SbF_6{}^- \rightarrow R_fSO_3{}^-NF_4{}^+ + Na^+SbF_6{}^- \qquad (3)$$

$$R_fSO_3{}^-NF_4{}^+ + Na^+BF_4{}^- \rightarrow R_fSO_3{}^-Na^+ + NF_4{}^+BF_4{}^- \qquad (4)$$

amounts of $NaSbF_6$ were detectable in the eluent of (3), treatment of the resulting solid with a $Na^+BF_4{}^-$ solution did not show any evidence for NF_4BF_4.

In our search for a suitable acid- and oxidizer-resistant anion-exchange medium, it was discovered that graphite salts are well suited for this purpose. Since the syntheses and properties of graphite salts are the subject of considerable controversy, our results on the preparation of these salts will be briefly summarized before presenting our data on the actual ion exchange reactions.

---

(10) Christe, K. O.; Wilson, W W.; Schack, C J *Inorg Synth* 1986, *24*, 3.

(11) Nikonorov, Yu. I. *Kinet. Katal.* 1979, *20*, 1598.

(12) Rosenthal, G L., Mallouk, T E., Bartlett, N *Synth Met* 1984, *9*, 433

(13) Brusilovsky, D., Selig, H., Vaknin, D, Ohana, I, Davidov, D *Synth Met.* 1988, *23*, 377.

(14) Bartlett, N., McQuillan, B., Robertson, A. S. *Mater. Res. Bull.* 1978, *13*, 1259.

(15) Bartlett, N.; McCarron, E. M.; McQuillan, B W. *Synth. Met.* 1979/80, *1*, 221.

(16) McCarron, E M Ph.D. Thesis, University of California, Berkeley, CA, 1981, 58.

(17) Christe, K O., Schack, C J., Wilson, R. D. *Inorg Chem* 1976, *15*, 1275.

Syntheses of Graphite Salts. In our study different types of graphite starting material were used, i.e. spectrographic graphite (SG) and two kinds of pyrolytic graphite (PG), one from a graphite slab used for rocket nozzle cones, and the second one from highly oriented, mirror-surfaced graphite pieces. The pyrolytic graphites are more highly graphitized, better oriented, and more easily intercalated than the spectrographic graphite and, therefore, have been used almost exclusively in the previously reported studies.[11-13]

In agreement with the previous studies,[11-13] the reaction

$$nC + 0.5F_2 + BF_3 \rightarrow C_n^+BF_4^- \qquad (5)$$

yielded a first-stage intercalate with n being very close to 8.0 and the same identity period. No particular effort was made in this study to determine whether in C_8BF_4 the boron is present exclusively as BF_4^- or if there might also be some free BF_3 and/or F_2 present.[13] It should be noted, however, that the addition of neat anhydrous HF to the (PG)- and (HOPG)C_8BF_4 generally resulted in gas evolution and a very pronounced swelling of the graphite salt, indicating the possible intercalation of some free BF_3.

For the synthesis of $C_n^+AsF_6^-$, the direct synthesis from graphite, AsF_5, and F_2 yielded for the two pyrolytic graphites n values close to 9.8 and for spectrographic graphite a value of 11.6. With $O_2^+AsF_6^-$ used as the oxidant[14] and spectrographic graphite

$$nC + O_2^+AsF_6^- \rightarrow C_n^+AsF_6^- + O_2 \qquad (6)$$

a composition of $C_{8.7}AsF_6$ was obtained. These salts were first-stage intercalates and approach the limiting composition C_8AsF_6, which has a close packing of the AsF_6^- anions in the galleries.[18] For C_nPF_6, the direct synthesis using pyrolytic graphite, PF_5, and F_2 produced a first-stage intercalate having the composition $C_{12.4}PF_6$. The fact that the limiting composition for C_nPF_6 appears to be about $C_{12}PF_6$, while that for C_nAsF_6 is about C_8AsF_6, cannot be due to steric effects because PF_6^- is smaller than AsF_6^-. It has been attributed[19] to the lower fluoride ion affinity of PF_5 relative to that of AsF_5. It, therefore, appears that PF_6^- cannot support a positive charge on carbon higher than that corresponding to a composition of about C_{12}^+. Further evidence for the limiting composition of C_nPF_6 being about $n = 12$ was obtained by a displacement reaction between (PG)$C_{8.1}BF_4$ and liquid PF_5 at room temperature. Although only half of the BF_3 was displaced by PF_5 in a single treatment, the stoichiometry of the displacement reaction was such that 1 mol of PF_5 liberated 1.54 mol of BF_3; i.e., the $C_{8.1}BF_4$ was converted to $C_{12.5}PF_6$ and BF_3. The $C_{12.5}PF_6$ composition observed for this displacement reaction is in excellent agreement with that of $C_{12.4}PF_6$ derived from the direct synthesis from graphite, PF_5, and F_2 (see above). It is noteworthy that the stoichiometry of the above displacement reaction resembles that previously observed for the $C_7SO_3F + AsF_5$ system.[20]

In conclusion, our syntheses of graphite salts are in good agreement with the previous literature data suggesting limiting compositions of about C_8BF_4, C_8AsF_6, and $C_{12}PF_6$ for these first-stage intercalates.

Ion-Exchange Reactions. Solutions of NF_4SbF_6 in HF, when passed through columns of either C_8BF_4 or C_8AsF_6, readily exchange the SbF_6^- anion for either BF_4^- or AsF_6^-.

$$C_8BF_4 + NF_4SbF_6 \rightarrow C_8SbF_6 + NF_4BF_4 \qquad (7)$$

$$C_8AsF_6 + NF_4SbF_6 \rightarrow C_8SbF_6 + NF_4AsF_6 \qquad (8)$$

In this manner, spectroscopically pure NF_4BF_4 or NF_4AsF_6 can be prepared. It is important to use a suitable column geometry, i.e. a large height to diameter ratio, and a sufficient molar excess of the graphite salt. The importance of the column geometry and of flow conditions was demonstrated by an experiment whereby a sample of (PG)$C_{8.1}BF_4$ was stirred with a large excess of NF_4SbF_6 dissolved in HF. Even after a contact time of 10 h, only an insignificant anion exchange had occurred. The importance of using a sufficient excess of graphite salt over NF_4SbF_6 was demonstrated in an experiment where the mole ratio of $C_{8.7}AsF_6$ to NF_4SbF_6 was only 1.57. In this case the conversion of NF_4SbF_6 to NF_4AsF_6 was only 72 mol %.

Another important point is that the graphite salt starting material is fully oxidized to a C_8^+ stage. If the graphite salt is not completely oxidized, it will be oxidized by NF_4SbF_6 in a reaction, analogous to (6), resulting in the loss of NF_4^+ values.

$$8C + NF_4^+SbF_6^- \rightarrow C_8^+SbF_6^- + NF_3 + 0.5F_2 \qquad (9)$$

This point was demonstrated in several experiments using C_nBF_4 compositions in which n ranged from 14 to 16 and the yields of NF_4BF_4 were less than quantitative.

For the synthesis of NF_4PF_6, the most highly oxidized graphite PF_6 salt available was $C_{12.4}PF_6$. In view of the incomplete oxidation state of the graphite, it was not surprising that a 40 mol % loss of NF_4^+ values occurred during the exchange reaction.

Conclusion. Graphite salts can be used as anion-exchange resins that are highly resistant toward strong acids and oxidizers. To our knowledge, these are the first anion exchangers capable of withstanding such harsh conditions for which previously only cation exchangers, such as Nafion, were available. The usefulness of graphite salts as anion exchangers was demonstrated by an improved method for the production of advanced NF_4^+ salts. This method eliminates most of the drawbacks of the previously used low-temperature, metathetical process[6] and provides the desired NF_4^+ salts in high purities and yields by a simple, one-step process under ambient conditions.

Acknowledgment. We are indebted to Drs. C. J. Schack and W. W. Wilson for their help, to Dr. A. Moore for a sample of HOPG graphite, and to the Office of Naval Research and the U.S. Army Research Office for financial support.

---

(18) Bartlett, N.; McQuillan, B. W. In *Intercalation Chemistry*; Wittingham, M. S., Jacobson, A. J., Eds.; Academic Press: New York, 1982.

(19) Hagiwara, R., Lerner, M., Bartlett, N. Presented at the ACS Ninth Winter Fluorine Conference, St Petersburg, FL, Feb 1989, paper 63.

(20) Karunanithy, S.; Aubke, F. *J. Fluorine Chem.* 1984, 25, 339.

APPENDIX E

Reprinted from Inorganic Chemistry, 1989, *28*, 675

Contribution from Rocketdyne, A Division of Rockwell International,
Canoga Park, California 91303

Reactions of Chlorine Fluorides and Oxyfluorides with the Nitrate Anion and Alkali-Metal Fluoride Catalyzed Decomposition of ClF_5

Karl O. Christe,* William W. Wilson, and Richard D. Wilson

Received July 12, 1988

The binary chlorine fluorides ClF_5, ClF_3, and ClF, when used in an excess, all undergo facile fluorine–oxygen exchange reactions with the nitrate anion, forming $FClO_2$, unstable FClO, and $ClONO_2$, respectively, as the primary products. Whereas $FClO_3$ does not react with $LiNO_3$ at temperatures as high as 75 °C, $FClO_2$ readily reacts with either $LiNO_3$ or N_2O_5 to give $ClONO_2$ and O_2 in high yield, probably via the formation of an unstable O_2ClONO_2 intermediate. With an excess of ClF, chlorine nitrate undergoes a slow reaction to give FNO_2 and Cl_2O as the primary products, followed by Cl_2O reacting with ClF to give Cl_2, ClF, and $FClO_2$. The alkali-metal fluorides CsF, RbF, and KF catalyze the decomposition of ClF_5 to ClF_3 and F_2, which can result in the generation of substantial F_2 pressures at temperatures as low as 25 °C.

Introduction

Ionic nitrates are surprisingly reactive toward the fluorides and oxyfluorides of bromine,[1,2] xenon,[3,4] and iodine.[5] The observed reaction chemistry is fascinating and often unpredictable. Thus, BrF_5 undergoes fluorine–oxygen exchange reactions that, depending on the choice of the nitrate salt or the reagent used in excess, yield either BrF_4O^- salts, free BrF_3O, or bromine nitrates. In the cases of XeF_6, $XeOF_4$, and IF_5, stepwise fluorine–oxygen exchange occurs, whereas for the closely related IF_7 molecule, reduction to IF_5 with simultaneous oxygen evolution was observed. In view of these results it was interesting to study the behavior of chlorine fluorides and oxyfluorides toward ionic nitrates.

The previous reports on reactions of ionic nitrates with chlorine fluorides are limited to a statement by Ruff and Krug that KNO_3 does not react with liquid ClF_3 while $AgNO_3$ does[6] and a synthesis of $ClONO_2$ from ClF and $M(NO_3)_2$ where M is either Ca, Sr, Ba, or Pb.[7] In addition, the reactions of ClF,[8,9] ClF_3,[9] ClF_5,[9] and $FClO_2$[9] with the covalent nitrate $HONO_2$ have previously been studied.

Experimental Section

Apparatus and Materials. The vacuum lines, handling techniques, and spectrometers used in this study have been described elsewhere.[3] Commercial $LiNO_3$ (J. T. Baker, 99.7%), $NaNO_3$ (J. T. Baker, 99.5%), KNO_3 (J. T. Baker, 99.1%), and $RbNO_3$ (K&K Labs, Inc., 99.9%) were dried in vacuo at 120 °C for 1 day prior to their use. $CsNO_3$ was prepared from Cs_2CO_3 and HNO_3 and dried in the same manner. N_2O_5,[10] ClF_5,[11] ClF,[12] and $FClO_2$[13] were prepared by literature methods. $FClO_3$ (Pennsalt) and ClF_3 (Matheson) were commercial materials and were purified by fractional condensation prior to their use.

Caution! Chlorine fluorides and oxyfluorides are powerful oxidizers and can react violently with most organic substances. The materials should be handled only in well-passivated metal–Teflon equipment with all the necessary safety precautions.

Reaction of ClF with an Excess of $NaNO_3$. A mixture of $NaNO_3$ (17.32 mmol) and ClF (11.53 mmol) in a 30-mL stainless steel cylinder was allowed to slowly warm in a dry ice–liquid N_2 slush bath from −196 to −78 °C and then toward 0 °C. The cylinder was recooled to −196 °C and did not contain any gas noncondensible at this temperature. The material volatile at room temperature was separated on warm up of the cylinder from −196 °C by fractional condensation through traps kept at −112, −126, −142, and −196 °C. The −112 °C trap contained $ClONO_2$[14] (8.89 mmol) and Cl_2O[15] (0.68 mmol), the one at −126 °C had $ClONO_2$ (0.09 mmol), the one at −142 °C had Cl_2 (0.35 mmol), while the one at −196 °C contained FNO_2[16] (1.01 mmol). The white solid residue in the cylinder was a mixture of NaF and $NaNO_3$ (1046 mg; weight calculated for 9.99 mmol of NaF and 7.33 mmol of $NaNO_3$ = 1043 mg). The yield of $ClONO_2$, based on ClF, was 76%.

Reaction of $NaNO_3$ with an Excess of ClF. Finely powdered $NaNO_3$ (5.15 mmol) was loaded in the drybox into a prepassivated 30-mL stainless steel cylinder equipped with a valve. On the vacuum line, ClF (8.00 mmol) was added at −196 °C. The cylinder was allowed to slowly warm to room temperature, where it was kept for 3 days. It was cooled again to −196 °C and did not contain any gas noncondensible at this temperature. The material volatile at room temperature was separated on warm up of the cylinder from −196 °C by fractional condensation through traps kept at −142 and −196 °C. The −196 °C trap contained FNO_2 (2.88 mmol) and the one at −142 °C had 5.14 mmol of a mixture

---

(1) Wilson, W. W.; Christe, K. O. *Inorg. Chem.* 1987, *26*, 916.
(2) Wilson, W. W.; Christe, K. O. *Inorg. Chem.* 1987, *26*, 1573.
(3) Christe, K. O.; Wilson, W. W. *Inorg. Chem.* 1988, *27*, 1296.
(4) Christie, K. O.; Wilson, W. W. *Inorg. Chem.*, in press.
(5) Christe, K. O.; Wilson, W. W.; Wilson, R. D. *Inorg. Chem.*, in press.
(6) Ruff, O.; Krug, H. *Z. Anorg. Allg. Chem* 1930, *190*, 270.
(7) Schmeisser, M., Eckermann, W., Gundlach, K. P., Naumann, D. *Z. Naturforsch.* 1980, *35B*, 1143.
(8) Schack, C. J. *Inorg. Chem.* 1967, *6*, 1938.
(9) Christe, K O *Inorg. Chem.* 1972, *11*, 1220.
(10) Wilson, W. W.; Christe, K. O. *Inorg. Chem.* 1987, *26*, 1631.
(11) Pilipovich, D.; Maya, W.; Lawton, E. A.; Bauer, H. F.; Sheehan, D. F.; Ogimachi, N. N.; Wilson, R. D.; Gunderloy, F. C.; Bedvell, V. E. *Inorg. Chem.* 1967, *6*, 1918.
(12) Schack, C. J.; Wilson, R. D. *Inorg. Synth.* 1986, *24*, 1.
(13) Christe, K. O.; Wilson, R. D.; Schack, C. J. *Inorg. Synth.* 1986, *24*, 3.
(14) Christe, K. O.; Schack, C. J.; Wilson, R. D. *Inorg. Chem.* 1974, *13*, 2811.
(15) Siebert, H. Anwendungen der Schwingungsspektroskopie in der Anorganischen Chemie. *Anorganische und Allgemeine Chemie in Einzeldarstellungen*; Springer Verlag: Berlin, Heidelberg, FRG, New York, 1966; Vol. VII.
(16) Bernitt, D. L.; Miller, R. J ; Hisatsune, I. C. *Spectrochim. Acta, Part A* 1967, *23*, 237.

consisting mainly of $ClONO_2$ and Cl_2O and small amounts of $FClO_2$[17] and Cl_2. The cylinder contained 215 mg of NaF (weight calculated for 5.15 mmol of NaF = 216 mg).

Reaction of $NaNO_3$ with an Excess of ClF_3. Finely powdered $NaNO_3$ (1.02 mmol) was loaded in the drybox into a prepassivated 30-mL stainless-steel reactor, and ClF_3 (5.36 mmol) was added at −196 °C on the vacuum line. The cylinder was allowed to slowly warm to room temperature where it was kept for 10 days. It was recooled to −196 °C and checked for noncondensible gas (0.26 mmol of O_2). The material volatile at room temperature was separated by fractional condensation through traps kept at −112, −126, and −196 °C. The −112 °C trap contained ClF_3[18] (4.36 mmol), and one at −126 °C had $FClO_2$[17] (0.25 mmol), and the one at −196 °C showed FNO_2[16] (1.02 mmol) and ClF[15] (0.77 mmol). The white solid residue (47 mg) consisted of NaF (weight calculated for 1.02 mmol of NaF = 43 mg).

Reaction of $LiNO_3$ with an Excess of ClF_3. A 30-mL stainless-steel cylinder was loaded in the drybox with $LiNO_3$ (2.68 mmol). ClF_3 (40.54 mmol) was added at −196 °C on the vacuum line. The cylinder was warmed from −196 °C to room temperature and kept at this temperature for 3 h with frequent agitation. The reactor was cooled back to −196 °C and did not contain any significant amount of noncondensible gas. The material volatile at room temperature was separated by fractional condensation through a series of traps kept at −95, −142, and −196 °C, while the cylinder was allowed to warm from −196 °C to room temperature. The −95 °C trap was empty, and the −196 °C trap contained FNO_2[16] (2.48 mmol). The contents of the −142 °C trap (40.67 mmol) consisted of unreacted ClF_3,[19] $FClO_2$,[17] and a very small amount of FNO_2.[16] The amount of $FClO_2$ and FNO_2 in the ClF_5 was estimated by infrared spectroscopy and verified by complexing with AsF_5 and weighing of the resulting $ClO_2^+AsF_6^-$[20] and $NO_2^+AsF_6^-$[13] (409 mg, weight calculated for 1.34 mmol of $ClO_2^+AsF_6^-$ and 0.20 mmol of $NO_2^+AsF_6^-$ = 391 mg). The white solid residue in the cylinder (71 mg; weight calculated for 2.68 mmol of LiF = 70 mg) consisted of LiF.

Reaction of $NaNO_3$ with ClF_5. The reaction between $NaNO_3$ and ClF_3 was carried out as described for the $LiNO_3$–ClF_5 system. After 10 days at 25 °C, the $NaNO_3$ had quantitatively reacted to yield 1 mol of NaF and FNO_2 and 0.5 mol of $FClO_2$/mol of $NaNO_3$.

Reaction of KNO_3 with ClF_5. The reaction between KNO_3 and ClF_5 was carried out as described above for $LiNO_3$. After 28 days at 25 °C, the KNO_3 had quantitatively reacted to yield FNO_2 and $FClO_2$ in a 2:1 mole ratio. About 16% of the byproduct KF had been converted to $KClF_4$,[21] and fluorine was found as noncondensible gas at −196 °C and identified by its reaction with mercury.

Reaction of $RbNO_3$ with ClF_5. The reaction between $RbNO_3$ and ClF_3 was carried out as described above. After 31 days at 25 °C, 90% of the $RbNO_3$ had reacted to yield FNO_2[16] and $FClO_2$[17] in a 2:1 mole ratio. About 35% of the byproduct RbF had been converted to $RbClF_4$,[21] and fluorine was identified as noncondensible gas at −196 °C.

Reaction of $CsNO_3$ with ClF_5. The reactions between $CsNO_3$ and ClF_3 were carried out as described above. After 32 days at 25 °C, 16% of the $CsNO_3$ had reacted to yield FNO_2[16] and $FClO_2$[17] in a 2:1 mole ratio. About half of the CsF byproduct had been converted to $CsClF_4$.[21] When the reaction was carried out at 0 °C for 2 h, the conversion of $CsNO_3$ was 4.4%, whereas at 70 °C for 3 days it was 46%. The amount of fluorine evolved in these reactions increased with increasing temperature.

Reaction of $CsNO_3$ with ClF_3 in the Presence of Excess CsF. A mixture of finely powdered $CsNO_3$ (0.97 mmol) and CsF (8.89 mmol) was placed in the drybox into a prepassivated stainless-steel reactor of 32.3-mL volume. On the vacuum line, ClF_5 (14.57 mmol) was added at −196 °C. The cylinder was agitated on a shaker at 25 °C for 18 days and then cooled to −196 °C. It contained 0.56 mmol of a noncondensible gas, which reacted quantitatively with Hg giving a weight increase of 21 mg (weight increase calculated for 0.56 mmol of F_2 = 21.3 mg). The material volatile at 25 °C was separated by fractional condensation through traps kept at −142 and −196 °C. The −196 °C trap contained FNO_2[16] (0.093 mmol) and $FONO_2$[14] (0.028 mmol), while the one at −142 °C had ClF_5[19] (13.97 mmol) corresponding to a ClF_3 consumption of 0.60 mmol. The white solid residue (1610 mg, weight calculated for the below given material balance = 1593 mg) was shown by Raman spectroscopy to contain significant amounts of $CsNO_3$ and $CsClF_4$.[21] These results are in excellent agreement with the following material balance:

$$0.59ClF_5 \rightarrow 0.59ClF_3 + 0.59F_2$$

$$0.028F_2 + 0.028CsNO_3 \rightarrow 0.028CsF + 0.028FONO_2$$

$$0.0465ClF_5 + 0.093CsNO_3 \rightarrow 0.093CsF + 0.093FNO_2 + 0.0465FClO_2$$

$$0.59ClF_3 + 0.59CsF \rightarrow 0.59CsClF_4$$

$$0.0465CsF + 0.0465FClO_2 \rightarrow 0.0465CsClF_2O_2$$

Reaction of $FClO_2$ with $LiNO_3$. Finely powdered $LiNO_3$ (2.41 mmol) was placed in the drybox into a prepassivated 30-mL stainless-steel reactor, and $FClO_2$ (1.62 mmol) was added at −196 °C on the vacuum line. The cylinder was allowed to slowly warm to room temperature where it was kept for 15 h. It was recooled to −196 °C, and the noncondensible gas (1.58 mmol of O_2) was pumped off. The material volatile at room temperature consisted of $ClONO_2$[14] (1.59 mmol). The white, solid residue (96 mg) was a mixture of LiF and $LiNO_3$ (weight calculated for 1.62 mmol of LiF and 0.79 mmol of $LiNO_3$ = 96 mg).

Reaction of $FClO_2$ with N_2O_3. N_2O_3 (0.83 mmol) was condensed at −31 °C in a dynamic vacuum into a 5-mm-o.d. glass NMR tube, which was attached to a flamed-out 96-mL Pyrex vessel equipped with two Teflon valves. $FClO_2$ (1.87 mmol) was added to the NMR tube at −196 °C. No appreciable reaction between N_2O_3 and $FClO_2$ was observed at temperatures as high as −31 °C. When the mixture was kept at 0 °C for 18 h, about 64% of the N_2O_3 had reacted with $FClO_2$ to yield $ClONO_2$[14] and O_2 as the main products. In addition, there was an attack of $FClO_2$ on the Pyrex vessel, resulting in substantial amounts of ClO_2 and SiF_4 and a trace amount of $NO_2^+ClO_4^-$.[22] The residue left behind at −78 °C in the NMR tube was identified by Raman spectroscopy as unreacted N_2O_3.[10]

Results and Discussion

MNO_3–ClF System. ClF readily reacts with $NaNO_3$ at subambient temperature to give NaF and $ClONO_2$ (eq 1). However,

$$NaNO_3 + ClF \rightarrow NaF + ClONO_2 \qquad (1)$$

the yield of $ClONO_2$ was found to be less than quantitative because of the competing reaction 2. Reaction 2 might be explained by

$$NaNO_3 + 2ClF \rightarrow NaF + Cl_2O + FNO_2 \qquad (2)$$

a secondary reaction of $ClONO_2$, formed in (1), with a second mole of ClF (eq 3). In a previous study,[9] $ClONO_2$ and ClF were

$$ClONO_2 + ClF \rightarrow Cl_2O + FNO_2 \qquad (3)$$

found not to interact appreciably below room temperature and with relatively short reaction times. However, it was shown in this study that at room temperature and with reaction times of several days reaction 3 slowly proceeds to give Cl_2O and FNO_2 as the main products with Cl_2 and $FClO_2$ as the byproducts. The byproducts are readily explained by the previously reported,[9,23] relatively fast reactions 4 and 5, which are summarized in (6).

$$2Cl_2O + 2ClF \rightarrow 2Cl_2 + 2FClO \qquad (4)$$

$$2FClO \rightarrow ClF + FClO_2 \qquad (5)$$

$$\text{net:}\quad 2Cl_2O + ClF \rightarrow 2Cl_2 + FClO_2 \qquad (6)$$

The fact that, for reaction 1, side reaction 2 could not be completely suppressed even at low temperatures indicates either acceleration of (3) under the conditions of (1) or a slightly different reaction path.

Obviously, reactions 2, 3, and 6 are favored by an excess of ClF. In order to maximize the yield of $ClONO_2$ in (1), it is, therefore, advantageous to employ an excess of $NaNO_3$. Furthermore, a lowering of the reaction temperature should also favor the formation of $ClONO_2$. By the use of about 100% excess of $NaNO_3$ and subambient reaction temperatures, a $ClONO_2$ yield of about 76%, based on ClF, was obtained. This yield is somewhat lower than the 92% previously reported[7] for the $Pb(NO_3)_2$ + ClF system,

---

(17) Smith, D. F.; Begun, G. M.; Fletcher, W. H. *Spectrochim. Acta* 1964, *20*, 1763.

(18) Claassen, H. H., Weinstock, B., Malm, J. G. *J. Chem. Phys.* 1958, *28*, 285.

(19) Begun, G. M.; Fletcher, W. H.; Smith, D. F. *J. Chem. Phys.* 1965, *42*, 2236. Christe, K. O. *Spectrochim. Acta, Part A* 1971, *27*, 631.

(20) Christe, K. O.; Schack, C. J.; Pilipovich, D.; Sawodny, W. *Inorg. Chem.* 1969, *8*, 2489.

(21) Christe, K. O.; Sawodny, W. *Z. Anorg. Allg. Chem.* 1970, *374*, 306.

(22) Nebgen, J. W., McElroy, A. D., Klodowski, H. F. *Inorg. Chem.* 1965, *6*, 1796.

(23) Christe, K. O.; Schack, C. J. *Adv. Inorg. Chem. Radiochem.* 1976, *18*, 319.

but is higher than those given for $Ca(NO_3)_2$ (63%), $Sr(NO_3)_2$ (44%), and $Ba(NO_3)_2$ (<10%). The main advantage of $NaNO_3$ over these other nitrates is its lower cost.

MNO_3–ClF_3 System. An excess of ClF_3 readily reacts with $NaNO_3$ at room temperature or below to give FNO_2, ClF, $FClO_2$, and O_2 as the main products. These are best rationalized in terms of the fluorine–oxygen exchange reaction 7, which generates FClO.

$$ClF_3 + NaNO_3 \rightarrow NaF + FNO_2 + FClO \qquad (7)$$

The thermally unstable FClO then undergoes either disproportionation (eq 8, or decomposition eq 9), with (8) and (9) contributing about equally.

$$2FClO \rightarrow ClF + FClO_2 \qquad (8)$$

$$2FClO \rightarrow 2ClF + O_2 \qquad (9)$$

In the presence of a large excess of $NaNO_3$ the FNO_2,[10] $FClO_2$, and ClF products can react further with $NaNO_3$ according to (10)–(12).

$$FNO_2 + NaNO_3 \rightarrow NaF + N_2O_5 \qquad (10)$$

$$FClO_2 + NaNO_3 \rightarrow NaF + ClONO_2 + O_2 \qquad (11)$$

$$ClF + NaNO_3 \rightarrow NaF + ClONO_2 \qquad (12)$$

MNO_3–ClF_5 System. From a preparative point of view, the reactions of ClF_5 were most interesting. For IF_5 and BrF_5 a stepwise fluorine–oxygen exchange was possible,[1,2,5] thus allowing the isolation of either XF_4O^- salts or the free XF_3O molecule. Since ClF_3O is rather difficult to synthesize,[23] a simpler synthesis of either ClF_3O or its ClF_4O^- salts is highly desirable. Consequently, the reactions of all alkali-metal nitrates with ClF_5 were studied by using a large excess of the latter to suppress, if possible, the second fluorine–oxygen exchange step leading to $FClO_2$. However, in all cases exclusively the two-step exchange reaction shown in (13) was observed. This suggests that the reaction of

$$2MNO_3 + ClF_5 \rightarrow 2MF + 2FNO_2 + FClO_2 \qquad (13)$$

$$M = Li, Na, K, Rb, Cs$$

the intermediately formed ClF_3O with MNO_3 is much faster than either that of ClF_5 with MNO_3 or the complexation of ClF_3O (eq 14). In one experiment a 10-fold excess of CsF was added to

$$MF + ClF_3O \rightarrow M^+ClF_4O^- \qquad (14)$$

the $CsNO_3$–ClF_5 reaction in an attempt to trap any intermediately formed ClF_3O as $Cs^+ClF_4O^-$. Although no evidence for the formation of $Cs^+ClF_4O^-$ was obtained, a detailed material balance of the reaction revealed two very interesting side reactions.

In the first side reaction, a significant amount of ClF_5 had decomposed at 25 °C to give equimolar amounts of F_2 and ClF_3 with the latter being complexed by CsF as $Cs^+ClF_4^-$. This side reaction had also been observed for $RbNO_3$ and KNO_3, but to a lesser extent. This decomposition of ClF_5 to ClF_3 and F_2 at room temperature was surprising in view of ClF_5 normally being completely stable at this temperature.[11] Although extrapolation of the degree of dissociation of ClF_5 at 25 °C from the known equlibrium constant temperature relationship[24] gives a value of 0.087%, this dissociation should require a significant activation energy and, therefore, not proceed under normal conditions. Our observation that in the presence of excess CsF more than 4% of the ClF_5 decomposed in 18 days at 25 °C while building up a fluorine pressure of about 340 Torr in the reactor, suggests that the alkali-metal fluorides (i) lower the activation energy required for the ClF_5 decomposition and (ii) effectively remove ClF_3 from the equilibrium given in (15), thereby shifting it to the right. The

$$ClF_5 \rightleftarrows ClF_3 + F_2 \qquad (15)$$

catalytic effect of alkali-metal fluorides for the backward reaction, i.e. the formation of ClF_5 from ClF_3 and F_2, has previously been recognized, and advantage of this has been taken for the ClF_5 synthesis[11] but to our knowledge has not been noted for the forward reaction.

The second side reaction observed for the $CsNO_3 + ClF_5 +$ CsF system was the formation of some fluorine nitrate, $FONO_2$. This can readily be explained by the known[16,25,26] reaction given in (16). The F_2 required for (16) is generated by (15).

$$CsNO_3 + F_2 \rightarrow CsF + FONO_2 \qquad (16)$$

MNO_3–$FClO_2$ System. When a large excess of MNO_3 is used in (13), the $FClO_2$ product can undergo further reaction with MNO_3. This was confirmed in a separate experiment between $LiNO_3$ and $FClO_2$, which reacted according to (17). The

$$LiNO_3 + FClO_2 \rightarrow LiF + ClONO_2 + O_2 \qquad (17)$$

quantitative formation of equimolar amounts of $ClONO_2$ and O_2 suggested the yet unknown O_2ClONO_2 molecule as an unstable intermediate. An attempt was made to isolate this intermediate at low temperature by reaction 18. By the use of an excess of

$$NO_2^+NO_3^- + FClO_2 \rightarrow O_2ClONO_2 + FNO_2 \qquad (18)$$

$FClO_2$, it was hoped that the only product of low volatility would be O_2ClONO_2, thus allowing a convenient product purification and isolation. Unfortunately, reaction 18 required a reaction temperature of 0 °C, well above the apparent thermal stability of the desired O_2ClONO_2. Consequently, the observed products were again $ClONO_2$ and O_2, formed according to (19). Since

$$NO_2^+NO_3^- + FClO_2 \rightarrow FNO_2 + ClONO_2 + O_2 \qquad (19)$$

this reaction was carried out in a Pyrex reactor to allow a low-temperature spectroscopic identification of the reaction product, side reactions of $FClO_2$ and N_2O_5 with the glass in the upper part of the reactor and each other also occurred, producing some SiF_4 and NO_2ClO_4.

Conclusion. All of the chlorine fluorides and oxyfluorides studied, except for the highly unreactive[23] $FClO_3$, undergo facile fluorine–oxygen exchange with ionic nitrates. The observed reaction chemistry is in general agreement with that previously found[9] for the analogous reactions with nitric acid, except for some minor deviations for $FClO_2$, which are attributed to thermally unstable intermediates. Depending on the exact reaction conditions, these unstable intermediates can decompose to different products.

Comparison of the nitrate–ClF_5 reactions with those of IF_5[5] and BrF_5[1,2] shows a noteworthy difference. Whereas for IF_5 and BrF_5 the fluorine–oxygen exchange could be halted at the XF_3O or XF_4O^- stage, this was not possible for ClF_5. This difference cannot be attributed to the thermal stability of the products (ClF_3O is thermally more stable than BrF_3O), but is most likely due to the extreme reactivity of ClF_3O.[23]

The alkali-metal fluoride catalyst decomposition of ClF_5 to ClF_3 and F_2 at room temperature was surprising and suggests a very low activation energy path for this reaction. It might possibly involve the attack of the free fluoride ion on a fluorine ligand of ClF_5, followed by fluorine elimination. If this assumption is indeed correct, this catalysis should be generally applicable to other high oxidation state fluorides of highly electronegative elements.

Acknowledgment. We thank Dr. C. J. Schack for helpful discussions and the Office of Naval Research and the U.S. Army Research Office for financial support.

Registry No. ClF_5, 13637-63-3; ClF_3, 7790-91-2; ClF, 7790-89-8; NO_3^-, 14797-55-8; $FClO_2$, 13637-83-7; FClO, 22363-68-4; $ClONO_2$, 14545-72-3; $FClO_3$, 7616-94-6; $LiNO_3$, 7790-69-4; N_2O_5, 10102-03-1; FNO_2, 10022-50-1; Cl_2O, 7791-21-1; Cl_2, 7782-50-5; CsF, 13400-13-0; RbF, 13446-74-7; KF, 7789-23-3; F_2, 7782-41-4; $NaNO_3$, 7631-99-4; KNO_3, 7757-79-1; $KClF_4$, 19195-69-8; $RbNO_3$, 13126-12-0; $CsNO_3$, 7789-18-6; $RbClF_4$, 15321-10-5; $CsClF_4$, 15321-04-7.

---

(24) Bauer, H. F; Sheehan, D. F. *Inorg. Chem.* 1967, *6*, 1736.

(25) Yost, D. M.; Beerbower, A. *J. Am. Chem. Soc.* 1935, *57*, 782.

(26) Viscido, L., Sicre, J. E., Schumacher, H. J. *Z. Phys. Chem.* (*Munich*) 1962, *32*, 182.

Journal of Fluorine Chemistry, *43* (1989) 125–129

Received: August 8, 1988; accepted: September 7, 1988

REACTIONS OF BrF_5 WITH THE AZIDE, NITRITE AND SULFATE ANIONS

KARL O. CHRISTE*, WILLIAM W. WILSON and CARL J. SCHACK

Rocketdyne, A Division of Rockwell International Corporation, Canoga Park, California
91303 (U.S.A)

SUMMARY

Bromine pentafluoride undergoes a facile fluorine-oxygen exchange reaction with the sulfate anion to yield an equimolar mixture of BrF_4O^- and SO_3F^- salts. With CsN_3 it ignites producing N_2 and a mixture of $CsBrF_4$ and $CsBrF_6$. With an excess of $NaNO_2$ it forms NaF, Br_2, and FNO_2. When BrF_5 is used in excess with KNO_2 its reduction is halted at the BrF_3 stage producing $KBrF_4$ and FNO_2 as the primary products. The FNO_2 can undergo a secondary reaction with KNO_2 to give N_2O_4 and KF which react further to FNO and KNO_3. The latter and excess BrF_5 yield some $KBrF_4O$ and FNO_2.

INTRODUCTION

The NF_4^+ and ClF_6^+ cations possess surprising kinetic stability and by metathesis in suitable solvents can be coupled with a variety of anions [1,2]. Since one of the best solvents for this purpose is BrF_5, its compatibility with the N_3^-, NO_2^-, and SO_4^{2-} anions was studied. Although these anions were found to be unstable in BrF_5, the observed reactions are interesting and are reported in this paper.

EXPERIMENTAL

Apparatus and Materials. The vacuum lines, handling techniques and spectrometers used in this study have been described elsewhere [3]. The BrF_5 (Matheson) was treated with 35 atm

0022-1139/89/$3.50

of F_2 at 100°C for 24 hours in the presence of NaF and then purified by fractional condensation through traps kept at -64° and -95°C, with the material retained at -95°C being used. The KNO_2 (J.T. Baker, 99.0%) and $NaNO_2$ (J.T. Baker, 98.0%) were dried in vacuo at 120°C for one day prior to their use. The Cs_2SO_4 was prepared from Cs_2CO_3 and H_2SO_4 and dried in vacuo at 200°C for one day. The CsN_3 (Eastman Kodak) was used as received.

Reaction of Cs_2SO_4 with BrF_5. A mixture of Cs_2SO_4 (1.30 mmol) and BrF_5 (106.4 mmol) in a 3/4" o.d. Teflon ampule was kept at 25°C for one hour. The material volatile at 25°C was pumped off and consisted of 105.1 mmol of BrF_5. The white solid residue (698.4 mg, weight calcd for 1.30 mmol of $CsBrF_4O$ and 1.30 mmol of $CsSO_3F$ = 698.2 mg) was identified by infrared and Raman spectroscopy as a mixture of $CsBrF_4O$ and $CsSO_3F$.

Reaction of CsN_3 with BrF_5. When a mixture of CsN_3 and a fivefold excess of BrF_5 in a Teflon-FEP ampule was warmed from -196°C towards ambient temperature, the mixture ignited on melting of the BrF_5 and burned with a bright red flame breaching the container. To achieve better temperature control, the experiment was repeated in a 95 ml Monel cylinder. CsN_3 (2.41 mmol) was added to the cylinder in the drybox, and BrF_5 (12.36 mmol) was added at -196°C on the vacuum line. The cylinder was allowed to slowly warm to room temperature and then cooled back again to -196°C. The gas noncondensible at -196° (N_2, 3.65 mmol) was pumped off, and the excess of unreacted BrF_5 (9.98 mmol) was removed at 25°C. The white solid residue (730 mg, weight calcd for 1.20 mmol each of $CsBrF_4$ and $CsBrF_6$ = 739 mg) was shown by Raman and infrared spectroscopy to be an about equimolar mixture of $CsBrF_4$ and $CsBrF_6$.

Reaction of BrF_5 with an Excess of $NaNO_2$. To a prepassivated 30 ml stainless steel cylinder that contained $NaNO_2$ (10.3 mmol), BrF_5 (2.54 mmol) was added at -196°C. The cylinder was allowed to warm to room temperature where it was kept for two hours. The material volatile at 25°C was separated by fractional condensation through -142°C and -196°C traps. The -142° trap contained Br_2 (1.27 mmol), and the one at -196° had FNO_2 (5.33 mmol, corresponding to an 84% yield based on BrF_5). The white solid residue was shown to be a mixture of NaF and unreacted $NaNO_2$.

Reaction of KNO_2 with an Excess of BrF_5. A mixture of KNO_2 (2.55 mmol) and BrF_5 (12.06 mmol) in a 30 ml stainless steel cylinder was kept at 25°C for four hours. Then, the cylinder was cooled to -196°C and shown to contain no material noncondensible at this temperature. The material volatile at 25°C was pumped off and separated by fractional condensation. It consisted of FNO_2, FNO and BrF_5. The light yellow-orange residue (290 mg) was identified by spectroscopic methods as a mixture of $KBrF_4$, KNO_3, $KBrF_4O$ and KF.

RESULTS AND DISCUSSION

At room temperature Cs_2SO_4 readily undergoes the following quantitative reaction with BrF_5.

$$Cs_2SO_4 + BrF_5 \rightarrow CsBrF_4O + CsSO_3F$$

Even in the presence of a large excess of BrF_5, a further fluorine-oxygen exchange to a second mole of $CsBrF_4O$ and SO_2F_2 does not take place. Although the above reaction is quantitative, it is not as useful as that of $CsNO_3$ with BrF_5 [4] for the preparation of pure $CsBrF_4O$ because of the difficulty of separating $CsBrF_4O$ from $CsSO_3F$.

The reaction of CsN_3 with an excess of BrF_5 is quite violent and, unless carefully controlled, results in ignition upon melting of the BrF_5. With careful temperature control, the following quantitative reaction is observed:

$$2CsN_3 + BrF_5 \rightarrow 2CsF + 3N_2 + BrF_3$$

The CsF product reacts with the BrF_3 and excess of BrF_5 to give $CsBrF_4$ [5] and $CsBrF_6$ [6], respectively:

$$CsF + BrF_3 \rightarrow CsBrF_4$$

and

$$CsF + BrF_5 \rightarrow CsBrF_6$$

Since BrF_3 is a stronger Lewis Acid than BrF_5 [7], all of the BrF_3 reacts with half of the CsF available leaving the other half for complexing with excess BrF_5. The reaction of CsN_3 with BrF_5 can, therefore, be regarded as a redox reaction in which N_3^- is oxidized to N_2 and BrF_5 is reduced to BrF_3.

The products observed for the reaction of BrF_5 with NO_2^- depend on which reagent is used in excess. As with the N_3^- anion, the NO_2^- anion acts as a reducing agent toward BrF_5. If an excess of NO_2^- is used, BrF_5 is reduced all the way to Br_2 as shown by the following equation:

$$5NaNO_2 + 2BrF_5 \rightarrow 5NaF + Br_2 + 5FNO_2$$

This reaction has potential as a relatively simple, high yield synthesis for FNO_2.

If an excess of BrF_5 is used, the reaction products are $KBrF_4$, KNO_3, $KBrF_4O$, KF, FNO, and FNO_2. These products are best rationalized by the following reaction sequence in which not all of the steps may go to completion:

$$KNO_2 + BrF_5 \rightarrow KBrF_4 + FNO_2$$

$$KNO_2 + FNO_2 \rightarrow KF + N_2O_4$$

$$KF + N_2O_4 \rightarrow KNO_3 + FNO$$

$$KNO_3 + BrF_5 \rightarrow KNO_3 + FNO_2$$

Of these reactions, the third one involving $KF + N_2O_4$ and the last one involving $KNO_3 + BrF_5$ have previously been demonstrated [8,4] in separate experiments.

In summary, BrF_5 is not only capable of undergoing smooth fluorine-oxygen exchange reactions, as for example with NO_3^- [4], SO_4^{2-}, BrO_3^- [9], BrO_4^- [10], or IO_4^- [11], but also can act as an oxidative fluorinator toward anions of lower oxidizing power such as N_3^- or NO_2^-

ACKNOWLEDGEMENT

The authors wish to thank Mr. R.D. Wilson for his help and to the Office of Naval Research and the U.S. Army Research Office for financial support.

REFERENCES

1 For a recent review of NF_4^+ chemistry, see I.V. Nikitin and V.Ya. Rosolovskii, Russ. Chem. Rev., 54, (1985) 426.

2 K.O. Christe and W.W. Wilson, Inorg. Chem., 22, (1983) 1950.

3 K.O. Christe and W.W. Wilson, Inorg. Chem., 27, (1988) 1296.

4 K.O. Christe and W.W. Wilson, Inorg. Chem., 26, (1987) 916.

5 K.O. Christe and C.J. Schack, Inorg. Chem., 9, (1970) 1852.

6 G. Tantot and R. Bougon, C.R. Seances Acad. Sci., Ser. C, 281, (1975) 271.

7 K.O. Christe, C.J. Schack, and D. Pilipovich, Inorg. Chem., 11, (1972) 2205.

8 C.T. Ratcliffe and J.M. Shreeve, J.C.S. Chem. Commun., (1966) 674.

9 R. Bougon, T. Bui Huy, P. Charpin, and G. Tantot, C.R. Seances Acad. Sci., Ser. C, 283 (1976) 71.

10 K.O. Christe, R.D. Wilson, E.C. Curtis, W. Kuhlmann, and W. Sawodny, Inorg. Chem. 17, (1978) 533.

11 K.O. Christe, R.D. Wilson, and C.J. Schack, Inorg. Chem., 20, (1981) 2104.

Reprinted from Inorganic Chemistry, 1989, *28*, 904
Copyright © 1989 by the American Chemical Society and reprinted by permission of the copyright owner.

Contribution from Rocketdyne, A Division of Rockwell International,
Canoga Park, California 91303

Fluorine-Oxygen Exchange Reactions in IF_5, IF_7, and IF_5O

Karl O. Christe,* William W. Wilson, and Richard D. Wilson

Received June 7, 1988

When reacted with alkali-metal nitrates, IF_5 readily exchanges two fluorine ligands for a doubly bonded oxygen atom. In all cases MIF_4O salts (M = Li, K, Cs) and FNO_2 are formed as the primary products. The FNO_2 byproduct undergoes a fast secondary reaction with MNO_3 to yield equimolar amounts of N_2O_5 and MF. The N_2O_5 decomposes to N_2O_4 and 0.5 mol of O_2, while the MF, depending on the nature of M, does or does not undergo complexation with the excess of IF_5. Pure MIF_4O salts, free of MF or $MF{\cdot}nIF_5$ byproducts, were prepared from MF, I_2O_5, and IF_5 in either CH_3CN or IF_5 as a solvent. The new compounds $LiIF_4O$, $NaIF_4O$, $RbIF_4O$, and $NOIF_4O$ were characterized by vibrational spectroscopy. It was also shown that, contrary to a previous report, FNO_2 does not form a stable adduct with IF_5 at temperatures as low as −78 °C. An excess of IF_7 reacts with MNO_3 (M = Li, Na) to give MF, FNO_2, IF_5, and 0.5 mol of O_2, but surprisingly no IF_5O. With $CsNO_3$, the reaction products are analogous, except for the CsF reacting with both the IF_5 product and the excess of IF_7 to give $CsIF_6{\cdot}2IF_5$ and $CsIF_8$, respectively. When in the IF_7 reaction an excess of $LiNO_3$, is used, the IF_5 product undergoes further reaction with $LiNO_3$, as described above. The IF_5O molecule was found to be rather unreactive. It does not react with either LiF or CsF at 25 or 60 °C or with $LiNO_3$ or $CsNO_3$ at 25 °C. At 60 °C with $LiNO_3$, it slowly loses oxygen, with the IF_5 product reacting to yield $LiIF_4O$, as described above.

Introduction

Recent work from our laboratory has shown that the nitrate ion is an excellent reagent for replacing two fluorine ligands by one doubly bonded oxygen atom in compounds such as BrF_5,[1,2] XeF_6,[3] and $XeOF_4$.[4] A logical extension of this work was a study of analogous fluorine–oxygen exchange reactions in iodine fluorides.

Although the reaction of KNO_3 with a large excess of IF_5 at its boiling point has previously been reported[5] to yield NO_2 and KIF_6, no mention of any fluorine–oxygen exchange was made. Some evidence for hydrolytic fluorine–oxygen exchange in $CsIF_6$ was observed during its recrystallization from CH_3CN solution. It resulted in the isolation of small amounts of single crystals of $CsIF_4O$, which were used for a crystal structure determination.[6] Attempts to utilize this reaction or the reactions of either MIO_3 or MIO_2F_2 (M = K or Cs) with IF_5 for the preparation of MIF_4O salts, however, resulted only in mixtures of MIF_4O and MIO_2F_2.[7] Finally, pure KIF_4O was prepared from a 5:1 mixture of $KF{:}I_2O_5$ in a large excess of IF_5, and its vibrational spectra have been recorded.[8]

In the case of IF_7, fluorine–oxygen exchange has been achieved by its reaction with either silica at 100 °C,[9] Cab-O-Sil at ambient temperature,[10] or Pyrex,[11,12] I_2O_5,[12] or small amounts of water[11-13] at room temperature with IF_5O being the principal product. Most likely, the reactions with silica or Pyrex also involve the hydrolysis of IF_7, with traces of HF continuously regenerating the required H_2O according to (1) and (2). However, most of these reactions

$$SiO_2 + 4HF \rightarrow SiF_4 + 2H_2O \qquad (1)$$

$$IF_7 + H_2O \rightarrow IF_5O + 2HF \qquad (2)$$

are slow and are difficult to control and scale up. It was, therefore, interesting to examine whether nitrates could be used advantageously to achieve fluorine–oxygen exchange in iodine fluorides and to prepare new iodine oxyfluoride salts.

Experimental Section

Apparatus and Materials. The vacuum lines, handling techniques, and spectrometers used in this study have been described elsewhere.[3] Commercial $LiNO_3$ (J. T. Baker, 99.7%), $NaNO_3$ (J. T. Baker 99.5%) and KNO_3 (J. T. Baker, 99.1%) were dried in vacuo at 120 °C for 1 day prior to their use. The $CsNO_3$ were prepared from Cs_2CO_3 and HNO_3 and dried in the same manner. The heavier alkali-metal fluorides (K, Rb, Cs) were dried by fusion in a platinum crucible and powdered in a drybox prior to use, while the lighter ones (Li, Na) were dried in vacuo at 120 °C. The N_2O_5,[14] FNO_2,[1] FNO,[15] IF_7,[10] and IF_5O,[10] were prepared by literature methods. The IF_5 (Matheson Co.) was treated with ClF_3 (Matheson) at 25 °C until the originally dark brown liquid was colorless. Pure IF_5 was obtained by fractional condensation at −64 °C in a dynamic vacuum. A commercial sample of I_2O_5 (Mallinckrodt), which actually was HI_3O_8, was converted to I_2O_5 by heating to 210 °C in a dynamic vacuum for 12 h. Its purity was verified by Raman spectroscopy.[16] The CH_3CN (Baker, UV grade, <0.001% H_2O) was stored over Linde 3A molecular sieves prior to use.

Caution! ClF_3 is a powerful oxidizer and contact with organic materials must be avoided.

Reaction of $LiNO_3$ with an Excess of IF_7. A 30-mL stainless-steel cylinder was loaded in the drybox with $LiNO_3$ (4.32 mmol). On the vacuum line, IF_7 (12.94 mmol) was added at −196 °C. The cylinder was allowed to warm to room temperature slowly and was kept at this temperature for 3 days. It was recooled to −196 °C, and the noncondensible gas (2.16 mmol of O_2 based on *PVT* measurements and the weight change of the cylinder) was pumped off. The material volatile at 30 °C was separated by fractional condensation through a series of traps at −95, −126, and −196 °C. These traps contained the following materials: −196 °C, 4.26 mmol of FNO_2; −126 °C, 8.6 mmol of IF_7; −95 °C, 4.3 mmol of IF_5. In its Raman spectrum, the white solid residue (120 mg; weight calculated for 4.32 mmol of LiF = 112 mg) showed no evidence for the presence of unreacted $LiNO_3$.

Reaction of $NaNO_3$ with an Excess of IF_7. The reaction was carried out in the same manner as described for $LiNO_3$. After 15 h at 25 °C, no noticeable reaction had occurred, but after 60 h at 60 °C, IF_5, NaF, FNO_2, and 0.5 mol of oxygen were formed in quantitative yield.

Reaction of $CsNO_3$ with an Excess of IF_7. A 75-mL stainless steel cylinder was loaded in the drybox with $CsNO_3$ (2.47 mmol). On the vacuum line, IF_7 (12.48 mmol) was added at −196 °C. The cylinder was kept for 3 days at 25 °C and then recooled to −196 °C. It contained 0.44 mmol of a gas (O_2) noncondensible at −196 °C. The material volatile at 25 °C was separated by fractional condensation through a series of traps kept at −45, −95, −126, and −196 °C while the cylinder was allowed

---

(1) Wilson, W. W.; Christe, K. O. *Inorg. Chem.* **1987**, *26*, 916.
(2) Wilson, W. W.; Christe, K. O. *Inorg. Chem.* **1987**, 26, 1573
(3) Christe, K. O.; Wilson, W. W. *Inorg. Chem.* **1988**, *27*, 1296
(4) Christe, K. O.; Wilson, W. W. *Inorg. Chem.*, in press.
(5) Aynsley, E. E.; Nichols, R.; Robinson, P. L. *J. Chem. Soc.* **1953**, 623
(6) Ryan, R. R.; Asprey, L. B. *Acta Crystallogr.* **1972**, *B28*, 979.
(7) Milne, J. B.; Moffett, D. M. *Inorg. Chem.* **1976**, *15*, 2165.
(8) Christe, K. O., Wilson, R. D., Curtis, E. C., Kuhlmann, W.; Sawodny, W. *Inorg. Chem.* **1978**, *17*, 533.
(9) Gillespie, R. J.; Quail, J. W. *Proc. Chem. Soc.* **1963**, 278.
(10) Schack, C. J., Pilipovich, D., Cohz, S. N., Sheehan, D. F. *J. Phys Chem.* **1968**, *72*, 4697.
(11) Alexakos, L. G., Cornwell, C. D., Pierce, S. B. *Proc Chem Soc* **1963**, 341.
(12) Bartlett, N., Levchuk, L. E. *Proc Chem Soc* **1963**, 342
(13) Selig, H.; Elgad, U. *J. Inorg. Nucl. Chem. Suppl.* **1976**, 91.
(14) Wilson, W. W.; Christe, K. O. *Inorg. Chem.* **1987**, *26*, 1631.
(15) Christe, K. O., Wilson, R. D., Goldberg, I. A. *Inorg. Chem.* **1976**, *15*, 1271.
(16) Sherwood, P. M. A., Turner, J. J. *Spectrochim. Acta, Part A* **1970**, *26A*, 1975.

to warm from −196 to 25 °C. The −45 °C trap was empty, the −95 and −126 °C traps contained IF_7 (11.07 mmol), and the −196 °C trap had FNO_2 (0.86 mmol). The white solid residue (764 mg; weight calculated 0.54 mmol of $CsIF_8$, 1.61 mmol of $CsNO_3$, 0.27 mmol of $CsIF_6{\cdot}2IF_5$, and 0.04 mmol of $CsIF_6$ = 770 mg) was shown by vibrational spectroscopy to consist of $CsNO_3$, $CsIF_8$,[17] $CsIF_6{\cdot}2IF_5$,[18] and a small amount of $CsIF_6$.[18]

Reaction of an Excess of $LiNO_3$ with IF_7. A 30-mL stainless-steel cylinder was loaded with $LiNO_3$ (8.62 mmol) and IF_7 (1.90 mmol) at −196 °C. The cylinder was allowed to slowly warm to ambient temperature and was kept at this temperature for 3 days. It was recooled to −196 °C and the noncondensible gas (2.71 mmol of O_2) was pumped off. The material volatile at 30 °C consisted of N_2O_4 (3.47 mmol) and IF_5 (0.30 mmol). The white solid residue (601 mg; weight calculated for a mixture of 1.62 mmol of $LiNO_3$, 1.60 mmol of $LiIF_4O$, and 5.40 mmol of LiF = 613 mg) was shown by its infrared and Raman spectra to contain LiF_4O and unreacted $LiNO_3$.

Reaction of $LiNO_3$ with an Excess of IF_5. A 30-mL stainless-steel cylinder containing $LiNO_3$ (5.55 mmol) was cooled to −196 °C, and IF_5 (62.94 mmol) was added. The cylinder was kept for 15 h on a shaker at ambient temperature. After the cylinder was recooled to −196 °C, noncondensible material (0.51 mmol of O_2) was pumped off. The material volatile at 35 °C consisted of FNO_2 (0.34 mmol), N_2O_4 (1.03 mmol), and IF_5 (61.5 mmol). The white solid residue (589 mg; weight calculated for a mixture of 3.15 mmol of $LiNO_3$, 1.37 mmol of $LiIF_4O$, and 1.03 mmol of LiF = 553 mg) was shown by vibrational spectroscopy to contain $LiIF_4O$ and unreacted $LiNO_3$.

Reaction of KNO_3 with an Excess of IF_5. A 30-mL stainless-steel cylinder containing KNO_3 (3.17 mmol) and IF_5 (42.45 mmol) was shaken for 12 h at 25 °C and then kept in an oven at 50 °C for 5 days. The cylinder was cooled to −196 °C and noncondensible material (0.75 mmol of O_2) was pumped off. The material volatile at 35 °C consisted of N_2O_4 (1.6 mmol), IF_5 (39.2 mmol) and a small amount of $IONO_2$ (see Results and Discussion). The white solid residue (850 mg; weight calculated for a mixture of 1.58 mmol of KIF_4O and 1.58 mmol of KIF_6 = 847 mg) contained according to its vibrational spectra KIF_4O,[5] KIF_6,[18] and a small amount of unreacted KNO_3.

Reaction of $CsNO_3$ with an Excess of IF_5. When $CsNO_3$ was reacted with a 5-fold excess of IF_5 at 25 °C for 40 h, the main reaction products were N_2O_4, O_2, $CsIF_4O$, and $CsIF_6{\cdot}2IF_5$[18] in addition to unreacted IF_5 and $CsNO_3$, and a smaller amount of FNO_2. Harsher reaction conditions (70 °C for 6 days, 20-fold excess of IF_5, and vacuum pyrolysis of the solid product at 100 °C) resulted in complete conversion of $CsNO_3$ to $CsIF_4O$ and $CsIF_6$.

Synthesis of $LiIF_4O$. A prepassivated 30-mL stainless-steel cylinder was loaded in the glovebox with LiF (4.85 mmol) and I_2O_5 (0.97 mmol). On the vacuum line IF_5 (31.84 mmol) was added at −196 °C. The cylinder was shaken for 20 h at ambient temperature and then kept at 50 °C for 3 days with occasional agitation. The material volatile at 25 °C was pumped off and consisted of IF_5 (29 mmol). The white solid residue (1030 mg; weight calculated for 4.85 mmol of $LiIF_4O$ = 1095 mg) consisted of a mixture of mainly $LiIF_4O$, LiF, and IF_3O and a small amount of IO_2F. The IF_3O and IO_2F were concentrated in the material found in the bottom of the reactor, whereas essentially pure $LiIF_4O$ was obtained from the upper walls of the reactor.

Synthesis of $NOIF_4O$. A 30-mL stainless-steel cylinder was loaded in the drybox with I_2O_5 (1.43 mmol). On the vacuum line, IF_5 (154.8 mmol) and FNO (12.66 mmol) were added at −196 °C. The cylinder was placed on a shaker at ambient temperature for 2 days and then reconnected to the vacuum line. The volatile material was removed in a dynamic vacuum at 20 °C. After several hours of pumping, the weight of the residue (1.80 g) approached that predicted for 7.15 mmol of $NOIF_4O$ (1.78 g), but after an additional 14 h of pumping further decreased to 886 mg, indicating that the complex was not completely stable at ambient temperature. Inspection of the residue in the reactor revealed in its bottom a white, sticky solid and on its upper walls a white, dry solid. More of the white, dry solid had also sublimed to a −196 °C cold trap used to collect the volatile material during the final stages of the pumping. Its Raman and infrared spectra were in good agreement with a predominantly ionic $NO^+IF_4O^-$ salt, whereas the sticky white solid exhibited, in addition to the $NOIF_4O$ absorptions, broad bands in the range characteristic for iodine oxyfluorides and/or their polyanions

Syntheses of MIF_4O (M = Li, Na, Rb) in CH_3CN Solution. All reactions were carried out in a similar manner by loading within the drybox a mixture of MF (5 mmol) and I_2O_5 (1 mmol), followed by about 20 mL of dry CH_3CN into a 12 in. long, $^3/_4$ in. o.d. Teflon FEP ampule, equipped with a stainless-steel valve and a Teflon-coated magnetic stirring bar. On the vacuum line, IF_5 (3 mmol) was added at −196 °C, and the mixture was stirred at 25 °C for 20 h. All volatile material was removed in a dynamic vacuum at room temperature, leaving behind the desired MIF_4O salts in almost quantitative yield. The color of the solid products was sometimes off-white causing a strong fluorescence background when their laser Raman spectra were recorded.

The FNO_2–IF_5 System. A mixture of IF_5 (4.42 mmol) and FNO_2 (6.9 mmol) was kept in a 30-mL stainless-steel cylinder at 25 °C for 24 h. Then, the cylinder was cooled to −78 °C, and the volatile material (FNO_2, 6.7 mmol) was collected in a −196 °C trap. Therefore, FNO_2 does not form a stable adduct with IF_5 at temperatures as low as −78 °C. The slight discrepancy in the observed FNO_2 material balance is attributed to FNO_2 trapped in the solid IF_5.

Results and Discussion

Fluorine–Oxygen Exchange in IF_7. An excess of IF_7 reacted quantitatively with either $LiNO_3$ at ambient temperature or $NaNO_3$ at 60 °C according to (3). In the case of $CsNO_3$ for

$$\begin{gathered} MNO_3 + IF_7 \rightarrow MF + FNO_2 + IF_5 + 0.5O_2 \\ M = Li, Na \end{gathered} \tag{3}$$

3 days at 25 °C, reaction 3 proceeded with a yield of about 35%. However, the CsF formed in (3) underwent the secondary reactions (4)–(6), thus resulting in a mixture of $CsIF_8$,[17] $CsIF_6{\cdot}2IF_5$,[18]

$$CsF + IF_7 \rightarrow CsIF_8 \tag{4}$$

$$CsF + 3IF_5 \rightarrow CsIF_6{\cdot}2IF_5 \tag{5}$$

$$CsF + IF_5 \rightarrow CsIF_6 \tag{6}$$

$CsIF_6$,[18] and unreacted $CsNO_3$ as the solid products. The fact that reaction 3 produced exclusively IF_5 and O_2 and no IF_5O was surprising in view of the previously observed ease of fluorine–oxygen exchange in BrF_5,[1,2] XeF_6,[3] and $XeOF_4$[4] and the ready formation of IF_5O from IF_7 by controlled hydrolysis.[9-13]

One possible explanation for the lack of IF_5O observation in (3) could be that IF_5O is formed initially, but one of the starting materials or byproducts catalyzes its decomposition to IF_5 and O_2. To test this hypothesis, we have examined the stability of IF_5O in the presence of $LiNO_3$, $CsNO_3$, LiF, CsF, FNO_2, or $LiNO_3$ + FNO_2. There was no reaction of IF_5O with either LiF or CsF at 25 °C and LiF at 60 °C. Furthermore, neither $LiNO_3$ nor $CsNO_3$ reacted with a large excess of IF_5O at 25 °C. A temperature of 60 °C was required to achieve the very slow reaction (7). The formation of MIF_4O in (7) and the absence of any

$$\begin{gathered} 2MNO_3 + IF_5O \rightarrow MIF_4O + MF + N_2O_4 + O_2 \\ M = Li \text{ or } Cs \end{gathered} \tag{7}$$

MIF_4O_2[19] in the products suggest that IF_5O does not undergo a fluorine–oxygen exchange with MNO_3, but decomposes first to O_2 and IF_5, which then reacts with MNO_3 (see below). For M in (7) being Cs, the secondary reaction 5, i.e. the formation of $CsIF_6{\cdot}2IF_5$, was also observed. Since in the $LiNO_3$–IF_7 system IF_5 and O_2 are being rapidly generated at 25 °C, the slow decomposition of IF_5O at 60 °C in the presence of MNO_3 does not provide a satisfactory explanation for (3).

This conclusion was further supported by a ^{19}F NMR study of the $LiNO_3$–IF_7 system between −20 and +25 °C. Besides a very broad signal at ϕ of about 170 due to IF_7, the only other signals observed were those of IF_5 (quintet at $\phi = 65$ and doublet at $\phi = 11$),[20] which grew with increasing temperature and time.

The effect of FNO_2 on the decomposition of IF_5O was also studied, but again no O_2 evolution was observed at 25 °C. Finally, the effect of FNO_2 in the presence of $LiNO_3$ at 25 °C was investigated. Since $LiNO_3$ is known[14] to react with FNO_2 (eq 8), and the formed N_2O_5 slowly decomposes at 25 °C to N_2O_4 and O_2 (eq 9), a sequence such as (8)–(10) might explain the formation of IF_5 and O_2, as shown by the overall equation (11). Although

---

(17) Adams, C. J. *Inorg. Nucl. Chem. Lett* 1974, *10*, 831.
(18) Christe, K. O. *Inorg. Chem.* 1972, *11*, 1215.
(19) Christe, K. O.; Wilson, R. D., Schack, C. J. *Inorg. Chem.* 1981, *20*, 2104
(20) Dungan, C. H.; Van Wazer, J R *Compilation of Reported F*^{19} *NMR Chemical Shifts*; Wiley-Interscience: New York, 1970.

$$\mathrm{LiNO_3 + FNO_2 \rightarrow LiF + N_2O_5} \qquad (8)$$

$$\mathrm{2N_2O_5 \rightarrow 2N_2O_4 + O_2} \qquad (9)$$

$$\mathrm{N_2O_4 + IF_5O \rightarrow N_2O_5 + IF_5} \qquad (10)$$

$$\text{net:}\quad \mathrm{LiNO_3 + FNO_2 + IF_5O \rightarrow LiF + N_2O_4 + IF_5 + O_2} \qquad (11)$$

an experiment at 25 °C using a mole ratio of FNO_2:$LiNO_3$:IF_5O ≐ 1:1.2:3.4 resulted in IF_5, N_2O_4, and O_2 formation, the rate was very slow and even after 5 days only about half of the excess of IF_5O used had decomposed to IF_5 and O_2. This finding together with the above described NMR experiment, which showed no detectable IF_5O signal, mitigates against (11) being the cause for the rapid IF_5 formation in the $LiNO_3$–IF_7 system.

Finally, one might argue that in the $LiNO_3$ + IF_7 reaction the IF_7 acts simply as a fluorinating agent (eq 12), similar to the

$$\mathrm{MNO_3 + IF_7 \rightarrow MF + FONO_2 + IF_5} \qquad (12)$$

known reaction of F_2 with alkali-metal nitrates.[21,22] The $FONO_2$ could then undergo decomposition to FNO_2 and O_2 (eq 13). The

$$\mathrm{FONO_2 \rightarrow FNO_2 + 0.5O_2} \qquad (13)$$

summation of (12) and (13) is identical with the observed reaction 3. Arguments against this reaction path are that (13) is extremely slow at 25 °C,[23] that the above NMR experiment showed no signal due to $FONO_2$,[24] and that the stronger fluorinating agents ClF_5[25] and BrF_5[1,2] undergo fluorine–oxygen exchange with MNO_3 and not O_2 elimination.

Since IF_5O by itself is a stable molecule[10] and there is no evidence for its catalytic decomposition at 25 °C (see above), the lack of IF_5O formation cannot be attributed to instability of the final product. This conclusion is further supported by the case of BrF_3O, which in spite of its well-known instability[26,27] is formed in high yield from BrF_5 and $LiNO_3$.[1]

Possible explanations for the different behavior of IF_7 and BrF_5 include (i) the difference in stability of their oxo anions, IF_6O^- and BrF_4O^-. Whereas BrF_4O^- can form stable salts,[1,26,27] there is no evidence for the formation of IF_6O^- salts (see above). If these anions are crucial intermediates, required for the formation of IF_5O and BrF_3O, respectively, then the nonexistence of IF_6O^- could explain the lack of IF_5O formation. Another explanation is that (ii) the mechanism, previously proposed[1] for the formation of BrF_3O from BrF_5, involves an ionic intermediate formed by the attack of BrF_5 on the nitrate anion (eq 14 and 15).

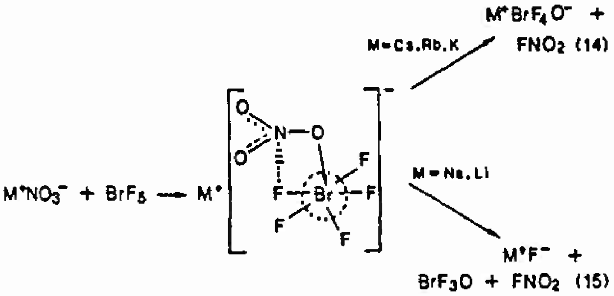

A crucial part of this mechanism is the existence of a free valence electron pair on the bromine atom that can easily be shifted to open up a required coordination site for the approach of an oxygen atom. If, however, the halogen central atom of the halogen fluoride does not possess a free valence electron pair, as is the case in IF_7 or IF_5O, then the mechanism in (14) and (15) becomes more difficult and O_2 elimination (eq 3) might take place.

When IF_7 was reacted with a large excess of $LiNO_3$, reaction 3, i.e. formation of LiF, FNO_2, IF_5, and 0.5 mol of O_2, occurred in quantitative yield. However, the products FNO_2 and IF_5 underwent further high-yield reactions (eq 16–18) with $LiNO_3$,

$$\mathrm{LiNO_3 + IF_5 \rightarrow LiIF_4O + FNO_2} \qquad (16)$$

$$\mathrm{LiNO_3 + FNO_2 \rightarrow LiF + N_2O_5} \qquad (17)$$

$$\mathrm{N_2O_5 \rightarrow N_2O_4 + 0.5O_2} \qquad (18)$$

resulting in (19) as the overall reaction. Reaction 17 has previously

$$\mathrm{4LiNO_3 + IF_7 \rightarrow LiIF_4O + 3LiF + 2N_2O_4 + 1.5O_2} \qquad (19)$$

been demonstrated,[14] and the decomposition of N_2O_5 to N_2O_4 and O_2 (eq 18) is well-known.

Fluorine–Oxygen Exchange in IF_5. In the case of IF_5, which contains a free valence electron pair on iodine, fluorine–oxygen exchange was observed in high yield with $LiNO_3$, KNO_3 and $CsNO_3$ (eq 20). Reaction 20 was always accompanied by the

$$\mathrm{MNO_3 + IF_5 \rightarrow MIF_4O + FNO_2} \qquad \mathrm{M = Li, K, Cs} \qquad (20)$$

secondary reactions (21) and (18). The fact that the secondary

$$\mathrm{MNO_3 + FNO_2 \rightarrow MF + N_2O_5} \qquad (21)$$

reaction (21) always consumed as much MNO_3 as (20) did, strongly indicates that (21) must be considerably faster than (20). Furthermore, if the MF byproduct, formed in (21), can complex with the excess of IF_5, reaction 22 or 23 ensues. These sequences

$$\mathrm{MF + IF_5 \rightarrow MIF_6} \qquad \mathrm{M = K} \qquad (22)$$

$$\mathrm{MF + 3IF_5 \rightarrow MIF_6{\cdot}2IF_5} \qquad \mathrm{M = Cs} \qquad (23)$$

explain the observed overall reactions (24)–(26). These results

$$\mathrm{2LiNO_3 + IF_5 \rightarrow LiIF_4O + LiF + N_2O_4 + 0.5O_2} \qquad (24)$$

$$\mathrm{2KNO_3 + 2IF_5 \rightarrow KIF_4O + KIF_6 + N_2O_4 + 0.5O_2} \qquad (25)$$

$$\mathrm{2CsNO_3 + 4IF_5 \rightarrow CsIF_4O + CsIF_6{\cdot}2IF_5 + N_2O_4 + 0.5O_2} \qquad (26)$$

are in excellent agreement with our expectations based on the known reaction chemistry of BrF_5[1] and deviate from the previous report[5] that KNO_3 reacts with a large excess of IF_5 to give KIF_6 and NO_2. Furthermore, the previous claim[28] that FNO_2 and IF_5 produce a white, solid $NO_2^+IF_6^-$ adduct of marginal stability at room temperature could not be verified. In our study it was shown that at temperatures as low as −78 °C, IF_5 does not form a stable adduct with FNO_2.

It should be noted that in one of the fractions of the volatile products from the KNO_3–IF_5 reactions a small amount of material was observed that, on the basis of its gas-phase infrared spectrum, is attributed to iodine mononitrate, $IONO_2$. It exhibited very strong absorption bands at 1686, 1271, and 795 cm^{-1}, that are assigned to the antisymmetric NO_2 stretch, the symmetric NO_2 stretch, and the NO_2 scissoring modes, respectively. The observed frequency trends are in excellent agreement with those predicted from the known series $FONO_2$, $ClONO_2$, and $BrONO_2$.[2]

Alternate Syntheses of IF_4O^- Salts. The only previously known IF_4O^- salts had been $CsIF_4O$[6,7] and KIF_4O.[7,8] The successful synthesis of a stable $LiIF_4O$ salt in this study and the fact that the stability of this type of salt generally decreases with decreasing cation size suggested that all alkali metals and probably also NO^+ should be capable of forming stable IF_4O^- salts. Since the above reactions of alkali-metal nitrates with IF_5 always yielded other solid byproducts in addition to MIF_4O, the synthesis (eq 27)

$$\mathrm{5MF + I_2O_5 + 3IF_5 \xrightarrow{solvent} 5MIF_4O} \qquad (27)$$

previously demonstrated[8] for KIF_4O was used for the preparation of essentially pure IF_4O^- salts of Li, Na, Rb, and NO. With CH_3CN used as a solvent, the new compounds $LiIF_4O$, $NaIF_4O$, and $RbIF_4O$ were prepared. Alternatively, an excess of IF_5 can be used as a solvent in (27). In this manner KIF_4O had previously

---

(21) Yost, D. M.; Beerbower, A. *J. Am. Chem. Soc.* 1935, *57*, 782.
(22) Viscido, L.; Sicre, J. E.; Schumacher, H. J. *Z. Phys. Chem. (Munich)* 1962, *32*, 182.
(23) Bruna, P. J., Sicre, J. E. *An. Asoc. Quim. Argent.* 1971, *59*, 205.
(24) Ghibaudi, E.; Colussi, A. J.; Christe, K. O. *Inorg. Chem.* 1985, *24*, 2869.
(25) Christe, K. O.; Wilson, W. W. Unpublished results.
(26) Bougon, R.; Bui Huy, T. *C. R. Seances Acad. Sci., Ser. C* 1976, *283*, 461.
(27) Gillespie, R. J.; Spekkens, P. *J. Chem. Soc., Dalton Trans.* 1976, 2391.
(28) Aynsley, E. E.; Hetherington, G.; Robinson, P. L. *J. Chem. Soc.* 1954, 1119.

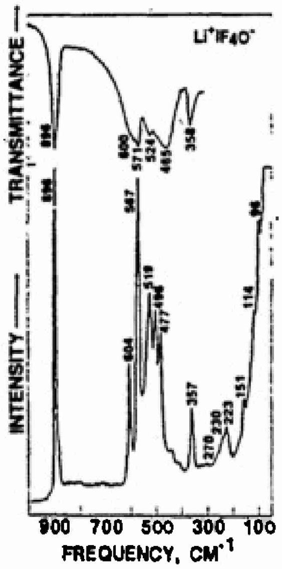

Figure 1. Vibrational spectra of solid $LiIF_4O$.

been prepared,[8] and $LiIF_4O$ and $NOIF_4O$ were synthesized in this study. On the basis of the vibrational spectra, the products prepared in CH_3CN solution appeared to be of better purity than those from IF_5 solution, which, in the case of $LiIF_4O$, showed some IF_3O and IO_2F as impurities. In the case of CH_3CN, however, the products sometimes were off-white, and trace residues of organic materials caused a strong fluorescence background when the laser Raman spectra were recorded. All of the alkali-metal IF_4O^- salts are white solids, stable at room temperature, while the $NO^+IF_4O^-$ salt slowly dissociates at room temperature.

^{19}F NMR Spectra. The IF_4O^- salts were of low solubility in IF_5, but were quite soluble in CH_3CN. The IF_4O^- anion in CH_3CN showed in the ^{19}F NMR spectrum a singlet at $\phi = 3$–9 ppm depending on the nature of the cation. The observation of a singlet confirms the presence of a pseudooctahedral IF_4O^- anion with four equivalent equatorial fluorine atoms.

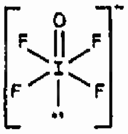

For comparison, the ^{19}F NMR spectrum of IF_3O in CH_3CN was also recorded and showed a broad singlet at $\phi = 14$.

Vibrational Spectra. The infrared and Raman spectra of solid $LiIF_4O$, $NaIF_4O$, KIF_4O, $RbIF_4O$, $CsIF_4O$, and $NOIF_4O$ are shown in Figures 1–6, and the observed frequencies and their assignments are summarized in Table I. As in the case of the closely related BrF_4O^- anion,[1,8] the number of observed Raman bands strongly depends on the cation and indicates strong interaction between anions and cations in the crystal lattice. As expected, this interaction is stronger for the smaller cations.

The assignments given in Table I are in very good agreement with those previously made for KIF_4O.[8] The only correction proposed with respect to the previous work is the location of the band center for the antisymmetric IF_4 stretching vibration ν_7(E). The frequency of this band is difficult to determine from the infrared spectra because of the broadness of the bands in the 450–600-cm^{-1} region. Since in $LiIF_4O$ and $NaIF_4O$ one of the degenerate components of this mode is also observable in the Raman spectra, which exhibit much narrower line widths, its frequency can be located more precisely. An averaged value of about 560 cm^{-1} appears much more plausible for ν_7(E) than the previously proposed[8] value of 482 cm^{-1}. This revised frequency for ν_7(E) of IF_4O^- is in much better agreement with the value of 608 cm^{-1} found for isoelectronic $XeOF_4$[29,30] and should alleviate

Table I. Vibrational Spectra of $M^+IF_4O^-$ Salts (M = NO, Li, Na, K, Rb, Cs) Compared to Those of $XeOF_4$

assigns for IF_4O^- in point group C_{4v}				obsd freq, cm^{-1} (rel intens)													
				$NO^+IF_4O^-$		$LiIF_4O$		$NaIF_4O$		KIF_4O		$RbIF_4O$		$CsIF_4O$		$XeOF_4$[b] gas	
				IR	RA	IR	RA	IR	RA	IR	RA	IR	RA	IR	RA	IR	RA
A_1	ν_1	ν_{IO}		868 vs	864 (100)	896 vs	896 (100)	895 vs	896 (100)	885 vs	883 (100)	895 vs	898 (100)	888 vs	889 (90)	926 s	926 m
	ν_2	ν_{sym}	IF_4 in phase	540–460	530 (20) 508 (2)	524 w	567 (90) 519 (55)		541 (85)		540 (98)		531 (80)		528 (100)	576 m	577 vs
	ν_3	δ_{sym}	IF_4 out of plane		286 (1)		270 sh		284 (2)	279 ms[a]	278 sh				270 sh	294 s	286 mw
B_1	ν_4	ν_{sym}	IF_4 out of phase	540–460	484 (17) 460 sh	465 vs	496 (50) 477 (43)	455 vs	513 (30) 457 (30)	500 vs 460 s	492 (30) 465 sh	570–440 vs, br	478 (60)	475 vs	475 (64)		543 m
	ν_5	δ_{asym}	IF_4 out of plane				230 sh										
B_2	ν_6	δ_{sym}	IF_4 in plane		225 (10)		223 (10)		230 (6)		224 (5)[a]				220 sh		225 mw
E	ν_7	ν_{asym}	IF_4	540–460 vs, br	540 sh	600 sh 571 vs	604 (35)	580 sh 540 vs	584 (20)	580 sh 550 vs		570–440 vs, br		530 vs		608 vs	
	ν_8	δ	OIF_4	391 m 350 m	393 (17) 351 (5)	358 m	357 (19)	350 ms	354 (20)	380 m 366 sh[a]	366 (20)	365 m	370 (20)	360 ms	360 (25)	361 s	360 mw
	ν_9	δ_{asym}	IF_4 in plane		159 (3)		151 (4)		150 sh		140 (2)[a]						161 vw

[a] Values from ref 8. [b] Values from ref 29 and 30.

---

(29) Tsao, P.; Cobb, C. C.; Claassen, H. H. *J. Chem. Phys.* **1971**, *54*, 5247.
(30) Begun, G. M.; Fletcher, W. H.; Smith, D. F. *J. Chem. Phys.* **1965**, *42*, 2236.

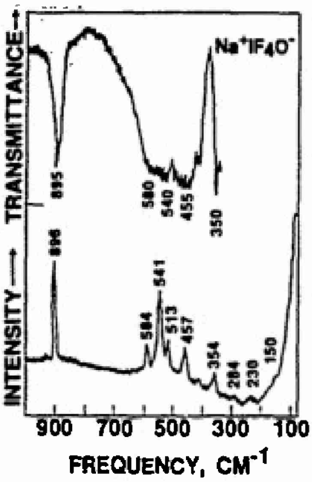

Figure 2. Vibrational spectra of solid $NaIF_4O$.

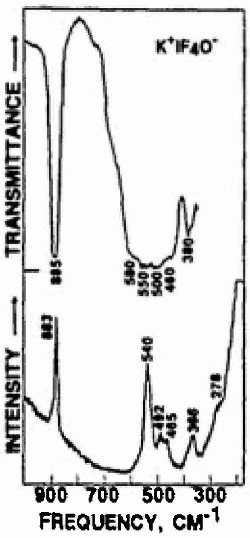

Figure 3. Vibrational spectra of solid KIF_4O.

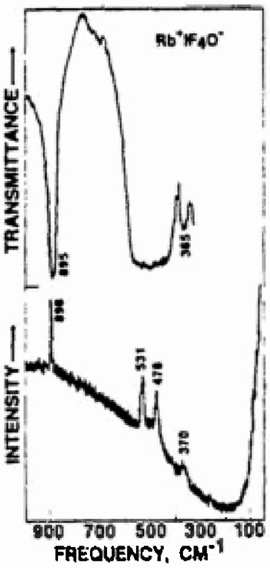

Figure 4. Vibrational spectra of solid $RbIF_4O$.

the anomaly found for $f_{rr'}$ in the normal-coordinate analysis of IF_4O^-.[8]

The vibrational spectra of the solid product obtained from the reaction of FNO with I_2O_5 and IF_5 demonstrate that the compound has the predominantly ionic composition $NO^+IF_4O^-$. The infrared and Raman spectra show an intense band at about 2302 cm^{-1}, which is characteristic for NO^+,[31] in addition to bands that

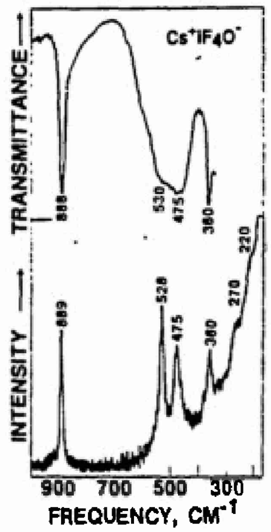

Figure 5. Vibrational spectra of solid $CsIF_4O$.

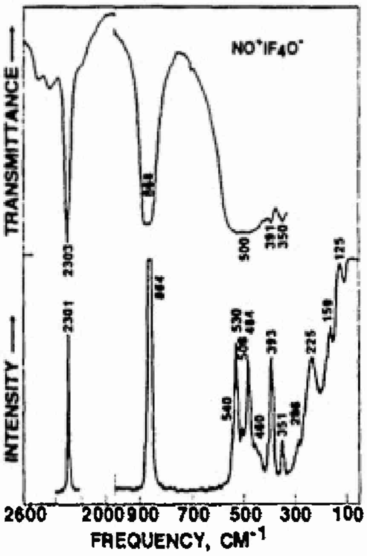

Figure 6. Vibrational spectra of solid $NOIF_4O$.

are quite similar to those of the alkali-metal IF_4O^- salts. The slight frequency shifts are attributed to weak covalent contributions to the bonding.

Conclusions. The nitrate ion is a useful reagent for fluorine-oxygen exchange in IF_5. The resulting IF_4O^- anion is capable of forming stable salts, even with cations as small as Li^+. It also forms a marginally stable, highly ionic NO^+ salt. With IF_7, the NO_3^- anion does not undergo a fluorine–oxygen exchange but causes a surprising reductive deoxygenation, which is attributed to the absence of a free valence electron pair on the iodine central atom of IF_7. With IF_5O, again no fluorine–oxygen exchange was observed. At elevated temperatures, oxygen loss occurred first, followed by the reaction of the resulting IF_5 with NO_3^- to give IF_4O^- salts.

Acknowledgment. We thank Dr. C. J. Schack for helpful discussions and the Office of Naval Research and the U.S. Army Research Office for financial support.

Registry No. $LiNO_3$, 7790-69-4; $NaNO_3$, 7631-99-4; KNO_3, 7757-79-1; $CsNO_3$, 7789-18-6; FNO_2, 10022-50-1; FNO, 7789-25-5; IF_7, 16921-96-3; IF_5O, 16056-61-4; I_2O_5, 12029-98-0; O_2, 7782-44-7; IF_5, 7783-66-6; NaF, 7681-49-4; $CsIF_8$, 54988-13-5; $CsIF_6 \cdot 2IF_5$, 36949-61-8; $CsIF_6$, 20115-52-0; N_2O_4, 10544-72-6; $LiIF_4O$, 118867-55-3; $IONO_2$, 14696-81-2, KIF_4O, 59654-71-6, KIF_6, 20916-97-6, $CsIF_4O$, 36374-06-8, LiF, 7789-24-4; IF_3O, 19058-78-7; IO_2F, 28633-62-7; $NOIF_4O$, 118867-56-4, $NaIF_4O$, 118831-04-2, $RbIF_4O$, 118831-05-3; RbF, 13446-74-7.

---

(31) Griffiths, J. E., Sunder, W. A., Falconer, W. E. *Spectrochim Acta, Part A* 1975, *31A*, 1207.

APPENDIX I

Reprinted from the Journal of the American Chemical Society, 1990, *112*.

Syntheses, Properties, and Structures of Anhydrous Tetramethylammonium Fluoride and Its 1:1 Adduct with *trans*-3-Amino-2-butenenitrile

Karl O. Christe,*,† William W. Wilson,† Richard D. Wilson,† Robert Bau,‡ and Jin-an Feng‡

Contribution from Rocketdyne, A Division of Rockwell International, Canoga Park, California 91303, and the Department of Chemistry, University of Southern California, Los Angeles, California 90007.

Received February 26, 1990

Abstract: A simple method for the preparation of anhydrous and essentially HF_2^--free $N(CH_3)_4F$ is described. The compound was characterized by X-ray diffraction, NMR, infrared, and Raman spectroscopy. It crystallizes in the hexagonal system with a hexagonal closest packing of the $N(CH_3)_4^+$ cations. It is shown that the free F^- anion is a very strong Lewis base and chemically reacts with most of the solvents, such as CH_3CN or chlorinated hydrocarbons, previously used for studies of the fluoride anion. As a result, some of the properties previously reported for F^- were due to HF_2^- or other secondary reaction products. Its relatively simple synthesis and lower cost, combined with its good solubility and the high chemical inertness of the $N(CH_3)_4^+$ cation, make $N(CH_3)_4F$ an excellent substitute for presently used fluoride ion sources, such as either $[(CH_3)_2N]_3S^+F_2Si(CH_3)_3^-$, which is commonly referred to as tris(dimethylamino)sulfonium fluoride, or CsF. The reaction of $N(CH_3)_4F$ with CH_3CN results in the dimerization of CH_3CN and the formation of a 1:1 adduct of $N(CH_3)_4F$ with this dimer, *trans*-3-amino-2-butenenitrile. The crystal structure and vibrational spectra of this adduct are reported.

Introduction

The free fluoride anion is a very strong base and plays an important role in many organic and inorganic reactions.[1] Although alkali-metal fluorides are readily available, their low solubilities in most of the common solvents have rendered them of very limited practical use. Since the solubility of an ionic fluoride generally increases with increasing size of its countercation, the solubility limitations of the alkali-metal fluorides could be overcome by the use of a larger countercation. However, this large countercation must be chemically inert toward the fluoride anion, solvents, and other reagents, and its fluoride salt must be readily accessible to make it of practical use.

Although tetraalkylammonium fluorides would appear to be ideally suited for this purpose, they have not been developed into widely used reagents because of the great experimental difficulties encountered with their syntheses in anhydrous form. Thus, the tetraalkylammonium fluorides are generally available only as hydrates that, upon attempted water removal, undergo an E_2 elimination reaction with the formation of bifluoride and an olefin. The observation of the following reaction

$$2(n\text{-}C_4H_9)_4N^+F^- \rightarrow (n\text{-}C_4H_9)_4N^+HF_2^- + (n\text{-}C_4H_9)_3N + CH_3CH_2CH{=}CH_2$$

has prompted Sharma and Fry to conclude[2] that "it is very unlikely that pure, anhydrous tetraalkylammonium fluoride salts have ever, in fact, been produced in the case of ammonium ions susceptible to E_2 elimination, rather, reactions which have been reported to proceed in the presence of naked fluoride ion generated from such sources have probably actually been caused either by hydrated fluoride ion or by bifluoride ion". Although tetramethylammonium fluoride does not contain any carbon–carbon bond and, therefore, cannot undergo an E_2-type elimination reaction, Sharma and Fry's conclusion has also been applied to this compound, as evidenced by a recent statement[3a] that $N(CH_3)_4F$ "has never been obtained anhydrous and that removal of water results in decomposition". Similarly, Rieux and co-workers recently concluded[3b] that "the naked fluoride is still a myth and not yet a reality". In view of these reports, it is not surprising that $N(CH_3)_4F$ has not been exploited as a readily accessible, chemically inert, and highly soluble form of naked fluoride and that costly alternatives, such as tris(dimethylamino)sulfonium difluorotrimethylsilicate,[4] $[(CH_3)_2N]_3S^+F_2Si(CH_3)_3^-$, have been developed. Although the latter compound does not contain a free fluoride ion per se, the $F_2Si(CH_3)_3^-$ anion serves as an excellent fluoride ion donor toward stronger Lewis acids.

Recent work in our laboratory on the synthesis of the ClF_6^- anion[5] required a countercation that was larger and more soluble than cesium and at the same time resisted chemical attack by ClF_5. Since ClF_5 reacts violently with H_2O and is a much weaker Lewis acid than HF, incapable of displacing it from HF_2^-, we needed H_2O- and HF_2^--free $N(CH_3)_4F$.

Numerous reports[6-12] on the synthesis of tetramethylammonium fluoride can be found in the literature. They are based on two approaches. The first one dates back to 1888 and involves the neutralization of $N(CH_3)_4OH$ with HF in aqueous solution, followed by water removal in vacuo at temperatures up to 160 °C.[6] If the water is removed at various temperatures, intermediate $N(CH_3)_4F\cdot nH_2O$-type hydrates can be isolated with n ranging from 1 to 5.[13] The difficulty with this process is the removal of the last amounts of water from the $N(CH_3)_4F$, because at 160 °C the removal rate is still slow while the $N(CH_3)_4F$ already begins to undergo a very slow decomposition.[6] Thus, the products obtained by this method have been reported to contain significant amounts of impurities, attributed to either HF_2^-[9] or the monohydrate.[10] In a minor modification[8] of this method, the bulk of the water was removed from the aqueous $N(CH_3)_4F$ solution in vacuo on a rotating evaporator. The resulting syrupy oils were converted to an $N(CH_3)_4F\cdot CH_3OH$ solvate by repeated treatment

---

† Rocketdyne

‡ University of Southern California.

(1) Young, J. A. *Fluorine Chem. Rev.* 1967, *1*, 359.

(2) Sharma, R. K., Fry, J. L. *J. Org. Chem.* 1983, *48*, 2112.

(3) (a) Emsley, J. *Polyhedron* 1985, *4*, 489. (b) Rieux, C., Langlois, B., Gallo, R. *C. R. Acad. Sci., Ser. 2*, 1990, *310*, 25.

(4) (a) Middleton, W. J. U.S. Patent 3 940 402, Feb 1976. (b) Middleton, W. J. *Org. Synth.* 1985, *64*, 221.

(5) Christe, K. O., Wilson, W. W., Schrobilgen, G. J., Chirakal, R. *Inorg. Chem.*, in press.

(6) Lawson, A. T.; Collie, N. *J. Chem. Soc.* 1888, *53*, 624.

(7) Musker, W. K. *J. Org. Chem.* 1967, *32*, 3189.

(8) Klanberg, F., Muetterties, E. L. *Inorg. Chem.* 1968, *7*, 155.

(9) Tunder, R., Siegel, B. *J. Inorg. Nucl. Chem.* 1963, *25*, 1097.

(10) Harmon, K. M., Gennick, I., Madeira, S. L. *J. Phys. Chem.* 1974, *78*, 2585.

(11) Urban, G., Dötzer, R. German Patent 1 191 813, May 1965.

(12) Cunico, R. F., Han, Y. K. *J. Organomet. Chem.* 1978, *162*, 1.

(13) Gennick, I., Harmon, K. M.; Hartwig, J. *Inorg. Chem.* 1977, *16*, 2241.

0002-7863/90/1512-7619$02.50/0

with CH_3OH and drying in vacuo at 100 °C.

The second approach utilizes metathetical reactions,[9-12] such as

$$N(CH_3)_4Cl + KF \xrightarrow{CH_3OH} N(CH_3)_4F + KCl\downarrow$$

The resulting crude $N(CH_3)_4F$ was purified by recrystallization from isopropyl alcohol.[9] This synthetic method has frequently been used but, according to Klanberg and Muetterties,[8] the $N(CH_3)_4F$ prepared in this manner always contained at least 1–2% of chloride, while commercially available $N(CH_3)_4F$ had an even higher Cl^- content of 6.6%.

Another metathesis that has been described in a German patent[11] is based on the reaction of $N(CH_3)_4Cl$ with HF and $NaOCH_3$ in CH_3OH to give $N(CH_3)_4F{\cdot}2CH_3OH$. This solvate is then converted to $N(CH_3)_4F$ by vacuum pyrolysis at 150 °C. The reaction of $N(CH_3)_4Cl$ with HF and $NaOCH_3$ must be carried out in two separate steps. Reacting the $N(CH_3)_4Cl$ first with $NaOCH_3$ according to

$$N(CH_3)_4Cl + NaOCH_3 \xrightarrow{CH_3OH} N(CH_3)_4OCH_3 + NaCl\downarrow$$

$$N(CH_3)_4OCH_3 + HF + CH_3OH \xrightarrow{CH_3OH} N(CH_3)_4F{\cdot}2CH_3OH$$

results in a more efficient use of the starting materials than the reverse sequence

$$N(CH_3)_4Cl + 10HF \rightarrow N(CH_3)_4H_2F_3 + 7HF + HCl$$

$$N(CH_3)_4H_2F_3 + 2NaOCH_3 \xrightarrow{CH_3OH} N(CH_3)_4F{\cdot}2CH_3OH + 2NaF\downarrow$$

According to Klanberg and Muetterties[8] these $NaOCH_3$–HF-based processes suffer from the same drawback, i.e., Cl^- impurities, as the $N(CH_3)_4Cl$ + KF metathesis and the use of excess HF will generate HF_2^- impurities.

Although some of the above chemistry dates back for more than 100 years,[6] reliable analytical data, such as water analyses, detailed spectroscopic or structural data, and physical and chemical properties have not been reported for “anhydrous” $N(CH_3)_4F$. Therefore, it was also highly desirable to better characterize this important compound.

Experimental Section

Materials. The CH_3CN (Baker, Bio-analyzed, having a water content of 40 ppm) was treated with P_2O_5 and freshly distilled prior to use, thereby reducing its water content to <4 ppm. The $N(CH_3)_4OH$ (Baker, analyzed, 10% aqueous solution), HF (Baker, analyzed, 50% aqueous solution), CH_3OH (Baker, absolute, 0.003% H_2O), and $(CH_3)_2CHOH$ (Mallinckrodt, A.R., 0.03% H_2O) were used as received.

Apparatus. Volatile materials were handled either in a flamed-out Pyrex vacuum line equipped with Kontes Teflon valves or in the dry nitrogen atmosphere of a glovebox. Solids were manipulated exclusively in the drybox.

Raman spectra were recorded on either a Cary Model 83 or a Spex Model 1403 spectrophotometer by use of the 488-nm exciting line of an Ar ion or the 647.1-nm line of a Kr ion laser, respectively. Baked-out Pyrex melting point capillaries were used as sample holders. Infrared spectra were recorded as KBr disks on a Perkin-Elmer Model 283 spectrophotometer. For the exclusion of moisture, only KBr that had been fused and finely ground in the drybox was used. The KBr disks were pressed in a Wilks minipress inside the drybox, with the sample in a powdered KBr matrix being sandwiched between two prepressed layers of neat KBr, and the resulting sandwiches were left in the press for the recording of the spectra. The spectra obtained in this manner were identical with those obtained for pressed AgCl disks, indicating that no reaction between KBr and $N(CH_3)_4F$ had occurred during the pressing operation.

The ^{19}F and ^1H NMR spectra were measured at 84.6 and 90 MHz, respectively, on a Varian Model EM390 spectrometer, with 5-mm Teflon-FEP tubes (Wilmad Glass Co.) as sample containers and $CFCl_3$ and TMS, respectively, as internal standards, with negative shifts being upfield from the standards. A Perkin-Elmer differential scanning calorimeter, Model DSC-1B, was used to determine the thermal stability and to check for phase transitions. The samples were crimp sealed in aluminum pans, and a heating rate of 10 °C/min in N_2 was used. The instrument was calibrated with the known melting points of *n*-octane and indium. Water contents were measured by the Karl Fischer method[14] on a Photovolt Model Aquatest IV, with Teflon ampules as sample containers and plastic syringes for the sample injection.

Table I. Summary of Crystal Data and Refinement Results for the Tetramethylammonium Fluoride–3-Amino-2-butenenitrile Adduct

space group	$P2_1/C$ (monoclinic)
a (Å)	10.252 (3)
b (Å)	8.579 (2)
c (Å)	13.324 (3)
β (deg)	111.65 (2)
V (Å^3)	1089.2 (5)
molecules/unit cell	4
molecular weight	174.99
crystal dimensions (mm)	0.5 × 2.0 × 1.2
calculated density (g cm^{-3})	1.071
wavelength (Å) used for data collection	0.71069
$(\sin \theta)/\lambda$ limit (Å^{-1})	0.539
total number of reflections measured	1493
number of independent reflections	1492
number of reflections used in structural analysis $I > 3\sigma(I)$	1141
number of variable parameters	181
final agreement factors	$R(F) = 0.0387$ $R_w(F) = 0.0529$

Table II. Bond Distances in the Tetramethylammonium Fluoride–3-Amino-2-butenenitrile Adduct

C2···N1	1.486 (2)	C3′···C2′	1.489 (2)
C3···N1	1.485 (2)	C4′···C2′	1.357 (1)
C4···N1	1.491 (2)	C5′···C4′	1.408 (2)
C5···N1	1.503 (2)	N6′···C5′	1.150 (2)
C2′···N1′	1.337 (2)		

Table III. Bond Angles (deg) in the Tetramethylammonium Fluoride–3-Amino-2-butenenitrile Adduct

C3–N1–C2	110.4 (1)	C3′–C2′–N1′	115.9 (1)
C4–N1–C2	109.3 (1)	C4′–C2′–N1′	122.6 (1)
C4–N1–C3	111.5 (1)	C4′–C2′–C3′	121.5 (1)
C5–N1–C2	108.1 (1)	C5′–C4′–C2′	121.8 (1)
C5–N1–C3	109.1 (1)	N6′–C5′–C4′	179.6 (1)
C5–N1–C4	108.3 (1)		

X-ray diffraction patterns of powdered samples in sealed 0.5-mm quartz capillaries were obtained by using a General Electric Model XRD-6 diffractometer, Ni-filtered Cu Kα radiation, and a 114.6-mm-diameter Philips camera.

Crystal Structure of $N(CH_3)_4F$–*trans*-$NH_2C(CH_3)$═CHCN. Single crystals of $N(CH_3)_4F$–*trans*-$NH_2C(CH_3)$═CHCN were grown by allowing *n*-hexane vapors to diffuse slowly into a saturated solution of $N(CH_3)_4F$ in CH_3CN. A rocklike crystal was mounted in a quartz capillary in the glovebox. A Nicolet/Syntex $P2_1$ automated four-circle diffractometer, with Mo Kα radiation and a graphite crystal monochromator, was used for the intensity data collection. The unit cell parameters were determined by least-squares refinement of 15 centered reflections. Data were collected with the ω-scan technique for all reflections such that $4.0° < 2\theta < 45.0°$. Throughout the data collection, three reflections were monitored periodically and no decay was observed. Of 1493 reflections collected, 1141 reflections with $I > 3\sigma(I)$ were retained for the ensuing structure analysis.

The structure was solved by direct methods with the SHELXS86 system[15] of crystallographic programs. The positions of all atoms were revealed after direct method analysis of the data. Subsequent least-squares refinements of the atomic coordinates, including positions of the hydrogen atoms, and thermal parameters resulted in final agreement values of R = 3.87% and R_w = 5.29%. Details of the data collection parameters and other crystallographic information are given in Table I, and the final atomic coordinates are listed in Table A (supplementary material). Interatomic distances and angles are given in Tables II and III, respectively. Figures 1 and 2 show a packing diagram for the $N(CH_3)_4F$ adduct and the interactions of the fluorine atoms, respectively.

---

(14) Scholz, E. *Karl Fischer Titration, Methoden zur Wasserbestimmung*, Springer Verlag: Berlin, 1984.

(15) Sheldrick, G. M. *SHELX System of Crystallographic Programs*, University of Goettingen: West Germany, 1986.

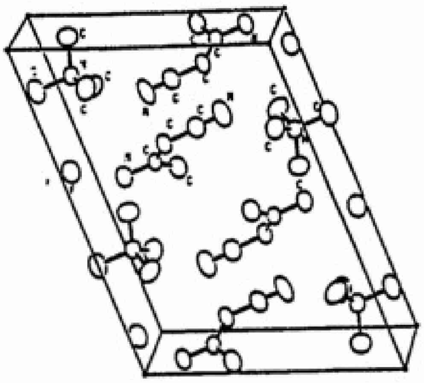

Figure 1. Packing diagram of $N(CH_3)_4F$-*trans*-$H_2NC(CH_3)CHCN$ viewed along the *b* axis.

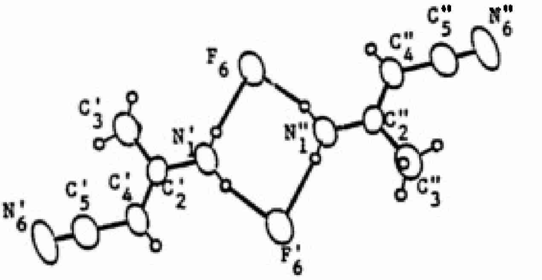

Figure 2 View of the molecular $N(CH_3)_4F$–$H_2NC(CH_3)CHCN$ unit showing the interactions of the fluorine atoms.

Synthesis of $N(CH_3)_4F$. The following generalized procedure was found to yield the purest samples of $N(CH_3)_4F$. Inside a glovebag purged by nitrogen or CO_2-free air, a measured amount of a 10% aqueous $N(CH_3)_4OH$ solution was placed into a polyethylene beaker. With a pH electrode as an indicator and a Teflon-coated magnetic stirring bar for mixing, the $N(CH_3)_4OH$ solution was titrated with 50% aqueous HF to the exact equivalence point. Plasticware was used exclusively for the handling of the HF solution. The last few percent of the required HF was added slowly with a more dilute HF solution to avoid overshooting the end point. The resulting $N(CH_3)_4F$ solution was transferred into a round-bottom Pyrex flask, and the water was pumped off with a rotary film evaporator while the temperature was slowly raised toward 150 °C. After most of the water had been removed at 150 °C, the solid white residue was finely ground in a porcelain mortar in the dry N_2 atmosphere of a glovebox and then further pumped on at 150 °C for several days until the weight became essentially constant, and the infrared absorption bands of $N(CH_3)_4F{\cdot}H_2O$[16] at 822 and 895 cm^{-1} showed an intensity comparable to or less than that of the weak $N(CH_3)_4^+$ band at 1203 cm^{-1} (see later text). The other main impurities present at this stage were small amounts of HF_2^- and, if glass equipment had been used, SiF_6^{2-}, which were readily monitored by their characteristic infrared absorptions[17,18] at 1256 and at 708 and 728 cm^{-1}, respectively. In the drybox, the crude $N(CH_3)_4F$ was recrystallized by dissolving it in dry isopropyl alcohol and pumping off enough of the solvent to precipitate most of the $N(CH_3)_4F$, in the form of its alcoholate, out of the solution. The $N(CH_3)_4HF_2$ and $[N(CH_3)_4]_2SiF_6$ impurities were enriched in the mother liquer, and the solvated isopropyl alcohol was removed from the recrystallized material in a dynamic vacuum at 80 °C. The yield of purified $N(CH_3)_4F$ was about 80%, and material with a water content ≤ 0.06 wt % and a trace of HF_2^- as the only detectable impurity was obtained in this manner. The quality of the product was checked for H_2O, isopropyl alcohol, HF_2^-, and SiF_6^{2-} contamination by Karl Fischer titration and infrared, Raman, and ^{19}F and ^1H NMR spectroscopy.

Thermal Decomposition of $N(CH_3)_4F$. Anhydrous $N(CH_3)_4F$ (7.08 mmol) was placed inside the glovebox into a flamed-out Pyrex vessel equipped with a Teflon valve. The vessel was connected to a Pyrex vacuum line and gradually heated in a dynamic vacuum to 230 °C. The volatile products were separated by passage through two cold traps kept at −126 and −196 °C. After 4 h, the pyrolysis was essentially complete. The Pyrex vessel contained 18 mg (0.06 mmol) of a white solid residue that was identified by its infrared spectrum as $[N(CH_3)_4]_2SiF_6$. The −126 °C trap contained $N(CH_3)_3$ (7.01 mmol), and the −196 °C trap contained CH_3F (7.03 mmol).

Results and Discussion

Synthesis of Anhydrous $N(CH_3)_4F$. Our synthesis of anhydrous $N(CH_3)_4F$ is based on the method of Lawson and Collie from 1888, but incorporates the following improvements: (i) the neutralization step

$$N(CH_3)_4OH + HF \xrightarrow{H_2O} N(CH_3)_4F + H_2O$$

is carried out in a CO_2-free atmosphere to avoid the formation of carbonate or bicarbonate impurities; (ii) a pH electrode is used as an indicator to titrate exactly to the equivalence point of aqueous $N(CH_3)_4F$; (iii) only plastic (polyethylene or Teflon) equipment is used for the handling of the HF solution to avoid SiF_6^{2-} formation; (iv) the water is removed in a dynamic vacuum with a rotary film evaporator; (v) the bath temperature is precisely controlled to 150 °C for the final water removal that is periodically monitored by the weight loss of the sample and by infrared spectroscopy; (vi) the crude product is azeotroped with isopropyl alcohol for additional water removal; and (vii) the azeotroped product is purified by recrystallization from dry isopropyl alcohol.

This process is capable of producing $N(CH_3)_4F$ in very high yield. The only significant loss of material is that retained in the mother liquor during the final recrystallization step. Water contents, based on Karl Fischer titrations of methanol solutions, as low as 0.06 wt % were obtained, with no detectable SiF_6^{2-} and only a trace of HF_2^- as an impurity. Since the process does not involve any chlorine-containing reagents, chloride contamination is precluded. The process is also readily scalable and was carried out on a 100-g scale without any complications.

Recrystallizations of the crude $N(CH_3)_4F$ from either CH_3CN or CH_3OH were also studied, but are inferior to that using isopropyl alcohol. Methanol does not form an azeotrope with H_2O, and its solvate with $N(CH_3)_4F$ is considerably more stable than that of isopropyl alcohol, thus rendering the CH_3OH removal more difficult. Acetonitrile reacts with the free fluoride ion (see later text), resulting in significant material losses and the formation of $N(CH_3)_4HF_2$ and $N(CH_3)_4F$–$NH_2C(CH_3)$=$CHCN$ as potential contaminants.

Properties of $N(CH_3)_4F$. The compound is a white, crystallinic, hygroscopic solid that starts to decompose slowly in a dynamic vacuum at about 170 °C. The previously postulated[6] decomposition path

$$N(CH_3)_4F \rightarrow N(CH_3)_3 + CH_3F$$

was confirmed by a quantitative vacuum pyrolysis at 210–230 °C. The only byproduct obtained in the pyrolysis was a trace of $[N(CH_3)_4]_2SiF_6$ that had been formed by handling of the material in glass. The $N(CH_3)_4F$ is highly soluble in water and alcohols with which it tends to form solvates, in partially chlorinated hydrocarbons with which it undergoes a ready chlorine–fluorine exchange,[19] and in CH_3CN from which it readily abstracts a proton resulting in the formation of CH_2CN^-, $NH_2C(CH_3)$=$CHCN$, and HF_2^-.[20] It is also soluble in formamide; however, the ^{19}F NMR signal in this solvent is very broad (about 200 Hz at 25 °C), indicating strong interaction with the solvent. Furthermore, $N(CH_3)_4F$ dissolves exothermically in acetone, exhibiting originally a signal at about −103.6 ppm that rapidly decays giving rise to a new signal at about −103.0 ppm. It dissolves also in nitromethane with a faint yellow color showing a ^{19}F signal at −150 ppm. It thus appears that in most solvents in which $N(CH_3)_4F$ is soluble, strong interactions with the solvent occur. The most inert solvent found to date is CHF_3 (bp −84.4 °C, mp −160 °C). At −80 °C, CHF_3 dissolves 4.4 wt % of $N(CH_3)_4F$ and the only ^{19}F signal observed in addition to the solvent peak is a singlet with a line width of about 7 Hz at −107 ppm for the fluoride ion. There was no evidence for hydrogen abstraction and HF_2^- for-

---

[16] Harmon, K. M.; Gennick, I. *Inorg. Chem.* 1975, *14*, 1840.

[17] Wilson, W. W.; Christe, K. O.; Feng, J.; Bau, R. *Can. J. Chem.* 1989, 67, 1898.

[18] Siebert, H. *Anwendungen der Schwingungsspektroskopie in der Anorganischen Chemie*, Springer Verlag: Berlin, 1966.

[19] Christe, K. O.; Wilson, W. W. *J. Fluorine Chem.* 1990, *46*, 339.

[20] Christe, K. O.; Wilson, W. W. *J. Fluorine Chem.* 1990, *47*, 117.

Table IV. ^{19}F NMR Shifts (ppm Upfield from $CFCl_3$) of Tetramethylammonium Fluoride in Various Solvents

$(CH_3)_2SO$	−73	CH_3COCH_3	−103	$(CH_3)_2CHOH$	−122
CH_3CN	−74	CHF_3	−107	C_2H_5OH	−137
H_2NCHO	−96	$CHCl_3$	−113	CH_3OH	−148
CH_2Cl_2	−97	H_2O	−119	CH_3NO_2	−150

mation under these conditions. When the CHF_3 solvent is pumped off from the $N(CH_3)_4F$ at −78 °C, a CHF_3 adduct of approximately a 1:1 composition was obtained that dissociates at a higher temperature reversibly to $N(CH_3)_4F$ and CHF_3. Low-temperature Raman spectra of this adduct showed only minor frequency shifts compared to the starting materials, indicating weak interaction. In some other solvents such as hexane, dimethoxyethane, ethyl acetate, propylene carbonate, dimethylformamide, benzene, 1,2-difluorobenzene, tetrahydrofuran, dioxane, trichlorofluoromethane, sulfuryl chloride fluoride, sulfolane, or carbon disulfide, however, little or no solubility of $N(CH_3)_4F$ was observed by ^{19}F NMR spectroscopy. Whereas the proton resonance of the $N(CH_3)_4^+$ cation exhibits the expected chemical shift and coupling constant ($\delta = 3.1$, $J_{^1H^{14}N} = 0.6$ Hz),[20] the observed ^{19}F NMR shifts of the fluoride anion are highly solvent dependent,[20] as can be seen in Table IV, and strongly deviate from those previously reported.[21] The trend in chemical shifts for $^{19}F^-$ in different solvents relative to those of $^{35}Cl^-$ ions in the same solvents is similar to that observed for ^{129}Xe relative to Cl^-. Therefore, this solvent dependency cannot be attributed to varying degrees of hydrogen bonding between F^- and protons of the solvents.[22]

Chemically, the free fluoride anion in $N(CH_3)_4F$ acts, as expected, as a very strong Lewis base and readily complexes with suitable Lewis acids, such as BF_3,[23] PF_5,[23] SbF_5,[24] HF,[17] SiF_4, SF_4,[9] etc., forming the corresponding complex fluoro anions. In the absence of good fluoride acceptor molecules, it can abstract even relatively firmly bound protons from compounds such as CH_3CN.[19] The $N(CH_3)_4^+$ cation is coordinatively saturated and, due to the relatively high strength of the carbon–nitrogen bond, possesses a high activation energy toward chemical reactions. Compared to the tris(dimethylamino)sulfonium cation, TAS^+,[4] the $N(CH_3)_4^+$ cation is chemically much more inert as shown, for example, by its ability to form a stable ClF_4^- salt.[25] On the other hand, TAS^+ salts are more soluble and are also thermally more stable. This was shown by complexing $N(CH_3)_4F$ with $SiF(CH_3)_3$.

$$N(CH_3)_4F + SiF(CH_3)_3 \rightarrow N(CH_3)_4^+SiF_2(CH_3)_3^-$$

The resulting $N(CH_3)_4^+SiF_2(CH_3)_3^-$ salt was found to be of only marginal stability at room temperature, whereas $TAS^+SiF_2(CH_3)_3^-$ is stable up to its melting point of 98–101 °C.[4] Thus, the main advantages of $N(CH_3)_4^+$ over $[(CH_3)_2N]_3S^+$ are its lower cost and increased chemical inertness.

Crystal Structure of Tetramethylammonium Fluoride. Although the crystal structures of $N(CH_3)_4Cl$, $N(CH_3)_4Br$, and $N(CH_3)_4I$ are well-known[26-29] and exhibit interesting polymorphism, no crystal data were previously available for $N(CH_3)_4F$. Our attempts failed to grow single crystals of pure $N(CH_3)_4F$ that were suitable for an X-ray diffraction study. With CH_3CN, hydrogen abstraction occurs[19] resulting in the formation of CH_2CN^-

$$2F^- + CH_3CN \rightarrow HF_2^- + CH_2CN^-$$

Table V. X-ray Powder Data[a] for $N(CH_3)_4F$

d(obsd), Å	d(calcd), Å	intens	h	k	l
5.35	5.356	vs	1	0	0
4.57	4.577	s	1	0	1
4.40	4.406	ms	0	0	2
3.398	3.403	mw	1	0	2
3.092	3.092	m	1	1	0
2.677	2.678	m	2	0	0
2.565	2.562	ms	2	0	1
2.530	2.531	ms	1	1	2
2.290	2.289	mw	2	0	2
2.202	2.203	w	0	0	4
1.979	1.979	m	2	0	3
1.838	1.839	mw	2	1	2
1.794	1.794	w	1	1	4
1.751	1.750	w	3	0	1
1.667	1.667	mw	2	1	3

[a] Hexagonal; $a = 6.185$ Å, $c = 8.812$ Å, Cu Kα radiation, Ni filter.

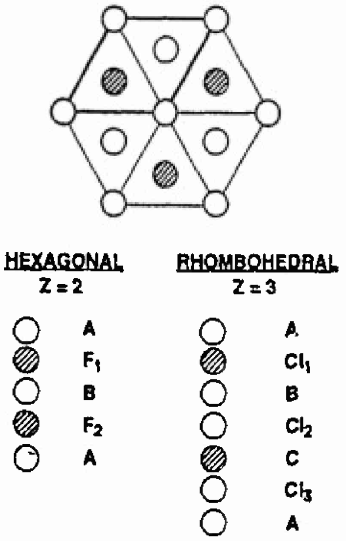

Figure 3. Packing arrangements for the hexagonal anion and cation layers in hexagonal $N(CH_3)_4F$ and rhombohedral $N(CH_3)_4Cl$, viewed along the c axis. The actual unit cell is marked by a heavier line.

followed by its reaction with CH_3CN to give *trans*-3-amino-2-butenenitrile[30]

which forms a 1:1 adduct with $N(CH_3)_4F$ (see later text). Thus, all the single crystals obtained during this study from CH_3CN solutions were either the tetramethylammonium bifluoride[17] or the 1:1 adduct of $N(CH_3)_4F$ with *trans*-3-amino-2-butenenitrile (see later text). In chlorinated solvents, rapid halogen exchange was observed,[20] while from alcoholic solutions only solvates of $N(CH_3)_4F$ were obtained. Therefore, our structure determination of $N(CH_3)_4F$ was limited to powder data.

The observed powder pattern is given in Table V. It can be indexed for a hexagonal unit cell with $a = 6.185$, $c = 8.812$ Å, $Z = 2$, and a calculated density of 1.058 g cm^{-3}. The hkl indices show no restrictions indicating a primitive lattice, and the presence of two molecules per unit cell precludes the possibility of a rhombohedral unit cell. Since the observed c/a value of 1.42 strongly deviates from 1.63, a zincite-type structure is highly unlikely[29,31] and $N(CH_3)_4F$ most likely possesses an *anti*-NiAs-type structure. In the latter, the $N(CH_3)_4^+$ cation would be surrounded by six fluoride anions located at the corners of a trigonal prism, while the fluoride anion would be surrounded by six $N(CH_3)_4^+$

---

(21) Hudlicky, M. *J. Fluorine Chem.* 1985, *28*, 461.

(22) Carmona, C.; Eaton, G.; Symons, M. C. R. *J. Chem. Soc., Chem Commun.* 1987, 873.

(23) Köksal, F.; Celik, F.; Cakır, O. *Radiat Phys. Chem.* 1989, *33*, 135 and references cited therein.

(24) Heyns, A. M.; De Beer, W. H. *Spectrochim. Acta, Part A* 1983, *39A*, 601.

(25) Wilson, W. W.; Christe, K. O. *Inorg Chem.* 1989, *28*, 4172.

(26) Cheban, Yu. M.; Dvorkin, A. A.; Rotaru, V. K.; Malinovskii, T. I. *Sov. Phys.-Crystallogr.* 1987, *32*, 604.

(27) Pistorius, C. W. F. T.; Gibson, A. A. V. *J. Solid State Chem* 1973, *8*, 126.

(28) Dufourcq, J.; Haget-Bouillaud, Y.; Chanh, N. B.; Lamanceau, B. *Acta Crystallogr., Sect. B* 1972, B28, 1305.

(29) Wyckoff, R. W. G. *Crystal Structures*, 2nd ed.; John Wiley & Sons: New York, 1962; Vol. 1.

(30) Krüger, C. *J. Organomet Chem* 1967, *9*, 125.

(31) Krebs, H. *Grundzüge der Anorganischen Kristallchemie*, Ferdinand Enke Verlag: Stuttgart, 1968; p 122.

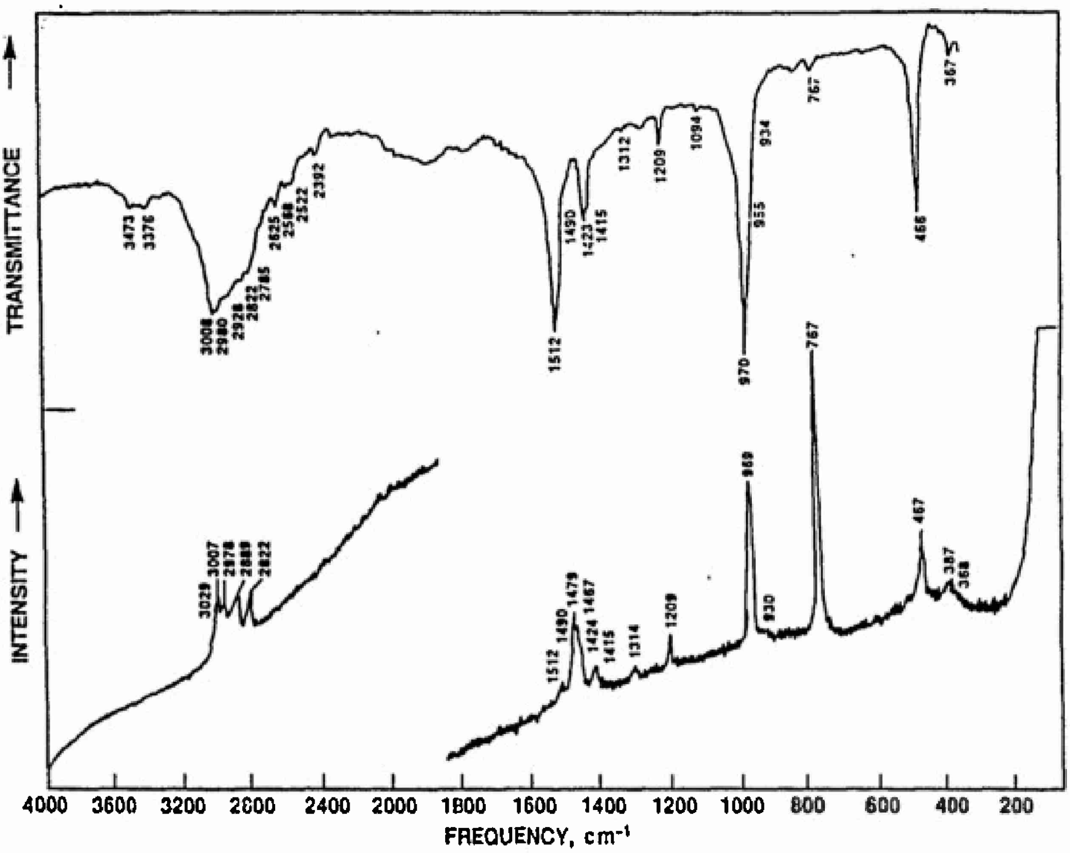

Figure 4. Infrared and Raman spectra of solid $N(CH_3)_4F$.

cations and two other fluoride anions.[29,31]

It is interesting to compare the structure of $N(CH_3)_4F$ with that of $N(CH_3)_4Cl$. The latter exhibits five phases: two low-temperature phases and a tetragonal room-temperature phase that is irreversibly transformed at 140 °C to a room-temperature stable, rhombohedral phase, which in turn reversibly changes at 263 °C to a face-centered cubic high-temperature phase.[27] The tetragonal room-temperature phase is a hydrated phase that exists only in the presence of a small amount of water.[28]

The main difference between the rhombohedral $N(CH_3)_4Cl$ and the hexagonal $N(CH_3)_4F$ phases consists of the stacking arrangements of the hexagonal anion and cation layers. In $N(CH_3)_4F$, the cations are arranged in a hexagonal closest packing with $Z = 2$ and alternating AB layers, while in rhombohedral $N(CH_3)_4Cl$ they are stacked in a cubic closest packing with $Z = 3$ and alternating ABC layers[31] (see Figure 3). In $N(CH_3)_4F$, the two fluoride anions are located above each other within the unit cell, while in $N(CH_3)_4Cl$ the three chloride anions occupy all three possible positions. This difference can be explained by the larger radius and space requirement of Cl^- versus F^-.

No evidence was found by DSC measurements between 30 and 330 °C for a phase transition from the hexagonal to a higher temperature phase. The only observed effect was the onset of endothermic decomposition at about 210 °C.

Vibrational Spectra of $N(CH_3)_4F$. The infrared and Raman spectra of solid $N(CH_3)_4F$ are shown in Figure 4. The observed frequencies and their assignments[17,32-35] are summarized in Tables VI and G (supplementary material).

The previous literature data on the vibrational spectra of $N(CH_3)_4F$ had been limited to incomplete infrared spectra of Nujol and Fluorolube mulls in the NaCl region.[10,16] Whereas the antisymmetric NC_4 stretching and the CH_3 deformation modes had been properly assigned,[10] the CH_3 rocking mode, $\nu_{17}(F_2)$, had been incorrectly attributed to an HF_2^- impurity band at 1263 cm⁻¹.

Table VI. Vibrational Spectra of Solid $N(CH_3)_4F$ and Their Assignment

obsd freq, cm⁻¹ (rel intens)		
IR	Raman	assgnt in pt gp T_d
3473 w, br		$\nu_{CH_3} + \nu_{19}$
3376 w, br		$\nu_{CH_3} + \nu_8$
3030 sh	3029 sh	ν_{CH_3} and binary bands
3008	3007 (2)	
2980	2978 (1.3)	
2928 s, br		
	2889 (1.9)	
2822	2822 (1.4)	
2785		
2625 w		$\nu_7 + \nu_{16}$, $2\nu_{17}$
2568 w		$\nu_3 + \nu_8 + \nu_{16}$
2522 w		$\nu_7 + \nu_{17}$
2392 w		$\nu_{16} + \nu_{18}$
1880 w, vbr		$\nu_8 + \nu_{15}$
1770 w, br		$\nu_{17} + \nu_{19}$
1512 s	1512 (0.4)	ν_{15}
1490 sh	1490 sh	
	1479 (2.9)	ν_6
	1467 sh	ν_2
1423 m	1424 (0.7)	ν_{16}
1415 sh	1415 sh	
1312 vvw	1314 (0.4)	ν_{17}
1209 w	1209 (1.3)	ν_7
1094 vw		3 × 367 or ν_{11}
970 vs	969 (5.8)	ν_{18}
955 sh		
934 sh	930 (0.2)	$2\nu_{19}$
767 vw	767 (10)	ν_3
466 ms	467 (2.4)	ν_{19}
	387 (0.4)	ν_8
367 w	368 (0.3)	ν_8 or ν_{12}

As shown by our study, this mode occurs at 1312 cm⁻¹, in excellent agreement with the values of 1293, 1297, and 1299 cm⁻¹ observed for the corresponding iodide, bromide, and chloride salts.[33]

Furthermore, the previous predictions made from these partial IR data, that $N(CH_3)_4F$ should be tetragonal,[10] were ill founded,

---

(32) Berg, R. W. *Spectrochim. Acta, Part A* 1978, *34A*, 655.
(33) Bottger, G. L., Geddes, A. L. *Spectrochim. Acta* 1965, *21*, 1708.
(34) Kabisch, G., Klose, M. *J. Raman Spectrosc.* 1978, *7*, 312.
(35) Kabisch, G. *J. Raman Spectrosc.* 1980, *9*, 279.

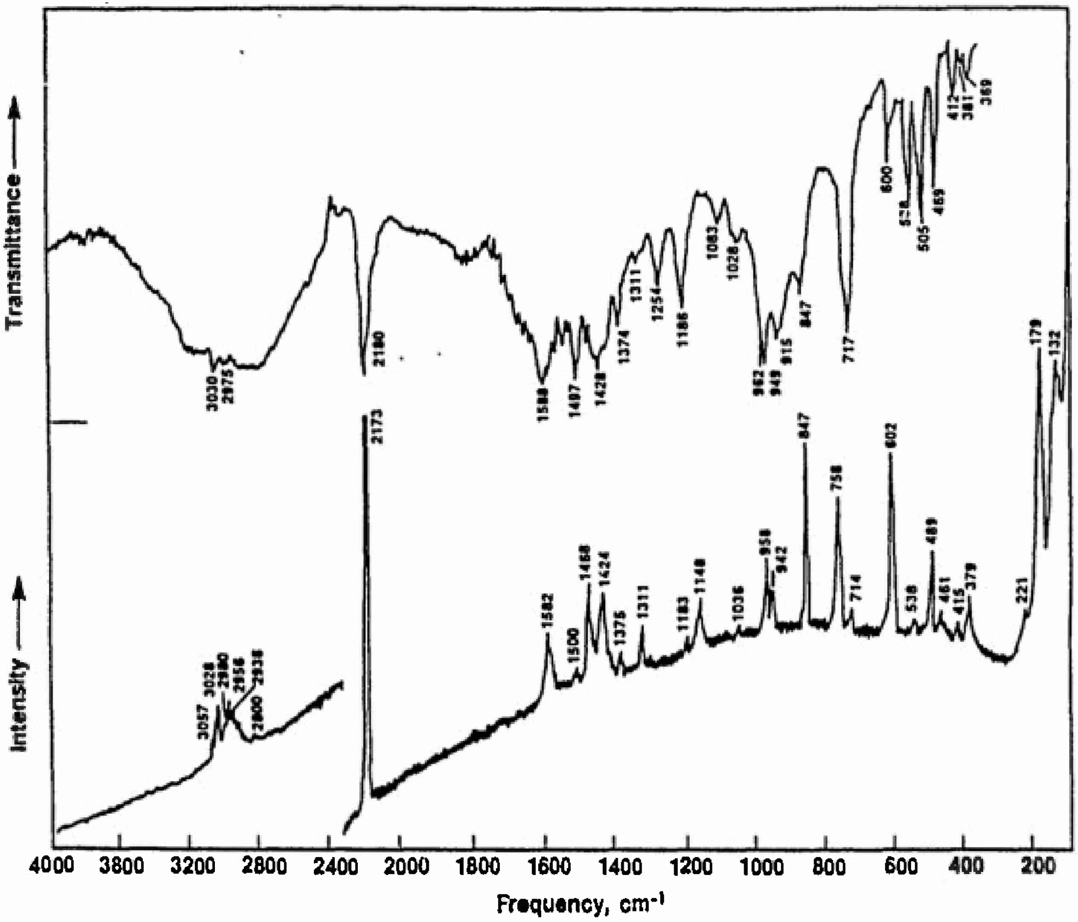

Figure 5. Infrared and Raman spectra of solid $N(CH_3)_4F-H_2NC(CH_3)CHCN$.

as demonstrated by the above X-ray diffraction data showing the compound to be hexagonal.

The assignments for $N(CH_3)_4F$ can be derived from those of the free $N(CH_3)_4^+$ cation. As a free ion, $N(CH_3)_4^+$ belongs to the point group T_d and has 19 fundamental vibrations that are classified as $3A_1 + A_2 + 4E + 4F_1 + 7F_2$. Of these, only the F_2 modes are infrared and the A_1, E, and F_2 modes Raman active.[32] In the solid state, the number of fundamentals can increase and the selection rules be violated due to effects, such as distortion of the $N(CH_3)_4^+$ tetrahedron, site symmetries lower than T_d, and factor group splittings. Thus, the deviations of the observed spectra from the T_d selection rules, coupled with crystallographic information, can be used to judge the degree of deformation of the $N(CH_3)_4^+$ from tetrahedral symmetry.[35] On the basis of a comparison of the Raman spectrum of the free $N(CH_3)_4^+$ ion with those of cubic $[N(CH_3)_4]_2SnCl_6$, hexagonal $N(CH_3)_4CdCl_3$, monoclinic $N(CH_3)_4HgCl_3$, and tetragonal $N(CH_3)_4ClO_4$, $N(CH_3)_4NO_3$, $N(CH_3)_4Cl$, $N(CH_3)_4Br$, and $N(CH_3)_4I$, Kabisch has derived empirical rules for estimating, from the vibrational spectra, the degree of distortion of the $N(CH_3)_4^+$ cation.[35]

A comparison of our $N(CH_3)_4F$ spectra (see Figure 4 and Table VI) with the data[35] of Kabisch shows that the spectrum of the $N(CH_3)_4^+$ cation in solid $N(CH_3)_4F$ is very similar to those of the free $N(CH_3)_4^+$ cation and of the very weakly distorted $N(CH_3)_4^+$ cation in $[N(CH_3)_4]_2SnCl_6$. Therefore, it can be concluded that in $N(CH_3)_4F$ the distortion of the $N(CH_3)_4^+$ cation from tetrahedral symmetry must also be minimal. This finding is not unexpected since Kabisch had also shown that within the $N(CH_3)_4I$, $N(CH_3)_4Br$, and $N(CH_3)_4Cl$ series the cation distortion decreases with decreasing anion size.[35] Therefore, repulsion effects are more important than electrostatic effects, and fluoride should be the least distorting.

On the basis of the broadness of the CH_3 stretching bands in its infrared spectrum, CH--F hydrogen bonding has previously been postulated for $N(CH_3)_4F$.[10] This postulate requires further substantiation since the CH_3 deformation modes show no evidence for similar broadenings and the widths of the CH_3 stretching infrared bands can be readily explained by the Fermi resonance bands also observed in the Raman spectra of the free $N(CH_3)_4^+$ ion.[32,34,35]

Since infrared spectroscopy is a very useful technique to analyze $N(CH_3)_4F$ for impurities, we have scrutinized all the weak infrared features. In our opinion, essentially all of the weak bands shown in Figure 4 belong to $N(CH_3)_4F$. The most common impurities in $N(CH_3)_4F$ are HF_2^-, SiF_6^{2-}, $F^- \cdot nH_2O$, and different solvates. All of these are readily detected by their characteristic absorptions, most of which are given in the Experimental Section.

$N(CH_3)_4F$-*trans*-$H_2NC(CH_3)$=CHCN Adduct. As already mentioned, the fluoride anion can abstract a proton from CH_3CN, and the resulting CH_2CN^- anion can react with a second CH_3CN molecule and a proton to give the rearranged acetonitrile dimer, 3-amino-2-butenenitrile. During attempts to grow single crystals of $N(CH_3)_4F$ by allowing *n*-hexane to slowly diffuse into a saturated CH_3CN solution, large single crystals were obtained that were characterized by X-ray diffraction and vibrational spectroscopy as a 1:1 adduct between $N(CH_3)_4F$ and *trans*-3-amino-2-butenenitrile (1).

The crystal structure of 1 is shown in Figures 1 and 2, and the pertinent crystallographic data are summarized in Tables I–III and A–F. The monoclinic unit cell of 1 consists of layers of $N(CH_3)_4F$ that are separated by four molecules of the aminobutenenitrile. To maximize the packing density, the four aminobutenenitrile molecules are arranged in four different orientations, with the linear C—C≡N groups pointing alternatingly to the left and to the right and the

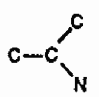

groups forward and backward (see Figure 1). The F^- anion forms two weak bridges to two hydrogen atoms from two different $-NH_2$ groups at 1.806 and 1.856 Å, respectively, with the remaining distances to other hydrogens being considerably longer than the sum of the van der Waals radii. As a result, the tetramethylammonium cation shows little distortion and is essentially tetrahedral.

The bond distances and angles found for the $H_2N{-}C(CH_3){=}CH{-}CN$ part of the adduct agree well with those predicted from the known structures of the similar molecules, CH_3CN, $NC{-}CN$, $CH_2{=}CH_2$, CH_3CHO, H_2NCHO, and CH_3COCN.[36]

The infrared and Raman spectra of the $N(CH_3)_4F{-}H_2NC(CH_3)CHCN$ adduct are given in Figure 5. The sizes of the molecules involved, the low crystal symmetry, and the large unit cell make detailed assignments difficult. However, the following vibrations can be readily assigned: $\nu(C{\equiv}N)$, 2173; $\nu(C{=}C)$, 1582; $\nu_{as}(NC_4)$, 958, 942; $\nu_s(NC_4)$, 758; $\delta_{as}(NC_4)$, 469 cm^{-1}. The intense and narrow $C{\equiv}N$ stretching vibration at 2173–2180 cm^{-1} is very useful for checking for the presence of the nitrile adduct in $N(CH_3)_4F$ that has been handled in CH_3CN.

Conclusion

Contrary to the general belief that $N(CH_3)_4F$ cannot be obtained anhydrous and that removal of water results in decomposition,[3] it was shown in this study that $N(CH_3)_4F$ with a water content of ≤ 0.06 wt % can be prepared with relative ease. This synthesis of anhydrous $N(CH_3)_4F$ provides a relatively cheap source of highly soluble fluoride containing a chemically very inert countercation. Thus, anhydrous $N(CH_3)_4F$ might become an attractive substitute for the more expensive and less inert fluoride ion source, (TAS)F, $[(CH_3)_2N]_3S^+F_2Si(CH_3)_3^-$. A characterization of anhydrous $N(CH_3)_4F$ also revealed that the properties of the "naked" fluoride ion in solution are poorly understood and that some of the properties previously attributed to the fluoride ion are due to other anions, such as HF_2^-. Furthermore, it was shown that certain solvents, such as CH_3CN or partially chlorinated hydrocarbons, which in the past have been preferred for fluoride ion reactions,[37,38] undergo chemical reactions with F^-. Finally, a novel 1:1 adduct of $N(CH_3)_4F$ with a dimer of CH_3CN was isolated from CH_3CN solution, and its crystal structure was determined.

Acknowledgment. We thank Dr. Carl Schack for helpful discussions and the preparation of a sample of $SiF(CH_3)_3$. The work at Rocketdyne was financially supported by the Air Force Astronautics Laboratory and the Army Research Office.

Supplementary Material Available: Tables A–G listing final atomic coordinates, hydrogen atom positions, N–H and C–H bond distances, hydrogen bond distances, final temperature factors, and mode descriptions for the $N(CH_3)_4^+$ cation, respectively (6 pages); observed and calculated structure factors (5 pages). Ordering information is given on any current masthead page.

---

[36] Harmony, M. D.; Laurie, V. W.; Kuczkowski, R. L.; Schwendeman, R. H.; Ramsay, D. A.; Lovas, F. J.; Lafferty, W. J.; Maki, A. G. *J. Phys. Chem. Ref. Data* **1979**, *8*, 619.

[37] Miller, W. T.; Fried, J. H.; Goldwhite, H. *J. Am. Chem. Soc.* **1960**, *82*, 3091.

[38] Fawcett, F. S.; Tullock, C. W.; Coffman, D. D. *J. Am. Chem. Soc.* **1962**, *84*, 4275.

Journal of Fluorine Chemistry, *47* (1990) 117–120

Received: April 28, 1989; accepted: June 28, 1989

REACTION OF THE FLUORIDE ANION WITH ACETONITRILE, CHLOROFORM AND METHYLENE CHLORIDE

KARL O. CHRISTE* AND WILLIAM W. WILSON

Rocketdyne, a Division of Rockwell International Corporation, Canoga Park, California 91303 (USA)

SUMMARY

^{19}F and ^{1}H NMR spectra of the F^- anion in CH_3CN and CD_3CN solutions show that the F^- anion can abstract a proton from CH_3CN resulting in the slow formation of the bifluoride and acetonitrile anions. With chloroform or methylene chloride the F^- anion undergoes halogen exchange reactions at room temperature. These reactions demonstrate the exceptional reactivity of the free fluoride anion when present as a highly soluble salt.

INTRODUCTION

During recent work in our laboratory on the synthesis and characterization of anhydrous, HF_2^- free tetramethylammonium fluoride, we have used a combination of Karl Fischer titration and infrared and NMR spectroscopy to check for water and HF_2^- impurities. It was found that samples of $[N(CH_3)_4]F$, which based on their infrared spectra were free of H_2O and HF_2^-, showed significant amounts of HF_2^- in the NMR spectra of their CH_3CN solutions. The fact that the concentration of HF_2^- increased with increasing time, suggested that the HF_2^- might be generated by attack on the solvent by F^-. Since CH_3CN is frequently used as a solvent in fluorine chemistry, it is important to know whether CH_3CN undergoes a reaction with the F^- anion. Furthermore, it was interesting to examine whether polar, chlorinated hydrocarbons such as $CHCl_3$ or CH_2Cl_2 could be used as inert solvents for $[N(CH_3)_4]F$.

EXPERIMENTAL

The synthesis of anhydrous, HF_2^- free $[N(CH_3)_4]F$ will be described elsewhere [1]. The CH_3CN (Baker, Bio-analyzed, having an H_2O content of 40 ppm) was treated with P_2O_5

0022-1139/90/$3.50

and freshly distilled in a flamed out Pyrex vacuum system prior to use, thereby reducing its water content to ≤ 4 ppm. The CD_3CN (99.96%D, Stohler) was used as received and showed only a trace of CHD_2CN as the only impurity detectable by NMR spectroscopy. The CH_2Cl_2 and the $CHCl_3$ (J.T. Baker, Analyzed) were dried by storage over Linde 4A molecular sieves. The $CHCl_3$ contained 1% of CH_3CH_2OH as a stabilizer and had a water content of 0.006% before treatment with the molecular sieves. The NMR spectra were recorded on a Varian EM 390 spectrometer operating at 90 MHz for ^1H and 84.6 MHz for ^{19}F. Tetramethylsilane or $CFCl_3$ was used as an external standard with negative shifts being upfield from the standard. Teflon-FEP sample tubes (Wilmad Glass Co.) were used for the CH_3CN reactions and glass tubes for the experiments involving $CHCl_3$ or CH_2Cl_2.

RESULTS AND DISCUSSION

Samples of $[N(CH_3)_4]F$, which based on their infrared spectra and Karl Fischer titrations were HF_2^- free and had less than 0.06 weight percent water, were dissolved in either CH_3CN or CD_3CN. Their saturated solutions in Teflon-FEP tubes were periodically monitored by ^{19}F and ^1H NMR spectroscopy for their HF_2^- content.

The ^{19}F NMR spectra of $[N(CH_3)_4]F$ in CH_3CN showed two signals: one intense singlet at ϕ -74 to -79 for F^- [2], and a doublet at ϕ -145 to -148 with $J_{^1H^{19}F}$ = 121 Hz for HF_2^- [2, 3]. In fresh solutions, the HF_2^- concentrations were very low but increased in the course of several hours to the 5 to 10 mol% range and after standing at room temperature for several days reached a level of 30 mol%. In addition to an increase in the intensity of the HF_2^- signal, the originally colorless CH_3CN solutions also developed a yellow color on standing.

The ^1H NMR spectra of the CH_3CN solutions of $[N(CH_3)_4]F$ showed, besides the CH_3CN (δ = 1.96) and $[N(CH_3)_4]^+$ (δ = 3.1, $J_{^1H^{14}N}$ = 0.6 Hz [4]) signals, a triplet at δ = 16.3 with $J_{^1H^{19}F}$ = 121 Hz characteristic for HF_2^- [3] and a broad singlet at δ = 9.1 characteristic for the CH_2CN^- anion [5]. The relative intensities of the HF_2^- and CH_2CN^- signals increased together with increasing time.

Based on the above evidence, it must be concluded that at room temperature the F^- anion was slowly reacting with CH_3CN according to:

$$2F^- + CH_3CN \rightarrow HF_2^- + CH_2CN^-$$

Although the NMR spectra showed no evidence for the presence of free HF, the above reaction almost certainly involves at least two steps. The first one is the slow abstraction of a proton from CH_3CN by the strong base F^-

$F^- + CH_3CN \rightarrow HF + CH_2CN^-$

followed by the rapid reaction of HF with the large excess of F^- present.

$HF + F^- \rightarrow HF_2^-$

Conclusive proof for the generation of the HF_2^- anion from the acetonitrile solvent was obtained by substitution of the CH_3CN by CD_3CN. If the bifluoride anion is, indeed, generated from the reaction of F^- with CH_3CN, replacement of CH_3CN by CD_3CN in the reaction

$2F^- + CD_3CN \rightarrow DF_2^- + CD_2CN^-$

should result in the following spectroscopic changes: the ^{19}F NMR spectrum should show a triplet at Ø -147 with $J_{^2D^{19}F}$ = 18 Hz for DF_2^- [6] instead of the HF_2^- doublet, and the ^1H spectrum should show no new resonances since only deuterated species are being formed. These predictions were experimentally confirmed (the only new signal was a triplet at Ø -147 with a coupling constant of 17.6 Hz), and no evidence for the formation of either HF_2^- or CH_2CN^- was detected in the CD_3CN experiment. If some bifluoride had been present in the $[N(CH_3)_4]F$ starting material, it could have only been in the form of HF_2^- and, therefore, both an HF_2^- and a DF_2^- signal should have been observed since HF_2^- and DF_2^- do not undergo a fast exchange in CH_3CN [6].

The possibility of using either methylene chloride or chloroform as a solvent for $[N(CH_3)_4]F$ was also examined. It was found that at room temperature both solvents undergo a halogen exchange reaction with $[N(CH_3)_4]F$. Whereas the reaction with CH_2Cl_2 is relatively slow and CH_2ClF is the main reaction product, the reaction with $CHCl_3$ is quite fast and all three possible exchange products, $CHCl_2F$, $CHClF_2$, and CHF_3 in a mol ratio of about 2:3:1 were observed by NMR spectroscopy. Thus, the ^{19}F and ^1H NMR spectra of a saturated CH_2Cl_2 solution containing some undissolved $[N(CH_3)_4]F$ exhibited, in addition to intense signals due to the free fluoride anion (singlet at Ø -97.0 with a line width of 3 Hz) and the $[N(CH_3)_4]^+$ cation (singlet at δ 3.44), a triplet at Ø -169.4 and a doublet at δ 5.93 with J_{HF} = 49 Hz which are characteristic for CH_2ClF [7]. For a saturated $CHCl_3$ solution containing some undissolved $[N(CH_3)_4]F$, the F^- anion signal at Ø -120.3 was weak and disappeared quickly giving rise to doublets at Ø -78.3 with J_{HF} = 79.1 Hz, Ø -80.8 with J_{HF} = 54.3 Hz, and Ø -84.3 with J_{HF} = 75.0 Hz, which are characteristic for CHF_3 [8], $CHCl_2F$ [9, 10], and $CHClF_2$, respectively. Although halogen exchange reactions involving chlorinated hydrocarbons and ionic fluorides are well known [11, 12], the mild conditions under which the above described reactions proceed are surprising.

CONCLUSION

Although CH_3CN is an excellent solvent for $[N(CH_3)_4]F$, it is not chemically inert. The strongly basic F^- anion can abstract a proton from CH_3CN with the formation of the HF_2^- and CH_2CN^- anions. Similarly, $CHCl_3$ and CH_2Cl_2 readily react with $[N(CH_3)_4]F$ at room temperature undergoing halogen exchange reactions thus demonstrating the high reactivity of the free fluoride anion.

ACKNOWLEDGMENT

The authors are grateful to the Office of Naval Research and the Army Research Office for financial support and to Dr. C. J. Schack and Mr. R. D. Wilson for their help.

REFERENCES

1 W. W. Wilson and K. O. Christe, to be published.

2 K. O. Christe and W. W. Wilson, J. Fluorine Chem., 46 (1990) 339.

3 J. S. Martin and F. Y. Fujiwara, Can. J. Chem., 49 (1971) 3071.

4 D. J. Brauer, H. Buerger, M. Grunwald, G. Pawelke, and J. Wilke, Z. Anorg. Allg. Chem., 537 (1986) 63.

5 C. Krueger, J. Organometall. Chem., 9 (1967) 125; I. N. Juchnovski and I. G. Binev, ibid. 99 (1975) 1.

6 F. Y. Fujiwara and J. S. Martin, J. Am. Chem. Soc., 96 (1974) 7625.

7 P. Resnick, private communication.

8 R. H. Cox and S. L. Smith, J. Magn. Res., 1 (1969) 432.

9 G. V. D. Tiers, J. Am. Chem. Soc., 84 (1962) 3972.

10 J. W. Emsley, L. Phillips, and V. Wray, 'Fluorine Coupling Constants,' Pergamon, Oxford, 1977.

11 W. A. Sheppard and C. M. Sharts, 'Organic Fluorine Chemistry,' W. A. Benjamin, New York, 1969.

12 M. Hudlicky, 'Chemistry of Organic Fluorine Compounds,' Wiley, New York, 1976.

APPENDIX J

Reprinted from Inorganic Chemistry, 1990, *29*.

Contribution from Rocketdyne, A Division of Rockwell International Corporation, Canoga Park, California 91303,
Department of Chemistry, McMaster University, Hamilton, Ontario L8S 4M1, Canada,
and Department of Nuclear Medicine, Chedoke-McMaster Hospitals, Hamilton, Ontario L8N 3Z5, Canada

The Hexafluorochlorate(V) Anion, ClF_6^-

Karl O. Christe,*[,1a] William W. Wilson,[1a] Raman V. Chirakal,[1b,c] Jeremy C. P. Sanders,[1b]
and Gary J. Schrobilgen*[,1b]

Received February 12, 1990

The low-temperature reactions of either $N(CH_3)_4F$ or CsF with ClF_5 in CH_3CN solutions produce white solids, which on the basis of material balances and low-temperature Raman spectra, contain the ClF_6^- anion. The similarity of the Raman spectrum of ClF_6^- to that of the octahedral BrF_6^- ion indicates that ClF_6^- is also octahedral and that the free valence electron pair on chlorine is sterically inactive. The existence of the ClF_6^- anion was further supported by an ^{18}F exchange experiment between ClF_5 and ^{18}F-labeled FNO that showed complete randomization of the ^{18}F isotope among the two molecules. A high-field ^{19}F NMR study of neat ClF_5 and ClF_5 in anhydrous HF solution in the presence and absence of excess CsF has provided accurate measurements of the ClF_5 NMR parameters including, for the first time, both $^{37/35}Cl$ secondary isotopic ^{19}F NMR shifts. Moreover, the NMR study also supports the existence of ClF_6^-, showing that ClF_5 undergoes slow chemical exchange with excess CsF in anhydrous HF at room temperature.

Introduction

The hexafluorohalate(V) anions belong to the interesting class of AX_6E compounds,[2] which possess six X ligands and a free valence electron pair E. Depending on the size of the central atom A, the free valence electron pair E can be either sterically active or inactive. Thus, a recent study has shown that in IF_6^- the free valence electron pair is sterically active, while in BrF_6^- it is not.[3] Whereas the ClF_5 molecule was discovered 27 years ago,[4] and the BrF_6^- and IF_6^- anions have been known for about as long,[5,6]

---

(1) (a) Rocketdyne. (b) McMaster University. (c) Chedoke-McMaster Hospitals.

(2) Gillespie, R. J. *Molecular Geometry*; Van Nostrand Reinhold Co.: London, 1972.

(3) Christe, K. O.; Wilson, W. W. *Inorg. Chem.* 1989, *28*, 3275.

(4) Maya, W.; Bauer, H. F. U.S. Pat. 3,354,646, 1967.

(5) Emeleus, H. J.; Sharpe, A. G. *J. Chem. Soc.* 1949, 2206.

(6) Whitney, E. D.; MacLaren, R. O.; Fogle, C. E.; Hurley, T. J. *J. Am. Chem. Soc.* 1964, *86*, 2583.

0020-1669/90/1329-3506$02.50/0 © 1990 American Chemical Society

the ClF_6^- anion has so far proven elusive. For example, ClF_5 does not form any stable adducts with alkali-metal fluorides and the only reaction observed is a catalytic decomposition of ClF_5 to ClF_3 and F_2.[7] Furthermore, a ^{18}F radiotracer study of the CsF–ClF_5 system did not provide any evidence for fluorine exchange and, thereby, for the formation of a ClF_6^- intermediate.[8] The well-established existence of the ClF_6^+ cation[9-12] and of the $ClF_6^\bullet$ radical,[13] combined with the recent finding that in BrF_6^- the bromine free valence electron pair is sterically inactive,[3] indicated that the weak Lewis acidity of ClF_5 and the low solubilities of CsF and $CsClF_6$ in ClF_5 are the most likely reasons for the previous failures[7,8] to isolate the ClF_6^- anion. Our recent success[14] with handling ClF_3 in CH_3CN solution and the surprisingly high thermal stability of $N(CH_3)_4ClF_4$, combined with its high solubility in CH_3CN, suggested that similar reaction conditions, i.e., the use of $N(CH_3)_4^+$ as a large, stabilizing counterion, of CH_3CN as a solvent, and of low temperature, might provide the long sought after ClF_6^- anion.

Experimental Section

Caution! Mixtures of ClF_5 or ClF_6^- salts with organic materials, such as CH_3CN or $[N(CH_3)_4]^+$ salts, are highly explosive and must be handled on a small scale with appropriate safety precautions, such as barricades, face shields, heavy leather gloves, and protective clothing.

Materials. The CH_3CN (Baker, Bio-analyzed, having a water content of 40 ppm) was treated with P_2O_5 and freshly distilled in a flamed-out Pyrex vacuum system prior to use, thereby reducing its water content to ≤4 ppm. The CsF (KBi) was dried by fusion in a platinum crucible and ground in the drybox. The ClF_5 (Rocketdyne) was purified by fractional condensation prior to its use. The synthesis of HF_2^-- and H_2O-free $N(CH_3)_4F$ is described elsewhere.[15]

Apparatus. All reactions were carried out in well-passivated (with ClF_3) Teflon-FEP or Kel-F ampules that were closed by stainless steel valves. The ClF_5 was handled in a stainless steel–Teflon–FEP vacuum line,[16] and the CH_3CN was transferred on a baked-out Pyrex vacuum line equipped with Teflon stopcocks. Nonvolatile materials were handled in the dry N_2 atmosphere of a glovebox.

Fluorine-18 Exchange Reaction between FNO and ClF_5. A 50-mL nickel can was heated to red heat four times with 2 atm of H_2, followed by pumping each time. The procedure was repeated four times with F_2, followed by treatment with 3 atm of FNO at room temperature for 1 day and pumping for 4 h. Nitric oxide (0.62 mmol) was combined at −196 °C in the can with a Ne/^{18}F-labeled F_2 mixture, which was accelerator produced under conditions previously described.[17] The Ne was pumped off at −196 °C, and F_2 (0.31 mmol) was added to the can. The can was briefly warmed to 20 °C, and the resulting ^{18}F-labeled FNO was condensed, for the removal of any HF, at −196 °C into a U-tube containing 0.5 g of NaF, followed by warming to −78 °C. It was then combined at −196 °C in a $^1/_4$ in. o.d. Teflon–FEP ampule with ClF_5 (0.62 mmol). The resulting mixture was warmed to 20 °C for several minutes and then vacuum-distilled through two U-traps kept at −120 and −196 °C. The −120 °C trap contained the ClF_5, and the −196 °C one, the FNO. Individual activity measurements were corrected for the elapsed time by correcting to zero time of the experiment. At the end of the experiment, the −120 °C trap, containing ClF_5, showed a zero time activity of 71.6 mCi (84.9%), whereas that in the −196 °C trap, containing the FNO, was 12.7 mCi (15.1%).

Synthesis of $N(CH_3)_4ClF_6$. In a typical experiment, $N(CH_3)_4F$ (150.9 mg, 1.62 mmol) was transferred in the drybox into a prepassivated Teflon–FEP ampule that was closed by a stainless steel valve. Dry CH_3CN (5.96 mL, 4.702 g) was added at −196 °C on the Pyrex vacuum line, and the mixture was warmed to room temperature. ClF_5 (1.62 mmol) was added at −196 °C on the stainless steel vacuum line, and the mixture was kept at −31 °C for 3 h with occasional very careful agitation. All material volatile at −31 °C was pumped off and trapped in a −196 °C trap and consisted of 4.70 g of CH_3CN. The white solid residue was highly shock sensitive and consistently exploded when either exposed to a laser beam at low temperature or warmed to room temperature.

When the above experiment was repeated at room temperature, gas evolution set in at about 0 °C, and after solvent removal at 20 °C, a stable white solid was obtained, which, on the basis of its weight and vibrational spectrum, was identified as $N(CH_3)_4ClF_4$.[14]

When CsF was substituted for $N(CH_3)_4F$ in the reaction with ClF_5 in CH_3CN at −31 °C, the volatile materials at −31 °C consisted of the CH_3CN and ClF_5 starting materials, and the nonvolatile residue was unreacted CsF.

For the recording of the low-temperature Raman spectrum of $CsClF_6$, a solution of ClF_5 in CH_3CN was kept in contact with excess CsF for several hours at −40 °C and then slowly cooled to −110 °C. The Raman spectrum of the product in the bottom of the tube was recorded at −110 °C and indicated the presence of $CsClF_6$ (see below) and solid CH_3CN.

Nuclear Magnetic Resonance Spectroscopy. The ^{19}F NMR spectra were recorded unlocked (field drift < 0.1 Hz h^{-1}) by using a Bruker WM-250 or AM-500 spectrometer equipped with a 5.8719 or 11.744 T cryomagnet, respectively. On both instruments, spectra were obtained by using 5-mm combination $^1H/^{19}F$ probes operating at 235.361 MHz (WM-250) or 470.599 MHz (AM-500).

The 5.8719-T ^{19}F spectra were typically accumulated in a 16K memory. Spectral width settings of 5 and 10 kHz were employed, yielding data point resolutions of 0.62 and 1.22 Hz and acquisition times of 1.638 and 0.819 s, respectively. No relaxation delays were applied. The number of free-induction decays accumulated was typically between 2000 and 10000 transients.

The 11.744-T ^{19}F spectra were accumulated in a 16K memory. Spectral width settings of 5 and 30 kHz were employed, yielding data point resolutions of 0.61 and 3.59 Hz and acquisition times of 1.638 and 0.278 s, respectively. No relaxation delays were applied. Typically 80–1000 transients were accumulated.

On both instruments the pulse width corresponding to a bulk magnetization tip angle, θ, of approximately 90° was equal to 1 μs. No line-broadening parameters were applied in the exponential multiplication of the free-induction decays prior to Fourier transformation.

The spectra were referenced to neat $CFCl_3$. The chemical shift convention used is that a positive (negative) sign signifies a chemical shift to high (low) frequency of the reference compound.

Low-temperature studies were carried out by using Bruker temperature controllers. The temperature was measured with a copper–constantan thermocouple inserted directly into the sample region of the probe and was considered accurate to ±1 °C.

Fluorine-19 NMR samples were prepared in 25-cm lengths of AWG 9 (ca. 4-mm o.d., 0.8-mm wall) FEP plastic tubing heat sealed at one end with the open end flared (45° SAE) and joined, by means of a compression fitting, to a Kel-F valve. The assembly was seasoned overnight with ca. 1 atm of F_2 gas, evacuated, and weighed. A weighed amount of CsF was transferred into a sample tube in a drybox. Both ClF_5 and HF were distilled into NMR tubes through a metal line fitted with a pressure transducer that had been previously seasoned overnight with ca. 1 atm of ClF_5 vapor. The ClF_5 pressure was measured (±0.5% accuracy) in a calibrated portion of the metal vacuum line with a pressure transducer (0–1000 Torr range), whose wetted surfaces were Inconel, and condensed at −196 °C into the FEP NMR sample tube. The amount of HF solvent used was determined by direct weighing of the tube assembly. The FEP tube was heat sealed under dynamic vacuum with its contents frozen at −196 °C. The FEP sample tubes were placed in 5-mm thin-walled precision NMR tubes (Wilmad) in order to run their spectra.

Raman Spectroscopy. Low-temperature Raman spectra were recorded on a Cary Model 83 spectrophotometer using the 488-nm exciting line of an Ar ion laser.

Results and Discussion

Synthesis of ClF_6^- Salts. It was found that the activation energy for the ClF_5–CH_3CN reaction is sufficiently high to permit the judicious handling of ClF_5 in a large excess of dry CH_3CN. Although ClF_5 is a more powerful oxidizer than ClF_3, its pseudooctahedral structure with five fluorine ligands and one free valence electron pair renders it less reactive than the pseudotrigonal-bipyramidal ClF_3.

To take advantage of the high activation energy of the ClF_5–CH_3CN reaction, $N(CH_3)_4F$ was carefully combined with ClF_5 in this solvent at −31 °C. Removal of the solvent at −31 °C resulted in a white, highly sensitive solid that violently exploded

---

(7) Christe, K. O.; Wilson, W. W.; Wilson, R. D. *Inorg. Chem.* 1989, *28*, 675.
(8) Bougon, R. *Bull. Inf. Sci. Tech., Commis. Energ. At. (Fr.)* 1971, *161*, 9.
(9) Christe, K. O. *Inorg. Nucl. Chem. Lett.* 1972, *8*, 741.
(10) Roberto, F. Q. *Inorg. Nucl. Chem. Lett.* 1972, *8*, 737.
(11) Christe, K. O. *Inorg. Chem.* 1973, *12*, 1580.
(12) Christe, K. O.; Wilson, W. W. *Inorg. Chem.* 1983, *22*, 1950.
(13) Boate, A. R.; Morton, J. R.; Preston, K. F. *Inorg. Chem.* 1975, *14*, 3127.
(14) Wilson, W. W.; Christe, K. O. *Inorg. Chem.* 1989, *28*, 4172.
(15) Wilson, W. W.; Christe, K. O.; Feng, J.; Bau, R. To be published.
(16) Christe, K. O.; Wilson, R. D.; Schack, C. J. *Inorg. Synth.* 1986, *24*, 3.
(17) Chirakal, R.; Firnau, G.; Schrobilgen, G. J.; McKay, J.; Garnett, E. S. *Int. J. Appl. Radiat. Isot.* 1984, *35*, 401.
(18) Bougon, R.; Charpin, P.; Soriano, J. *C. R. Hebd. Seances Acad. Sci., Ser. C* 1971, *272*, 565.

either on exposure to a laser beam at low temperature or on warming to room temperature, thereby preventing its direct identification. It was shown, however, by quantitative material balances that most of the ClF_5 starting material had been retained by the $N(CH_3)_4F$ at −31 °C.

When the reaction between $N(CH_3)_4F$ and ClF_5 was carried out at temperatures above −31 °C, gas evolution was observed at about 0 °C and, after solvent removal at 20 °C, a stable, white solid was isolated, which was identified by vibrational spectroscopy as $N(CH_3)_4ClF_4$.[14] Since the latter compound is stable up to 100 °C and is not shock sensitive,[14] the explosive material from the −31 °C reaction could not have been $N(CH_3)_4ClF_4$ but most likely was $N(CH_3)_4ClF_6$.

To overcome the experimental difficulties associated with the characterization of $N(CH_3)_4ClF_6$, the $N(CH_3)_4F$ starting material in the $N(CH_3)_4F-ClF_5-CH_3CN$ system was substituted by CsF. It was hoped that $CsClF_6$ would be stable at −31 °C, the lowest temperature at which the CH_3CN solvent could be pumped off at a reasonable rate. However, it was found that $CsClF_6$ is thermally unstable even at −31 °C, and all the ClF_5 was pumped off at −31 °C, together with the CH_3CN solvent. Since CH_3CN is a much weaker Raman scatterer than the chlorine fluorides,[14] it was possible to record the low-temperature Raman spectrum of $CsClF_6$ without removal of the CH_3CN and, thereby, to identify the ClF_6^- anion A detailed discussion of the observed spectrum will be given below.

^{18}F Radiotracer Study. Further evidence for the formation of the ClF_6^- anion was obtained by an ^{18}F radiotracer study of the $ClF_5-^{18}FNO$ system. It was found that ClF_5 undergoes rapid fluorine exchange with ^{18}FNO (eq 1). Within several minutes

$$^{18}FNO + ClF_5 \rightleftharpoons [NO^+ClF_5{}^{18}F^-] \rightleftharpoons FNO + ClF_4{}^{18}F \qquad (1)$$

at room temperature, complete randomization of the ^{18}F isotope had occurred. The measured values of 84.9% for the radioactivity in ClF_5 and 15.1% in FNO are in excellent agreement with the values 83.3 and 16.7% predicted for a random distribution of ^{18}F involving an unstable $NO^+ClF_6^-$ intermediate. The rapid fluorine exchange in the $FNO-ClF_5$ system is in marked contrast to the results from the previous study of the $CsF-ClF_5$ system for which no evidence of exchange was reported.[8] The lack of exchange in the $CsF-ClF_5$ system is probably due to the very low solubility of CsF in ClF_5 and not to the lack of ClF_6^- formation (see below).

^{19}F NMR Study of Chemical Exchange Behavior between F^- and ClF_5. Chlorine pentafluoride has previously been shown in two ^{19}F NMR studies to possess a square-pyramidal (C_{4v}) AX_4E structure in the liquid state[19,20] as predicted by the VSEPR model.[2] Alexandre and Rigny[20] demonstrated that, unlike the equatorial X_4 part of the ^{19}F NMR spectrum, which showed a secondary isotopic shift arising from ^{19}F bonded to ^{35}Cl and ^{37}Cl, the axial A part of the spectrum was broadened significantly and showed no evidence for an isotopic shift.[20] This study concluded that chemical exchange between the axial (F_{ax}) and equatorial (F_{eq}) fluorines could be disregarded and that the line broadening of F_{ax} arises from partially quadrupole-collapsed scalar couplings between $^{19}F_{ax}$ and the spin-$^3/_2$ quadrupolar nuclei ^{35}Cl and ^{37}Cl, $^1J(^{19}F_{ax}-^{35/37}Cl)$, which are significantly larger than $^1J(^{19}F_{eq}-^{35/37}Cl)$. Nuclear relaxation time measurements in the same study have confirmed this and have provided estimates of the magnitudes of the scalar couplings ($^1J(^{19}F_{ax}-^{35}Cl) = 192$ and $^1J(^{19}F_{eq}-^{35}Cl) \leq 20$ Hz). The larger value for $^1J(F_{ax}-^{35}Cl)$ is in accord with the shorter $F_{ax}-Cl$ bond observed in this molecule.[21] The temperature behavior of the ^{19}F NMR spectrum of liquid ClF_5 was investigated in the previous study, but it does not report any variations of line widths as a function of temperature. We have recorded the ^{19}F NMR spectra of neat ClF_5 at 25, −56, and −90 °C (Figure 1). While there is little effect upon the line width of the F_{eq} resonance on lowering the temperature, a significant narrowing of the F_{ax} resonance line width is observed together with partial resolution of its chlorine isotopic shift. The observed line narrowing for the F_{ax} resonance is attributable to the increased quadrupolar relaxation rates of ^{35}Cl and ^{37}Cl at low temperatures where the isotropic molecular tumbling correlation time (τ_c) for ClF_5 is greater.[22] This behavior is consistent with the dominant contribution of scalar relaxation of the second kind, via $^1J(F_{ax}-^{35/37}Cl)$, to the spin–spin relaxation time (T_2) of the F_{ax} nuclei, as found in the previous study.[20]

The ^{19}F NMR spectra of a solution of ClF_5 (0.536 m) in anhydrous HF and a solution of ClF_5 (0.619 m) in anhydrous HF containing CsF (5.60 m) were investigated. The ^{19}F NMR spectrum of ClF_5 recorded in HF solvent at 25 °C consists of two well-resolved doublets corresponding to equatorial fluorines on ^{35}Cl and ^{37}Cl spin coupled to the axial fluorine environment (Figure 2). The latter environment, as in the neat sample of ClF_5 at 24.4 °C, is broadened significantly owing to partial quadrupole collapse of the $^1J(^{35/37}Cl-^{19}F)$ scalar couplings so that resolution of the isotopically shifted quintets (Figure 2, also cf. Figure 1) is precluded. The line broadening on the quintets is again dominated by scalar coupling and not by fluorine exchange, as has been established for neat ClF_5 in the present and earlier studies.[20] The addition of F^- to HF solutions of ClF_5 results in pronounced broadening of the doublet resonances at 25 °C, preventing resolution of the isotope shift, whereas the appearance of the axial fluorine resonance remains essentially unchanged (Figure 3). The line broadening is consistent with slow intermolecular ^{19}F exchange arising from equilibrium 2 and the intermediacy of ClF_6^- in the

$$ClF_5 + F(HF)_x^- \rightleftharpoons ClF_6^- + xHF \qquad (2)$$

exchange process. Cooling of the ClF_5-F^- sample to −56 °C slowed ^{19}F chemical exchange sufficiently to allow resolution of the equatorial fluorine doublets (Figure 3) and the axial fluorine quintets. This is the first time the two quintet patterns arising from the $^{35}Cl-^{37}Cl$ secondary isotope effect have been observed in ClF_5. The sharpening of the axial fluorine resonance is not, however, attributed to slowing of the ^{19}F chemical exchange process but is primarily attributed to the dominant effect of the increased quadrupole relaxation rates of the ^{35}Cl and ^{37}Cl nuclei on $^1J(^{35/37}Cl-^{19}F)$ at low temperatures where τ_c for ClF_5 is greater. The addition of CsF presumably increases the viscosity of the solvent medium owing to $F(HF)_x^-$ formation and hence increases τ_c for ClF_5, leading to collapse of the $^1J(^{35/37}Cl-^{19}F)$ couplings. In contrast, the ^{19}F resonances associated with ClF_5 dissolved in HF do not sharpen as significantly, although the quintet pattern clearly possesses a narrower line width than at 25 °C (Figure 2). The broader lines can be attributed to the low viscosity of the HF solvent medium, even at −56 °C, allowing the partially collapsed $^1J(^{35/37}Cl-^{19}F)$ couplings to persist in the slow chemical exchange limit.

The secondary isotope shifts, $^1\Delta^{19}F_{ax}(^{37/35}Cl) = -0.189$ ppm and $^1\Delta^{19}F_{eq}(^{37/35}Cl) = -0.085$ ppm for ClF_5/CsF in HF at −56 °C (Figure 3), follow the usual trend and are negative; i.e., the observed NMR nucleus bonded to the heavier of two isotopes has its NMR resonance to lower frequency.[23] They are comparable in magnitude to those for closely related species in the same row of the periodic table; i.e., for ClF_6^+, $^1\Delta^{19}F(^{37/35}Cl) = -0.15$ ppm,[24] for SF_6, $^1\Delta^{19}F(^{34/32}S) = -0.0552$ ppm,[25] and for SF_4, $^1\Delta^{19}F_{ax}(^{34/32}S) = -0.0690$ ppm and $^1\Delta^{19}F_{eq}(^{34/32}S) = -0.0330$ ppm[25] with the ^{19}F bonded to the heavier isotope occurring at lower frequency. The relative sizes of isotopic shifts are known to be larger for shorter bonds,[26] and this is also true for the secondary isotopic shifts of ClF_5 [$r(Cl-F_{ax}) = 1.58$, $r(Cl-F_{eq}) = 1.67$ Å[21] and $f_{Rax} = 3.01$, $f_{Req} = 2.57$ mdyn Å^{-1}][27] and BrF_5 [$r(Br-F_{ax}) = 1.689$,

---

(15) Pilipovich, D., Maya, W., Lawton, E. A., Bauer, H. F., Sheehan, D. F., Ogimachi, N. N., Wilson, R. D., Gunderloy, F. C., Bedwell, V. E. *Inorg Chem* 1967, *6*, 1918

(20) Alexandre, M., Rigny, P. *Can J Chem* 1974, *52*, 3676

(21) Goulet, P., Jurek, R.; Chanussot, J. *J Phys* 1976, *37*, 495

(22) Boeré, R. T., Kidd, R. G. *Annu Rep NMR Spectrosc* 1982, *13*, 320

(23) Jameson, C. J., Osten, H. J. *J Am Chem Soc* 1985, *107*, 4158

(24) Christe, K. O., Hon, J. F., Pilipovich, D. *Inorg Chem* 1973, *12*, 84

(25) Gombler, W. *Z Naturforsch* 1985, *40b*, 782

(26) Jameson, C. J. *J Chem Phys* 1977, *66*, 4983

(27) Begun, G. M., Fletcher, W. H., Smith, D. F. *J Chem Phys* 1965, *42*, 2236

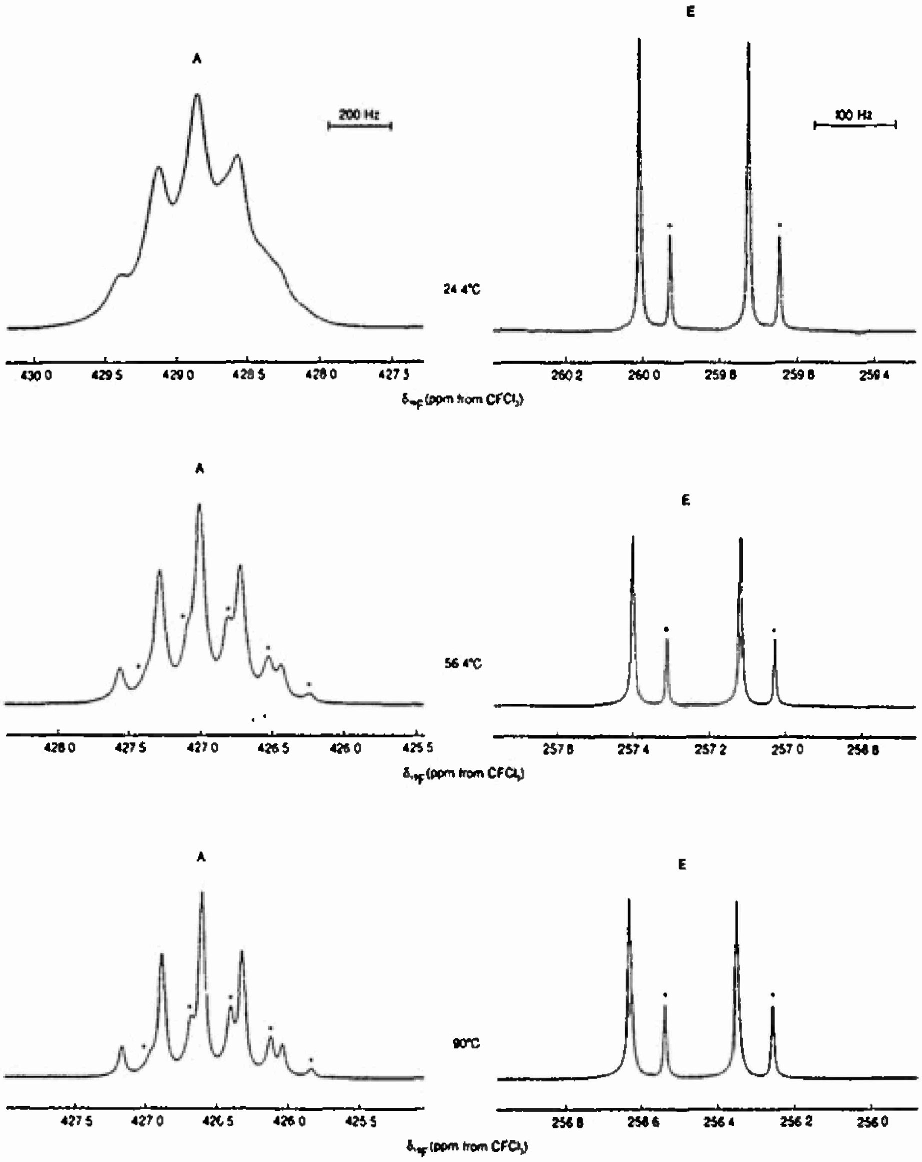

Figure 1. Variable-temperature ^{19}F NMR spectra (470.599 MHz) of neat ClF$_5$. A and E denote resonances for the axial and equatorial fluorine environments, respectively; asterisks denote resonances arising from the ^{37}Cl isotopomer.

Table I. ^{19}F NMR Data for Neat ClF$_5$ and ClF$_5$–HF and ClF$_5$–CsF–HF Solutions

sample compn	T, °C	chem shift δ, ppm[a]		^2J(F$_{ax}$–F$_{eq}$), Hz	line width, Hz		secondary isotopic shift[b] $^1\Delta^{19}$F($^{37/35}$Cl), ppm	
		F$_{eq}$	F$_{ax}$		F$_{eq}$	F$_{ax}$	F$_{eq}$	F$_{ax}$
neat ClF$_5$	24.4	259.8	428.8	133	3.5	~110	−0.079	e
	−56.4	257.2	426.9	133	4.0	44	−0.088	−0.1977
	−90.0	256.4	426.6	133	5.2	26	−0.091	−0.199
ClF$_5$ in HF solv[c]	25	256.4	424.6	130	5.7	~140	−0.078	e
	−56.3	253.9	422.6	130	2.5	71	−0.087	e
ClF$_5$/CsF in HF solv[d]	25	253.6	420.9	123	28	~100	e	e
	−56.3	250.8	418.8	124	6.9	18	−0.085	−0.189

[a] Spectra were referenced with respect to external CFCl$_3$ at 25 °C. [b] $^1\Delta^{19}$F($^{37/35}$Cl)/ppm = δ(F(^{37}Cl)) − δ(F(^{35}Cl)). [c] Concentration of ClF$_5$ = 0.536 m. [d] Concentration of ClF$_5$ = 0.619 m, and that of CsF = 5.60 m. [e] Isotopic shift not resolved.

r(Br–F$_{eq}$) = 1.774 Å[28] and $f_{R_{ax}}$ = 4.07, $f_{R_{eq}}$ = 3.19 mdyn Å^{-1}],[27] where $^1\Delta^{19}$F$_{ax}$($^{81/79}$Br) = −0.030 and $^1\Delta^{19}$F$_{eq}$($^{81/79}$Br) = −0.015 ppm.[29] Moreover, the ratio $^1\Delta^{19}$F$_{ax}$($^{37/35}$Cl)/$^1\Delta^{19}$F$_{eq}$($^{37/35}$Cl) = 2.22 is remarkably similar to those found for the axial and equatorial secondary isotopic shifts of SF$_4$, $^1\Delta^{19}$F$_{ax}$($^{34/32}$S)/$^1\Delta^{19}$F$_{eq}$($^{34/32}$S) = 2.09, and BrF$_5$, $^1\Delta^{19}$F$_{ax}$($^{81/79}$Br)/$^1\Delta^{19}$F$_{eq}$($^{81/79}$Br) = 2.0.[29] NMR data are summarized in Table I.

Raman Spectrum of CsClF$_6$. The Raman spectrum of the product from the low-temperature reaction of CsF with ClF$_5$ in CH$_3$CN solution was recorded at −110 °C in frozen CH$_3$CN. In the region of the Cl–F fundamental vibrations, three bands were observed at 525, 384, and 289 cm^{-1} (Figure 4, trace A, which, under the influence of the laser beam, rapidly decayed giving rise to new bands at 507, 418, and 290 cm^{-1} (Figure 4, trace B). These new bands are due to the ClF$_4^-$ anion, as shown by the Raman spectrum of N(CH$_3$)$_4$ClF$_4$ in CH$_3$CN recorded under identical

---

(28) Robiette, A. G., Bradley, R. H., Brier, P. N. *J. Chem. Soc., Chem. Commun.* 1971, 1567.
(29) Sanders, J. C. P., Schrobilgen, G. J. Unpublished results.

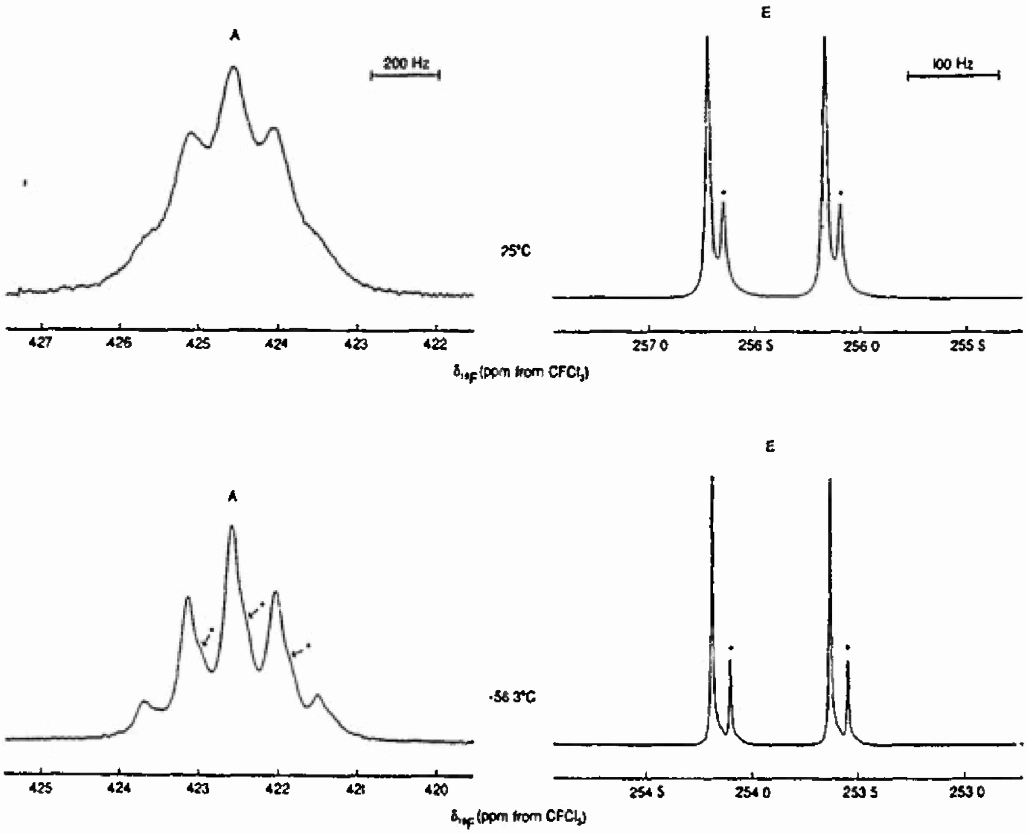

Figure 2 Variable-temperature ^{19}F NMR spectra (235.361 MHz) of ClF_5 (0.536 m) in HF solution. A and E denote resonances for the axial and equatorial fluorine environments, respectively; asterisks denote resonances arising from the ^{37}Cl isotopomer.

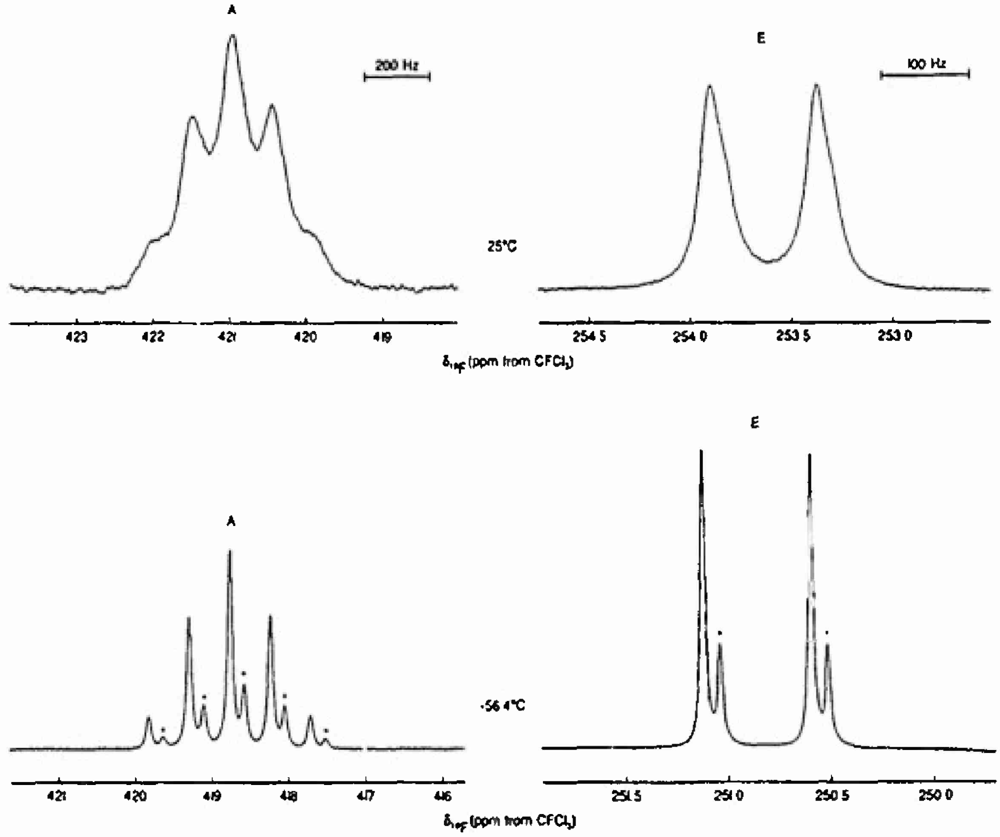

Figure 3 Variable-temperature ^{19}F NMR spectra (235.361 MHz) of ClF_5 (0.619 m)–CsF (5.60 m) in HF solution. A and E denote resonances for the axial and equatorial fluorine environments, respectively, asterisks denote resonances arising from the ^{37}Cl isotopomer.

conditions (Figure 4, trace C) The new set of bands at 525, 384, and 289 cm^{-1} are attributable to ClF_6^- for the following reasons. (i) the bands cannot be assigned to either CH_3CN, ClF_5, or ClF_4^-, (ii) they must be due to a species that on photolysis can produce ClF_4^-, (iii) the relative intensities of these Raman bands are very similar to those observed for solid $Cs^+BrF_6^-$,[18] and (iv) the observed frequencies are in excellent agreement with our expectations for ClF_6^-.

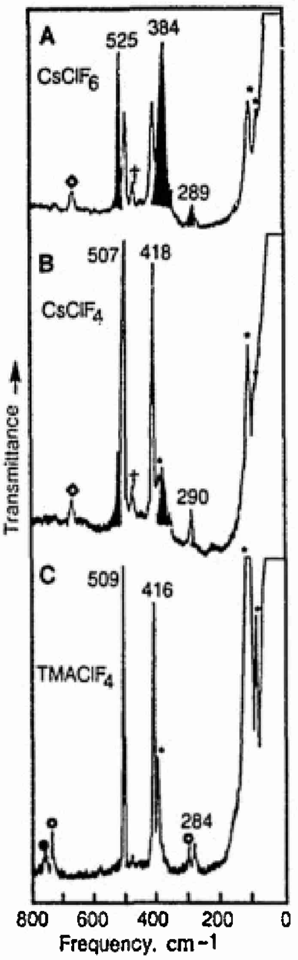

Figure 4. Raman spectra of CsClF$_6$ (trace A), CsClF$_4$ (trace B), and N(CH$_3$)$_4$ClF$_4$ (trace C) recorded at −110 °C for the solids in frozen CH$_3$CN. The bands assigned to the anions of the title compounds are marked by their frequency values. Bands due to ClF$_5$, CH$_3$CN, Kel-F, Teflon-FEP, and the N(CH$_3$)$_4^+$ cation have been marked by daggers, stars, diamonds, hollow circles, and full circles, respectively. Traces A and B are the first and second scan of the same sample and demonstrate the rapid decay of ClF$_6^-$ (solid peaks) to ClF$_4^-$ (hollow peaks) under the influence of the laser beam.

The last point needs some amplification. By analogy with octahedral BrF$_6^-$,[3] the ClF$_6^-$ anion, which possesses a smaller central atom than BrF$_6^-$, should also be octahedral; i.e., the free valence electron pair on chlorine should be sterically inactive. Octahedral ClF$_6^-$ should possess six fundamental vibrations of which only the $\nu_1(A_{1g})$, $\nu_2(E_g)$, and $\nu_5(F_{2g})$ modes would be Raman active. Since in all the Raman active modes the central Cl atom is at rest, the observed frequencies should depend only on the force constants and should be independent of the mass of the central atom. Furthermore, the F-matrix expressions of these modes contain the same elements as the corresponding modes of the closely related octahedral HalF$_6^+$ cations and the pseudooctahedral HalF$_5$ molecules and HalF$_4^-$ anions. Therefore, a plot of the frequencies of the modes should be mass independent and should exhibit smooth trends, with the frequencies decreasing with decreasing oxidation state of the central atom and increasing negative charge on the species. Plots of the sums of the frequencies of the symmetric in-phase and symmetric out-of-phase stretching modes and of those of the scissoring deformation mode for the series BrF$_4^-$,[30] BrF$_6^-$,[3] BrF$_5$,[26,31] and BrF$_6^+$[32,33] and ClF$_4^-$,[34] ClF$_6^-$, ClF$_5$,[21,26,35] and ClF$_6^+$[36] are shown in Figure 5. With the exception of the ClF$_6^-$ values, all the other frequencies had previously been established experimentally. As can be seen from Figure 5, the frequencies observed in this study for ClF$_6^-$ perfectly fit the expected trends and strongly support their assignment to an octahedral ClF$_6^-$ anion.

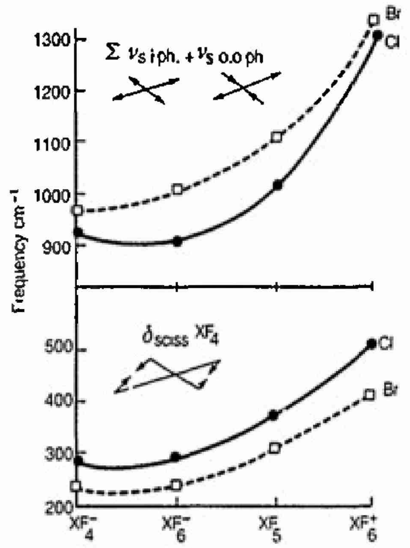

Figure 5. Plots of the sums of the frequencies of the two symmetric stretching modes and of those of the scissoring deformation mode for the different octahedral and pseudooctahedral halogen fluoride ions and molecules. The symmetry coordinates of each mode are depicted by the arrow diagrams.

Conclusion. The results from this study, i.e., Raman spectroscopy and the ^{18}F radiotracer study, provide strong evidence for the existence of the ClF$_6^-$ anion and its octahedral structure. As previously suggested, the past failures[7,8] to isolate the ClF$_6^-$ anion are due to its thermal and photolytic instability, combined with the low solubility of CsF and CsClF$_6$ in liquid ClF$_5$. These problems were overcome by the use of the larger counterion N(CH$_3$)$_4^+$, which helps to stabilize the ClF$_6^-$ anion and increases the solubility of the resulting salt, the use of CH$_3$CN as a more effective solvent, and the use of low-temperature spectroscopic techniques. The obvious limitations of this approach are the horrendous incompatibility problems encountered when one works with one of the most powerful known oxidizers in an organic solvent with an organic counterion. In view of our previous work[3] on the structure of BrF$_6^-$, the steric inactivity of the free valence electron pair on the chlorine atom of ClF$_6^-$ is not surprising and is at variance with the conclusions reached from a theoretical study, which examined the Laplacian of the calculated electronic charge distribution of gaseous ClF$_6^-$ and predicted a fluxional structure having a distorted octahedral (C_{3v}) equilibrium geometry.[37]

Acknowledgment. We thank Dr. C. J. Schack and Mr. R. D. Wilson for their help, the U.S. Air Force Astronautics Laboratory, Edwards AFB (K.O.C. and G.J.S.), the U.S. Army Research Office (K.O.C.), and the Natural Sciences and Engineering Research Council of Canada (G.J.S.) for financial support, and Dr E. S. Garnett for the use of the facilities of the Nuclear Medicine Department, Chedoke-McMaster Hospitals.

---

(30) Christe, K O; Schack, C. J *Inorg Chem* 1970, 9, 1852

(31) Selig, H , Holzman, H. *Isr. J Chem* 1969, *7*, 417

(32) Gillespie, R J.; Schrobilgen, G J *Inorg Chem*. 1974, *13*, 1230.

(33) Christe, K. O., Wilson, R D. *Inorg. Chem* 1975, *14*, 694

(34) Christe, K O., Sawodny, W. *Z. Anorg. Allg. Chem* 1968, *357*, 127.

(35) Christe, K. O. *Spectrochim. Acta, Part A* 1971, *27a*, 631.

(36) Christe, K. O. *Inorg. Chem*. 1973, *12*, 1580.

(37) MacDougall, P. J *Inorg Chem*. 1986, *25*, 4400

Journal of Fluorine Chemistry, *49* (1990) 167–169

Received: December 13, 1989; accepted: March 12, 1990

NEW SYNTHESIS OF IF_5O

C.J. SCHACK AND K.O. CHRISTE*

Rocketdyne, A Division of Rockwell International, Canoga Park, CA 91303 (USA)

SUMMARY

Phosphorus trifluoride oxide readily replaces two fluorine ligands in IF_7 for a doubly bonded oxygen atom, thereby providing a new and convenient synthesis for IF_5O. Attempts to extend this method to the syntheses of either IF_3O_2 or IFO_3 were unsuccessful due to competing deoxygenation reactions of the iodine oxyfluoride precursors. Furthermore, PF_3O does not undergo fluorine-oxygen exchange with the NF_4^+ cation.

INTRODUCTION

Recent work from our laboratory on fluorine-oxygen exchange reactions has shown that the nitrate ion is an excellent reagent for replacing two fluorine ligands by one doubly bonded oxygen atom in compounds such as BrF_5 [1, 2], XeF_6 [3], $XeOF_4$ [4], ClF_5, ClF_3 and ClF [5], and IF_5 [6]. However, IF_7 did not yield IF_5O but resulted in the formation of IF_5 and half a mol of oxygen [6]. This was unexpected since IF_7 is known to undergo fluorine-oxygen exchange with either silica at 100°C [7] or Cab-O-Sil [8], Pyrex [9, 10], I_2O_5 [10] or small amounts of water [9, 10] at ambient temperature. Recently, it was shown that PF_3O is also an effective reagent for accomplishing fluorine-oxygen exchange in XeF_6, UF_6, ClF_5, and BrF_5 [11]. It was, therefore, interesting to examine whether IF_7 and PF_3O undergo a fluorine-oxygen exchange reaction or are subject to deoxygenation as in the IF_7-NO_3^- case [6].

EXPERIMENTAL

Volatile materials were handled in a stainless steel vacuum line equipped with Teflon-FEP U-traps, stainless steel bellows-seal valves, and a Heise Bourdon tube-type gauge [12].

0022-1139/90/$3.50

All reactions were carried out either in stainless steel containers or sapphire tubes. Infrared spectra were recorded on a Perkin Elmer Model 283 spectrometer using a 5-cm path length Teflon cell with AgCl windows for gases, and AgCl disks, pressed in an Econo press (Barnes Engineering Co.), for solids. Raman spectra were recorded on a Spex Model 1403 spectrophotometer using the 647.1-nm exciting line of a Kr ion laser. Literature methods were used for the syntheses of IF_7 [8], PF_3O [13], IF_3O_2 [14], and NF_4BF_4 [15].

Synthesis of IF_5O

A 30 ml stainless steel cylinder was passivated first with ClF_3 and then with PF_3O. After evacuation and cooling to -196°C, the cylinder was loaded successively with IF_7 (1.04 mmol) and PF_3O (1.10 mmol) and allowed to warm to room temperature. After five days the volatile products were removed and separated by fractional condensation in U-traps cooled to -78, -126, and -196°C. Only a small amount of non-condensable gas was observed, presumably O_2. The -196°C trap contained PF_5 (1.03 mmol) and PF_3O (0.07 mmol). The -78°C trap contained IF_5 (0.08 mmol), while the -126°C trap contained IF_5O (0.91 mmol, 88% yield based on IF_7).

RESULTS AND DISCUSSION

Iodine heptafluoride and PF_3O readily undergo a fluorine-oxygen exchange reaction according to:

$$IF_7 + PF_3O \rightarrow IF_5O + PF_5$$

The reaction proceeds at room temperature and produces IF_5O in a yield of about 90%. In addition to IF_5O, small amounts of IF_5 and oxygen are formed due to some decomposition of IF_5O. Use of an excess of PF_3O does not result in further fluorine-oxygen exchange and the formation of either IF_3O_2 or FIO_3. This was confirmed by an examination of the IF_5O-PF_3O and the IF_3O_2-PF_3O systems. At room temperature, no fluorine-oxygen exchange was observed, while at elevated temperatures the iodine oxyfluoride starting materials underwent deoxygenation rather than fluorine-oxygen exchange with PF_3O.

Attempts to achieve fluorine-oxygen exchange in NF_4BF_4 with PF_3O did not produce any NF_3O. Instead, the NF_4BF_4 fluorinated the PF_3O to PF_5 and oxygen, followed by a partial displacement reaction of BF_4^- by PF_5.

$$NF_4BF_4 + PF_3O \rightarrow NF_3 + BF_3 + PF_5 + 0.5\,O_2$$

$$NF_4BF_4 + PF_5 \rightarrow NF_4PF_6 + BF_3$$

This result is not surprising in view of the previous findings that (+V) nitrogen exhibits a maximum coordination number of four toward fluorine [16] and PF_5 can displace BF_3 from NF_4BF_4 [17].

ACKNOWLEDGMENTS

The authors wish to thank Mr. R.D. Wilson and Dr. W.W. Wilson for their help, Dr. G.J. Schrobilgen for a sample of IF_3O_2 and the U.S. Army Research Office for financial support of the work at Rocketdyne.

REFERENCES

1 W. W. Wilson and K. O. Christe, Inorg. Chem., 26 (1987) 916.
2 W. W. Wilson and K. O. Christe, Inorg. Chem., 26 (1987) 1573.
3 K. O. Christe and W. W. Wilson, Inorg. Chem., 27 (1988) 1296.
4 K. O. Christe and W. W. Wilson, Inorg. Chem., 27 (1988) 3763.
5 K. O. Christe and W. W. Wilson, Inorg. Chem., 28 (1989) 675.
6 K. O. Christe, W. W. Wilson and R. D. Wilson, Inorg. Chem., 28 (1989) 904.
7 R. J. Gillespie and J. W. Quail, Proc. Chem. Soc., (1963) 278.
8 C. J. Schack, D. Pilipovich, S. N. Cohz, and D. F. Sheehan, J. Phys. Chem., 72 (1968) 4697.
9 L. G. Alexakos, C. D. Cornwell and S. B. Pierce, Proc. Chem. Soc., (1963) 341.
10 N. Bartlett and L. E. Levchuk, Proc. Chem. Soc., (1963) 342.
11 S. A. Kinkead and J. B. Nielsen, Paper 47 presented at the ACS Ninth Winter Fluorine Conference, St. Petersburg, FL (February, 1989).
12 K. O. Christe, R. D. Wilson, and C. J. Schack, Inorg. Synth., 24 (1986) 3.
13 W. Kwasnik in 'Handbook of Preparative Inorganic Chemistry,' 1 (1963) 193 (G. Brauer, Editor).
14 R. G. Syvret, Ph.D. Thesis, McMaster University (1987).
15 K. O. Christe, W. W. Wilson, C. J. Schack and R. D. Wilson, Inorg. Synth., 24 (1986) 39.
16 K. O. Christe, W. W. Wilson, G. J. Schrobilgen, R. V. Chirakal and G. A. Olah, Inorg.. Chem., 27 (1988) 879.
17 K. O. Christe, C. J. Schack and R. D. Wilson, Inorg. Chem., 15 (1976) 1275.

Journal of Fluorine Chemistry, 48 (1990) 361–366

SYNTHESES AND VIBRATIONAL SPECTRA OF CHLOROFLUORAMINES

J. V. GILBERT*, R. A. CONKLIN

Chemistry Department, University of Denver, Denver, CO 80208 (U.S.A.)

R.D. WILSON AND K.O. CHRISTE*

Rockeidyne Division of Rockwell International Corporation, Canoga Park, CA 91303 (U.S.A.)

SUMMARY

The chlorofluoramines $NFCl_2$ and NF_2Cl were prepared by fluorination of an NH_4Cl-$NaCl$ mixture and characterized by vibrational spectroscopy. For NF_2Cl, two fundamental vibrations were reassigned.

INTRODUCTION

The halogenated amines are in general highly energetic [1, 2]. This characteristic allows the production of excited state species such as nitrenes by either chemical reactions or photolysis [3]. Excited state nitrenes and particularly NF have been studied extensively as a lasing medium but required the use of either halogen azides [4-6] or NF_2 [7] as precursors. Since both of these are difficult to work with, a study was undertaken at the University of Denver to explore the use of chlorofluoramines as an alternate and more convenient source of excited nitrenes. This interest in chlorofluoramines prompted a search for a convenient and safe synthesis of $NFCl_2$ and NF_2Cl, and a reinvestigation of their spectroscopic properties.

0022-1139/90/$3.50

$NFCl_2$ was first prepared [8] in 1963 from NaN_3 and ClF according to:

$$2ClF + NaN_3 \rightarrow NFCl_2 + NaF + N_2$$

However, the formation of highly explosive ClN_3 [9] as a by-product makes this method unattractive and may have been responsible for the reported instability [8] of condensed $NFCl_2$. An alternate synthesis of $NFCl_2$ was reported in 1968 and involved either the chlorination of NH_4F and NaCl-NaF mixtures or the fluorination of NH_4Cl and NaF mixtures [10]. Finally, the formation of $NFCl_2$ was mentioned in a 1969 paper on the chlorination of either ethyl fluorocarbamate or ethyl chlorofluorocarbamate by an excess of aqueous sodium hypochlorite [11]. In this paper, we would like to report on a modified fluorination reaction of NH_4Cl and some spectroscopic properties of $NFCl_2$ and NF_2Cl.

EXPERIMENTAL

Materials and Apparatus. Reagent grade NH_4Cl and NaCl (Barker) were finely ground together prior to use. Fluorine (Air Products) was premixed with dry N_2 in a mole ratio of 1:4, stored in a high pressure Monel cylinder at 1000 psi pressure, and its flowrate controlled by a flowmeter. Accidental overpressurization of the reactor was prevented by installing between the flowmeter and the reactor a blow-out bubbler filled with fluorocarbon oil. The fluorination reactor consisted of a 35 cm long, 3/4 inch o.d. copper tube which was kept at the desired temperature by means of an electric heating tape and temperature controller. The reactor was packed with a 1:1 mixture of NH_4Cl and NaCl dispersed between freshly cleaned dry copper shot. The reactor was followed by a stainless steel tube filled with activated NaF pellets (prepared from $NaHF_2$ pellets by heating to 300°C in a dry N_2 stream) for the removal of HF. The HF scrubber was followed by two Teflon-FEP stainless steel U-traps that were equipped with shut off valves and cooled to -78° and -183°C with a CO_2 bath and liquid Ar, respectively. The second Teflon cold trap was followed by another fluorocarbon oil filled bubbler to prevent back condensation of atmospheric moisture.

Infrared spectra were recorded on a Nicolet Model 5DXC FT IR spectrometer with a resolution of $2cm^{-1}$. The matrix isolation apparatus consisted of a RMC-Cryosystems LTS-22 closed cycle system operated at 8°K and 5×10^{-6} torr pressure. The samples were diluted with Ar to a MR of 100 and deposited through a needle valve on a cold KCl window. Typical deposition times used were two hours. Low temperature Raman spectra were recorded on a Spex Model 1403 spectrometer using the 647.1 nm line of a Kr ion laser and a previously described cooling device [12].

Synthesis of $NFCl_2$ and NF_2Cl. In a typical experiment, the reactor was loaded with 8 grams of NH_4Cl and 8 grams of NaCl dispersed on copper shot. Dry N_2 was passed through the reactor at 110°C for several hours to dry the reactor and the reagents. Then, the temperature was lowered to 55°C, and a mixture of 0.1 mol of F_2 and 0.4 mol of N_2 was passed through the reactor at a flow rate of 100cc/min, followed by a 10 min purge with pure N_2. The -183°C U-trap was transferred to a passivated (with ClF_3) stainless steel-Teflon FEP vacuum line [13], and the -183°C bath was replaced by liquid N_2 (-196°C). The products were separated by fractional condensation in a dynamic vacuum through a series of U-traps kept at -95° (toluene slush), -116° (ethanol slush), -142° (methylcyclopentane slush) and -196°C. The -196°C trap contained essentially pure NF_2Cl (1-2 mmol), the -142°C trap had mainly Cl_2 (6-8 mmol) and some $NFCl_2$ and a trace of NF_2Cl, the -116°C trap contained mainly $NFCl_2$ (~1 mmol) and some Cl_2, while the -95°C trap was essentially empty.

RESULTS AND DISCUSSION

Syntheses of $NFCl_2$ and NF_2Cl. Our synthesis of $NFCl_2$ and NF_2Cl is a modification of that originally reported by Pankratov and Sokolov [10]. It involves the fluorination of NH_4Cl with elemental F_2 in a flow reactor. In our study, it was found that the addition of NaCl to the NH_4Cl significantly increased the yields of the desired chlorofluoramines. Furthermore, careful drying of the reaction system is important to avoid the formation of $FClO_3$ and $FONO_2$. Although the yields of $NFCl_2$ and NF_2Cl are relatively low, and separation of the $NFCl_2$ from the main by-product Cl_2 is difficult and may require repeated careful fractionations, the method is a relatively convenient and safe way to produce moderate amounts of $NFCl_2$ and NF_2Cl. It avoids the hazards associated with the formation of chlorine azide as a potential by-product in the chlorofluorination of NaN_3 [8].

Vibrational Spectra. The infrared spectra of gaseous and Ar matrix isolated $NFCl_2$ and NF_2Cl and Raman spectra of liquid NF_2Cl and solid $NFCl_2$ were recorded. The infrared spectra of the gases were in excellent agreement with previous reports [14, 15]. Matrix infrared data had previously been reported only for NF_2Cl [16], and no Raman data had been available for either molecule. Our IR spectrum of matrix isolated NF_2Cl was in good agreement with the previous report [16], except for the antisymmetric NF_2 stretching mode, $\nu_5(a'')$, consisting only of a single band at 837 cm^{-1} and not a doublet at 842 and 837 cm^{-1}.

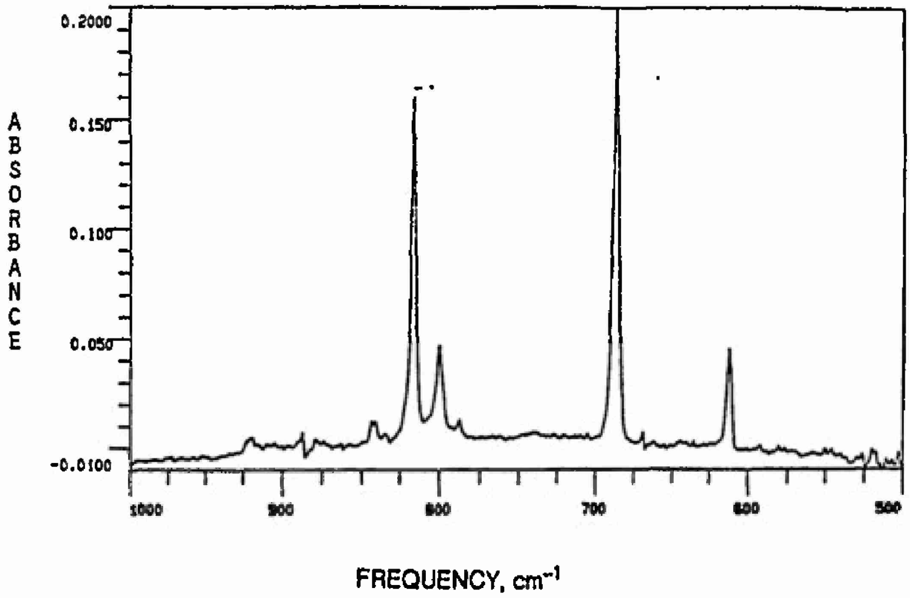

Fig. 1. Infrared Spectrum of Matrix Isolated $NFCl_2$. The absorption at 800 cm^{-1} was of variable relative intensity and is due to either an impurity or a matrix effect.

In our IR spectrum of matrix isolated $NFCl_2$ (see Figure 1) the NF stretching mode, $\nu_1(a')$, the symmetric NCl_2 stretch, $\nu_2(a')$, and the antisymmetric NCl_2 stretch, $\nu_5(a'')$, were observed at 816, 612 and 686 cm^{-1}, respectively. The slight frequency decreases relative to the corresponding gas phase values of 833, 619 and 694cm^{-1} are comparable to those found for NF_2Cl [15,16]. Our Raman spectrum of solid $NFCl_2$ at -130°C showed the following bands: 800 (5), $\nu_1(a')$, ν_{NF}; 689 (5), $\nu_5(a'')$, $\nu_{as}NCl_2$; 617 (33), $\nu_2(a')$, ν_sNCl_2; 430 (100), ν_3 (a'), δ_sFNCl_2; 348 (20), $\nu_6(a'')$, $\delta_{as}FNCl_2$; 281 (35), $\nu_4(a')$, δ_{sciss} NCl_2. The observed frequencies and relative intensities are in good agreement with the infrared data and confirm the assignments previously made [14] for the infrared spectrum of the gas.

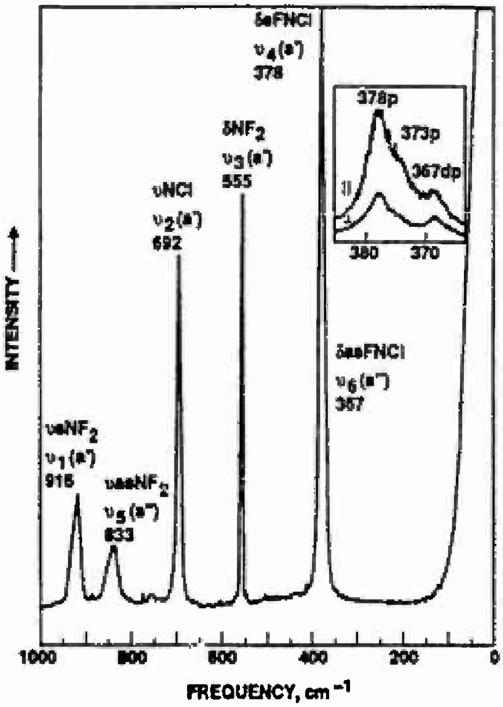

Fig. 2. Raman Spectrum of liquid NF_2Cl, recorded at -150°C. The insert shows polarization data for the 378 cm^{-1} band recorded with higher resolution and scale expansion.

The Raman spectrum of liquid NF_2Cl is shown in Figure 2. For the two FNCl deformation modes, the given assignment deviates from that [16] previously proposed. As recognized correctly in the previous matrix study, the two FNCl deformation modes nearly coincide, and three bands at 382, 377 and 366 cm^{-1} bad been observed. Since the antisymmetric NF_2 stretching mode, $\nu_5(a")$, had shown a 5 cm^{-1} splitting, it was assumed that the 382-377 cm^{-1} bands represent the second a" mode of NF_2Cl, with the 5cm^{-1} splittings being due to a site symmetry effect observable only for the a" modes [16]. The following observations in our study suggest that the previous assignments for the two FNCl deformations need to be reversed, i.e. that the a' FNCl deformation has a higher frequency than the a" one: (i) In our matrix IR spectrum, only a single band at 837 cm^{-1} was observed for the antisymmetric NF_2 stretching mode. (ii) The 378 cm^{-1} Raman band is clearly polarized, while the one at 367 cm^{-1} is depolarized; and (iii) the splitting of the 378 cm^{-1} band cannot be due to a matrix site symmetry effect because it was also observed for the Raman spectrum of the liquid. The splitting of the 378 cm^{-1} band might be attributed to the ^{35}Cl - ^{37}Cl isotopes, although the 5cm^{-1} separation appears rather large for a deformation mode, even if strong mixing with the N-Cl stretch is invoked.

ACKNOWLEDGMENTS

The work at the University of Denver was supported by the U.S. Air Force Office of Scientific Research and by the Petroleum Research Fund. The work at Rocketdyne was supported by the U.S. Army Research Office.

REFERENCES

1 J. Jander, Adv. Inorg. Chem. Radiochem., 19 (1976) 1.
2 F. P. Bowden and K. Sind, Proc. R. Soc. London, A277 (1984) 22.
3 J.V. Gilbert, X. L. Wu, D. H. Stedman, and R. D. Coombe, J. Phys. Chem., 91 (1987) 4265.
4 D. J. Benard, B. K. Winker, T. A. Seder, and R. H. Cohn, J. Phys. Chem., 93 (1989) 4790.
5 R. D. Coombe, D. Patel, A. T. Pritt Jr., and F. J. Wodarczyk, J. Chem. Phys., 75 (1981) 2177.
6 R. D. Coombe, J. Chem. Phys., 79 (1983) 254.
7 J. M. Herbelin and N. Cohen, Chem. Phys. Lett., 20 (1973) 605, and J. M. Herbelin, Chem. Phys. Lett., 42 (1976) 367.
8 B. Sukornick, R. F. Stahl, and J. Gordon, Inorg. Chem., 2 (1963) 875.
9 K. Dehnicke, Adv. Inorg. Chem. Radiochem., 26 (1983) 169.
10 A.V. Pankratov and O.M. Sokolov, Russ. J. Inorg. Chem., 13 (1968) 1481.
11 V. Grakauskas and K. Baum, J. Am. Chem. Soc., 91 (1969) 1679.
11 F. A. Miller and B. M. Harney, Appl. Spectrosc., 23 (1969) 8.
13 K. O. Christe, R. D. Wilson, and C. J. Schack, Inorg. Synth., 24 (1986) 3.
14 R. P. Hirschmann, L. R. Anderson, D. F. Harnish, and W. B. Fox, Spectrochim. Acta, Part A, 24A (1968) 1267.
15 R. Ettinger, J. Chem. Phys. 38 (1963) 2427.
16 J. J. Comeford, J. Chem. Phys., 45 (1966) 3463.

Revised JA901133V

The N_2F^+ Cation. An Unusual Ion Containing the Shortest Presently Known Nitrogen-Fluorine Bond

Karl O. Christe,*† Richard D. Wilson,† William W. Wilson,† Robert Bau,‡
Sunanda Sukumar ‡ and David A. Dixon◊

Contributions from Rocketdyne, A Division of Rockwell International Corporation, Canoga Park, California, 91303; and the Department of Chemistry, University of Southern California, Los Angeles, California, 90007; and the Central Research and Development Department, E.I. du Pont de Nemours and Company, Inc., Experimental Station, Wilmington, Delaware 19880.

Abstract

The $N_2F^+AsF_6^-$ salt was prepared in high yield from trans-N_2F_2 by thermal trans-cis isomerization in the presence of AsF_5 at 70°C. A displacement reaction between $N_2F^+AsF_6^-$ and FNO yields exclusively cis-N_2F_2. The Lewis acids BF_3 and PF_5 do not form a stable adduct with cis-N_2F_2 at temperatures as low as -78°C and do not catalyze the N_2F_2 trans-cis isomerization. A semi-empirical molecular orbital model is used to explain the puzzling differences in the reaction chemistry of cis- and trans-N_2F_2. The crystal structure of $N_2F^+AsF_6^-$ (monoclinic, C2/m, $a = 9.184(5)$Å, $b = 5.882(2)$Å, $c = 5.160(2)$Å, $\beta = 90.47(4)°$, Z = 2) was determined. Alternate space groups (Cm and C2) can be rejected based upon the observed vibrational spectra. Since in C2/m the N_2F^+ cations are disordered, only the sum of the N-F and N-N bond distances could be determined from the x-ray data. Local density

---

† Rocketdyne Division, Rockwell International Corporation

‡ University of Southern California, Los Angeles

◊ E.I. du Pont de Nemours and Company, Inc.

functional calculations were carried out for N_2F^+ and the well known isoelectronic FCN molecule. The results from these calculations allowed the sum of the N_2F^+ bond lengths to be partitioned into the individual bond distances. The resulting N-F bond length of 1.217Å is by far the shortest presently known N-F bond, while the N-N bond length of 1.099Å is comparable to the shortest presently known N-N bond length of 1.0976(2)Å in N_2. The surprising shortness of both bonds is attributed to the high s-character (sp hybrid) of the σ-bond orbitals on nitrogen and the formal positive charge on the cation. Thus, the shortening of the N-F bond on going from sp^3-hybridized NF_4^+ (1.30Å) to sp-hybridized N_2F^+ (1.22Å) parallels those found for the C-H and C-F bonds in the CH_4, $CH_2{=}CH_2$, $CH{\equiv}CH$ and CF_4, $CF_2{=}CF_2$, $FC{\equiv}N$ series, respectively. The oxidative power of N_2F^+ has also been studied. The N_2F^+ cation oxidized Xe and ClF to XeF^+ and ClF_2^+, respectively, but did not oxidize ClF_5, BrF_5, IF_5, XeF_4, NF_3 or O_2.

Introduction

The chemistry of N_2F_2 and its derivatives is fascinating and presents many mysteries.[1] Thus, N_2F_2 exists as two planar F-N=N-F isomers, a cis- and a trans- form. In spite of only a small enthalpy difference of 3.04 kcal/mol between the two isomers,[2] their properties and reaction chemistry are very different. For example, only the cis-isomer reacts with strong Lewis acids to form N_2F^+ salts. Furthermore, some of the synthetic methods for N_2F_2 produce exclusively the trans-isomer, and its slow and erratic isomerization to the more stable cis-isomer is poorly understood, as shown by recent ab initio calculations.[3]

The N_2F^+ cation[4-9] is also of great interest. Force field[9] and ab initio calculations[10-12] suggested that this cation should possess an unusually short N-F bond. Based on the previously published[9] NF stretching force constant value of 8.16 mdyn/Å and N-F bond length-force constant plots,[10,13] a value of about 1.23Å can be extrapolated for the N-F bond in N_2F^+. This surprisingly short N-F bond length value for N_2F^+ was also supported by ab initio calculations[10-12] which resulted in values of 1.28, 1.24 and 1.23Å, respectively. Considering that in covalent main group element fluorides the bond length generally decreases with an increase in the formal oxidation state of the central atom and that the shortest previously known N-F bond was 1.30Å in NF_4^+ (+V),[14] a value of about 1.23Å for N_2F^+ (+I) would be unique indeed.

On the other hand, if the N-F bond length in N_2F^+ were considerably longer than the value predicted from the force field computations, the N_2F^+ cation would be an ideal test case for "Gordy's Rule."[15] According to this rule, the bond stretching force constant k is related to the bond distance d by the equation

$$k_{AB} = aN\,(X_A X_B / d^2_{AB})^{3/4} + b$$

where X are the Pauling electronegativities, N the bond order, and a and b empirically determined constants. Although no a priori reason dictates such a relationship since bond lengths measure the position of the potential energy minimum whereas force constants indicate its curvature, only one exception to Gordy's Rule has previously been reported.[16] Thus, a knowledge of the N-F bond distance in N_2F^+ was of significant interest since it would either confirm the existence of an unusually short N-F bond or provide a rare example of a species not obeying Gordy's Rule.

Experimental Section

Materials. The following materials were commercial compounds and used without further purification: N_2F_4 (Air Products); Xe, O_2, IF_5, PF_5, and BF_3 (Matheson); ClF_5 and NF_3 (Rocketdyne); and ClF (Ozark Mahoning). Literature methods were used for the syntheses of trans-N_2F_2,[17] $N_2F^+AsF_6^-$,[4] FNO,[18] and XeF_4,[19] the purification of BrF_5,[20] and the drying of HF.[21]

Apparatus. Volatile materials were handled in a well-passivated (with ClF_3) stainless steel Teflon-FEP vacuum line.[22] Nonvolatile materials were manipulated under the dry nitrogen atmosphere of a glove box. Vibrational spectra were recorded as previously described.[20]

Reaction of $N_2F^+AsF_6^-$ with FNO. A sample of $N_2F^+AsF_6^-$ (1.84 mmol) was placed inside the dry box into a prepassivated 3/4 inch Teflon-FEP ampule that was closed by a stainless steel valve. On the vacuum line, FNO (4.14 mmol) was added at -196°C, and the resulting mixture was allowed to slowly warm from -196 to -78°C by the use of a liquid N_2-dry ice slush bath. The mixture was then allowed to slowly warm from -78°C to room temperature over a 12 hour period. The ampule was cooled to -196°C, and the volatile material was separated during warm up of the ampule to 25°C by fractional condensation through traps kept at -126 and -210°C. The -126°C trap contained unreacted FNO (2.29 mmol) and the -210°C trap contained cis-N_2F_2 (1.8 mmol). The white solid residue (401 mg, weight calcd for 1.84 mmol of $NO^+AsF_6^-$ = 403 mg) was identified by vibrational spectroscopy as $NO^+AsF_6^-$.[23]

Oxidation Reactions of $N_2F^+AsF_6^-$. All oxidation reactions of $N_2F^+AsF_6^-$ were carried out in the same manner. About 2 mmol of $N_2F^+AsF_6^-$ was placed in the dry box into a prepassivated 0.5 inch o.d. Teflon-FEP ampule that was closed by a stainless steel valve. On the vacuum line, about 2 ml of liquid anhydrous HF and about 5 mmol of the compound to be oxidized were added, and the resulting mixture was kept at room temperature for 24 hours. The ampule was cooled to -196°C and the amount of evolved nitrogen was measured by expansion into the vacuum line. The material volatile at room temperature was separated by fractional condensation through a series of cold traps kept at appropriate temperatures. The contents of these traps were measured by PVT and identified by infrared spectroscopy. The solid residues in the ampule were weighed and identified by infrared and Raman spectroscopy.

Crystal Structure Determination of $N_2F^+AsF_6^-$. Single crystals of $N_2F^+AsF_6^-$ were obtained by slowly cooling a saturated HF solution from 25 to 0°C and separating the resulting crystals from the cold solution by decantation. A suitable crystal was selected under a microscope inside the glove box and sealed in a quartz capillary.

Diffraction data were collected at room temperature using a Siemens/Nicolet/Syntex $P2_1$ diffractometer with Mo $K\alpha$ radiation up to a 2θ limit of 45°. A total of 1272 intensity values for an entire reflection sphere was collected and the four equivalent quadrants merged to give 364 unique reflections. An empirical ψ-scan absorption correction was applied, based on the variation in intensity of an axial reflection.[24]

The pattern of systematic absences was consistent with any one of the following centered monoclinic space groups: C2 (#5), Cm (#8), or C2/m (#12). The structure was solved for all three space groups. The positions of the atoms were obtained by direct methods using the computing package SHELX-86.[25] The structures were then refined using 362 reflections with $I > 3\sigma(I)$. Details of the data collection parameters and other crystallographic information are given in Table 1. The final atomic coordinates, thermal parameters, interatomic distances and bond angles for the preferred (see Discussion section) C2/m model are given in Tables 2-4, respectively.

Computational Methods. The geometry and vibrational frequencies of N_2F^+ and FCN were calculated in the local density functional approximation[26] by using the program system DMol.[27] The atomic basis functions are given numerically on an atom-centered, spherical-polar mesh. The radial portion of the grid is obtained from the solution of the atomic LDF equations by numerical methods. The radial functions are stored as sets of cubic spline coefficients so that the radial functions are piece-wise analytic, a necessity for the evaluation of gradients. The use of exact spherical atom results offers some advantages. The molecule will dissociate exactly to its atoms within the LDF framework, although this does not guarantee correct dissociation energies. Furthermore, because of the quality of the atomic basis sets, basis set superposition effects should be minimized and correct behavior at the nucleus is obtained.

Since the basis sets are numerical, the various integrals arising from the expression for the energy need to be evaluated over a grid. The integration points are generated in terms of angular functions and spherical harmonics. The number of radial points N_R is given as

$$N_R = 1.2 \times 14\,(Z - 2)^{1/3}$$

where Z is the atomic number. The maximum distance for any function is 12 a.u. The angular integration points N_0 are generated at the N_R radial points to form shells around each nucleus. The value of N_0 ranges from 14 to 302 depending on the behavior of the density.[28] The Coulomb potential corresponding to the electron repulsion term is determined directly from the electron density by solving Poisson's equation. In DMol, the form for the exchange-correlation energy of the uniform electron gas is that derived by von Barth and Hedin.[29]

All of the DMol calculations were done with a double numerical basis set augmented by polarization functions. This can be thought of in terms of size as a polarized double zeta basis set. However, because of the use of exact numerical solutions for the atom, this basis set is of significantly higher quality than a normal molecular orbital double zeta basis set. The fitting functions have angular momentum numbers one greater than that of the polarization function. Since all of the atoms have d polarization functions, the value of l for the fitting function is 3.

Geometries were optimized by using analytic gradient methods. There are two problems with evaluating gradients in the LDF framework which are due to the numerical methods that are used. The first is that the energy minimum does not necessarily correspond exactly to the point with a zero derivative.

The second is that the sum of the gradients may not always be zero as required for translational invariance. These tend to introduce errors on the order of 0.001Å in the calculation of the coordinates if both a reasonable grid and basis set are used. This gives bond lengths and angles with reasonable error limits. The difference of 0.001Å is about an order of magnitude smaller than the accuracy of the LDF geometries when compared to the experimental ones. The frequencies were determined by numerical differentiation of the gradient. A two point difference formula was used and a displacement of 0.01 a.u.

Results and Discussion

Trans-Cis Isomerization of N_2F_2 and the Synthesis of N_2F^+ Salts. Most of the known N_2F_2 syntheses produce exclusively the trans-isomer.[1] Since the trans-isomer is much less reactive than the cis-isomer and, for example, does not form N_2F^+ salts, conversion of the trans- to the cis-isomer is often required. This trans-cis isomerization is usually quite erratic. Although it proceeds at room temperature in stainless steel, it often exhibits long and irreproducible induction periods and requires numerous months to go to completion. This isomerization can be accelerated by increasing the temperature; however, the yields of cis-N_2F_2 sharply decrease at elevated temperature due to decomposition of N_2F_2 to $N_2 + F_2$.[30] In our study, aimed at the isomerization of N_2F_2 and its subsequent conversion to $N_2F^+AsF_6^-$, it was found advantageous to combine the trans-N_2F_2 with an excess of AsF_5 in a prepassivated, small volume stainless steel cylinder and to carry out the isomerization at about 70°C. In this manner, any cis-N_2F_2 formed is immediately removed from the cis-trans equilibrium by complexation and thereby protected against decomposition to N_2 and F_2. In this manner, yields of $N_2F^+AsF_6^-$ as high as 80% have been obtained from trans-N_2F_2 in three days at 70°C.

It was also of interest to study which N_2F_2 isomer is formed in the displacement reactions of $N_2F^+AsF_6^-$ with a strong Lewis base, such as FNO. It was found that exclusively cis-N_2F_2 is formed in quantitative yield according to

$$N_2F^+AsF_6^- + FNO \rightarrow NO^+AsF_6^- + \text{cis-}N_2F_2$$

Recent ab initio calculations[3] on the transition state structure for the N_2F_2 trans-cis isomerization resulted in the proposition of structure (I). A similar transition state might be expected for a fluoride abstraction from cis-N_2F_2 (III) by a strong Lewis acid leading to the N_2F^+ cation (II).

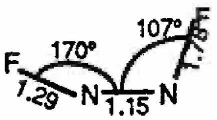

I

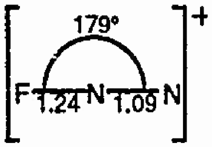

II

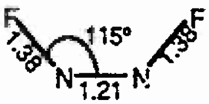

III

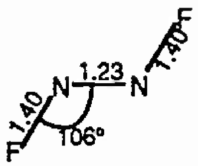

IV

These results suggested that Lewis acids which are capable of forming N_2F^+ salts might also promote the formation of the isomerization transition state and thereby catalyze the N_2F_2 trans-cis isomerization. In order to be an effective isomerization catalyst, the strength of the Lewis acid should be such that it interacts with N_2F_2 but does not form a stable complex at the desired isomerization temperature. To test the validity of this approach, we have studied the interaction of cis-N_2F_2 with BF_3 and PF_5. It was found that the resulting N_2F_2 adducts are indeed labile enough and exhibit some dissociation pressure at temperatures as low as -78°C. However, both PF_5 and BF_3 did not catalyze the isomerization of trans-N_2F_2 to cis-N_2F_2 in the temperature range of -78 to 25°C.

Thus, the chemistry of N_2F_2 raises numerous puzzling questions for which, to our best knowledge, no satisfactory answers have previously been given.[1] Among these questions are: (i) why does only cis-N_2F_2, but not trans-N_2F_2 form N_2F^+ salts, (ii) why do Lewis acids not catalyze the N_2F_2 trans-cis isomerization, and (iii) why is the cis-N_2F_2 isomer exclusively formed in the displacement reaction between N_2F^+ salts and FNO?

The great difference in reactivity between cis- and trans-N_2F_2 cannot be due to differences in thermodynamic properties or bond strengths because these values are very similar for both molecules.[1] Therefore, the difference in reactivity should be connected with the different spatial arrangement of the fluorine ligands and the free valence electron pairs on nitrogen. Using a semi-empirical molecular orbital model, the bonding in N_2F_2 can be described by two sp^2 hybridized nitrogen atoms resulting in one N-N and two N-F σ-bonds and two sterically active, free valence electron pairs on the two nitrogens. In addition, the remaining p orbitals on the nitrogen atoms form a [p-p] π-bond perpendicular to the plane of the sp^2 hybrids. In linear N_2F^+, the two nitrogens form a [sp-sp] σ-bond and two perpendicular [p-p] π-bonds.

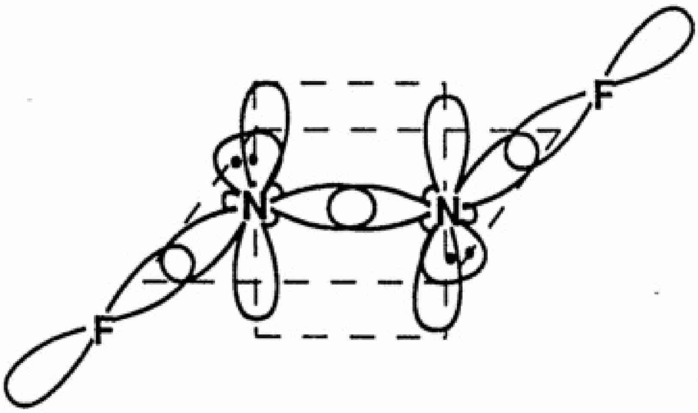

trans-N_2F_2

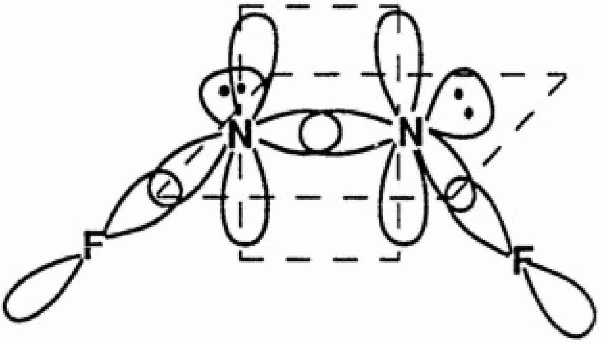

cis-N_2F_2

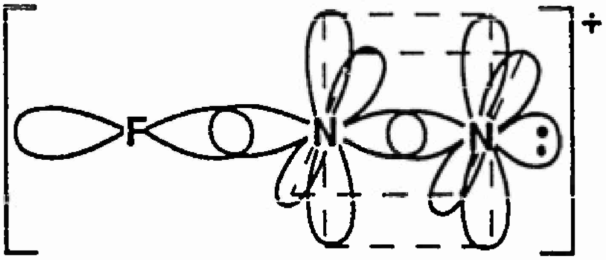

N_2F^+

When a Lewis acid, such as AsF_5, approaches a cis-N_2F_2 molecule, one of the fluorine ligands and hereby some electron density is pulled away from the remainder of the molecule. This results in an intermediate similar to the transition state (I) of the N_2F_2 trans-cis isomerization. This removal of electron density from one of the nitrogen atoms should result in the lowering of the electron density in the antibonding orbitals of the two free valence electron pairs on the two nitrogens. This enables them to form a partial triple bond, as demonstrated by the shortening of the N-N bond from 1.21Å in cis-N_2F_2 (III) to 1.15Å in the postulated trans-cis isomerization transition state (I). Therefore, the energy required for the elongation of one of the N-F bonds in (I) can be compensated for by the simultaneous formation of a partial N≡N triple bond thereby resulting in a very low energy barrier toward N_2F^+ formation. However, the formation of such a partial N≡N triple bond should be possible only for cis-N_2F_2, i.e. when the two free valence electron pairs on the nitrogens are on the same side of the molecule and can overlap. In trans-N_2F_2, migration of a nitrogen free valence electron pair from one side of the molecule to the other is blocked in the N_2F_2 plane by the fluorine ligands and in the perpendicular plane by the [p-p] π-bond. Furthermore, the N=N double bond in N_2F_2 does not permit free rotation around the N-N axis. Therefore, N_2F^+ formation from trans-N_2F_2 should be a high activation energy process requiring almost complete removal of one fluoride ion from N_2F_2, before the FNN angle in the remaining FN_2 fragment becomes large enough for the nitrogen free electron pair to tunnel through to the other side and form the second π-bond.

This rationale explains not only why trans-N_2F_2 does not form N_2F^+ salts, but also why Lewis acids do not catalyze the N_2F_2 trans-cis isomerization. As already pointed out above, the structure of the isomerization transition state closely resembles that of an expected intermediate in the N_2F^+ formation. If Lewis acids cannot abstract an F^- anion from trans-N_2F_2, it is then not surprising at all that they also do not promote the formation of the isomerization transition state.

The third question remaining to be answered was why in the FNO displacement reaction of $N_2F^+AsF_6^-$ exclusively the cis-N_2F_2 isomer is formed. In N_2F^+, the most important resonance structure is $[F\text{-}N^+{\equiv}N|]$ and, therefore, the formal positive charge resides mainly on the α-nitrogen atom. Furthermore, the free valence electron pair on the β-nitrogen atom is more diffuse than the N-F bond pair orbitals. Consequently, the attack of F^- on N_2F^+ should occur at the α-nitrogen atom resulting in the formation of an intermediate $F_2N{=}N$ molecule. The latter could easily undergo an α-fluorine migration to give FNNF.

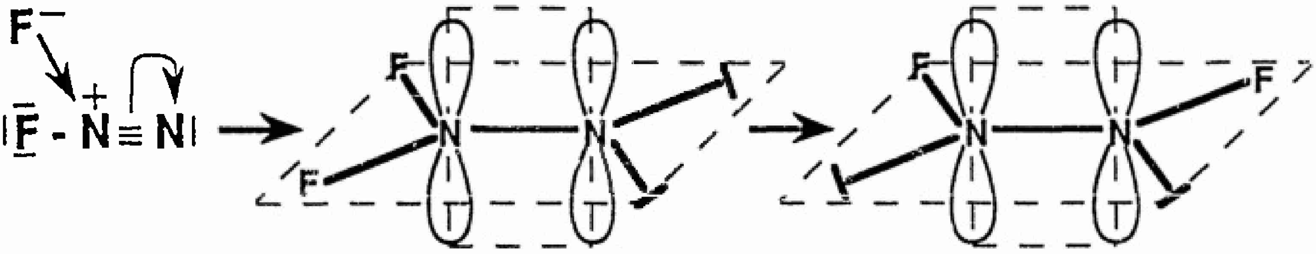

Since in all these steps a [p-p] π-bond between the two nitrogens is always retained, free rotation around the N-N axis is precluded and the rearrangement of the fluorine atoms and the nitrogen free valence electron pairs must take place in the plane perpendicular to the N-N π-bond. Therefore, the sequence of the fluorine ligands and the nitrogen free electron pairs in $F_2N{=}N$ (F,F,P,P) must also be retained in FNNF, resulting exclusively in the cis-FNNF isomer. The general ease of this type of α-migration could explain the failure to isolate the intermediate $F_2N{=}N$ isomer.

Structure of the N_2F^+ Cation. The crystal structure of $N_2F^+AsF_6^-$ can be solved either in the non-centrosymmetric space groups Cm or C2 with ordered or disordered N_2F^+ cations, respectively; or the centrosymmetric space group C2/m with disordered N_2F^+ cations. All three models resulted in acceptable agreement factors (Cm, R=2.96%; C2, R=2.68%; C2/m, R=4.04%) which to some extent are influenced by the number of variable parameters (Cm, 53; C2, 46; C2/m, 30). The Cm model resulted in an ordered almost linear N_2F^+ cation (r_{NF} = 1.221 (13)Å, r_{NN} = 1.099(13)Å, $\angle$ NNF = 177.2 (8)°) and a strongly distorted AsF_6^- anion with angles deviating by as much as 11.5° from those of an ideal octahedron. The C2 model resulted in a disordered bent N_2F^+ cation ($\Sigma r_{NF} + r_{NN}$ = 2.342(22)Å, $\angle$ NNF = 163.6(12)°) and again a strongly distorted AsF_6^- anion with angles deviating by as much as 13.8° from O_h symmetry. The C2/m model resulted in a disordered linear N_2F^+ cation ($\Sigma r_{NF} + r_{NN}$ = 2.316(12)Å) and an AsF_6^- anion which within experimental error is perfectly octahedral. Since the Raman spectra of $N_2F^+AsF_6^-$ crystals are in perfect agreement with O_h symmetry (only three narrow bands at 689 (ν_1, A_{1g}), 576 (ν_2, E_g), and 376cm^{-1} (ν_5, F_{2g}) with half widths of 10cm^{-1} or less at 25°C), models Cm and C2 must be rejected in spite of their lower R factors. This situation closely resembles that in isotypic $NS_2^+AsF_6^-$ for which the alternate Cm and C2 models could also be rejected based on the observed vibrational spectra.[31] The packing diagram for $N_2F^+AsF_6^-$ is shown in Figure 1. The AsF_6^- anions occupy the corners of the cell and the centers of the *a b* faces, while the NX_2 cations occupy the remaining faces of the cell.

As pointed out already in the introduction, a knowledge of the exact N-F and N-N bond distances in N_2F^+ is of great general interest. Since the above crystal structure determination provides only a value for the sum of the N-F and N-N bond lengths, a reliable method was sought to partition this sum into its individual components. This partitioning was achieved by local density functional (LDF) calculations providing both the geometry and the vibrational frequencies.

The accuracy of the LDF calculations was tested for FCN which is isoelectronic with FNN^+ and for which both the geometry[32] and the vibrational frequencies[33] are well known (see Table 5). As expected from a number of studies,[34] the LDF method slightly overestimates the bond distances and vibrational frequencies, but otherwise excellently reproduces the experimental values (see Table 5). Similarly, LDF calculations for the dinitrogen molecule, N_2, resulted in a bond length value (1.113Å) only slightly longer than the experimental one (1.098Å).[35]

The results of the LDF calculations for N_2F^+ are summarized in Table 6. As expected, the N_2F^+ cation is linear and the bond lengths are, as for isoelectronic FCN, slightly too long. To obtain better estimates for the actual bond lengths, the LDF values can be scaled in the following manner. Using the scaling factors from the FCN calculations, one obtains the values labelled LDFS1. Using the N_2 results for scaling r_{N-N} and the NF_4^+ results for scaling r_{N-F}, [r_{N-F}, LDF = 1.324Å,[36] experimental = 1.297Å[14]], one obtains the values labelled LDFS2. The sum of r_{N-N} and r_{N-F} of LDFS2 (2.331Å) is very close to that obtained from the crystal structure determination (2.316Å). If one partitions the experimentally determined sum of $r_{N-N} + r_{N-F}$ in the same ratio as that in LDFS2, final values of 1.217 and 1.099Å are obtained for r_{N-F} and r_{N-N}, respectively, in N_2F^+ (see Table 6). The close agreement between these values and those ($r_{NF} = 1.221$, $r_{NN} = 1.099$Å) obtained by the rejected Cm model with ordered N_2F^+ cations (see above) might be fortuitous.

Of the previously calculated[10-12] N-N and N-F bond lengths for N_2F^+, the SCF 6-31G* and MP-2 6-31G* values of Peters[11] (see Table 6) come the closest to the values from this study but appear to either underestimate or overestimate the r_{N-N} value. When comparing the calculated LDF vibrational frequencies of N_2F^+ with the observed ones (see Table 6), the agreement is very satisfactory, particularly if it is kept in mind that the LDF values are unscaled, harmonic, gas phase frequencies and the experimental values are anharmonic, solid state frequencies.

As shown above, the N_2F^+ cation is linear. This result confirms a recent theoretical study[12] which concluded that, contrary to P_2F^+, for N_2F^+ the linear $C_{\infty v}$ structure is favored by about 50 to 60 kcal over the symmetric, three membered ring structure of symmetry C_{2v}. As already pointed out in the introduction, the most interesting aspect of the N_2F^+ structure is its N-F bond distance. This distance (1.22Å) is by far the shortest distance found to date for any N-F bond. The previously known range for N-F bonds extended from 1.512Å in FNO to 1.30Å in NF_4^+.[13,14] The value of 1.22Å found for N_2F^+ is in good agreement with the value of 1.24Å estimated from a force field calculation[9] and force constant-bond distance plot extrapolations.[11,13] The excellent agreement between our experimental value and the value extrapolated from the stretching force constant demonstrates that N_2F^+ conforms with Gordy's rule.[15]

The nitrogen-nitrogen bond distance in N_2F^+ is also of interest. Its value of 1.099Å is comparable to those of 1.0976(2)Å[26] in N_2 and 1.118Å in N_2^+[38] and confirms its triple bond character. Thus the N_2F^+ cation is highly unusual. It possesses by far the shortest known N-F bond while at the same time exhibiting an N-N bond length comparable to the shortest known N-N bond. How can these unusually short bond distances be explained? It is tempting to invoke partial double bond character for the N-F bond by writing the following resonance structures:

$$[\,|\overline{\underline{F}}\text{-N}\equiv\text{N}\ ]^+ \leftrightarrow [\langle\text{F=N=N}\rangle]^+$$

If, however, the N-F bond assumes partial double bond character, the N≡N bond must lose some of its strength and lengthen accordingly. This is not the case, as evidenced by the short N≡N bond of 1.099Å in N_2F^+.

Although a formal positive charge and other highly electronegative ligands generally tend to increase the bond strength of an X-F bond, this effect alone is insufficient to explain the unusually short N-F and N≡N bonds in N_2F^+. For example, the N-F bond in NF_4^+ still has a value of 1.30Å,[14] in spite of a formal positive charge and three additional fluorine ligands which should be more electronegative than the nitrogen ligand in $N{\equiv}NF^+$.

The most plausible explanation for the shortening of the N-F bond in N_2F^+, compared to NF_4^+, is the change in hybridization of the nitrogen molecular orbitals. From carbon chemistry it is well known that the C-H and C-F bond lengths significantly decrease with increasing s-character of the carbon molecular orbital. Therefore, a similar bond shortening should be expected on going from sp^3-hybridized NF_4^+ to sp-hybridized $N{\equiv}NF^+$ (see Table 7). To our knowledge, this is the first example of hybridization induced, dramatic bond shortening outside of carbon chemistry.

The N_2F^+ Cation as an Oxidative Fluorinator. In view of N_2 having a higher ionization potential than Kr, i.e. 15.576 versus 13.999 eV,[40] and KrF^+ being the most powerful presently known oxidative fluorinator,[41] it was interesting to examine the oxidative power of the N_2F^+ cation. For this purpose, the reactions of $N_2F^+AsF_6^-$, dissolved in anhydrous HF, were studied at 25°C with the following substrates: ClF_5, BrF_5, IF_5, XeF_4, Xe, ClF, O_2, and NF_3. The KrF^+ cation is capable of oxidizing all of these substrates under comparable reaction conditions. For example, $HalF_5$ is oxidized to $HalF_6^+$ salts, XeF_4 to XeF_5^+, O_2 to O_2^+, and NF_3 to NF_4^+.[41] In the case of N_2F^+ the only substrates oxidized were Xe and ClF according to:

$$N_2F^+AsF_6^- + Xe \xrightarrow[25^\circ C]{HF} XeF^+AsF_6^- + N_2$$

$$N_2F^+AsF_6^- + ClF \longrightarrow ClF_2^+AsF_6^- + N_2$$

The first reaction was briefly mentioned in a previous paper,[42] but no experimental details were given.

To examine whether fluorination reactions with N_2F^+ might benefit from elevated temperatures, $N_2F^+AsF_6^-$ was heated with a large excess of either ClF_5 or BrF_5 in a small ullage stainless steel cylinder, in the absence of HF, to 70°C for three days. Again, no evidence for the formation of either ClF_6^+ or BrF_6^+ was detected. In the case of ClF_5, however, a small amount of the N_2F^+ starting material was fluorinated by ClF_5 to $N_2F_3^+$. A detailed analysis of the factors determining the relative strength of an oxidative fluorinator will be given in a separate paper.[43]

Acknowledgment. The authors thank Dr. Carl Schack for his help and the U.S. Army Research Office and U.S Air Force Astronautics Laboratory for financial support of the work at Rocketdyne.

Supplementary Material Available. Table SI listing observed and calculated structure factors (2 pages). Ordering information is given on any current masthead page.

References

1. For an exhaustive review of the properties and chemistry of N_2F_2 see Gmelin Handbook of Inorganic Chemistry, Fluorine, Supplement Volume 4, pages 385-403, Springer Verlag, Berlin (1986).
2. Craig, N. C.; Piper, L. G.; Wheller, V. L. J. Phys. Chem., 1971, 75, 1453.
3. Lee, T. J.; Rice, J. E.; Scuseria, G. E., Schaefer, H. F. III. Theor. Chim. Acta, 1989, 75, 81.
4. Moy, D.; Young, A. R. J. Amer. Chem. Soc., 1965, 87, 1889.
5. Ruff, J. K. Inorg. Chem., 1966, 5, 1791.
6. Roesky, H. W.; Glemser, O.; Bormann, D. Chem. Ber., 1966, 99, 1589.
7. Pankratov, A. V.; Savenkova, N. I. Russ. J. Inorg. Chem., 1968, 13, 1345.
8. Shamir, J.; Binenboym, J. J. Mol. Structure, 1969, 4, 100.
9. Christe, K. O.; Wilson, R. D.; Sawodny, W. J. Mol. Structure, 1971, 8, 245.
10. Pulay, P.; Ruoff, A.; Sawodny, W. Mol. Phys., 1975, 30, 1123.
11. Peters, N. J. S. Chem. Phys. Letters, 1987, 142, 76.
12. Yakobson, V. V.; Zyubina, T. S.; Charkin, O. P. Russ. J. Inorg. Chem., Engl., 1988, 33, 1727.
13. Christe, K. O. Spectrochim. Acta, Part A, 1986. 42A, 939.
14. Christe, K. O.; Lind, M. D.; Thorup, N.; Russell, D. R.; Fawcett, J.; Bau, R. Inorg. Chem., 1988, 27, 2450.
15. Gordy, W. J. Chem. Phys., 1946, 14, 305.
16. Mack, H. G.; Christen, D.; Oberhammer, H. J. Mol. Struct., 1988, 190, 215.
17. Münch, V.; Selig, H. J. Fluorine Chem., 1980, 15, 235.
18. Christe, K. O. Inorg. Chem., 1973, 12, 1580.
19. Bartlett, N.; Sladky, F. O. J. Amer. Chem. Soc., 1968, 90, 5316.
20. Wilson, W. W.; Christe, K. O. Inorg. Chem., 1987, 26, 1573.
21. Christe, K. O.; Wilson, W. W.; Schack, C. J. J. Fluorine Chem., 1978, 11, 71.

22. Christe, K. O.; Wilson, R. D.; Schack, C. J. Inorg. Synth., 1986, 24, 3.

23. Griffiths, J. E.; Sunder, W. A.; Falconer, W. E. Spectrochim. Acta, Part A, 1975, 31A, 1207.

24. For details on the ψ-scan empirical correction, see Churchill, M. R.; Hollander, F. J. Inorg. Chem., 1978, 17, 3548.

25. Sheldrix, G. M. SHELX System of Crystallographic Programs, University of Goettingen, West Germany, 1986.

26. a) Parr, R. G.; Yang, W. Density Functional Theory of Atoms and Molecules, Oxford Univeristy Press, New York, 1989.

b) Salahub, D. R. in Ab Initio Methods in Quantum Methods in Quantum Chemistry-II, ed. by Lawlwy, K. P.; J. Wiley & Sons, New York, 1987, p. 447.

c) Wimmer, E.; Freeman, A. J.; Fu, C. -L.; Cao, P. -L.; Chou S. -H.; Delley, B. in "Supercomputer Research in Chemistry and Chemical Engineering" ed. by Jensen, K. F.; Truhlar, D. G. ACS Symposium Series, American Chemical Society, Washington, D.C., 1987, p. 49.

d) Jones, R. O.; Gunnarsson, O. Rev. Mod. Phys. 1989, 61 689.

27. Delley, B. J. Chem. Phys. 1990, 92, 508. DMol is available commercially from BIOSYM Technologies, San Diego, CA.

28. This grid can be obtained by using the FINE parameter in DMol.

29. von Barth, U.; Hedin, L. J. Phys. Chem., 1972, 5, 1629.

30. Pankratov, A. V.; Sokolov, O. M. Russ. J. Inorg. Chem., 1966, 11, 943.

31. Johnson, J. P.; Passmore, J.; White, P. S.; Banister, A. J.; Kendrick, A. G. Acta Cryst. Part C 1987, C43, 1651.

32. Harmony, M.D.; Laurie, V. W.; Kuczkowski, R. L.; Schwendeman, R. H.; Ramsay, D.A.; Lovas, F.J.; Lafferty, W. J.; Maki, A. G. J. Phys. Chem. Ref. Data, 1979, 8, 619. See p. 640.

33. Shimanouchi, T. J. Phys. Chem. Ref. Data, 1977, 6, 993.

34. a) Dixon, D. A.; Andzelm, A.; Fitzgerald, Wimmer, E.; Delley, B. Science and Engineering on Cray Supercomputers Proceedings of the Fifth International Symposium, Cray Research, Minneapolis, MN, 1990.

b) Dixon, D. A.; Andzelm, A.; Fitzgerald, Wimmer, E.; Jasien, P. in "Theory and Applications of Density Functional Approaches to Chemistry," ed. by J. Labanowski, 1990, in press.

35. Huber, K. P.; Herzberg, G. "Constants of Diatomic Molecules", Van Nostrand Reinhold, New York, 1979.

36. Dixon, D. A.; Christe, K.O., unpublished work.

37. Wilkinson, P. G. J. Astrophys., 1957, 126, 1.

38. Wilkinson, P. G. Can. J. Phys., 1956, 34, 250.

39. "Tables of Interatomic Distances and Configuaration in Molecules and Ions," The Chemical Society, London, Special Publication No. 11, 1958.

40. CRC Handbook of Chemistry and Physics, 60th Edn., CRC Press, Boca Raton, FA 1979.

41. Christe, K. O.; Wilson, W. W.; Wilson, R. D. Inorg. Chem., 1984, 23, 2058.

42. Stein, L. Chemistry, 1974, 47, 15.

43. Christe, K.O.; Wilson, W. W.; Dixon, D. A. to be published.

Table 1. Summary of Crystal Data and Refinement Results for $N_2F^+AsF_6^-$

space group	C2/m (#12)
a (Å)	9.184(5)
b (Å)	5.882(2)
c (Å)	5.160(2)
β (deg)	90.47(4)
V (Å^3)	278.7(2)
molecules/unit cell	2
formula weight (g)	235.9
crystal dimensions (mm)	0.32 x 0.38 x 1.08
calculated density (g cm^{-3})	2.82
absorption coefficient (mm^{-1})	59.8
range in transmission factor (normalized to unity)	0.61 - 1.00
wavelength (Å) used for data collection	0.71069
sin θ/λ limit (Å^{-1})	0.6497
total number of reflections measured	1272
number of independent reflections	364
number of reflections used in structural analysis $I>3\sigma(I)$	362
number of variable parameters	30
final agreement factor	0.0404

Table 2. Final Atomic Coordinates for $N_2F^+AsF_6^-$

Atom	x	y	z	number[a]
As1	0	0	0.5	2
F2	0.1235(6)	0	0.2574(9)	4
F3	-0.0948(5)	0.2027(9)	0.3406(9)	8
N4	0	0.5	1	2
X5[b]	-0.1203(7)	0.5	0.9313(11)	4

(a) Number of times this atom appears in the unit cell

(b) X is the disordered terminal atom (50% N / 50% F) of the $[N_2F]^+$ cation in space group C2/m

Table 3. Final Temperature Factors for $N_2F^+AsF_6^-$

Atom	$U_{11} \times 10^4$	$U_{22} \times 10^4$	$U_{33} \times 10^4$	$U_{12} \times 10^4$	$U_{13} \times 10^4$	$U_{23} \times 10^4$
As1	416(5)	331(5)	333(4)	0(0)	9(4)	0(0)
F2	745(16)	935(17)	659(16)	0(0)	312(15)	0(0)
F3	1220(16)	1407(17)	1240(16)	715(16)	301(15)	716(16)
N4	723(18)	440(17)	532(17)	0(0)	146(17)	0(0)
X5[a]	655(17)	750(17)	809(17)	0(0)	7(16)	0(0)

(a) X is the disordered terminal atom (50% N / 50% F) of the $[N_2F]^+$ cation in space group C2/m

Table 4. Bond Distances (Å) and Bond Angles (deg) in $[N_2F]^+[AsF_6]^-$

As1-F2	1.696(4)
As1-F3	1.686(4)
N4-X5	1.158(6)
F2-As1-F3	89.2(2)
F2-As1-F2'	180.0(0)
F2'-As1-F3	90.8(2)

F3-As1-F3'	180.0(0)
F3-As1-F3"	90.0(2)
F3'-As1-F3"	90.0(2)
F3"-As1-F3'"	180.0(0)
X5-N4-X5'	180.0(0)

Table 5. Calculated and Experimental Bond Distances (Å) and Vibrational Frequencies (cm^{-1}) for FCN

	Expt	Calcd (LDF)
$r_{C\equiv N}$	1.159	1.169
r_{C-F}	1.262	1.274
C≡N stretch	2323	2355
C-F stretch	1077	1081
F-C≡N bend	451	465

Table 6. Calculated and Experimental Bond Distances (Å) and Vibrational Frequencies (cm^{-1}) for FNN^+

	Expt	Calcd (LDF)				
		LDF	LDFS1	LDFS2	SCF 6-31G*[a]	MP-2 6-31G*[a]
$r_{N\equiv N}$	$(1.099)^b$	1.121	1.111	1.106	1.072	1.138
r_{N-F}	$(1.217)^b$	1.248	1.236	1.225	1.240	1.256
$\Sigma r_{N-N} + r_{N-F}$	2.316(12)	2.369	2.347	2.331	2.312	2.394
N≡N stretch	2373	2409				
N-F stretch	1059	1100				
F-N≡N bend	388	438				

(a) data from ref. 11

(b) values obtained by partitioning the experimentally measured sum of $r_{N-N} + r_{N-F}$ according to their ratio in LDFS2

Table 7. Influence of Hybridization on Bond Lengths (Å) in Carbon and Nitrogen Compounds

	CH_4 (sp^3)	$H_2C=CH_2$ (sp^2)	HC≡CH (sp)
r_{C-H}	1.094^a	1.085^a	1.061^a

	CF_4 (sp^3)	$F_2C=CF_2$ (sp^2)	FC≡N (sp)
r_{C-F}	1.323^b	1.313^b	1.262^a

	NF_4^+	$[FN=NF_2]^+$	$[FN\equiv N]^+$
r_{N-F}	1.30^c	?	1.22^d

(a) data from ref. 32
(b) data from ref. 39
(c) data from ref. 14
(d) this work

Diagram Captions

Figure 1. A unit cell plot of $N_2F^+AsF_6^-$ viewed down the *c* axis. In addition to the mirror plane, two-fold rotational axes pass through As1 (bisecting the F3-As1-F3" angie) and N_4 (perpendicular to the X5-N4-X5' axis). The N_2F^+ cation is required by symmetry to be disordered, with the terminal X5, X5' positions being occupied equally by N and F atoms. This packing disorder causes the NX_2 cation to be linear and symmetric, and the central nitrogen atoms to be elongated along the molecular axis.

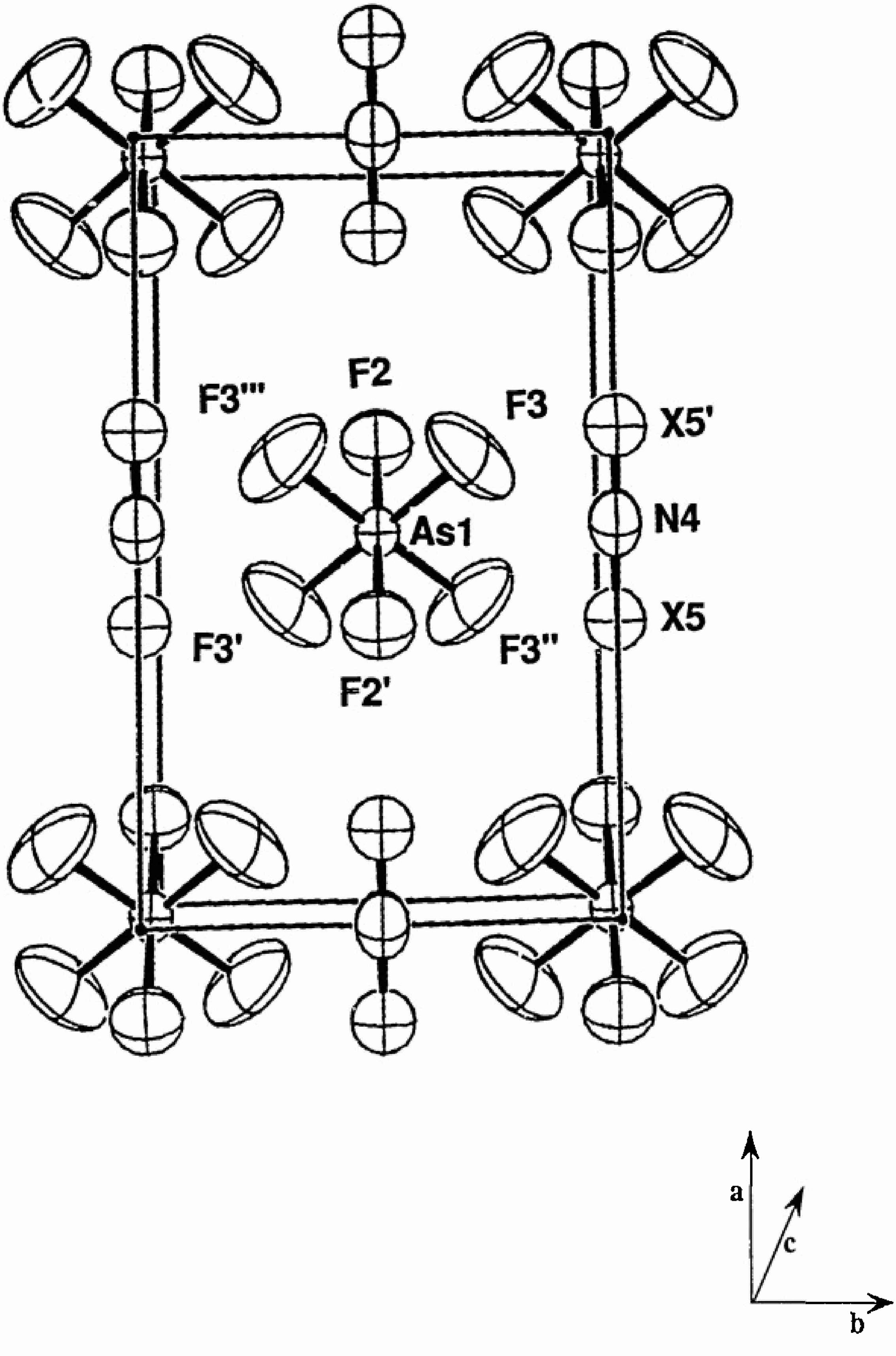

Figure 1

Supplementary Material

"The N_2F^+ Cation. An Unusual Ion Containing the Shortest Presently Known Nitrogen-Fluorine Bond"

Karl O. Christe, Richard D. Wilson, William W. Wilson, Robert Bau, Sunanda Sukumar, and David A. Dixon

Table S1

OBSERVED AND CALCULATED STRUCTURE FACTORS FOR (N2F)+(AsF8)-

PAGE 1

H	K	L	10FO	10FC	H	K	L	10FO	10FC	H	K	L	10FO	10FC	H	K	L	10FO	10FC	H	K	L	10FO	10FC
2	0	-6	138	129	4	4	-4	137	133	9	1	-2	73	74	9	3	-1	123	124	0	8	0	212	216
4	0	-6	140	127	6	4	-4	114	106	11	1	-2	80	84	0	4	-1	285	273	2	0	0	183	166
1	1	-6	103	102	1	5	-4	103	105	0	2	-2	421	429	2	4	-1	228	211	4	0	0	115	112
3	1	-6	113	98	3	5	-4	72	76	2	2	-2	371	362	4	4	-1	272	284	8	8	0	117	112
5	1	-6	102	95	5	5	-4	80	77	4	2	-2	304	300	6	4	-1	201	214	1	7	0	95	96
0	2	-6	91	88	0	6	-4	121	115	8	2	-2	216	212	8	4	-1	87	91	3	7	0	103	98
2	2	-6	119	116	2	6	-4	103	106	8	2	-2	171	181	10	4	-1	55	49	0	0	1	563	607
4	2	-6	138	126	2	0	-3	331	326	10	2	-2	123	119	1	5	-1	293	287	2	0	1	539	529
1	3	-6	73	72	4	0	-3	413	398	1	3	-2	164	164	3	5	-1	217	215	4	0	1	281	280
2	0	-5	89	80	6	0	-3	210	217	3	3	-2	239	235	5	5	-1	151	163	6	0	1	189	181
4	0	-5	101	98	8	0	-3	113	117	5	3	-2	266	273	7	5	-1	112	121	8	0	1	183	188
6	0	-5	160	152	10	0	-3	82	88	7	3	-2	153	155	0	6	-1	128	119	10	0	1	133	138
8	0	-5	105	96	1	1	-3	464	482	9	3	-2	84	83	2	8	-1	113	111	3	1	1	380	374
1	1	-5	184	187	3	1	-3	497	484	0	4	-2	301	300	4	6	-1	125	125	5	1	1	270	289
3	1	-5	152	150	5	1	-3	214	213	2	4	-2	353	348	8	6	-1	105	102	7	1	1	281	297
5	1	-5	159	152	7	1	-3	133	129	4	4	-2	289	287	1	7	-1	115	118	9	1	1	181	190
7	1	-5	128	122	9	1	-3	145	142	6	4	-2	164	173	3	7	-1	98	97	11	1	1	81	78
0	2	-5	161	179	0	2	-3	328	340	8	4	-2	97	104	4	0	0	84	98	0	2	1	64	47
2	2	-5	117	120	2	2	-3	297	306	1	5	-2	128	120	6	0	0	219	229	2	2	1	659	883
4	2	-5	124	119	4	2	-3	191	190	3	5	-2	198	195	8	0	0	313	321	4	2	1	577	668
6	2	-5	133	125	6	2	-3	108	107	5	5	-2	169	176	10	0	0	146	158	6	2	1	209	208
1	3	-5	135	148	8	2	-3	113	111	7	5	-2	81	87	3	1	0	288	295	8	2	1	85	109
3	3	-5	145	146	10	2	-3	95	95	0	6	-2	140	145	5	1	0	253	243	10	2	1	02	96
5	3	-5	141	128	1	3	-3	433	448	2	6	-2	152	149	7	1	0	249	247	1	3	1	614	826
0	4	-5	113	106	3	3	-3	339	340	4	6	-2	132	130	9	1	0	145	159	3	3	1	600	491
2	4	-5	70	74	5	3	-3	131	133	6	6	-2	90	90	11	1	0	82	83	5	3	1	260	241
4	4	-5	81	80	7	3	-3	106	108	1	7	-2	82	83	0	2	0	726	674	7	3	1	168	181
1	5	-5	91	94	9	3	-3	124	120	3	7	-2	78	81	2	2	0	393	400	9	3	1	118	122
2	0	-4	275	275	0	4	-3	168	168	2	0	-1	570	559	4	2	0	258	258	0	4	1	279	288
4	0	-4	186	185	2	4	-3	212	216	4	0	-1	538	535	8	2	0	379	366	2	4	1	348	366
6	0	-4	183	180	4	4	-3	188	190	6	0	-1	314	306	8	2	0	258	268	4	4	1	218	222
8	0	-4	164	165	6	4	-3	122	122	8	0	-1	118	117	10	2	0	94	106	6	4	1	101	94
1	1	-4	235	245	8	4	-3	03	85	10	0	-1	84	85	1	3	0	241	231	8	4	1	05	01
3	1	-4	122	125	1	5	-3	170	178	3	1	-1	380	385	3	3	0	352	363	10	4	1	88	89
5	1	-4	139	137	3	5	-3	186	180	5	1	-1	330	326	5	3	0	338	333	1	5	1	261	272
7	1	-4	164	162	5	5	-3	124	121	7	1	-1	302	295	7	3	0	192	189	3	5	1	153	165
9	1	-4	97	101	7	5	-3	66	85	9	1	-1	164	172	9	3	0	86	88	5	5	1	124	127
0	2	-4	339	351	0	6	-3	114	111	11	1	-1	83	85	0	4	0	578	567	7	5	1	138	136
2	2	-4	322	331	2	6	-3	98	97	0	2	-1	60	67	2	4	0	388	383	0	0	1	122	118
4	2	-4	164	161	4	6	-3	87	86	2	2	-1	156	166	4	4	0	180	193	2	6	1	148	147
6	2	-4	112	113	4	0	-2	723	725	4	2	-1	318	323	6	4	0	169	169	4	6	1	134	135
8	2	-4	123	123	6	0	-2	257	259	6	2	-1	408	404	8	4	0	148	143	6	6	1	102	97
1	3	-4	224	234	8	0	-2	119	114	8	2	-1	174	181	10	4	0	86	84	1	7	1	127	130
3	3	4	153	158	10	0	-2	110	117	10	2	-1	66	74	1	5	0	246	241	3	7	1	121	113
5	3	4	110	111	1	1	-2	51	61	1	3	-1	355	335	3	5	0	168	176	0	0	2	309	312
7	3	-4	112	110	3	1	-2	501	490	3	3	-1	216	211	5	5	0	113	128	2	0	2	141	152
0	4	-4	168	176	5	1	-2	449	452	5	3	-1	320	323	7	6	0	101	100	4	0	2	422	413
2	4	-4	181	189	7	1	-2	149	147	7	3	-1	268	269	9	5	0	79	77	6	0	2	398	391

Supplementary Material

"The N_2F^+ Cation. An Unusual Ion Containing the Shortest Presently Known Nitrogen-Fluorine Bond"

Karl O. Christe, Richard D. Wilson, William W. Wilson, Robert Bau, Sunanda Sukumar, and David A. Dixon

Table S1 (continued)

OBSERVED AND CALCULATED STRUCTURE FACTORS FOR [N2F]+[AsF6]-

H	K	L	10FO	10FC	H	K	L	10FO	10FC	H	K	L	10FO	10FC	H	K	L	10FO	10FC	H	K	L	10FO	10FC
8	0	2	203	205	5	5	2	148	145	1	3	3	279	278	7	1	4	108	103	3	1	5	174	175
10	0	2	89	89	7	5	2	101	101	3	3	3	171	161	9	1	4	92	86	5	1	5	127	122
3	1	2	544	531	0	6	2	138	140	5	3	3	176	177	0	2	4	335	349	7	1	5	98	88
5	1	2	386	371	2	6	2	140	142	7	3	3	159	166	2	2	4	198	195	0	2	5	183	171
7	1	2	141	148	4	6	2	148	141	9	3	3	98	102	4	2	4	138	138	2	2	5	154	160
9	1	2	101	99	6	6	2	117	112	0	4	3	162	170	6	2	4	151	151	4	2	5	103	107
11	1	2	81	79	1	7	2	106	99	2	4	3	147	143	8	2	4	122	117	6	2	5	93	87
0	2	2	417	425	3	7	2	109	103	4	4	3	148	145	1	3	4	205	208	1	3	5	127	129
2	2	2	503	506	0	0	3	89	118	6	4	3	133	133	3	3	4	124	123	3	3	5	132	126
4	2	2	436	424	2	0	3	246	256	8	4	3	97	100	5	3	4	106	109	5	3	5	128	124
6	2	2	236	242	4	0	3	373	360	1	5	3	117	127	7	3	4	114	114	0	4	5	106	104
8	2	2	127	132	6	0	3	228	240	3	5	3	139	137	0	4	4	165	175	2	4	5	131	123
10	2	2	91	87	8	0	3	116	114	5	5	3	163	155	2	4	4	131	128	4	4	5	100	101
1	3	2	367	375	10	0	3	77	71	7	5	3	108	110	4	4	4	143	137	1	5	5	110	102
3	3	2	443	423	1	1	3	227	241	0	6	3	109	106	6	4	4	135	135	0	0	6	120	122
5	3	2	200	191	3	1	3	280	267	2	6	3	128	122	1	5	4	132	127	2	0	6	119	124
7	3	2	76	78	5	1	3	325	333	4	6	3	113	109	3	5	4	129	121	4	0	6	117	106
9	3	2	93	98	7	1	3	201	204	0	0	4	317	324	5	5	4	90	91	1	1	6	111	118
0	4	2	290	308	9	1	3	98	89	2	0	4	289	279	0	6	4	117	116	3	1	6	100	100
2	4	2	215	221	0	2	3	329	342	4	0	4	236	239	0	0	5	210	208	5	1	8	82	72
4	4	2	191	179	2	2	3	327	324	6	0	4	180	185	2	0	5	244	244	0	2	6	85	88
6	4	2	170	165	4	2	3	229	235	8	0	4	109	100	4	0	5	128	132	2	2	6	90	94
8	4	2	124	132	6	2	3	124	129	1	1	4	318	322	6	0	5	82	68	4	2	8	112	108
1	5	2	116	122	8	2	3	104	105	3	1	4	233	229	1	1	5	206	214	1	3	6	85	84
3	5	2	162	169	10	2	3	87	87	5	1	4	123	132										

Contribution from Rocketdyne, A Division of Rockwell International, Canoga Park, California 91303, the Department of Chemistry, McMaster University, Hamilton, Ontario L8S 4M1, Canada, and the Central Research and Development Department, E.I. du Pont de Nemours and Company, Inc., Experimental Station, Wilmington, Delaware 19880 - 0328.

The Pentafluoroxenate(IV) Anion XeF_5^-; the First Example of a Pentagonal Planar AX_5 Species

Karl O. Christe,*[1] Earl C. Curtis,[1] David A. Dixon,[2] Hélène P. Mercier,[3] Jeremy C.P. Sanders[3] and Gary J. Schrobilgen,*[3]

Abstract. Xenon tetrafluoride forms stable 1:1 adducts with $N(CH_3)_4F$, CsF, RbF, KF and NaF, and an unstable 1:1 adduct with FNO. All these adducts are ionic salts containing pentagonal planar XeF_5^- anions as shown by a crystal structure determination of $N(CH_3)_4^+XeF_5^-$, Raman and infrared spectra, and ^{19}F and ^{129}Xe NMR spectroscopy. The X-ray crystal structure of $N(CH_3)_4^+XeF_5^-$ was determined at -86 °C. This compound crystallizes in the orthorhombic system, space group Pmcn, with four molecules in a unit cell of dimensions a = 6.340(2) Å, b = 10.244(3) Å, c =

13.896(4) Å with R = 0.0435 for 638 observed ($I > 3\sigma(I)$) reflections. In addition to four $N(CH_3)_4^+$ cations, the structure contains four pentagonal planar XeF_5^- anions per unit cell with D_{5h} symmetry. The Xe-F distances are 1.979(2) - 2.034(2) Å with F-Xe-F angles of 71.5(4) - 72.3(4)°. The D_{5h} structure of the XeF_5^- anion is highly unusual and represents the first example of an AX_5E_2 (E = valence electron lone pair) species in which all six atoms are coplanar. The results from the crystal structure determination and a normal coordinate analysis show that the XeF_5 plane of XeF_5^- is considerably more rigid than that in the fluxional IF_7 molecule due to the increased repulsion from the xenon free valence electron pairs. Local density functional calculations were carried out for XeF_5^- and XeF_4 with a double numerical basis set augmented by polarization functions and confirm the experimentally observed geometries and vibrational spectra. It is shown that the bonding in XeF_5^- closely resembles that in XeF_4. In a valence bond description, it can be visualized as the two axial positions being occupied by two sp-hybridized free valence electron pairs and the equatorial fluorines being bound by two Xe 5p electron pairs through semi-ionic multi center-four electron bonds.

INTRODUCTION

Recent work in our laboratories has shown that anhydrous $N(CH_3)_4F$[4] holds great potential for the synthesis and characterization of novel, high oxidation state, complex fluoro anions.[5-7] An area of special interest to us is the problem of maximum coordination numbers and their influence on the steric activity of free valence electron pairs. For example, it was shown that nitrogen(V) cannot accommodate five fluorine ligands,[8] whereas the iodine in IF_6^-, which had long been thought to have a distorted octahedral structure,[9,10] has recently been confirmed to possess a sterically active lone valence electron pair.[10] In contrast, the central atom free valence electron pairs in the smaller ClF_6^- and BrF_6^- anions become sterically inactive due to space limitations, as demonstrated in very recent vibrational[6,10] and single crystal X-ray structure studies.[11]

In this context, the likely structures of the XeF_5^- and XeF_6^{2-} anions posed an interesting problem, since both anions contain two free valence electron pairs on the xenon central atom. Therefore, they are representatives of the novel AX_5E_2 and AX_6E_2 geometries, respectively, where E stands for a free valence electron pair. Whereas no reports have been published on the existence or possible structure of XeF_5^- or any other AX_5E_2 species, Kiselev and coworkers[13-15] recently reported the synthesis of M_2XeF_6 salts (M = Cs, Rb, K, Na) from XeF_4 and MF. Based on vibrational spectra, they surprisingly assigned an octahedral structure to XeF_6^{2-}. However, a closer inspection of their published spectra[13] revealed that both the frequency separations and relative intensities of the observed bands are incompatible with an octahedral species.[16] Furthermore, it was noted that the Raman spectrum attributed to Cs_2XeF_6 was identical to that previously observed during the laser photolysis of $CsXeF_7$ and tentatively assigned to Cs_2XeF_8.[17] In view of these discrepancies we decided to investigate the fluoride acceptor properties of XeF_4 using $N(CH_3)_4F$ as a fluoride ion source and to re-investigate the XeF_4-MF systems.

EXPERIMENTAL

Apparatus and Materials. Volatile materials were handled in stainless steel-Teflon and Pyrex glass vacuum lines, as previously described.[18,19] Non-volatile materials were handled in the dry nitrogen atmosphere of a glove box.

Literature methods were used for the syntheses of anhydrous $N(CH_3)_4F$,[4] XeF_4[20] and FNO[21] and the drying of CH_3CN.[4,22] The LiF (Research Inorganic Chemicals, Research Organic Chemicals), NaF (Matheson) and BaF_2 (Baker and Adamson) were dried in a vacuum at 125 °C prior to their use. The KF (Allied), RbF (American Potash) and CsF (KBI) were dried by fusion in a platinum crucible, followed by transfer of the hot clinkers to the dry nitrogen atmosphere of the glove box where the fluoride samples were ground prior to use.

Syntheses of $M^+XeF_5^-$ (M = Cs, Rb, K, Na). The dry, finely powdered alkali metal fluorides (2 mmol) and XeF_4 (4 - 8 mmol) were loaded inside the dry box into prepassivated (with ClF_3), 10 mL stainless steel Hoke cylinders which were closed by metal valves. The cylinders were evacuated at -78 °C on the vacuum line and then heated in an oven to 190 °C for 14 hrs. Unreacted XeF_4 was pumped off at 30 °C and collected in a tared Teflon U-trap at -196 °C until the cylinders reached a constant weight. The combining ratios of MF with XeF_4 were obtained from the observed material balances, i.e., the weights of MF, XeF_4 used, XeF_4 recovered, and the products. Under the above conditions, the following combining ratios were observed: $CsF : XeF_4 = 1 : 0.99$, $RbF : XeF_4 = 1 : 0.95$, $KF : XeF_4 = 1 : 0.65$ and $NaF : XeF_4 = 1 : 0.32$. Additional heating of the $KF\text{-}XeF_4$ and $NaF\text{-}XeF_4$ adducts with more XeF_4 to 135 °C for 10 days increased the conversion of KF and NaF to the corresponding XeF_5^- salts to 73% and 36%, respectively.

Synthesis of $NO^+XeF_5^-$. In the drybox, XeF_4 (1.03 mmol) was loaded into a prepassivated 0.5 inch o.d. Teflon-FEP ampule which was closed by a stainless steel valve. On the vacuum line, FNO (6.77 mmol) was added to the ampule at -196 °C. The ampule was allowed to warm to 0 °C and was kept at this temperature for 10 min. with agitation, and the unreacted FNO was then pumped off at -78 °C. The white solid residue (265 mg, weight calculated for 1.03 mmol of $NO^+XeF_5^-$ = 264 mg) had a dissociation pressure of 10 torr at 0 °C.

Synthesis of $N(CH_3)_4^+XeF_5^-$. In a typical synthesis, $N(CH_3)_4F$ and XeF_4 (2.01 mmol each) were loaded into a Teflon-FEP ampule in a drybox and CH_3CN (3 mL liquid) was vacuum distilled onto the solid at -196 °C. The mixture was warmed to -40 °C for 30 min. with agitation; then allowed to warm to room temperature, followed by removal of the solvent in vacuo at this temperature. The white solid residue (605 mg, weight calculated for 2.01 mmol of $N(CH_3)_4^+XeF_5^-$ = 604 mg) was identified as $N(CH_3)_4^+XeF_5^-$ by vibrational and NMR spectroscopy and a crystal structure determination. When isolated from CH_3CN solution, the compound is stable indefinitely at room temperature. Caution! When solutions of $N(CH_3)_4^+XeF_5^-$ in CH_3CN are frozen in liquid nitrogen, they may detonate. Similar, but milder detonations were also found to occur when XeF_4 solutions were frozen at -196 °C. Exposure of solid samples of $N(CH_3)_4^+XeF_5^-$ to atmospheric moisture for even brief periods has resulted in the violent detonation of bulk samples.

Crystal Structure Determination of $N(CH_3)_4^+XeF_5^-$

Crystal Growing. Single crystals of $N(CH_3)_4^+XeF_5^-$ suitable for X-ray analysis were grown from CH_3CN solution by vacuum distilling ca. 2.5 mL of dry CH_3CN onto ca. 50 mg of $N(CH_3)_3^+XeF_5^-$ in a 1/4" o.d. FEP reaction vessel equipped with a Kel-F valve. The mixture was warmed to 65 °C to effect dissolution and allowed to cool slowly to room temperature (ca. 5 °C/hr.). Colorless crystals up to 5 mm in length, having a needle-like morphology, formed overnight. The mother liquor was syringed off the crystals in a dry nitrogen atmosphere and residual solvent was removed under dynamic vacuum. Several crystals were cleaved perpendicular to their long axes to give fragments measuring ca. 0.2 mm x 0.2 - 0.3 mm and transferred in a dry box to 0.2 mm o.d. Lindemann glass capillaries (previously dried under dynamic vacuum at 250 °C for 1 day) and sealed under a dry nitrogen atmosphere. The crystals were shown to be identical to the bulk sample prior to recrystallization by obtaining the single crystal Raman spectrum at room temperature (see Figure 5b) and were found to be stable at room temperature in glass indefinitely.

Collection and Reduction of X-ray Data. Crystals of $N(CH_3)_4{}^+XeF_5{}^-$ were centered on a Syntex P_3 diffractometer. Accurate cell dimensions were determined at T = 23 °C and at T = -86 °C from a least-squares refinement of the setting angles (χ, φ and 2θ) obtained from 15 accurately centered reflections (with $22.14° < 2\theta < 28.11°$) chosen from a variety of points in reciprocal space. At T = 23 °C, and after several hours in the X-ray beam, the crystal appeared to be totally decomposed, resulting in an opaque white coloration. Integrated diffraction intensities were collected on a new crystal at T = -86 °C using a $\theta:2\theta$ scan technique (slowest rate 5.0°/min) with $0 \le h \le 10$, $0 \le k \le 15$ and $-15 \le l \le 15$, using molybdenum radiation monochromatized with a graphite crystal (λ = 0.71069 Å). Throughout the data collection, two standard reflections were monitored every 48 reflections; a decay of 0.6% was observed; the intensities were adjusted accordingly. A total of 1414 reflections were collected out of which 641 reflections, satisfying the condition $I > 3\sigma(I)$, were chosen for structure solution. The intensities of these reflections were corrected for Lorentz polarization effects.

Solution and Refinement of the Structure. There were two space groups tnat were consistent with the reflection pattern: the non-centro-symmetric space group P21cn (No. 33) and the centro-symmetric space group Pmcn (No. 62). The structure has been solved in both centro-symmetric (Pmcn) and non-centro-symmetric (P21cn) space groups. The direct method of structure solution in the computer program SHELX-76 [23] was used to locate the positions of the Xe atom and the five F atoms. Successive Fourier synthesis yielded all the remaining non-hydrogen atoms. The structure was refined using the full-matrix least-squares technique with isotropic thermal parameters for individual atoms. In the case of the Pmcn space group and after full convergence of the isotropic refinement ($R = 0.1265$), the atoms were assigned anisotropic thermal parameters and further refined by the full-matrix least-squares technique ($R = 0.0714$). The positions of the hydrogen atoms were calculated and the fixed hydrogen atoms were given an isotropic temperature factor of 0.05 $Å^2$.[24] The R factor obtained was 0.0652 with unit weights. There was significant disagreement between the Fo and Fc values of three reflections, 110, 312 and 413, and were consequently omitted in a further refinement. This resulted in a global improvement of the structure and a final value for the R factor of 0.0435.

The same procedure was used for the P21cn space group which gave rise to a final R factor of 0.0763. The ratio of agreement factors R(7.63/4.35) = 1.75 is sufficient by Hamilton's R factor ratio test[7] to state that the correct space group is Pmcn.

An empirical absorption correction was also applied, but no significant improvement in the refinement was observed; in particular there was no change in the anisotropic thermal parameters.

Details of the data collection parameters and other crystallographic information for the Pmcn space group are given in Table 1, and the final atomic coordinates are summarized in Table 2. Programs used: XTAL,[24] data reduction; SHELX-76,[23] structure refinement; SNOOPI,[25] diagrams.

Vibrational Spectroscopy. Raman spectra were recorded on either a Cary Model 83 or a Spex Model 1403 spectrophotometer using a 488 nm exciting line of an Ar ion or the 647.1 nm line of a Kr ion laser, respectively. Baked-out Pyrex melting point capillaries or thin walled Kel-F tubes were used as sample containers. A previously described[26] device was used for recording the low-temperature spectra (at -150 °C). Single crystal spectra of $N(CH_3)_4^+XeF_5^-$ were recorded at room temperature on a Instruments S.A. Mole S-3000 triple spectrograph system equipped with a microscope for focusing the excitation laser to a one-micron spot. The Ar laser line at 514.5 nm was selected for excitation of the sample. Crystals were sealed in Lindemann glass capillaries as described below.

Infrared spectra were recorded using AgBr disks on a Perkin-Elmer Model 283 spectophotometer. The finely powdered samples were sandwiched between two thin AgBr disks and pressed together in a Wilks minipress inside the drybox.

Nuclear Magnetic Resonance Spectroscopy. The ^{19}F and ^{129}Xe NMR spectra were recorded unlocked (field drift < 0.1 Hz h^{-1}) using Bruker WM-250 and Bruker AM-500 spectrometers equipped with 5.8719 T and 11.744 T cryomagnets, respectively. Fluorine-19 spectra were obtained using a 5-mm combination $^{1}H/^{19}F$ probe operating at 235.36 MHz. The spectra were accumulated in 16 K memory. Spectral width settings of 5000 and 30000 Hz were employed, yielding data point resolutions of 0.61 and 3.6 Hz/data point and acquisition times of 1.638 and 0.279 s, respectively. No relaxation delays were applied. Typically 300 - 7000 transients were accumulated. The pulse width corresponding to a bulk magnetization tip angle, θ, of approximately 90° was equal to 1 μs. No line broadening parameters were applied in the exponential multiplication of the free induction decays prior to Fourier transformation.

Xenon-129 NMR spectra were obtained using a broad band VSP probe tunable over the range 23 - 202 MHz; spectra were recorded at 139.05 MHz. The spectra were accumulated in a 16 K memory. A spectral width setting of 50 kHz was employed, yielding a data point resolution of 6.1 Hz/data point and acquisition time of 0.164 s. No relaxation delays were applied. Typically 10000 transients were accumulated. The pulse width corresponding to a bulk magnetization tip angle, θ, of approximately 90° was equal to 18 μs. Line broadening parameters of 4 Hz were applied in the exponential multiplication of the free induction decays prior to Fourier transformation.

The ^{19}F and ^{129}Xe NMR spectra were referenced to neat external samples of $CFCl_3$ and $XeOF_4$, respectively, at ambient temperature. The chemical shift convention used is that a positive (negative) sign signifies a chemical shift to high (low) frequency of the reference compound.

The ^{129}Xe NMR samples of saturated solutions of $N(CH_3)_4^+XeF_5^-$ in CH_3CN were prepared in 25 cm-lengths of 3/8" o.d., 1/32" wall FEP plastic tubing that had been reduced to 9 mm o.d. by squeezing in a heated precision brass mold. The FEP tubing was heat sealed at one end with the open end flared (45° SAE) and joined, by means of compression fittings, to a Kel-F valve. The FEP tubes were heat sealed under dynamic vacuum with their contents frozen at -78 °C. The sealed FEP sample tubes were inserted into 10-mm thin-walled precision NMR tubes (Wilmad) in order to run their spectra.

The ^{19}F NMR samples were prepared in precision 5-mm glass NMR tubes (Wilmad). Solid $N(CH_3)_4^+XeF_5^-$ (or $N(CH_3)_4^+XeF_5^-$ and $N(CH_3)_4^+F^-$) was loaded into the NMR tube in the dry box and CH_3CN solvent distilled in vacuo into the tube at -78 °C. The tube was flame sealed. On warming to room temperature, a colorless saturated solution resulted containing some solid $N(CH_3)_4^+XeF_5^-$, which was decanted into the top of the tube prior to obtaining the NMR spectrum.

Computational Method.

The calculations described below were done using the local density functional theory[27-30] with the program system DMol[31]. DMol employs numerical functions for the atomic basis sets. The atomic basis functions are given numerically as an atom-centered, spherical-polar mesh. The radial portion of the grid is obtained from the solution of the atomic LDF equations by numerical methods. The radial functions are stored as sets of cubic spline coefficients so that the radial functions are piece-wise analytic, a necessity for the evaluation of gradients. The use of exact spherical atom results offers certain advantages. Because of the quality of the atomic basis sets, basis set superposition effects should be minimized, correct behavior at the nucleus is obtained, and radial nodal properties of the wavefunction are present.

Because the basis sets are numerical, the various integrals arising from the expression for the energy need to be evaluated over a grid. The integration points are generated in terms of angular functions and spherical harmonics. The number of radial points N_R is given as

$$N_R = 1.2 \times 14(Z + 2)^{1/3} \qquad (4)$$

where Z is the atomic number. The maximum distance for any function is 12 a.u. The angular integration points N_θ are generated at the N_R radial points to form shells around each nucleus. The value of N_θ ranges from 14 to 302 depending on the behavior of the density.[32] The Coulomb potential corresponding to the electron repulsion term could be solved by evaluation of integrals. However, since the method is based on the density, it was found to be more appropriate to determine the Coulomb potential directly from the electron density by solving Poisson's equation

$$-\nabla^2 V_e(r) = 4\pi e^2 \rho(r) \tag{5}$$

In DMol, the form for the exchange-correlation energy of the uniform electron gas is that derived by von Barth and Hedin.[33]

All of the DMol calculations were done with a double numerical basis set augmented by d polarization functions. This can be thought of in terms of size as a polarized double zeta basis set. However, because exact numerical solutions are employed for the atom, this basis set is of significantly higher quality than a normal molecular orbital polarized double zeta basis set. The fitting functions have an angular momentum number one greater than that of the polarization function resulting in a value of $l = 3$ for the fitting functions.

Geometries were determined by optimization using analytic gradient methods.[34] First derivatives in the LDF framework can be calculated efficiently and only take on the order of 3 - 4 SCF iterations or 10 - 25% of an energy evaluation. There are two problems with evaluating gradients in the LDF framework which are due to the numerical methods that are used. The first is that the energy minimum does not necessarily correspond exactly to the point with a zero derivative. The second is that sum of the gradients may not always be zero as required for translational invariance. These tend to introduce errors on the order of 0.001 Å in the calculation of the coordinates if both a reasonable grid and basis set are used. This gives bond lengths and angles with reasonable error limits. The difference of 0.001 Å is about an order of magnitude smaller than the accuracy of the LDF geometries as compared to experiment.

RESULTS AND DISCUSSION

Syntheses and Properties of XeF_5^- Salts

The reactions of the alkali metal fluorides with XeF_4 were studied under conditions (190 °C, 14 hrs.) very similar to those previously reported by Kiselev and coworkers.[13-15] It was found that XeF_4 combines with either CsF or RbF in a clean 1 : 1 mole ratio to form the corresponding, previously unidentified XeF_5^- salts. In the case of KF and NaF the same anion was formed; however, the percentage conversion of MF to $MXeF_5$ decreased with decreasing atomic weight of M (CsF = 99%, RbF = 95%, KF = 65% and NaF = 32%) and increased reaction times were required for higher conversions.

The interactions of LiF and BaF_2 with XeF_4 were also examined, but in neither case was evidence for the formation of a stable adduct obtained.

The XeF_5^- salts of Cs^+, Rb^+, K^+ and Na^+ are white, stable solids. Their physical properties, thermal stabilities, etc., are those previously attributed by Kiselev and coworkers to the corresponding M_2XeF_6 salts.[13-15] As will be shown below, they all contain pentagonal planar XeF_5^- anions.

Attempts to prepare $CsXeF_5$ from CsF and XeF_4 at room temperature in CH_3CN solutions were unsuccessful because of the very low solubility of CsF in this solvent. However, the highly soluble $N(CH_3)_4F$ readily forms $N(CH_3)_4^+XeF_5^-$ under these conditions. Even with a 2 : 1 molar ratio of $N(CH_3)_4F$: XeF_4 in CH_3CN solvent and a large excess of MF in the XeF_4-MF systems, only XeF_5^- and no XeF_6^{2-} was observed, indicating that XeF_5^- is the favored anion. The $N(CH_3)_4^+XeF_5^-$ salt is a white, stable solid whose structure was established by a crystal structure determination and vibrational and NMR spectroscopy (see below).

The lack of XeF_6^{2-} formation in these systems was further demonstrated by a study of the FNO-XeF_4 system. Even when a large excess of FNO was used, only $NO^+XeF_5^-$ and no $(NO^+)_2XeF_6^{2-}$ were formed at temperatures as low as -78 °C. The $NO^+XeF_5^-$ salt is a white solid having a dissociation pressure of 10 torr at 0 °C. It is ionic, containing NO^+ and XeF_5^- ions as shown by vibrational spectroscopy (see below).

In view of the above results and the structural evidence presented below, it appears quite clear that the salts obtained by the reactions of XeF_4 with fluoride ion sources are XeF_5^-, and not XeF_6^{2-}, salts. The fact that some of the products reported[13-15] by the Soviet workers gave elemental analyses approaching the M_2XeF_6 composition might be attributed to incomplete conversion of MF to $MXeF_5$ thus resulting in MF + $MXeF_5$. There is also no doubt that the products observed during the laser photolysis of either $CsXeF_7$ or NF_4XeF_7 were not XeF_8^{2-} but XeF_5^- salts.[17]

X-ray Crystal Structure of $N(CH_3)_4^+XeF_5^-$

The crystal structure consists of well-separated $N(CH_3)_4^+$ and XeF_5^- ions. The $N(CH_3)_4^+$ cation is tetrahedral with the expected bond lengths. Different views of the XeF_5^- anion are shown in Figures 1 and 2 while a stereoview of the packing in the unit cell is given in Figure 3 in which the hydrogen atoms have been omitted in the cation. Important bond lengths and angles are listed in Table 3. The xenon and five fluorines of the XeF_5^- anion and the nitrogen and two carbons of the cation are located on special positions which are on the mirror plane, resulting in an anion which is planar by crystal symmetry. The closest anion-cation distance occurs between F2 and C2, which lies in the anion plane, at 3.105(5) Å, whereas the remaining closest F...C distances occur at 3.237(5) (F5...C1), 3.354(5) (F3...C2), 3.370(5) (F1...C3) and 3.651(5) Å (F4...C2). The sum of the van der Waals radii of CH_3 (2.00 Å[35]) and F (1.35[35] - 1.40[36] Å) is 3.35 - 3.40 Å. The F2...C2 distance suggests weak hydrogen bonding between the C2-methyl group and F2 and is somewhat shorter than the shortest F...C distance in $N(CH_3)_4^+HF_2^-$ (3.313(5) Å),[7] which appears to be at the limit of the van der Waals distance. The short F2...C2 distance appears to account for the greater elongation of the thermal ellipsoid of F2 (in the direction of the C_5-axis of the anion; Figure 2).

Although the site symmetry of the XeF_5^- anion is C_s, the five fluorines are clearly equivalently bonded to the xenon, giving a pentagonal planar structure of D_{5h} symmetry. The average F-Xe-F angle of 72.0(4)° is essentially the ideal angle of 72°. The average Xe-F bond length (2.012(2) Å) is significantly longer than the average bond length of XeF_4 (1.953(2) Å)[37] and the average equatorial bond length of IF_7 (1.858(4) Å).[38] The nearest neighbor F...F contacts in the XeF_5^- anion are 2.35 - 2.38 Å, and are substantially less than twice the nominal van der Waals radius for fluorine, i.e., 2.70 [35] - 2.80 [38] Å, indicating that the fluorines of the pentagon are significantly congested, and are consistent with the long Xe-F bond length in XeF_5^-. This contrasts with the shorter Xe-F bond length of XeF_4 where the fluorines in the plane are not contacting, and the intramolecular F...F distances (2.76 Å) are at the limit of the sum of the fluorine van der Waals radii. The short I-F bond length for the equatorial belt of five fluorines in IF_7 relative to the Xe-F bond length of XeF_5^- may be attributed to relief of the congestion in the IF_5 belt by means of a 7.5° puckering, which has been deduced from electron diffraction studies,[38] but not corroborated by an independent study. The fact that XeF_5^- does not relieve its steric congestion by a puckering distortion may be attributed to the presence of the two axial lone pairs of electrons, which exert greater repulsive forces than the two axial fluorines in the IF_7 molecule, thus forcing the XeF_5^- anion to be planar. Moreover, the formal negative charge on XeF_5^- leads to a greater Xe-F bond polarity and elongation of the Xe-F bond, as is evident from a comparison with the Xe-F bond length of XeF_4, and serves to alleviate some of the steric congestion in the anion plane.

The steric crowding in the XeF_5^- molecular plane is further illustrated by the thermal parameters, which remain essentially unaltered before and after empirical absorption corrections. It is apparent that the principal axes of motion of the fluorine atoms in XeF_5^- and XeF_4 [37] are perpendicular to the bond directions producing the anticipated polar flattening of the thermal ellipsoids in the Xe-F bond directions. However, the thermal ellipsoids in XeF_5^- are elongated in the direction of the C_5-axis and flattened in the direction perpendicular to the Xe-F bonds in the molecular plane. In contrast to the fluorine thermal ellipsoids in XeF_5^-, those of XeF_4 are essentially isotropic in the directions perpendicular to the Xe-F bonds and in the molecular plane where the fluorine atoms are apparently not contacting one another to any significant extent. Steric congestion in XeF_5^- is additionally supported by vibrational force constant calculations (see below).

^{129}Xe and ^{19}F NMR Spectra of the XeF_5^- Anion

The ^{129}Xe NMR spectrum of $N(CH_3)_4^+XeF_5^-$ dissolved in CH_3CN containing a 1 molar excess of $N(CH_3)_4^+F^-$ at 24 °C (Figure 4) displays a well-resolved binomial sextet ($\Delta\nu_{1/2}$ = 15 Hz) consistent with the coupling of the ^{129}Xe nucleus to five chemically equivalent ^{19}F nuclei in the XeF_5^- anion ($\delta(^{129}Xe)$, -527.0 ppm from $XeOF_4$; $^1J(^{129}Xe-^{19}F)$, 3400 Hz). The ^{129}Xe chemical shift of XeF_5^- is significantly more shielded (i.e., by -843.9 ppm) than that of XeF_4 in CH_3CN at 24 °C ($\delta(^{129}Xe)$, 316.9 ppm from $XeOF_4$; $^1J(^{129}Xe-^{19}F)$, 3895 Hz). This behavior follows the expected trend of increased shielding which accompanies an increase in negative charge.[39] The ^{19}F NMR spectrum of a similar sample at 24 °C (Figure 5a) shows a narrow singlet ($\Delta\nu_{1/2}$ = 2.8 Hz) flanked by natural abundance (26.44%) ^{129}Xe satellites ($\delta(^{19}F)$, 38.1 ppm from $CFCl_3$; $^1J(^{129}Xe-^{19}F)$, 3398 Hz). A resonance due to unreacted fluoride was observed at -75 ppm. Interestingly, the ^{19}F chemical shift of XeF_5^- is deshielded by 56.8 ppm with respect to that of XeF_4 in CH_3CN at 24 °C ($\delta(^{19}F)$, -18.7 ppm from $CFCl_3$; $^1J(^{129}Xe-^{19}F)$, 3896 Hz). This result is somewhat surprising in view of the increased ionic character of the Xe-F bonds (i.e., greater bond length and smaller stretching force constant) compared with those in XeF_4; the reason for this is not clear but may be related to the congested environment of the fluorine ligands and the rather short nearest neighbor F...F contact distance. The ^{19}F NMR spectrum of a sample prepared from equimolar quantities of XeF_4 and $N(CH_3)_4^+F^-$ in CH_3CN showed a similar resonance, with accompanying ^{129}Xe satellites, at 38.1 ppm, however the linewidth was significantly broader, $\Delta\nu_{1/2}$ = 53 Hz (Figure 5b). This indicates that XeF_5^- undergoes dissociative fluorine exchange which can be suppressed by the presence of excess fluoride. There was no evidence for the formation of XeF_6^{2-} at XeF_4 : $N(CH_3)_4^+F^-$ ratios exceeding 1 : 1, thus casting further doubt on the previous claims[13-15] for the existence of stable salts of the XeF_6^{2-} anion.

The magnitude of the one-bond $^{129}Xe-^{19}F$ coupling constant drops from 3895 Hz in XeF_4 to 3400 Hz in XeF_5^- under the same conditions (i.e., solvent and temperature) of experimental measurement. If it is assumed that the Fermi-contact mechanism provides the dominant coupling contribution,[40] then the smaller value of $^1J(^{129}Xe-^{19}F)$ in XeF_5^- is in accord with the greater ionic character of the Xe-F bonds in the anion.

In the VSEPR notation, XeF_5^- is a seven-coordinate AX_5E_2 system, and is the first example of this geometry.[41] The solution structure proposed for the anion which is consistent with five equivalent fluorines is a pentagonal planar (D_{5h}) structure having five equivalent equatorial fluorines and two axial lone pairs of electrons. The dynamic behavior for related seven coordinate geometries is well established in the cases of XeF_6 and IF_7. In contrast to IF_7 and XeF_5^-, the gas phase structure of XeF_6 (AX_6E) is based upon a distorted octahedral geometry[42] in which the valence electron lone pair distorts the octahedral geometry to C_{3v} by occupying triangular faces of the octahedron, passing among adjacent faces via a transition state having intermediate C_s and C_{2v} geometries, with intramolecular exchange dynamics that are distinct from those of IF_7. The dynamic behavior of IF_7 (AX_7) is also well documented, based on gas phase electron diffraction measurements it is purported to have a puckered arrangement for the five equatorial fluorines[34] in the gas phase and it has been shown by ^{19}F NMR spectroscopy that axial and equatorial fluorine environments of IF_7 undergo rapid intramolecular exchange in solution.[43] The single fluorine environment observed in the NMR spectra of XeF_5^- could also be accounted for by assuming that the anion is fluxional. The VSEPR rules postulate that the valence shell lone pairs exert larger repulsive forces on adjacent electron pairs than do bonding pairs, so that, unlike IF_7, the transition state for exchange of axial lone pair positions with equatorial fluorine positions in XeF_5^- would presumably give rise to prohibitively large repulsive energies when a lone pair(s) occupies an equatorial position, suggesting that XeF_5^- is likely to be rigid in solution.

Vibrational Spectra and Normal Coordinate Analysis of XeF_5^-. The infrared and Raman spectra of $CsXeF_5$, $RbXeF_5$, $KXeF_5$, $NaXeF_5$, and $N(CH_3)_4XeF_5$ and the Raman spectra of $NOXeF_5$ have been recorded. The observed frequencies and their assignments are summarized in Table 4. Figure 6 shows, as typical examples, the vibrational spectra of $CsXeF_5$ and $N(CH_3)_4XeF_5$.

As shown above by the NMR data and the crystal structure determination, the XeF_5^- anion is pentagonal planar and, therefore, belongs to point group D_{5h}. After the removal of translational and rotational degrees of freedom, the irreducible representation of the molecule is

$$\Gamma_{vib} = 1A_1'(R) + 1A_2''(IR) + 2E_1'(IR) + 2E_2'(R) + E_2''(ia)$$

Since XeF_5^- is the first known example of an AX_5 species of symmetry D_{5h}, it is not surprising that a normal coordinate analysis had not previously been carried out for such a species. Force constants were calculated by the Wilson FG matrix method.[44] Figure 7 shows our choice of internal coordinates to describe the vibrations of such a molecule. Two imaginary ligands, E_6 and E_7, have been placed in the axial positions to define the angles γ, required for the definition of the out of plane deformation modes. The symmetry coordinates and approximate mode descriptions are given in Table 5 and are derived from those previously reported for the IF_7 molecule after correction for two apparent typographical errors.[45] The analytical G and F matrices, together with the computed numerical values, are given in Tables 6 and 7, respectively. The correctness of our G matrix was verified by an independent calculation of the numerical G-matrix using a computational method which gave identical values.

Vibrational Assignments. In agreement with the above predictions for XeF_5^- of symmetry D_{5h}, three mutually exclusive Raman and two infrared bands were observed in the 200 - 700 cm^{-1} region expected for the fundamental vibrations. The $N(CH_3)_4^+$ salt, containing the largest cation and, hence, the best isolated XeF_5^- anion, shows three narrow Raman lines at 502, 423 and 377 cm^{-1}. Based on their relative intensities and frequencies, which are similar to those of the three closely related Raman active modes of octahedral molecules, the 502, 423 and 377 cm^{-1} bands are assigned to the symmetric stretch, $\nu_1(A_1')$, the antisymmetric stretch, $\nu_5(E_2')$ and the symmetric in-plane deformation, $\nu_6(E_2')$, respectively. The rigorous adherence of the observed Raman spectrum to the vibrational selection rules for symmetry D_{5h} and the failure to observe further splittings of the vibrational bands serve to underscore that the vibrational modes of the XeF_5^- anion in its $N(CH_3)_4^+$ salt are only very weakly coupled.[46] It also justifies the use of the assumed free anion symmetry in the subsequent vibrational analysis and force field calculations.

In the salts with smaller cations, stronger coupling of the XeF_5^- motions or slight distortions of the anions can occur, resulting in a splitting of the two E_2' modes into their doubly degenerate components. As expected, the anion-cation interaction is strongest for the NO^+ salt causing some of the infrared active modes, such as $\nu_3(E_1')$ and $\nu_4(E_1')$, also to become weakly active in the Raman spectrum.

In the infrared spectra two strong anion bands were observed above 250 cm^{-1}. The first one was a very intense broad band extending from 400 to 550 cm^{-1} which must be due to the antisymmetric stretching mode $\nu_3(E_1')$. The second one is an intense band at 274 cm^{-1} which, based on its frequency and relative intensity, must be the symmetric out of plane (umbrella) deformation, $\nu_2(A_2'')$.

The third predicted infrared active mode is the anti-symmetric in-plane deformation, $\nu_4(E_1')$. Assuming the F_{66} and F_{44} symmetry force constants to be identical (both modes involve f_α and different combinations of $f_{\alpha\alpha}$ and $f_{\alpha\alpha}'$ with the latter being small due to the large mass of the xenon central atom), a frequency of 274 cm^{-1} was calculated for $\nu_4(E_1')$. Therefore, $\nu_4(E_1')$, which should be of medium infrared intensity, might be either hidden underneath the intense $\nu_2(A_2'')$ band at 274 cm^{-1} or occur just below the 250 cm^{-1} cut-off frequency of the AgBr windows used for our study. A frequency range of 240 to 290 cm^{-1} for $\nu_4(E_1')$ is also supported by the Raman spectrum of $NO^+XeF_5^-$ (see Table 4). In this compound, where anion-cation interaction is the strongest and the infrared active modes become also weakly Raman active, two weak Raman bands were observed at 244 and 282 cm^{-1}, respectively. Furthermore, the infrared spectra of $RbXeF_5$ and $CsXeF_5$ exhibit a 288 cm^{-1} shoulder on the strong 275 cm^{-1} band, and the Raman spectra of all the alkali metal XeF_5^- salts show an extremely weak band at about 290 cm^{-1}. Consequently, a frequency of 290 cm^{-1} was chosen by us for $\nu_4(E_1')$ and used for the force field computations. Our choice of 290 cm^{-1} for ν_4 is also supported by ab initio calculations for XeF_5^- (see below) and IF_7.[47] Assuming the frequency differences between calculated and observed frequencies to be the same for the two in-plane deformation modes in XeF_5^-, a value of 291 cm^{-1} is predicted for ν_4. Similarly, the transfer of the computed frequency difference of 102 cm^{-1} for the two in-plane deformation modes from IF_7 to XeF_5^- results in a ν_4 value of 275 cm^{-1} for XeF_5^-.

The only missing fundamental vibration is the ring puckering mode, $\nu_7(E_2'')$, which ideally is inactive in both the infrared and Raman spectra. Since no experimental frequency in available for this mode, the frequency of 79 cm^{-1} obtained by the ab initio calculation (see below) was used.

In addition to the fundamental vibrations, numerous Raman bands were observed in the low-frequency region which are attributed to lattice vibrations. The infrared spectra exhibit some weak bands above 600 cm^{-1} which can be readily assigned to different overtones or combination bands of XeF_5^- (see Table 4).

In $NO^+XeF_5^-$ and $N(CH_3)_4^+XeF_5^-$, cation bands were also observed (see Table 4) with frequency values that are in excellent agreement with previous literature data.[4,5,7,48]

Force Constants. The symmetry force constants of XeF_5^- are shown in Table 7. Except for the E_1' and E_2' blocks, all of the symmetry force constants are one-dimensional and well determined. In the two-dimensional E_2' block, G_{56} equals zero (see Table 6) resulting in F_{56} also becoming zero. Therefore, the only remaining underdetermined problem is the two-dimensional E_1' block. The range of possible solutions for this block was computed using the extremal conditions reported by Sawodny.[49] It has previously been pointed out[49-52] that in weakly coupled (heavy central atom) systems the values of the general valence force field tend to fall within the range given by $F_{34} = 0$ as the lower and $F_{34} = 1/2|F_{34}(\max) - F_{34}(\min)|$ as the upper limit with $F_{44} = \min$ being an excellent choice. The latter choice results in an F_{33} value of 1.830 mdyn/Å with an error limit of about 0.14 mdyn/Å and, therefore, F_{33} can be considered to be reasonably well determined.

The most important internal force constants of XeF_5^-, together with the known bond length, are given in Table 8 and are compared to those of the closely related XeF_2 [53] and XeF_4 [50] molecules and the IF_4^- anion.[50] As can be seen from Table 8, the force constants well reflect our expectations. Compared with XeF_2 and XeF_4, the increased $^{\delta+}$Xe-F$^{\delta-}$ polarity of the Xe-F bond in XeF_5^-, combined with the crowding effect in the equatorial plane, should decrease the Xe-F stretching (f_r), increase the in-plane deformation (f_α) and decrease the out of plane deformation (f_γ) force constants. Furthermore, ($f_{\alpha\alpha}$ - $f_{\alpha\alpha}'$) and ($f_{\gamma\gamma}$ - $f_{\gamma\gamma}'$) should exhibit positive signs as expected for adjacent angles interacting more strongly than non-adjacent angles. The excellent agreement between these expectations and the experimental values from Table 8 lends strong support to the above assignments for XeF_5^-.

The data of Table 8 demonstrate that the stretching force constants f_r are mainly influenced by the polarity of the Xe-F bonds, with increasing polarity decreasing the force constant. On the other hand, steric crowding has a strong impact on the deformation constants. If this crowding is anisotropic, as in the case of XeF_5^- where the crowding is concentrated in the equatorial plane, the deformation constants in the congested plane increase while the deformation constants out of the congested plane decrease significantly. The low value of the out-of-plane deformation constant f_γ, in combination with a comparable $f_{\gamma\gamma}$ value, implies a low energy barrier toward puckering of the equatorial plane. When the f_γ value approaches zero or becomes negative, spontaneous puckering should occur.

Computational Results. For a better understanding of the molecular structure of XeF_5^-, local density functional calculations were carried out for this ion and for XeF_4. The quality of these calculations for relatively large and heavy molecules, was first tested for the well characterized[54,55] and closely related XeF_4 molecule. The well known square planar (D_{4h}) symmetry and a Xe-F bond length of 1.998 Å (0.045 Å longer than that observed for the solid[54]) were obtained. The calculated vibrational frequencies are in excellent agreement with the experimental values[55] (Table 9), except for the in-plane deformation modes where the agreement is only fair.

For XeF_5^-, the computations confirmed that the pentagonal planar D_{5h} structure is indeed a minimum. Again, the computed bond length (2.077 Å) is slightly longer (0.065 Å) than the observed one (2.012 Å). A comparison between the observed and calculated spectra is given in Table 10. As for XeF_4, the agreement between computed and observed frequencies for XeF_5^- is quite good, with the largest discrepancies being found again for the in-plane deformation modes. These results confirm the assignments made above for XeF_5^-.

The influence of the bond length on the vibrational spectrum of XeF_5^- was also examined by computing the spectra for two shorter

Xe-F bond distances, one at the experimental bond length and one 0.01 Å longer (Table 10). As expected, the stretching frequencies are the most sensitive to changes in the bond length except for the equatorial ring puckering mode, ν_7, which is also very sensitive to the shortening of the bond length. At the experimental distance, the degenerate deformation frequency becomes imaginary showing that the molecule would assume a non-planar structure. As discussed above, increasing congestion in the equatorial ring will result in spontaneous puckering and an imaginary frequency for ν_7. The calculations at the experimental geometry are far enough from the theoretical minimum that the calculated frequencies should be employed only to show the expected trends as they do not refer to the minimum energy structure. The data of Table 10 also indicate that the frequency order of the Xe-F stretching modes is essentially independent of the Xe-F bond length. It should be noted that all of the calculated frequencies are harmonic values and were not scaled to include anharmonicity effects which are usually on the order of 5%.

The Mulliken charges for XeF_5^- are +1.48e for the Xe atom and -0.50e for the F atoms. This differs from the nominal assignments of -1.0e for each F and +4.0e for the Xe. The molecular orbitals (Table 11) provide some insight into the bonding in this molecule. If we consider only the valence p orbitals on F since the 2s orbitals are quite low in energy, the remaining orbitals can be qualitatively summed up as follows: there are 10 electrons in the $2p_y$ lone pairs on F orthogonal to the Xe-F bond. There are roughly

10 electrons in the $2p_z$ orbitals on F which are orthogonal to the molecular plane. The totally symmetric group of these orbitals interacts with the out-of-plane 5p orbital on Xe in a symmetric and antisymmetric way. The $2p_x$ orbitals on fluorine along the Xe-F bond have about 10e in them. These mix the $5p_x$ and $5p_y$ orbitals on Xe. Although the Xe 5s orbital does mix to some extent with the 2p orbitals on F, it is predominantly a lone pair. The basic description is thus a Xe with a $5s^2 5p_z^2$ occupancy surrounded by five F^- atoms. Delccalization of fluorine electron density into the Xe $5p_{x,y}$ orbitals with only a small participation of the d orbitals on Xe then reduces the charges on the F atoms. The HOMO is the antibonding combination of the in-plane lone pairs on the F atom orthogonal to the Xe-F axis. The NHOMO is almost degenerate in energy with the HOMO and is the antibonding out-of-plane combination of the F $2p_z$ and the Xe $5p_z$ orbitals (Figure 8).

Both the orbitals and the bonding in XeF_5^- are quite similar to those of XeF_4 which were calculated for comparison. In XeF_4, the Mulliken charges on Xe and F are +1.65e and -0.41e, respectively. The Xe 5s orbital participates in two orbitals with most of its density in the orbital at 22.02 eV just as in XeF_5^-. The $5p_z$ orbital of Xe and the out-of-plane $2p_z$ orbitals on the fluorines interact to give bonding and antibonding molecular orbitals. The orbital configuration at Xe is thus dominated by the $5s^2 5p_z^2$ configuration just as in the anion. The HOMO in XeF_4 is at 9.15 eV and is the $5p_y$ antibonding orbital as found in XeF_5^-. Its significantly higher value, compared with XeF_5^-, is in agreement with our expectations for an anion and its parent molecule.

It is important to note that the calculations provide a molecular orbital description of the bonding in XeF_5^- and XeF_4. The orbitals reported above are the canonical orbitals with the molecular symmetry. Because of the molecular symmetry, the 5s and $5p_z$ orbitals cannot mix and thus give separate s^2 and p^2 occupancies. In contrast, in the VSEPR model used elsewhere in this work, the valence electron lone pairs may be described as two doubly occupied sp hybrids above and below the plane, but this is not required by the VSEPR model. The two models are equivalent as the VSEPR model is derived from a localized orbital approach whereas the calculations are based on a molecular orbital approach. The sum and difference of the $5s^2$ and $5p_z^2$ orbitals will lead to the two sp hybrid lone pairs. However, the total electron density, which is the invariant quantity, is independent of the choice of models used to describe it. (In a formal sense, the wave function is invariant to a unitary transformation.)

CONCLUSIONS

Xenon tetrafluoride indeed forms stable adducts with strong Lewis bases, such as tetramethylammonium fluoride and the heavier alkali metal fluorides. However, contrary to previous reports,[13-15] these salts do not contain the XeF_6^{2-} dianion, but the XeF_5^- anion.

The XeF_5^- anion has a highly unusual pentagonal planar structure for which no other examples were previously known. It can be derived from that of a pentagonal bipyramid, such as IF$_7$,[38] in which the two axial fluorine ligands have been replaced by two sterically active free valence electron pairs. Compared with IF$_7$,

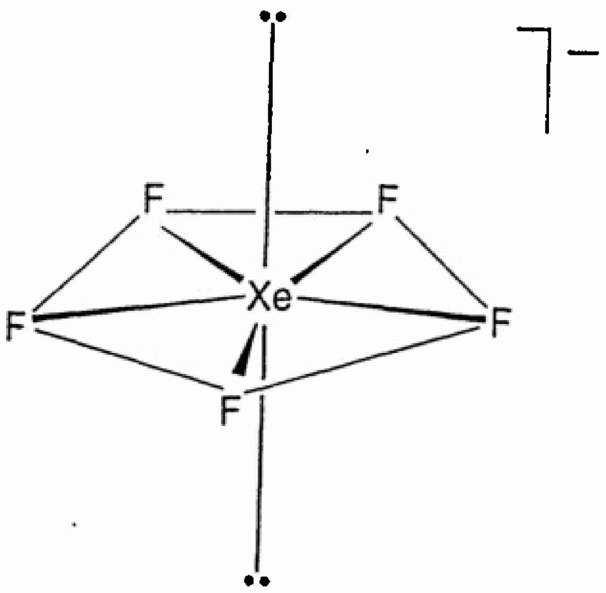

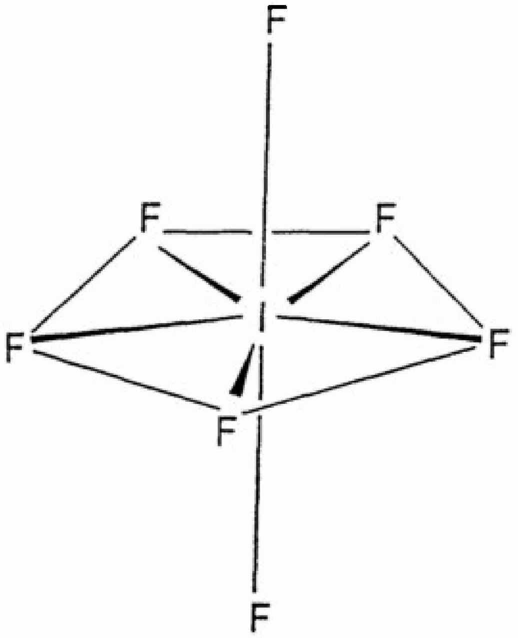

which is a fluxional molecule undergoing with relative ease a dynamic ring-puckering pseudorotation,[38,47] the equatorial XeF$_5$ plane of XeF$_5^-$ appears to be considerably more rigid. The increased rigidity of the XF$_5$ plane in XeF$_5^-$ is attributed to the stabilizing effect of the two free valence electron pairs on xenon. These free pairs are more diffuse and hence repulsive than the axial I-F bond pairs in IF$_7$, thereby offering more resistance toward the puckering of the equatorial XeF$_5$ plane.

Acknowledgements. The authors thank C.J. Schack, W.W. Wilson, R.D. Wilson and S.S. Tsai for their help; F. Adar, Instruments S.A., Edison, N.J. for recording the single crystal Raman spectrum of $N(CH_3)_4^+XeF_5^-$; the U.S. Air Force Astronautics Laboratory, Edwards AFB (K.O.C. and G.J.S.); the U.S. Army Research Office (K.O.C.) and the Natural Sciences and Engineering Research Council of Canada (G.J.S.) for financial support; Ministry of Foreign Affairs, France for a Lavoisier Fellowship (H.P.M.) and C.N.R.S. Laboratoire des Agrégats Moléculaires et Matériaux Inorganiques, Montpellier, France for granting a leave of absence to H.P.M.

Supplementary Material Available: Tables of anisotropic thermal parameters (Supplementary Table 1), hydrogen atomic coordinates (Supplementary Table 2) and a tabulation of calculated and observed structure factor amplitudes (Supplementary Table 3) (XX pages). Ordering information is given on any current masthead page.

REFERENCES

1. Rockwell International, Rocketdyne Division.
2. E. I. du Pont de Nemours and Company, Inc.
3. McMaster University.
4. Christe, K.O.; Wilson, W.W.; Wilson, R.D.; Bau, R.; Feng, J. J. Am. Chem. Soc. 1990, 112, 7619..
5. Wilson, W.W.; Christe, K.O. Inorg. Chem. 1989, 28, 4172.
6. Christe, K.O.; Wilson, W.W.; Chirakal, R.V.; Sanders, J.C.P.; Schrobilgen, G.J. Inorg. Chem. 1990, 29, 3506.
7. Wilson, W.W,; Christe, K.O.; Feng, J.; Bau, R. Can. J. Chem. 1989, 67, 1988.
8. Christe, K.O.; Wilson, W.W; Schrobilgen, G.J., Chirakal, R.V.; Olah, G.A. Inorg. Chem. 1988, 27, 789.
9. Klamm, H.; Meinert, H.; Reich, P.; Witke, P. Z. Chem., 1968, 8, 469.
10. Christe, K.O.; Wilson, W.W. Inorg. Chem. 1989, 28, 3275 and references cited therein.
11. Mahjoub, A.R.; Hoser, A.; Fuchs, J.; Seppelt, K. Angew. Chem. Int. Ed. Engl., 1989, 28, 1526.
12. Christe, K.O.: Wilson, W.W. Inorg. Chem. 1939, 28, 3275.
13. Spitzin, V.I.; Kiselev, Yu. M.; Fadeeva, N.E.: Popov, A.I.; Tchumaevsky, N.A. Z. Anorg. Allg. Chem. 1988, 559, 171.
14. Kiselev, Yu. M.; Goryachenkov, S.A.; Martynenko, L.I.; Spitsyn, V.I. Dokl. Akad. Nauk SSSR 1984, 278, 881.

15. Kiselev, Yu. M.; Fadeeva, N.E.; Popov, A.I.; Korobov, M.V.; Nikulin, V.V.; Spitsyn, V.I. Dokl. Akad. Nauk SSSR 1987, 295, 378.

16. Weidlein, J.; Müller, U.; Dehnicke, K.; "Schwingungsspektroskopie", Georg Thieme Verlag, Stuttgart, Germany, 1982.

17. Christe, K.O.; Wilson, W.W. Inorg. Chem. 1982, 21, 4113.

18. Christe, K.O.; Wilson, R.B.; Schack, C. J. Inorg. Synth. 1986, 24, 3.

19. Syvret, R.G.; Schrobilgen, G.J. Inorg. Chem. 1989, 28, 1564.

20. (a) Bartlett, N.; Sladky, F.O. J. Am. Chem. Soc. 1968, 90, 5316. (b) Malm, J.G.; Chernick, C.L. Inorg. Synth. 1966, 8, 254.

21. Christe, K.O. Inorg. Chem. 1972, 12, 1580.

22. Winfield, J.M. J. Fluorine Chem. 1984, 25, 91.

23. Sheldrick, G.M. "SHELX-76 Program for Crystal Structure Determination"; University of Cambridge: Cambridge, England, 1976.

24. Hall, S.R.; Stewart, J.H. "XTAL 2.6 User's Manual", University of Western Australia and University of Maryland.

25. Davies, K. "CHEMGRAF Suite: SNOOPI", Chemical Design Ltd. Oxford, England, 1983.

26. Miller, F.A; Harney, B.M. Appl. Spectrosc. 1969, 23, 8.

27. Parr, R.G.; Yang, W. Density Functional Theory of Atoms and Molecules, Oxford University Press, New York, 1989.

28. Salahub, D.R. in "Ab Initio Methods in Quantum Methods in Quantum Chemistry", Lawley, K.P.; J. Wiley & Sons, New York, 1987, 2nd ed., p. 447.

29. Wimmer, E.; Freeman, A.J.; Fu, C.-L.; Cao, P.-L.; Chou, S.-H.; Delley, B. in "Supercomputer Research in Chemistry and Chemical Engineering" Jensen, K.F.; Truhlar, D.G., Eds.; ACS Symposium Series, American Chemical Society, Washington, D.C., 1987, p. 49; (b) Dixon, D.A.; Andzelm, J.; Fitzgerald, G.; Wimmer, E.; Delley, B. in Science and Engineering on Cray Supercomputers Proceedings of the Fifth International Symposium, Cray Research, Minneapolis, MN, 1990, p. 285.

30. Jones, R.O.; Gunnarsson, O. Rev. Mod. Phys. 1989, 61, 689.

31. Delley, B. J. Chem. Phys. 1990, 92, 508. DMol is available commercially from BIOSYM Technologies, San Diego, CA.

32. This grid can be obtained by using the FINE parameter in DMol.

33. von Barth, U.; Hedin, L. J. Phys. C 1972, 5, 1629.

34. (a) Versluis, I.; Ziegler, T. J. Chem. Phys. 1988, 88, 3322; (b) Andzelm, J.; Wimmer, E.; Slahub, D.R. in "The Challenge of d and f Electrons: Theory and Computation"; Eds Salahub, D.R.; Zerner, M.C. ACS Symposium Series, No. 394, American Chemical Society, Washington, D.C. 1989, p. 228; (c) Fournier, R.; Andzelm, J.; Salahub, D.R. J. Chem. Phys. 1989, 90, 6371.

35. Pauling, L. "The Nature of the Chemical Bond", 3rd ed.; Cornell University Press: Ithaca, N.Y., 1960; p. 260.

36. Bondi, A. J. Phys. Chem. 1964, 68, 441.

37. Burns, J.H.; Agron, P.A.; Levy, H.A. Science, 1963, 139, 1208.

38. Adams, W.J.; Thompson, H.B.; Bartell, L.S. *J. Chem. Phys.* 1970, *53*, 4040.

39. Jameson, C.J.; Mason, J. In "Multinuclear NMR", J. Mason, ed., Plenum Press: New York, 1987; Chapter 3, pp. 66-68.

40. (a) Jameson, C.J. In "Multinuclear NMR", J. Mason, ed., Plenum Press: New York, 1987; Chapter 4, pp. 97 - 101; Chapter 18. (b) Schrobilgen, G.J. In "NMR and the Periodic Table", R.K. Harris and B.E. Mann, eds., Academic Press: New York, 1978; Chapter 14.

41. Gillespie, R.J. "Molecular Geometry", Van Nostrand Reinhold Co.: London, 1972.

42. (a) Bartell, L.S.; Gavin, R.M.; Thompson, H.B. *J. Chem. Phys.* 1965, *43*, 2547. (b) Bartell, L.S.; Gavin, R.M. *J. Chem. Phys.* 1968, *48*, 2466.

43. Gillespie, R.J.; Quail, J.W. *Can. J. Chem.* 1964, *42*, 2671.

44. Wilson, E.B. *J. Chem. Phys.* 1941, *9*, 76.

45. Khanna, R.K. *J. Mol. Spectrosc.* 1962, *8*, 134.

46. A factor-group analysis of the vibrational modes of the unit cell was carried out using the correlation chart method (Carter, R.L. *J. Chem. Educ.* 1971, *48*, 297 and references therein). The free anion symmetry (D_{5h}) was correlated to the site symmetry of the anion (C_s) which, in turn, was correlated to the crystal symmetry (D_{2h}). Assuming complete vibrational coupling occurs in the unit cell of $N(CH_3)_4^+XeF_5^-$, all the vibrational modes of the XeF_5^- anion are found to be Raman and infrared active under the crystal symmetry. Moreover, ν_3, ν_4,

ν_5, ν_6 and ν_7 will be split into four and three components in their Raman (A_g, B_{1g}, B_{2g}, B_{3g}) and infrared (B_{1u}, B_{2u}, B_{3u}) spectra, respectively; ν_1 will be split into two components in both the Raman (A_g, B_{3g}) and infrared (B_{1u}, B_{2u}) spectra and ν_2 will not be split in the infrared (B_{3u}) but will be split into two components in the Raman (B_{1g}, B_{2g}) spectrum.

47. Bartell, L.S.; Rothman, M.J.; Gavezzotti, A. J. Chem. Phys. 1982, 76, 4136, and references cited therein.
48. Christe, K.O.; Wilson, W.W.; Bougon, R.A. Inorg. Chem. 1986, 25, 2163.
49. Sawodny, W. J. Mol. Spectrosc. 1969, 30, 56.
50. Christe, K.O.; Naumann, D. Inorg. Chem. 1973, 12, 59.
51. Pfeiffer, M. J. Mol. Spectrosc. 1969, 21, 181.
52. Thakur, S.N.; Rai, S.N. J. Mol. Struct. 1970, 5, 320.
53. Siebert, H. "Anwendungen der Schwingungsspektroskopie in der Anorganischen Chemie", Anorganische und Allgemeine Chemie in Einzeldarstellung, VII, Springer Verlag: Berlin, Germany, 1966.
54. Burns, J.H.,; Agron, P.A.; Levy, H.A. Science 1963, 139, 1208; Templeton, D.H.; Zalkin, A.; Forrester, J.D.; Williamson, S.M. J. Am. Chem. Soc. 1963, 85, 242; Ibers, J.A., Hamilton, W.C. Science 1963, 139, 106.
55. Claassen, H.H.; Chernick, C.L.; Malm, J.G. J. Am. Chem. Soc. 1963, 85, 1927.

FIGURE CAPTIONS

Figure 1. Atom numbering scheme, bond lengths (Å) and angles (deg) for XeF_5^- at -86 °C in $[N(CH_3)_4]^+[XeF_5]^-$. Projection of the XeF_5^- anion on (111). Esd's are given in parentheses; thermal ellipsoids are shown at the 50% probability level.

Figure 2. Projections of the XeF_5^- anion on (130) (left) and (010) (right). Thermal ellipsoids are shown at the 50% probability level.

Figure 3. Stereoview [111] of the unit cell of $[N(CH_3)_4]^+[XeF_5]^-$; hydrogen atoms are excluded.

Figure 4. The ^{129}Xe NMR spectrum (139.05 MHz) at 24 °C of a saturated solution of $N(CH_3)_4^+XeF_5^-$ in CH_3CN containing a 1 molar excess of $N(CH_3)_4^+F^-$.

Figure 5. The ^{19}F NMR spectrum (235.36 MHz) at 24 °C of (a) a saturated solution of $N(CH_3)_4^+XeF_5^-$ in CH_3CN containing a 1 molar excess of $N(CH_3)_4^+F^-$ and (b) a saturated solution of pure $N(CH_3)_4^+XeF_5^-$ in CH_3CN. Asterisks (*) denote ^{129}Xe satellites.

Figure 6. (a) Vibrational spectra of solid $Cs^+XeF_5^-$. Upper trace, infrared spectrum recorded at room temperature using an AgBr disk; lower trace, Raman spectrum recorded in a glass capillary at 25 °C using 647.1 nm excitation. (b) Single crystal Raman spectrum of $N(CH_3)_4^+XeF_5^-$ recorded in a glass capillary at room tempertature using 514.5 nm excitation.

Figure 7. Internal coordinates for pentagonal planar AX_5.

Figure 8. Selected molecular orbitals for XeF_5^-.

(a) HOMO, antibonding combination of in-plane p_y's on F; (b) Bonding out-of-plane orbital combination between Xe $5p_z$ and p_z's on F; (c) Antibonding out-of-plane orbital combination between Xe $5p_z$ and p_z's on F.

Table 1. Summary of Crystal Data and Refinement Results for $[N(CH_3)_4]^+[XeF_5]^-$ [a]

Space group	Pmcn (orthorhombic)
a (Å)	6.340(2)
b (Å)	10.244(3)
c (Å)	13.896(4)
V (Å^3)	902.55
Molecules/unit cell	4
Molecular weight (g mol^{-1})	300.44
Calculated density (g cm^{-3})	2.153
T (°C)	-86
Color	colorless
Crystal decay (%)	0.6
μ (cm^{-1})	35.77
Wavelength (Å) used for data collection	0.71069
sin θ/λ limit (Å^{-1})	0.538
Total number of reflections measured	1414
Number of independent reflections	641
Number of reflections used in structural analysis $I > 3\sigma(I)$	638
Number of variable parameters	83
Final agreement factors	R(F) = 0.0435
	R(WF) = 0.0435

[a] Unit cell parameters obtained at 23 °C were: a = 6.400 Å, b = 10.321 Å, c = 14.029 Å; Volume, 926.71 Å^3.

Table 2. Final Atomic Coordinates for $[N(CH_3)_4]^+[XeF_5]^-$

Atom	x	y	z	pop[a]
Xe1	0.2500	0.1233(1)	0.0155(1)	0.5
F1	0.2500	0.1876(9)	0.1497(6)	0.5
F2	0.2500	-0.0324(8)	0.1025(6)	0.5
F3	0.2500	-0.0399(8)	-0.0673(6)	0.5
F4	0.2500	0.1799(9)	-0.1236(6)	0.5
F5	0.2500	0.3217(8)	0.0110(6)	0.5
N1	0.2500	-0.403(1)	0.172(1)	0.5
C1	0.2500	0.628(2)	0.068(1)	0.5
C2	0.2500	-0.281(2)	0.231(1)	0.5
C3	0.437(5)	-0.483(2)	0.196(1)	1.0

a The site occupation factor.

Table 3. Bond distances (Å) and Bond Angles (deg) in $[N(CH_3)_4]^+[XeF_5]^-$

Bond Lengths

Xe1-F1	1.979(2)
Xe1-F2	2.001(2)
Xe1-F3	2.030(2)
Xe1-F4	2.018(2)
Xe1-F5	2.034(2)
N1-C1	1.481(6)
N1-C2	1.488(6)
N1-C3	1.524(4)

Bond Angles

F2-Xe1-F1	72.3(4)
F3-Xe1-F2	71.7(4)
F4-Xe1-F3	72.2(4)
F5-Xe1-F1	72.3(4)
F5-Xe1-F4	71.5(4)
C2-N1-C1	110.7(3)
C3-N1-C1	108.9(5)
C3-N1-C2	109.6(4)

Table 4. Vibrational Spectra of the XeF_5^- Anion in Different Salts

observed frequencies,[a] cm^{-1}												
$NOXeF_5$[b]		$N(CH_3)_4XeF_5$[c]		$NaXeF_5$		$KXeF_5$		$RbXeF_5$		$CsXeF_5$		assignments for XeF_5^- in point group D_{5h}
RA		RA	IR	RA	IR	RA	IR	RA	IR	RA	IR	
25 °C	-150 °C											
									970 vw		955 vw	$\nu_1 + \nu_3$ (E_1')
									882 vw		870 sh	$\nu_3 + \nu_5$ ($E_1' + E_2'$)
							860 vw				850 vw	$2\nu_3$ ($A_1' + E_2' + A_2'$)
							800 vw		808 vw		795 vw	$\nu_5 + \nu_6$ ($A_1' + E_1' + A_2'$)
									752 vw		740 sh	$2\nu_6$ ($A_1' + E_1'$)
							740 vw		728 vw		724 vw	$\nu_4 + \nu_5$ ($E_1' + E_2'$)
											705 sh	
									668 vw		650 sh	$\nu_4 + \nu_6$ ($E_1' + E_2'$)
						544(0.1)		550(0.1)		547(0.1)		$2\nu_2$ (A_1')
503(10)	506(10)	502(10)		519(10)	525 sh	505(10)		509(10)		504(10)		ν_1 (A_1')
	498(1)		509 sh			498 sh		489 sh				
482(0+)			465 vs	473(0.1)	450 vs,br		490 vs	471(0.1)	470 vw,br		450 vs,br	ν_3 (E_1')
	475(0.5)		420 sh		415 s		410 s	453 sh	418 s		415 s	
440 sh	445(1.0)	423(2.1)		444(1.0)		439(1.4)		440(1.6)		432(1.5)		ν_5 (E_2')
429(1.1)	424(1)			422(1.3)		424(1.2)		437 sh		422(1.6)		
382 sh	384(1)	377(3.3)		386(2.0)		388(2.4)	379 sh	389(2.2)	372 w	380(2.2)		ν_6 (E_2')
374(2.3)	373(2.5)			393 sh		381(1.9)		379(1.6)		369(2.3)		
290(0+)	282(0.5)			293(0+)		290(0+)		299(0+)	288 sh	312(0+)	288 sh	ν_4 (E_1')
240(0.2)	244(0.6)		278 s		276 s		275 s	278(0+)	275 s		274 s	ν_2 (A_2'')
								169(0.7)				
						147(1.5)		131(1.1)				
						113 sh		107(0.4)				
135(1)	144(1.5)					102(0.5)		91(1.3)		124(1.2)		
97(0.9)	100(1.5)	90(1)		144(1.4)		90(2)		77(1)		104(1.5)		lattice vibrations
75(1.5)	82(3.0)					65 sh		59(1.4)		57(0.3)		
35(0.5)	42(1)					52 sh		52 sh				
						42 sh		47 sh				
								35(0.6)				

a Values in parentheses denote relative intensities; sh denotes a shoulder; s, strong and w, weak.

b The NO^+ stretching mode was observed at 2314 cm^{-1} with a relative intensity of 1.0.

c Only the bands due to the XeF_5^- anion have been listed in the Table. In addition to these bands, the following bands due to the $N(CH_3)_4^+$ cation were observed. RA: 3035(0.2), 2990(0.1), 2970(0.1), 2930(0.2), 2920(0.1), 1494(0.1), 1458(0.3), 1185(0+), 954(0.5), 758(0.9), 480(0.2), 468(0.2), 456(0.1); IR: 3040m, 2968w, 1491s, 1423w, 954s, 462s. For their assignment see ref. (3).

Table 5. Symmetry Coordinates and Approximate Mode Descriptions for a Pentagonal Planar XY_5 Molecule.

$$S_1 = \frac{1}{\sqrt{5}} (\Delta r_1 + \Delta r_2 + \Delta r_3 + \Delta r_4 + \Delta r_5)$$

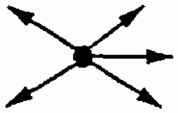

symmetric stretch

$$S_2 = \frac{1}{\sqrt{10}} [\sum_{i=1}^{5} (\Delta\gamma_{i6} - \Delta\gamma_{i7})]$$

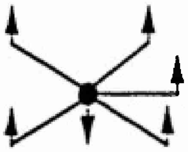

symmetric out of plane (umbrella) deformation.

$$S_{3a} = \sqrt{\frac{2}{5}} [\Delta r_1 + \cos\alpha (\Delta r_2 + \Delta r_5) + \cos2\alpha (\Delta r_3 + \Delta r_4)]$$

$$S_{3b} = \sqrt{\frac{2}{5}} [\sin\alpha (\Delta r_2 - \Delta r_5) + \sin2\alpha (\Delta r_3 - \Delta r_4)]$$

asymmetric stretch

$$S_{4a} = \sqrt{\frac{2}{5}} [\Delta\alpha_{34} + \cos\alpha (\Delta\alpha_{45} + \Delta\alpha_{23}) + \cos2\alpha (\Delta\alpha_{15} + \Delta\alpha_{12})]$$

$$S_{4b} = \sqrt{\frac{2}{5}} [\sin\alpha (\Delta\alpha_{45} - \Delta\alpha_{23}) + \sin2\alpha (\Delta\alpha_{15} - \Delta\alpha_{12})]$$

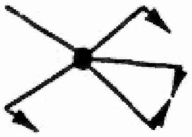

asymmetric in plane deformation

$$S_{5a} = \sqrt{\frac{2}{5}} [\Delta r_1 + \cos2\alpha (\Delta r_2 + \Delta r_5) + \cos\alpha (\Delta r_3 + \Delta r_4)]$$

$$S_{5b} = \sqrt{\frac{2}{5}} [\sin2\alpha (\Delta r_2 + \Delta r_5) + \sin\alpha (\Delta r_3 + \Delta r_4)]$$

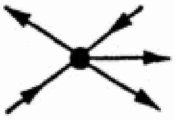

asymmetric stretch

$$S_{6a} = \sqrt{\frac{2}{5}} [\Delta\alpha_{34} + \cos2\alpha (\Delta\alpha_{45} + \Delta\alpha_{23}) + \cos\alpha (\Delta\alpha_{15} + \Delta\alpha_{12})]$$

$$S_{6b} = \sqrt{\frac{2}{5}} [\sin2\alpha (\Delta\alpha_{45} - \Delta\alpha_{23}) - \sin\alpha (\Delta\alpha_{15} - \Delta\alpha_{12})]$$

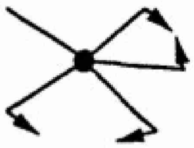

in plane (scissor) deformation

$$S_{7a} = \frac{1}{\sqrt{5}} [(\Delta\gamma_{16} - \Delta\gamma_{17}) + \cos2\alpha (\Delta\gamma_{26} - \Delta\gamma_{27} + \Delta\gamma_{56} - \Delta\gamma_{57}) + \cos\alpha (\Delta\gamma_{36} - \Delta\gamma_{37} + \Delta\gamma_{46} - \Delta\gamma_{47})]$$

$$S_{7b} = \frac{1}{\sqrt{5}} [\sin2\alpha (\Delta\gamma_{26} - \Delta\gamma_{27} - \Delta\gamma_{56} + \Delta\gamma_{57}) - \sin\alpha (\Delta\gamma_{36} - \Delta\gamma_{37} - \Delta\gamma_{46} + \Delta\gamma_{47})]$$

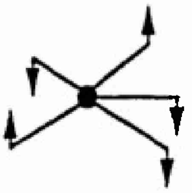

asymmetric out of plane deformation

Table 6. G-Matrix[a] for Pentagonal Planar XeF_5^- of Symmetry D_{5h}.

A_1' $G_{11} = \mu_y = 5.2637 \times 10^{-2}$

A_2'' $$G_{22} = \frac{2}{r^2}(\mu_y + 5\mu_x) = 4.4802 \times 10^{-2}$$

E_1' $$G_{33} = \mu_y + \frac{5\mu_x}{2} = 7.1677 \times 10^{-2}$$

$$G_{34} = \frac{5\sqrt{5}\ \mu_x}{4r\sin\alpha} = 1.1123 \times 10^{-2}$$

$$G_{44} = \frac{1}{r^2}(5\mu_y\sin^2 2\alpha + \mu_x) = 2.4333 \times 10^{-2}$$

E_2' $G_{55} = \mu_y = 5.2637 \times 10^{-2}$

$G_{56} = 0$

$$G_{66} = \frac{1}{r^2}(4\mu_y\sin^2\alpha) = 4.7026 \times 10^{-2}$$

E_2'' $$G_{77} = \frac{2\mu_y}{r^2} = 2.5995 \times 10^{-2}$$

[a] The following geometry was used for the calculation of the G-matrix: $r = 2.0124$ Å and $\alpha = 72°$.

Table 7. F-Matrix and Force Field for Pentagonal Planar XeF_5^- of Symmetry D_{5h}

Assignment	Freq (cm^{-1})	Symmetry Force Constants[a]
A_1' ν_1	502	$F_{11} = f_r + 2f_{rr} + 2f_{rr}' = 2.820$
A_2'' ν_2	274	$F_{22} = r^2(f_\gamma + 2f_{\gamma\gamma}\cos\alpha + 2f_{\gamma\gamma}'\cos2\alpha) = 0.996$
E_1' ν_3	465	$F_{33} = f_r + 2f_{rr}\cos\alpha + 2f_{rr}'\cos2\alpha = 1.830$
		$F_{34} = r(f_{r\alpha} + 2f_{r\alpha}'\cos\alpha + 2f_{r\alpha}''\cos2\alpha) = -0.342$
ν_4	290	$F_{44} = r^2(f_\alpha + 2f_{\alpha\alpha}\cos\alpha + 2f_{\alpha\alpha}'\cos2\alpha) = 2.212$
E_2' ν_5	423	$F_{55} = f_r + 2f_{rr}\cos2\alpha + 2f_{rr}'\cos\alpha = 2.003$
		$F_{56} = r(f_{r\alpha} + 2f_{r\alpha}'\cos2\alpha + 2f_{r\alpha}''\cos\alpha) = 0$
ν_6	377	$F_{66} = r^2(f_\alpha + 2f_{\alpha\alpha}\cos2\alpha + 2f_{\alpha\alpha}'\cos\alpha) = 1.797$
E_2'' ν_7	79[b]	$F_{77} = r^2(f_\gamma + 2f_{\gamma\gamma}\cos2\alpha + 2f_{\gamma\gamma}'\cos\alpha) = 0.143$

[a] Stretching constants in mdyn/Å, deformation constants in mdyn Å/rad^2, and stretch-bend interaction constants in mdyn/rad.

[b] Value taken from the ab initio calculation.

Table 8. Internal Force Constants (mdyn/Å) and Bond Length (Å) of XeF_5^- Compared to those of XeF_2, XeF_4 and IF_4^-

Force Constant	XeF_2[a]	XeF_4[b]	IF_4^- [b]	XeF_5^- [c]
f_r	2.83	3.055	2.221	2.096
f_{rr}	0.14	0.120	0.183	0.143
f_{rr}'	--	0.007	0.466	0.219
$f_\alpha\ (-f_{\alpha\alpha}')$	0.20	0.193	0.182	0.458
$f\ \ (-f\ \ ')$	--	0.299	0.257	0.072
$f_{\alpha\alpha} - f_{\alpha\alpha}'$	--	--	--	0.045
$f_\alpha - f_{\alpha\alpha}$	--	--	--	0.413
$f\ \ - f\ \ '$	--	--	--	0.093
$f\ \ - f$	--	--	--	-0.021
r	1.98	1.953	--	2.012

a Data from ref. (53).

b Data from ref. (50). The f values in ref. (50) have not been properly normalized and must be divided by two to correspond to the values from this work.

c This work.

Table 9. Calculated and Experimental Vibrational Frequencies (cm^{-1}) of XeF_4

Assignment		Calculated frequency	Observed frequency	Approximate mode description
A_{1g}	ν_1	532	543	ν_{sym} (in phase)
A_{2u}	ν_2	271	291	δ_{sym} (out of plane)
B_{1g}	ν_3	498	502	ν_{sym} (out of phase)
B_{2g}	ν_4	182	235	δ_{sym} (in plane)
B_{2u}	ν_5	156	inactive	δ_{asym} (out of plane)
E_u	ν_6	591	586	ν_{asym}
E_u	ν_7	143	123	δ_{asym} (in plane)

Table 10. Calculated and Experimental Vibrational Frequencies (cm^{-1}) for XeF_5^-

Assignment	Calculated frequency			Observed frequency	Approximate mode description
	a	b	c		
A_1' ν_1	467	537	551	502	ν_{sym} (in plane)
A_2'' ν_2	270	274	275	274	δ_{sym} (out of plane)
E_1' ν_3	502	574	585	400 - 550	ν_{asym}
E_1' ν_4	248	255	254	290	δ_{asym} (in plane)
E_2' ν_5	413	477	489	423	ν_{asym}
E_2' ν_6	335	356	361	377	δ_{sym} (in plane)
E_2'' ν_7	79	21	28i	-	δ_{asym} (out of plane)

a With the calculated Xe-F bond length of 2.077 Å.

b With an assumed Xe-F bond length of 2.022 Å.

c With the observed Xe-F bond length of 2.012 Å.

Table 11. Valence Molecular Orbitals for XeF_5^-

Symmetry	Orbital[a]	Energy (eV)
A_2'	p_y anti on F	3.00
A_2''	p_z anti 0.67 Xe, 0.40 F	3.15
E_1'	p_y on F	3.71
A_1'	0.43 p_x on F, 0.57 s on Xe, anti	4.00
E_2''	p_z on F	4.06
E_1''	p_z on F some Xe d	4.69
E_2'	$p_{x,y}$ on F	4.78
E_2'	$\rho_{x,y}$ on F	5.72
A_2''	0.77 p_z Xe, 0.21 p_z F	7.38
E_1'	0.56 p_x, p_y Xe 0.40 p_x on F	9.01
A_1'	0.89 Xe s	16.02

[a] x = Xe - F bond axis, y = orthogonal to Xe - F axis in-plane, z = out-of-plane

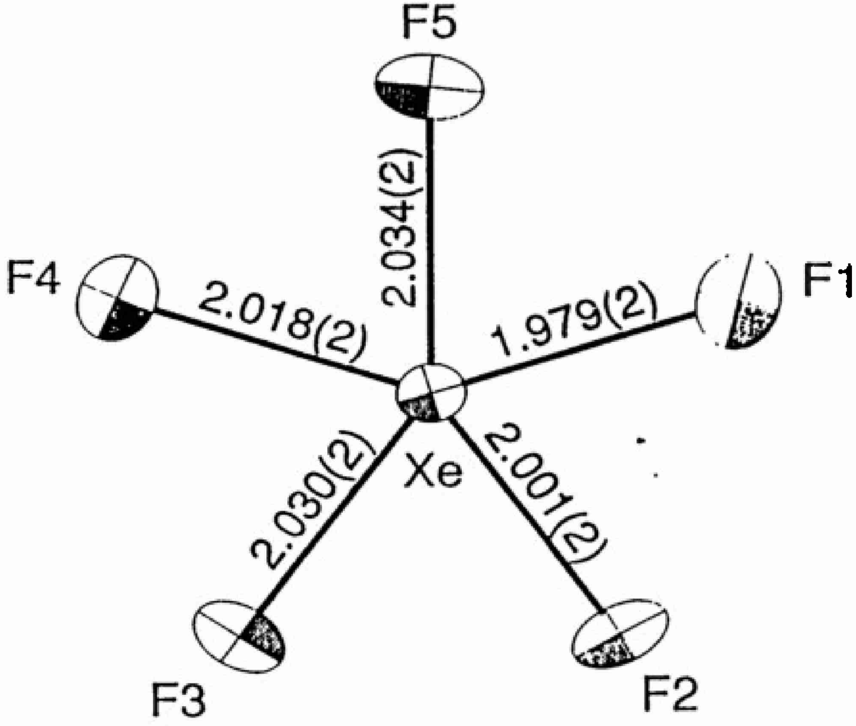
F5
2.034(2)
F4
2.018(2)
1.979(2)
F1
Xe
2.030(2)
2.001(2)
F3
F2

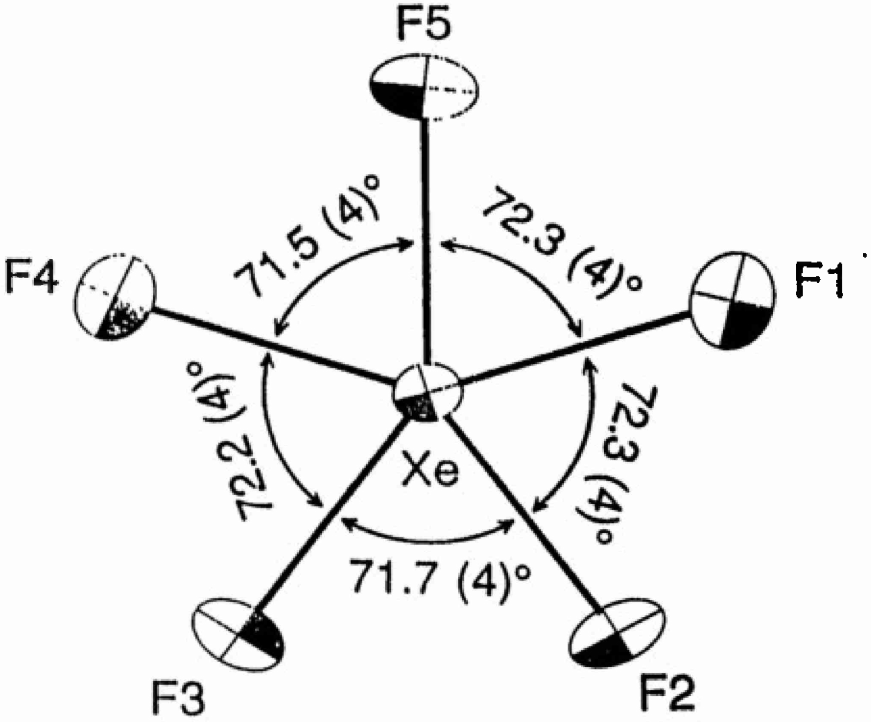
F5
71.5 (4)°
72.3 (4)°
F4
F1
72.2 (4)°
Xe
72.3 (4)°
71.7 (4)°
F3
F2

Figure 2

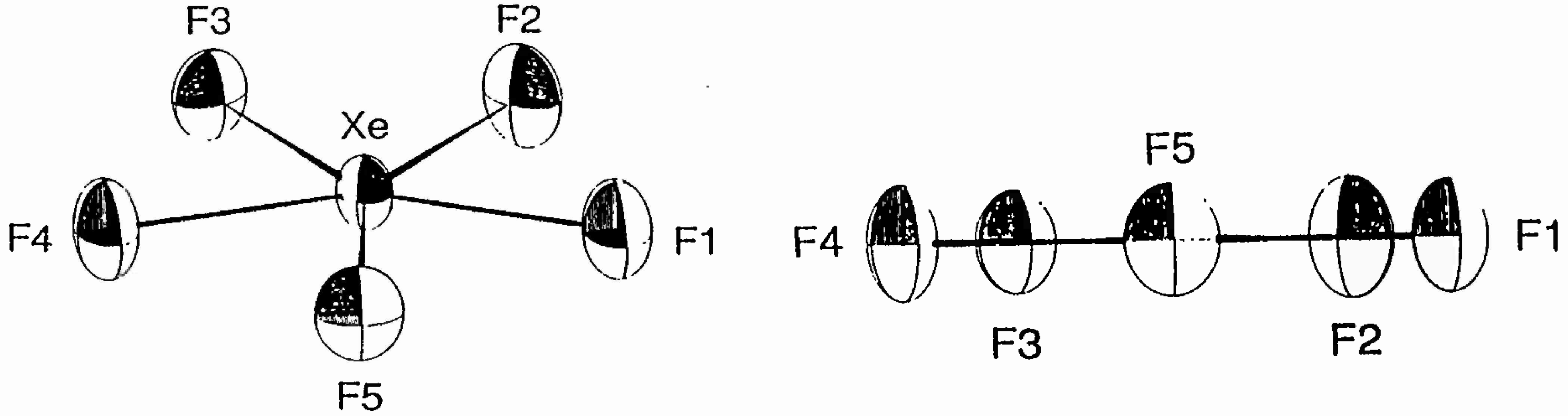

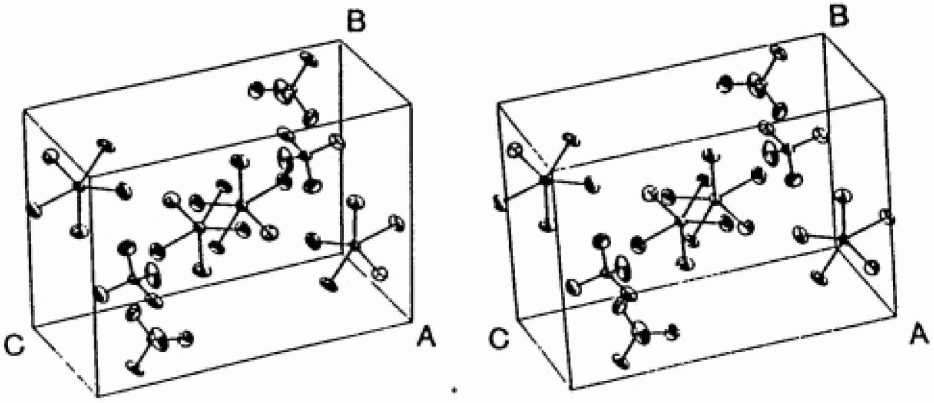
B
C
A
B
C
A

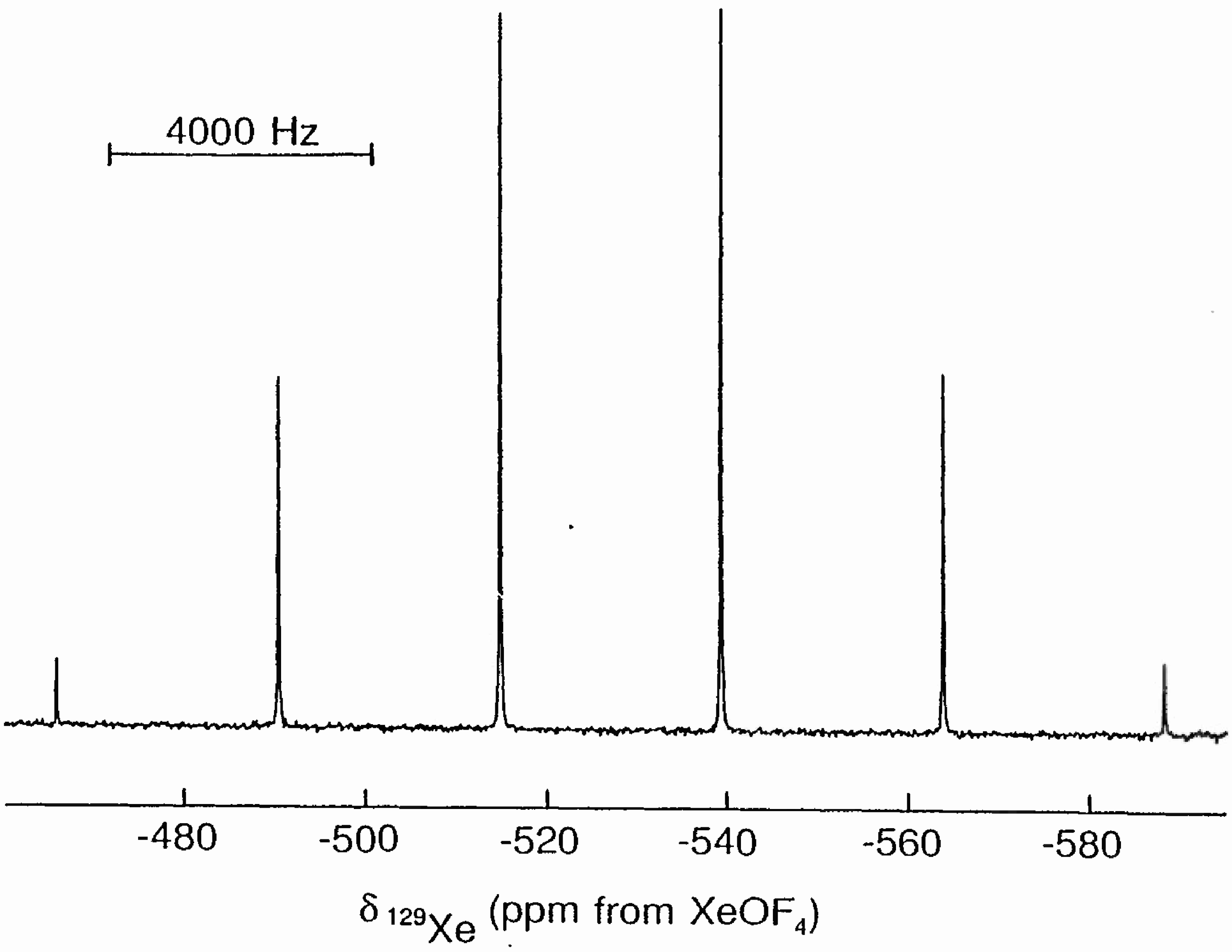
4000 Hz
-480
-500
-520
-540
-560
-580
δ 129Xe (ppm from XeOF4)

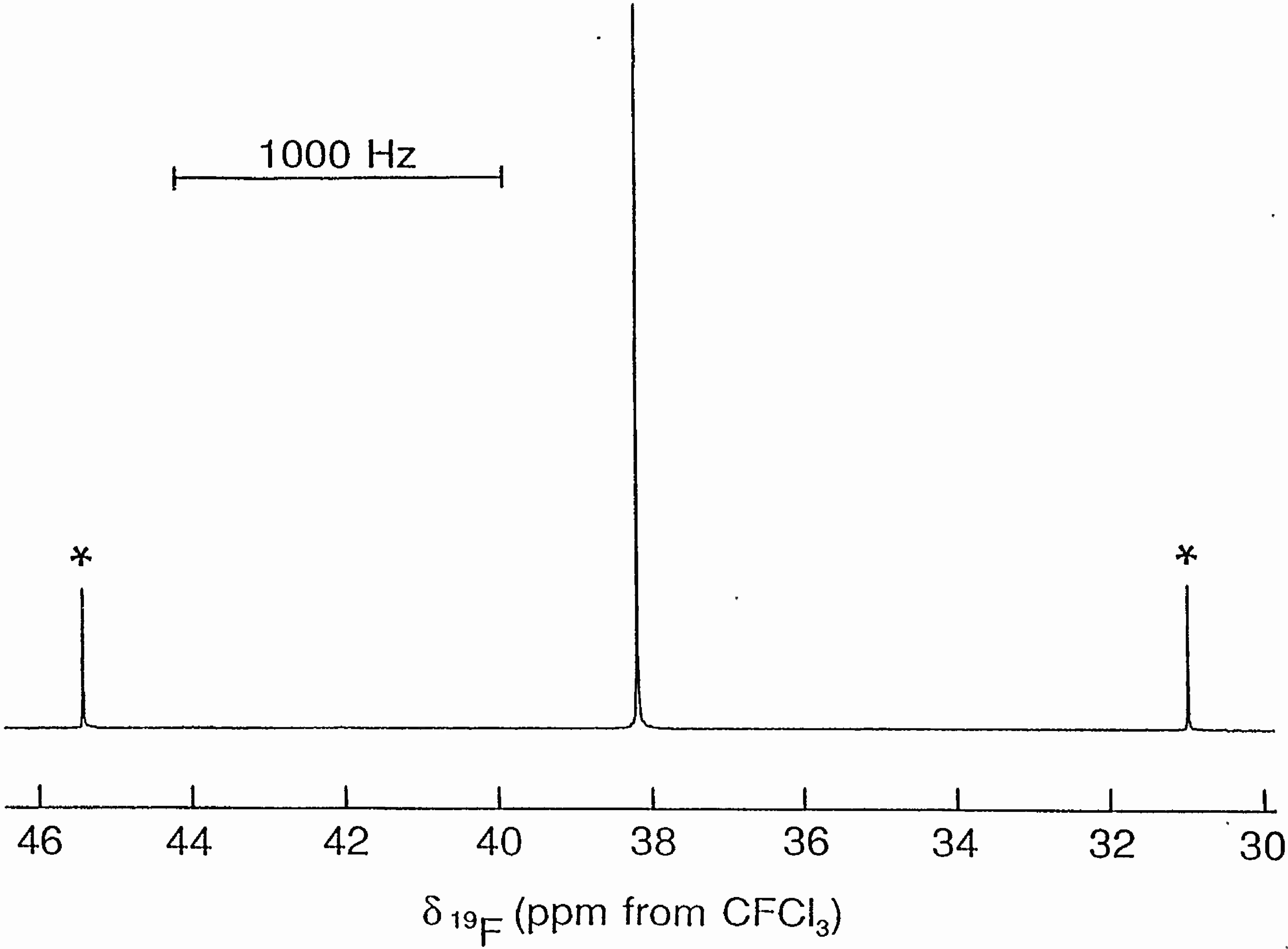
1000 Hz
*
*
46
44
42
40
38
36
34
32
30
$\delta_{^{19}F}$ (ppm from $CFCl_3$)

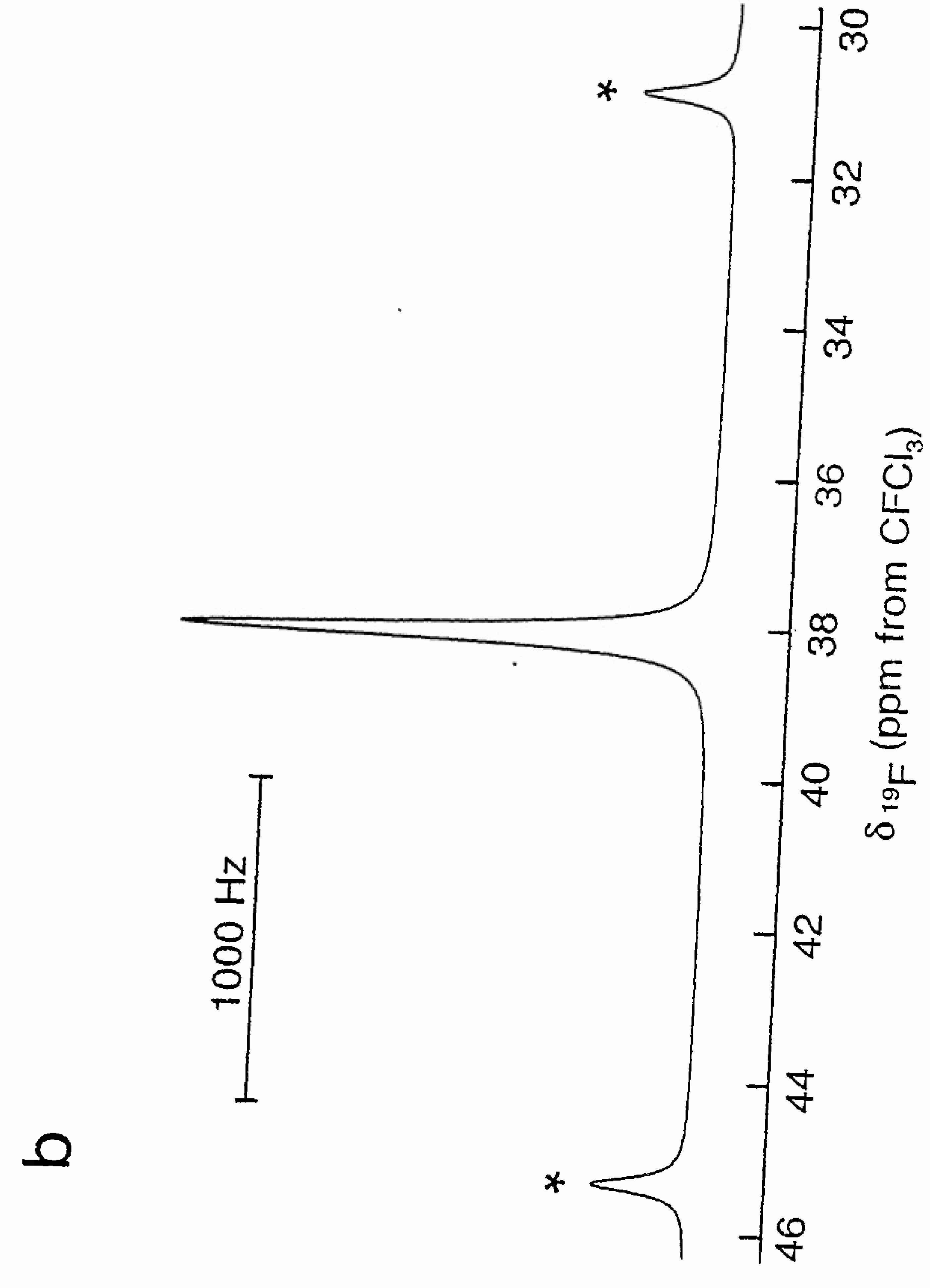
b
1000 Hz
*
*
46
44
42
40
38
36
34
32
30
$\delta_{^{19}F}$ (ppm from $CFCl_3$)

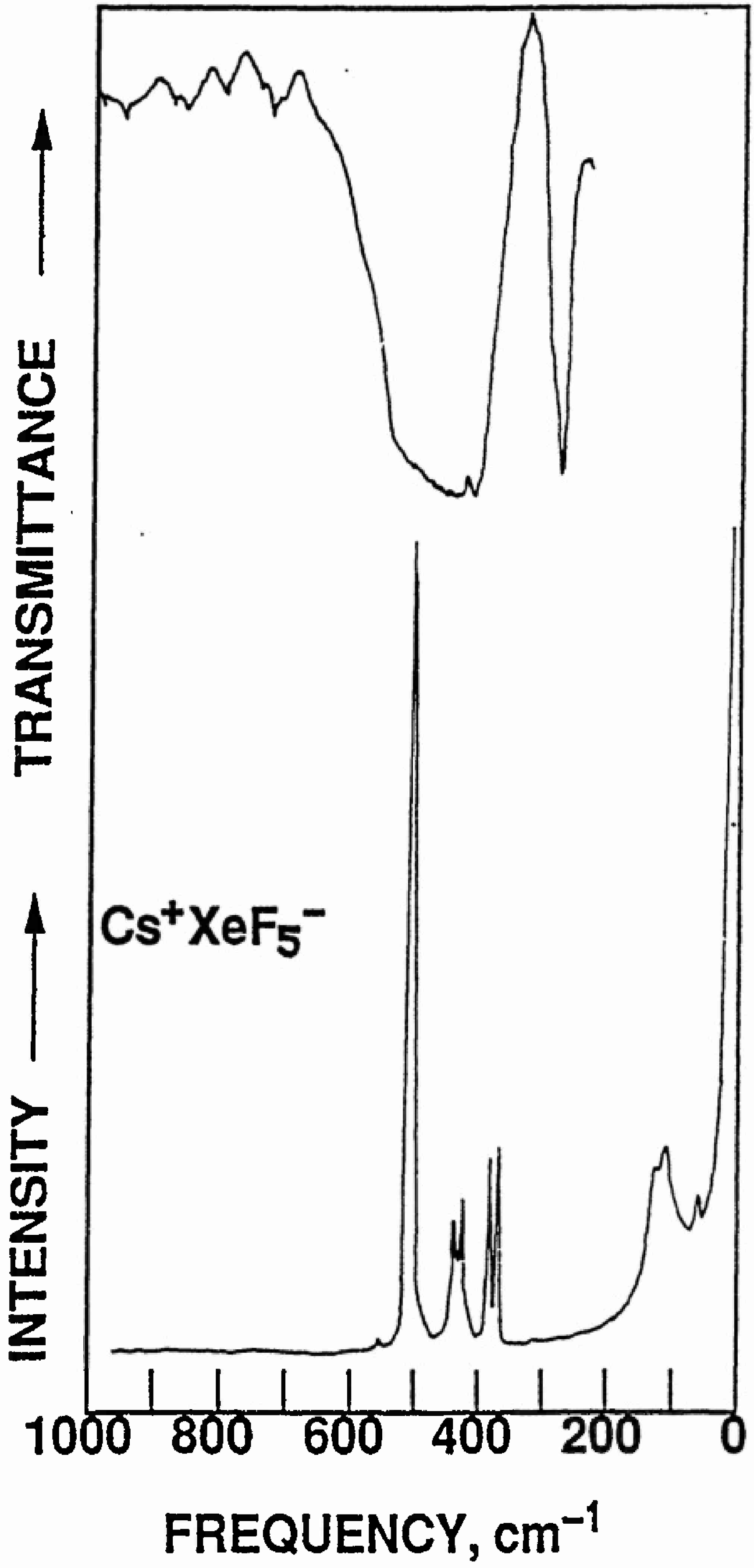
TRANSMITTANCE
Cs$^+$XeF$_5^-$
INTENSITY
1000
800
600
400
200
0
FREQUENCY, cm^{-1}

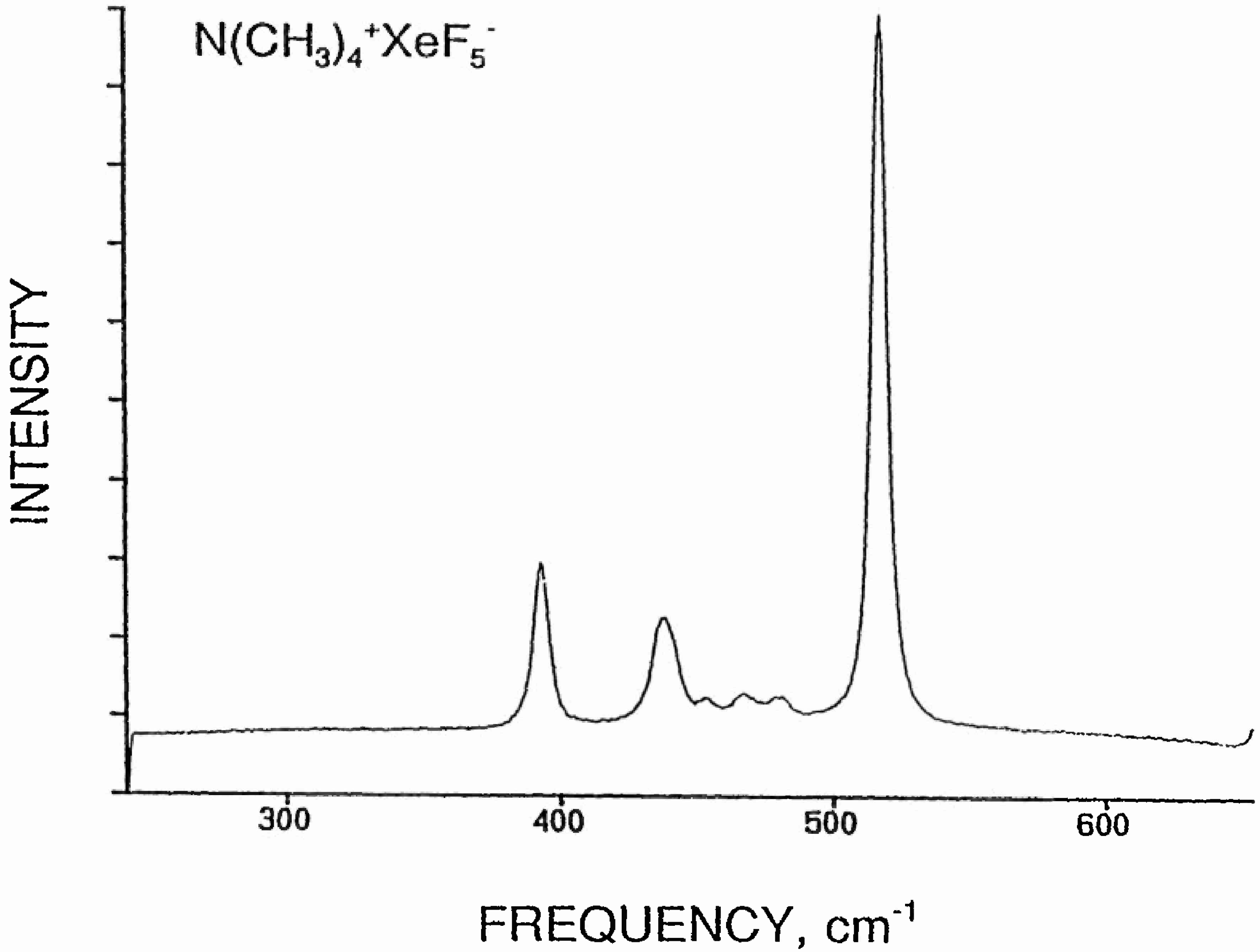

$N(CH_3)_4^+XeF_5^-$
INTENSITY
300
400
500
600
FREQUENCY, cm^{-1}

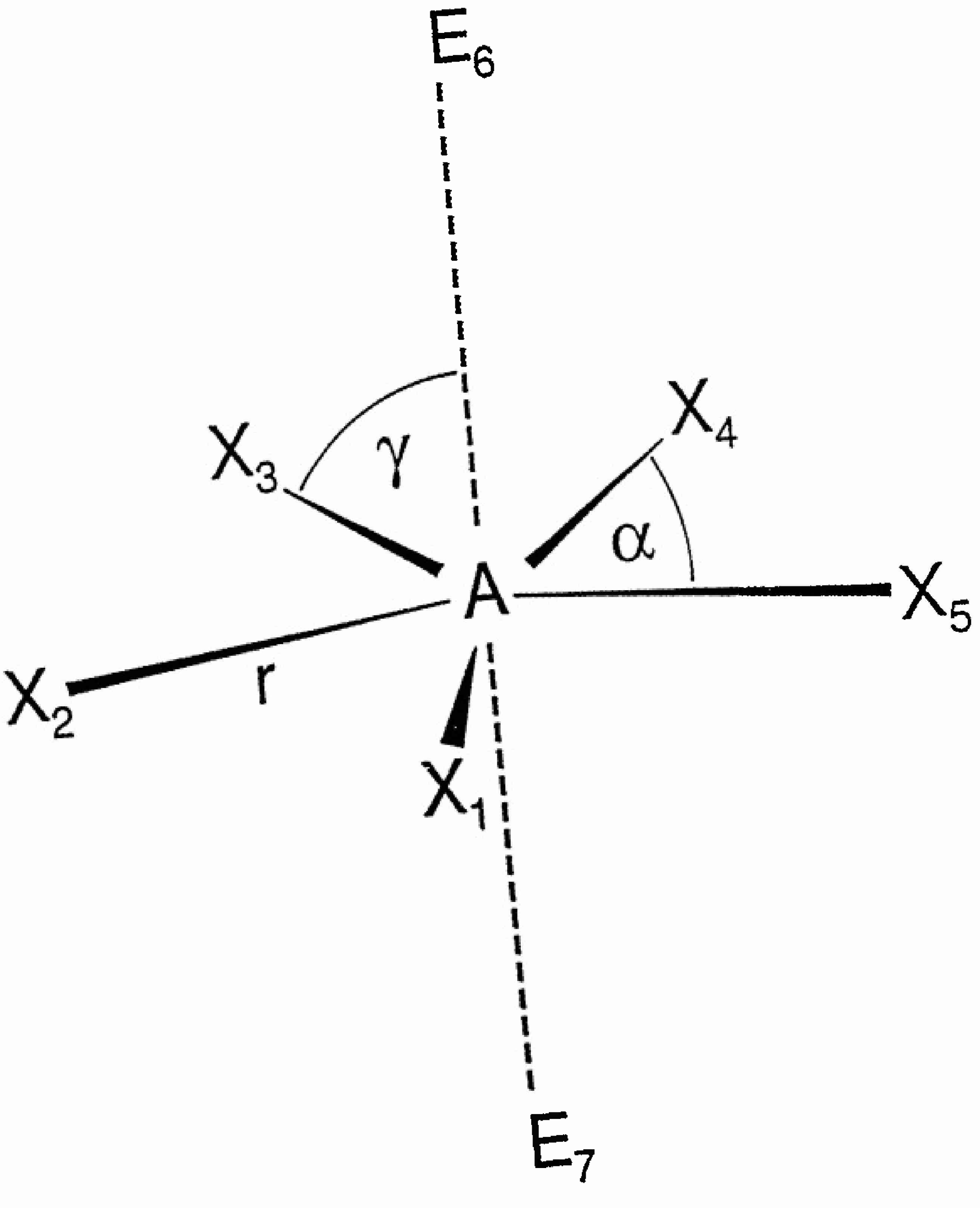
E6
X3
γ
X4
α
A
X5
X2
r
X1
E7

a

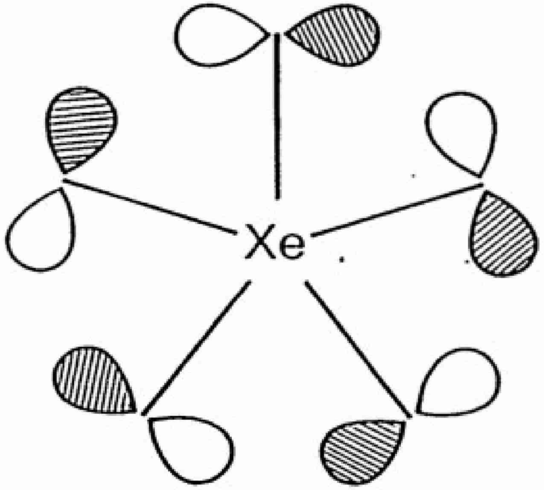

HOMO (a_2')

b

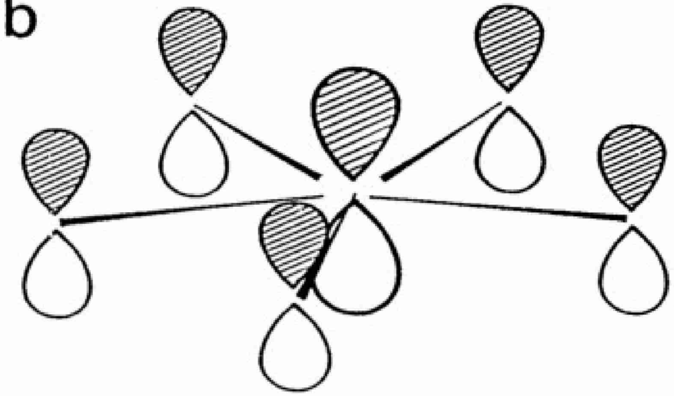

a_2'' (bonding)

c

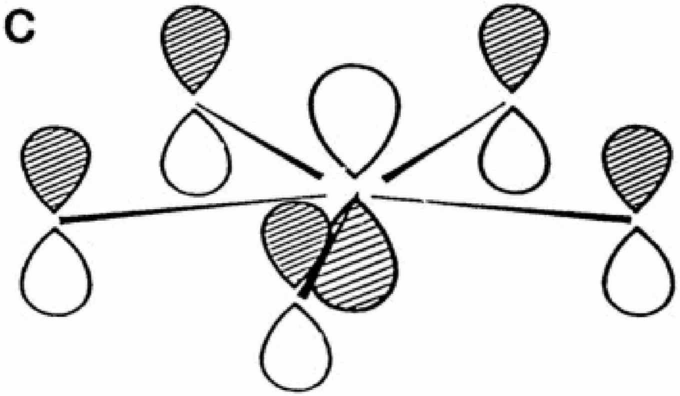

NHOMO a_2'' (antibonding)

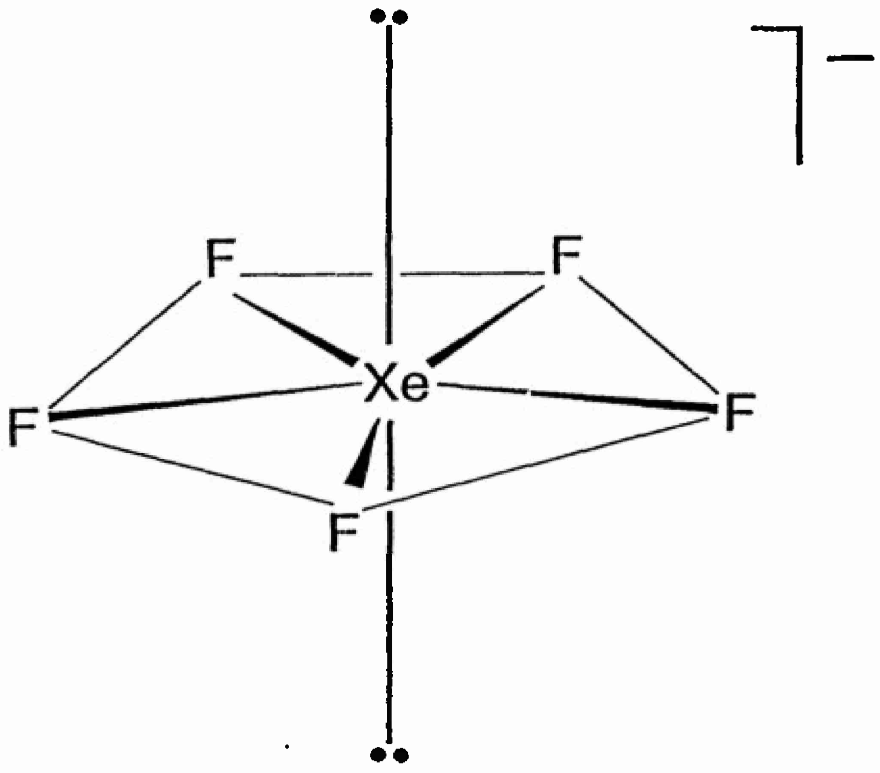
Xe
F
F
F
F
F
−

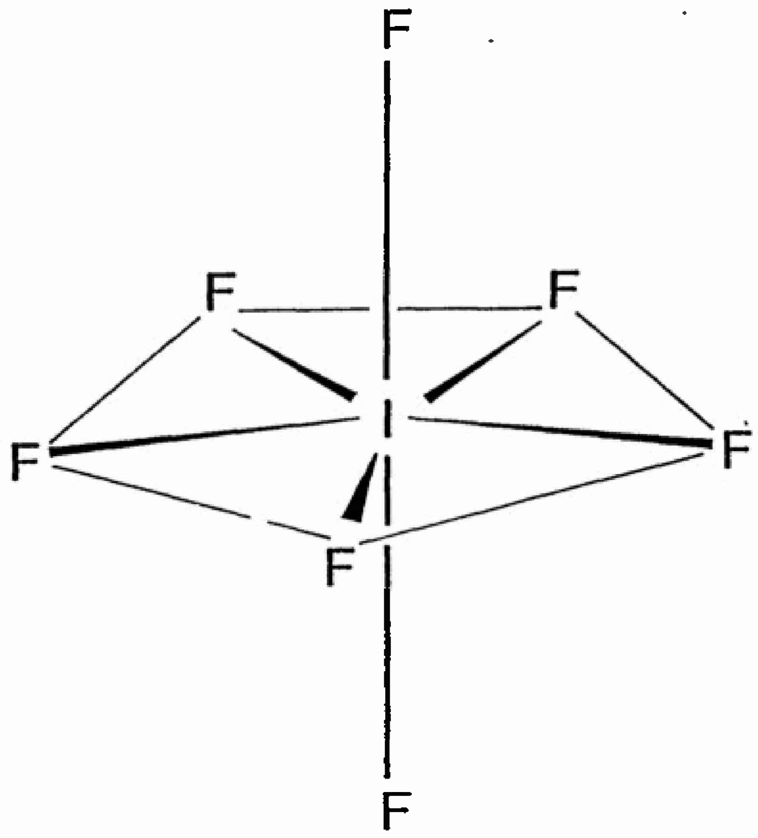
F
F
F
I
F
F
F
F

SUPPLEMENTARY MATERIAL

Contribution from Rocketdyne, A Division of Rockwell International, Canoga Park, California 91303 and the Department of Chemistry, McMaster University, Hamilton, Ontario L8S 4M1, Canada, and the Central Research and Development Department, E.I. du Pont de Nemours and Company, Inc., Experimental Station, Wilmington, Delaware 19880 - 0328.

The Pentafluoroxenate(IV) Anion XeF_5^-; the First Example of a Pentagonal Planar AX_5 Species

Karl O. Christe,*[1] Earl C. Curtis,[1] David A. Dixon[2], Hélène P. Mercier[3], Jeremy C.P. Sanders[3] and Gary J. Schrobilgen*[3]

Supplementary Material Available:

Table 1. Anisotropic Thermal Parameters with Standard Deviations for $[N(CH_3)_4]^+[XeF_5]^-$

Table 2. Hydrogen Atomic Coordinates in the $[N(CH_3)_4]^+$ cation

Table 3. Final Structure Factor Amplitudes for $N(CH_3)_4^+XeF_5^-$

Supplementary Table 1

Anisotropic Thermal Parameters (Å^2) with Standard Deviations for $[N(CH_3)_4]^+[XeF_5]^-$

Atom	U_{11}[a]	U_{22}	U_{33}	U_{23}	U_{13}	U_{12}
Xe1	470(7)	158(6)	187(6)	8(4)	0.0	0.0
F1	919(9)	426(6)	232(5)	30(4)	0.0	0.0
F2	900(8)	241(5)	344(5)	124(4)	0.0	0.0
F3	696(7)	240(5)	391(5)	142(4)	0.0	0.0
F4	999(9)	364(5)	178(4)	79(4)	0.0	0.0
F5	617(7)	199(4)	460(5)	3(4)	0.0	0.0
N1	308(9)	156(7)	275(7)	46(6)	0.0	0.0
C1	459(12)	489(12)	288(9)	90(9)	0.0	0.0
C2	578(13)	108(9)	371(11)	25(8)	0.0	0.0
C3	618(11)	714(10)	552(8)	11(7)	-73(8)	450(9)

[a] $U_{ij} \times 10^4$ is listed. The thermal parameter expression is $\exp\{-2\pi^2(U_{11}h^2a^{*2} + U_{22}k^2b^{*2} + U_{33}l^2c^{*2} + 2U_{12}hka^*b^* + 2U_{13}hla^*c^* + 2U_{13}klb^*c^*)\}$

Supplementary Table 2

Hydrogen Atomic Coordinates in the $[N(CH_3)_4]^+$ cation.

Thermal parameters are all fixed at 0.05

Atom	x	y	z	pop[a]	U
H1	0.250	0.534	0.002	0.5	0.05
H2	0.353	0.660	0.063	1.0	0.05
H3	0.250	0.700	0.329	0.5	0.05
H4	0.321	0.795	0.222	1.0	0.05
H5	0.592	0.481	0.155	1.0	0.05
H6	0.293	0.682	0.261	1.0	0.05
H7	0.335	0.556	0.189	1.0	0.05

[a] The site occupation factor.

Supplementary Table 3

Final Structure Factor Amplitudes for $N(CH_3)_4^+XeF_5^-$; Pmcn; -86 °C

H	K	L	FO	FC	H	K	L	FO	FC
4	0	0	161.47	170.48	5	7	0	40.34	35.63
6	0	0	83.91	75.73	0	8	0	83.26	79.64
3	1	0	93.97	103.44	2	8	0	68.04	67.69
5	1	0	53.46	53.70	4	8	0	52.86	51.29
0	2	0	35.41	25.05	1	9	0	28.38	28.97
2	2	0	30.52	28.98	3	9	0	30.83	30.12
1	3	0	53.87	49.71	0	10	0	17.70	15.97
3	3	0	41.55	48.91	2	10	0	13.59	12.27
5	3	0	22.10	29.67	1	1	1	22.58	26.31
0	4	0	137.28	131.65	2	1	1	114.92	145.39
2	4	0	143.33	144.89	3	1	1	8.21	8.47
4	4	0	84.13	89.32	4	1	1	73.01	78.13
6	4	0	48.55	46.00	5	1	1	6.59	7.18
1	5	0	166.77	162.35	6	1	1	41.65	35.58
3	5	0	106.43	103.34	0	2	1	69.57	68.35
5	5	0	58.35	57.49	2	2	1	31.56	36.89
0	6	0	40.77	41.66	3	2	1	113.41	124.30
2	6	0	14.81	14.73	5	2	1	69.78	70.91
4	6	0	5.80	4.62	6	2	1	9.37	9.29
1	7	0	70.27	69.32	0	3	1	90.57	87.65
3	7	0	49.01	48.99	1	3	1	2.36	6.19

H	K	L	FO	FC	H	K	L	FO	FC
2	3	1	56.25	60.96	2	7	1	63.21	63.18
3	3	1	14.50	14.27	3	7	1	15.17	15.15
4	3	1	46.76	46.57	4	7	1	43.03	43.30
5	3	1	5.57	5.76	5	7	1	7.43	2.50
6	3	1	11.34	26.38	0	8	1	14.22	14.32
0	4	1	4.13	5.51	1	8	1	31.73	31.38
1	4	1	28.61	24.30	2	8	1	18.72	19.36
2	4	1	7.07	7.97	3	8	1	23.63	23.53
3	4	1	11.55	11.26	4	8	1	7.37	5.71
4	4	1	4.28	4.59	0	9	1	64.31	62.70
5	4	1	2.19	0.21	1	9	1	1.78	1.26
0	5	1	88.36	83.22	2	9	1	57.24	56.87
1	5	1	5.60	3.92	3	9	1	4.93	3.24
2	5	1	65.69	66.24	0	10	1	15.54	15.19
3	5	1	8.08	7.49	1	10	1	76.69	76.36
4	5	1	49.24	49.61	2	10	1	8.13	7.99
5	5	1	4.60	3.97	0	11	1	54.59	55.24
6	5	1	32.99	29.12	1	0	2	94.90	96.41
0	6	1	5.90	4.64	4	0	2	99.96	107.46
1	6	1	161.25	155.96	5	0	2	27.56	26.82
2	6	1	15.02	16.28	6	0	2	61.12	52.47
3	6	1	112.20	115.98	0	1	2	5.59	5.26
4	6	1	6.86	4.62	2	1	2	8.35	6.84
5	6	1	66.21	65.01	4	1	2	8.16	6.98
0	7	1	71.57	67.35	5	1	2	56.38	54.34
1	7	1	12.23	12.47	6	1	2	10.31	4.42

H	K	L	FO	FC
0	2	2	5.77	7.22
1	2	2	10.62	11.80
2	2	2	36.37	37.81
3	2	2	2.38	2.50
4	2	2	6.28	7.25
5	2	2	5.23	5.05
6	2	2	3.01	0.38
0	3	2	5.59	9.42
1	3	2	85.69	88.07
2	3	2	5.04	3.38
3	3	2	63.53	66.73
4	3	2	4.47	0.88
5	3	2	45.38	45.43
6	3	2	1.33	2.76
1	4	2	33.95	34.25
2	4	2	115.90	122.85
3	4	2	30.91	32.28
4	4	2	78.88	82.94
5	4	2	14.53	13.83
6	4	2	50.12	45.96
0	5	2	19.80	19.62
1	5	2	108.34	104.84
2	5	2	10.76	9.54
3	5	2	78.10	81.22
4	5	2	9.39	11.38
5	5	2	41.52	41.90
6	5	2	6.61	3.30
0	6	2	9.16	6.84
1	6	2	4.71	4.38
2	6	2	15.09	14.27
3	6	2	7.88	8.58
4	6	2	4.74	5.55
5	6	2	2.51	0.67
0	7	2	13.85	14.09
1	7	2	90.30	87.88
2	7	2	7.34	5.24
3	7	2	68.99	69.42
4	7	2	7.41	6.47
5	7	2	40.19	37.28
0	8	2	90.00	90.41
1	8	2	27.25	26.28
2	8	2	84.24	83.83
3	8	2	17.96	16.90
4	8	2	60.34	58.42
0	9	2	5.29	6.90
1	9	2	40.94	40.70
2	9	2	10.34	10.65
3	9	2	31.03	30.86
0	10	2	6.85	3.06
1	10	2	9.02	9.40
2	10	2	4.20	0.79
1	1	3	29.34	27.69

H	K	L	FO	FC	H	K	L	FO	FC
2	1	3	63.40	71.60	1	5	3	20.74	21.09
3	1	3	8.96	8.51	2	5	3	131.06	134.34
5	1	3	15.74	13.29	3	5	3	22.87	22.81
6	1	3	41.48	35.01	4	5	3	73.55	77.43
0	2	3	48.95	44.91	5	5	3	9.78	9.03
1	2	3	95.53	94.35	0	6	3	59.50	56.10
2	2	3	42.14	41.87	1	6	3	139.14	135.44
3	2	3	70.07	78.26	2	6	3	39.36	39.66
4	2	3	24.92	24.70	3	6	3	93.57	95.28
5	2	3	52.92	48.92	4	6	3	27.86	27.81
6	2	3	16.45	15.27	5	6	3	61.23	58.84
0	3	3	21.94	21.53	0	7	3	73.78	70.47
1	3	3	6.50	7.32	1	7	3	15.52	14.83
2	3	3	58.22	59.14	2	7	3	55.25	54.15
3	3	3	21.77	21.11	3	7	3	8.33	8.78
4	3	3	38.23	40.13	4	7	3	38.09	37.68
5	3	3	8.87	7.30	5	7	3	9.80	9.02
6	3	3	22.65	22.84	0	8	3	1.90	1.07
0	4	3	16.33	16.56	1	8	3	7.66	6.02
1	4	3	49.96	45.04	2	8	3	4.52	3.41
2	4	3	21.64	21.31	3	8	3	3.49	1.43
3	4	3	29.40	30.82	4	8	3	2.74	0.77
4	4	3	7.92	7.36	0	9	3	85.97	87.43
5	4	3	8.75	8.25	1	9	3	31.06	30.99
6	4	3	8.82	3.47	2	9	3	71.19	73.00
0	5	3	154.21	142.84	3	9	3	19.62	19.85

H	K	L	FO	FC
0	10	3	23.98	22.53
1	10	3	89.32	90.50
2	10	3	24.64	23.30
1	0	4	29.77	27.23
2	0	4	97.24	103.03
3	0	4	39.40	39.90
4	0	4	70.69	71.98
5	0	4	12.74	13.82
6	0	4	30.57	40.45
0	1	4	50.54	47.24
1	1	4	79.23	78.29
2	1	4	34.40	35.62
3	1	4	62.78	66.36
4	1	4	26.75	26.19
5	1	4	36.28	43.18
6	1	4	9.16	12.70
0	2	4	16.83	18.45
1	2	4	11.88	11.89
2	2	4	11.68	15.34
3	2	4	8.00	6.89
4	2	4	4.21	4.47
5	2	4	7.67	8.09
6	2	4	2.33	1.00
0	3	4	69.72	66.26
1	3	4	138.60	137.87
2	3	4	44.00	44.02

H	K	L	FO	FC
3	3	4	87.28	92.16
4	3	4	31.51	33.56
5	3	4	49.40	48.62
6	3	4	14.26	14.59
0	4	4	140.61	136.29
1	4	4	69.54	67.63
2	4	4	116.46	119.08
3	4	4	33.24	35.29
4	4	4	75.60	76.99
5	4	4	29.51	28.93
6	4	4	44.26	39.53
0	5	4	7.42	6.46
1	5	4	71.17	67.45
2	5	4	20.62	20.35
3	5	4	50.78	53.37
4	5	4	11.81	9.40
5	5	4	35.39	34.76
0	6	4	17.47	18.78
1	6	4	5.90	5.52
2	6	4	16.37	15.28
3	6	4	9.08	10.35
4	6	4	9.26	6.98
5	6	4	3.07	0.66
0	7	4	30.59	29.72
1	7	4	72.68	73.64
2	7	4	33.25	34.21

H	K	L	FO	FC
3	7	4	56.40	55.58
4	7	4	18.50	16.48
0	8	4	98.59	96.70
1	8	4	42.71	43.07
2	8	4	80.39	83.46
3	8	4	37.38	37.17
4	8	4	56.88	55.47
0	9	4	23.66	22.68
1	9	4	62.60	62.69
2	9	4	13.00	13.77
3	9	4	46.27	46.54
0	10	4	8.90	7.60
1	10	4	5.55	3.62
2	10	4	5.91	6.45
0	1	5	14.03	14.46
1	1	5	24.07	23.23
2	1	5	54.65	54.72
3	1	5	24.93	23.86
4	1	5	36.27	34.05
5	1	5	19.67	17.31
6	1	5	24.09	20.46
0	2	5	87.46	80.26
1	2	5	125.78	123.38
2	2	5	62.71	64.48
3	2	5	87.88	90.09
4	2	5	40.55	39.03
5	2	5	59.81	56.03
6	2	5	22.25	20.71
0	3	5	108.69	105.69
1	3	5	40.35	39.44
2	3	5	59.69	61.87
3	3	5	31.03	31.21
4	3	5	46.05	47.14
5	3	5	21.06	18.42
6	3	5	32.52	27.23
0	4	5	15.90	14.94
1	4	5	63.43	63.03
2	4	5	11.07	13.13
3	4	5	31.62	33.42
4	4	5	7.21	6.32
5	4	5	16.84	17.27
0	5	5	129.50	126.49
1	5	5	70.36	67.39
2	5	5	88.24	91.22
3	5	5	44.98	46.83
4	5	5	58.06	59.36
5	5	5	25.81	25.00
0	6	5	46.64	46.41
1	6	5	87.77	87.68
2	6	5	40.44	40.78
3	6	5	71.59	72.43
4	6	5	27.87	29.69

H	K	L	FO	FC
5	6	5	44.07	40.84
0	7	5	65.18	63.33
1	7	5	35.33	34.92
2	7	5	61.10	61.95
3	7	5	25.97	25.78
4	7	5	41.04	41.19
0	8	5	8.37	7.87
1	8	5	6.82	5.99
2	8	5	7.56	6.61
3	8	5	10.03	8.33
4	8	5	3.64	3.14
0	9	5	64.86	65.30
1	9	5	30.61	32.22
2	9	5	59.28	59.59
3	9	5	24.23	25.15
0	10	5	46.54	47.92
1	10	5	79.91	84.57
1	0	6	103.04	102.15
2	0	6	101.05	101.74
3	0	6	52.55	53.53
4	0	6	75.85	73.66
5	0	6	44.39	40.76
6	0	6	47.17	39.70
0	1	6	63.56	60.74
1	1	6	137.88	132.32
2	1	6	59.33	57.01
3	1	6	90.20	86.72
4	1	6	36.97	35.08
5	1	6	47.35	44.27
6	1	6	22.36	18.05
0	2	6	22.83	20.22
1	2	6	29.87	27.23
2	2	6	33.04	31.16
3	2	6	24.86	26.45
4	2	6	9.76	11.79
5	2	6	3.01	1.27
6	2	6	6.03	2.88
0	3	6	63.34	61.39
1	3	6	78.50	77.20
2	3	6	59.44	59.73
3	3	6	57.92	60.18
4	3	6	33.37	32.25
5	3	6	35.43	34.25
0	4	6	136.05	128.13
1	4	6	84.18	83.54
2	4	6	114.85	118.41
3	4	6	69.05	70.92
4	4	6	71.20	72.75
5	4	6	34.51	32.90
0	5	6	48.94	45.53
1	5	6	62.34	62.85
2	5	6	29.49	30.44

H	K	L	FO	FC	H	K	L	FO	FC
3	5	6	44.69	46.69	3	1	7	34.27	34.51
4	5	6	25.19	26.17	4	1	7	40.68	40.02
5	5	6	31.77	30.71	5	1	7	18.40	15.82
0	6	6	2.69	2.47	6	1	7	28.04	22.79
1	6	6	2.99	3.93	0	2	7	128.63	118.88
2	6	6	5.45	3.67	1	2	7	115.82	113.81
3	6	6	5.72	5.10	2	2	7	94.37	94.46
4	6	6	2.61	2.69	3	2	7	84.39	83.40
5	6	6	3.06	1.94	4	2	7	60.88	60.97
0	7	6	22.43	21.81	5	2	7	50.35	45.42
1	7	6	31.14	29.19	0	3	7	104.21	97.66
2	7	6	13.53	13.34	1	3	7	80.42	81.05
3	7	6	25.20	25.43	2	3	7	88.21	90.57
4	7	6	16.47	16.70	3	3	7	48.87	48.63
0	8	6	65.48	67.96	4	3	7	52.83	51.06
1	8	6	48.29	49.70	5	3	7	33.65	30.71
2	8	6	56.46	58.06	0	4	7	22.68	21.41
3	8	6	34.32	35.27	1	4	7	13.79	12.70
0	9	6	29.52	31.31	2	4	7	12.33	11.82
1	9	6	48.07	49.87	3	4	7	12.24	11.20
2	9	6	30.99	32.42	4	4	7	9.65	10.81
0	10	6	21.18	21.23	5	4	7	4.07	4.81
1	10	6	10.12	10.89	0	5	7	55.00	55.73
0	1	7	79.62	78.92	1	5	7	40.01	40.37
1	1	7	30.75	30.14	2	5	7	54.74	56.88
2	1	7	55.39	52.48	3	5	7	26.54	27.24

H	K	L	FO	FC
4	5	7	38.81	38.98
5	5	7	22.75	21.84
0	6	7	53.81	54.24
1	6	7	60.34	60.71
2	6	7	53.25	54.71
3	6	7	46.77	47.95
4	6	7	36.26	35.68
0	7	7	53.25	52.00
1	7	7	34.91	36.18
2	7	7	40.83	42.44
3	7	7	30.81	32.56
4	7	7	29.80	29.66
0	8	7	4.42	4.47
1	8	7	2.19	1.92
2	8	7	3.01	1.92
3	8	7	3.34	1.56
0	9	7	59.07	58.39
1	9	7	36.36	36.92
2	9	7	48.40	50.01
0	0	8	98.10	95.35
1	0	8	103.33	98.11
2	0	8	100.32	99.78
3	0	8	79.32	80.65
4	0	8	59.26	55.17
5	0	8	45.25	42.98
0	1	8	103.58	97.26

H	K	L	FO	FC
1	1	8	108.83	102.93
2	1	8	76.36	77.89
3	1	8	70.14	70.65
4	1	8	47.72	46.64
5	1	8	41.43	39.19
0	2	8	46.50	45.68
1	2	8	16.42	15.85
2	2	8	18.12	18.35
3	2	8	5.34	3.42
4	2	8	13.15	12.82
5	2	8	4.90	4.07
0	3	8	52.61	51.02
1	3	8	75.72	75.62
2	3	8	41.66	42.32
3	3	8	54.33	54.73
4	3	8	32.69	31.61
5	3	8	36.85	34.44
0	4	8	83.90	81.99
1	4	8	91.67	91.87
2	4	8	59.98	60.13
3	4	8	62.12	63.42
4	4	8	45.14	44.48
5	4	8	42.89	40.25
0	5	8	47.85	48.35
1	5	8	59.45	60.42
2	5	8	46.12	46.81

H	K	L	FO	FC
2	7	9	35.65	36.76
3	7	9	31.48	31.41
0	8	9	15.70	13.61
1	8	9	6.73	7.00
2	8	9	7.94	6.20
0	0	10	68.21	66.89
1	0	10	85.44	85.27
2	0	10	47.87	46.06
3	0	10	66.64	66.31
4	0	10	36.97	36.51
5	0	10	41.69	37.67
0	1	10	61.67	58.88
1	1	10	43.50	42.80
2	1	10	52.63	52.80
3	1	10	34.24	33.45
4	1	10	39.46	38.98
5	1	10	21.76	20.18
0	2	10	18.63	20.67
1	2	10	6.70	7.91
2	2	10	5.90	4.34
3	2	10	7.76	6.05
4	2	10	3.94	4.38
0	3	10	74.34	73.82
1	3	10	42.74	42.06
2	3	10	61.34	62.78
3	3	10	35.43	34.03

H	K	L	FO	FC
4	3	10	44.49	43.00
0	4	10	46.13	44.14
1	4	10	58.55	58.70
2	4	10	47.97	47.87
3	4	10	46.94	46.62
4	4	10	33.08	31.03
0	5	10	60.76	61.64
1	5	10	38.43	37.27
2	5	10	53.65	54.87
3	5	10	26.25	26.75
4	5	10	36.12	35.92
0	6	10	3.51	4.09
1	6	10	2.49	2.10
2	6	10	3.07	1.31
3	6	10	3.24	0.50
0	7	10	61.63	64.58
1	7	10	38.96	40.28
2	7	10	56.09	57.48
0	8	10	44.06	44.38
1	8	10	55.16	57.49
0	1	11	23.49	24.12
1	1	11	72.17	71.59
2	1	11	29.11	28.07
3	1	11	61.77	60.82
4	1	11	17.51	16.49
0	2	11	56.61	54.69

H	K	L	FO	FC
3	5	8	46.21	46.14
4	5	8	30.74	30.80
0	6	8	11.93	13.44
1	6	8	1.92	1.93
2	6	8	15.67	17.05
3	6	8	3.20	2.84
4	6	8	5.86	7.76
0	7	8	26.92	27.03
1	7	8	32.66	32.92
2	7	8	28.06	28.46
3	7	8	31.80	30.60
0	8	8	42.44	44.07
1	8	8	44.84	47.98
2	8	8	41.57	42.74
3	8	8	40.24	40.26
0	9	8	34.33	34.04
1	9	8	26.67	26.20
0	1	9	71.32	65.73
1	1	9	72.41	71.48
2	1	9	54.18	55.52
3	1	9	44.77	44.23
4	1	9	38.81	36.52
5	1	9	38.20	34.83
0	2	9	75.65	75.75
1	2	9	58.89	56.38
2	2	9	71.51	71.13

H	K	L	FO	FC
3	2	9	45.44	44.55
4	2	9	47.81	45.91
5	2	9	31.20	27.15
0	3	9	44.12	44.42
1	3	9	50.72	49.47
2	3	9	40.24	38.80
3	3	9	46.96	47.48
4	3	9	27.38	26.66
5	3	9	23.39	22.57
0	4	9	1.54	0.39
1	4	9	3.79	2.86
2	4	9	7.65	6.49
3	4	9	2.94	1.83
4	4	9	2.92	0.28
0	5	9	62.10	60.88
1	5	9	59.30	59.05
2	5	9	53.86	53.76
3	5	9	51.45	51.62
4	5	9	36.30	36.71
0	6	9	68.14	69.26
1	6	9	50.54	50.75
2	6	9	52.39	54.79
3	6	9	39.30	39.70
4	6	9	43.09	42.69
0	7	9	40.63	42.78
1	7	9	45.47	46.12

H	K	L	FO	FC
1	2	11	33.95	33.83
2	2	11	48.06	48.19
3	2	11	29.07	28.68
4	2	11	40.71	38.26
0	3	11	15.64	12.25
1	3	11	34.26	34.01
2	3	11	7.86	7.26
3	3	11	24.74	24.41
4	3	11	11.37	10.08
0	4	11	15.21	14.56
1	4	11	19.60	19.57
2	4	11	6.95	6.99
3	4	11	12.51	12.62
0	5	11	34.30	35.57
1	5	11	66.66	68.81
2	5	11	25.84	27.10
3	5	11	46.98	48.48
0	6	11	79.88	83.55
1	6	11	50.95	52.37
2	6	11	73.66	76.30
0	7	11	19.59	20.95
1	7	11	42.09	43.74
0	0	12	43.75	41.87
1	0	12	87.75	88.78
2	0	12	41.60	42.60
3	0	12	63.89	64.47
4	0	12	30.05	28.27
0	1	12	56.94	56.47
1	1	12	16.65	16.07
2	1	12	51.47	50.87
3	1	12	12.37	13.26
4	1	12	35.84	34.79
0	2	12	3.90	3.67
1	2	12	25.10	24.80
2	2	12	5.41	7.59
3	2	12	10.73	10.93
0	3	12	45.04	47.86
1	3	12	17.64	18.20
2	3	12	44.55	45.89
3	3	12	13.31	13.44
0	4	12	37.70	37.73
1	4	12	66.61	68.51
2	4	12	30.20	29.97
3	4	12	58.14	57.57
0	5	12	62.58	62.84
1	5	12	20.37	20.25
2	5	12	49.78	51.32
0	6	12	7.68	8.68
1	6	12	4.59	2.03
0	1	13	20.47	19.99
1	1	13	60.78	62.96
2	1	13	9.81	10.29

H	K	L	FO	FC
3	1	13	45.02	45.71
0	2	13	72.90	74.90
1	2	13	23.83	24.85
2	2	13	65.34	67.13
3	2	13	19.80	19.97
0	3	13	5.15	4.95
1	3	13	41.52	42.98
2	3	13	9.62	10.86
0	4	13	3.41	1.35
1	4	13	3.05	0.50
2	4	13	2.55	0.56
0	5	13	15.90	17.08
1	5	13	42.44	46.48
0	0	14	22.62	23.08
1	0	14	87.96	93.69
2	0	14	19.14	20.08
0	1	14	59.78	62.07
1	1	14	14.90	15.96
2	1	14	50.01	53.02
0	2	14	4.45	6.35
1	2	14	9.04	8.18
2	2	14	2.96	4.64
0	3	14	44.81	47.41
1	3	14	9.75	10.67

APPENDIX O

X-ray Crystal Structure and Raman Spectrum of Tribromine(1+) Hexafluoroarsenate(V), $Br_3^+AsF_6^-$, and Raman Spectrum of Pentabromine(1+) Hexafluoroarsenate(V), $Br_5^+AsF_6^-$

K.O. Christe
Rocketdyne Division, Rockwell International
Canoga Park, CA (USA)
- and -
R. Bau and D. Zhao
Department of Chemistry, University of Southern California
Los Angeles, CA (USA)

Dedicated to Professor Josef Goubeau on his 90th Birthday*

Abstract

A single crystal of $Br_3^+AsF_6^-$ was isolated from a sample of $BrF_2^+AsF_6^-$ which had been stored for 20 years. It was characterized by x-ray diffraction and Raman spectroscopy. It is shown that $Br_3^+AsF_6^-$ (triclinic, a = 7.644(7)Å, b = 5.641(6)Å, c = 9.810(9)Å, α = 99.16(8)°, β = 86.61(6)°, γ = 100.11(7)°, space group $P\bar{1}$ R (F) = 0.0608) is isomorphous with $I_3^+AsF_6^-$. The structure consists of discrete Br_3^+ and AsF_6^- ions with some cation-anion interaction causing distortion of the AsF_6^- octahedron. The Br_3^+ cation is symmetric with a bond distance of 2.270(5)Å and a bond angle of 102.5(2)°. The three fundamental vibrations of Br_3^+ were observed at 297 (ν_3), 293 (ν_1), and 124 cm^{-1} (ν_2). The Raman spectra of $Cl_3^+AsF_6^-$ and $I_3^+AsF_6^-$ were reinvestigated and ν_3 (B_1) of I_3^+ was reassigned. General valence force fields are given for the series Cl_3^+, Br_3^+, and I_3^+. Reactions of excess Br_2 with either $BrF_2^+AsF_6^-$ or $O_2^+AsF_6^-$ produce mixtures of $Br_3^+AsF_6^-$ and $Br_5^+AsF_6^-$. Based on its Raman spectra, the Br_5^+ cation possesses a planar, centrosymmetric structure of C_{2h} symmetry with three semi-ionically bound, collinear, central Br atoms and two more covalently, perpendicularly bound, terminal Br atoms.

Kristall Struktur und Raman Spektrum von Tribrom(1+) Hexafluoroarsenat(V), $Br_3^+AsF_6^-$, und Raman Spektrum von Pentabrom(1+) Hexafluoroarsenat(V), $Br_5^+AsF_6^-$

Inhaltsübersicht

Ein Einkristall von $Br_3^+AsF_6^-$, gebildet während 20 jähriger Aufbewahrung einer $BrF_2^+AsF_6^-$ Probe, wurde isoliert und mittels Röntgenstrukturanalyse und Raman Spektren charakterisiert. Es wird gezeigt, dass $Br_3^+AsF_6^-$ (triklin, a = 7.644 (7)Å, b = 5.641 (6)Å, c = 9.810 (9)Å, α = 99.16 (8)°, β = 86.61 (6)°, γ = 100.11 (7)°, Raumgruppe $P\bar{1}$, R (F) = 0.0608) isomoph mit $I_3^+AsF_6^-$ ist. Die Struktur besteht aus diskreten Br_3^+ und AsF_6^- Ionen mit schwachen Anion-Kation Wechselwirkungen die in einer Verzerrung der AsF_6^- Oktaeder resultieren. Das Br_3^+ Kation ist symmetrisch mit einem Bindungsabstand von 2.270 (5)Å und einem Bindungswinkel von 102.5 (2)°. Die drei Grundschwingungen von Br_3^+ wurden bei 297 (ν_3), 293 (ν_1), und 124 cm^{-1} (ν_2) gefunden. Raman Spektren von $Cl_3^+AsF_6^-$ und $I_3^+AsF_6^-$ wurden neu aufgenommen, und ν_3 (B_1) von I_3^+ wurde neu zugeordnet. Allgemeine Valenzkraftkonstanten wurden für die Reihe Cl_3^+, Br_3^+, und I_3^+ berechnet. Umsetzumgen von überschüssigem Brom mit $B\overset{F}{r}_2^+AsF_6^-$ oder $O_2^+AsF_6^-$ resultieren in einem Gemisch von $Br_3^+AsF_6^-$ und $Br_5^+AsF_6^-$. Auf Grund der beobachteten Raman Spektren besitzt das Br_5^+ Kation eine planare, zentrosymmetrische C_{2h} Struktur mit drei halb-ionisch gebundenen,kollinearen Brom zentralatomen und zwei mehr kovalent und rechtwinklig gebundenen Brom Endatomen.

One of us (KOC) is deeply indebted to Prof. Goubeau for the profound influence he has had on his professional and personal career. Prof. Goubeau has given him much more than a solid chemical education, he has instilled in him an everlasting love and enjoyment of chemistry.

Introduction

Homopolyatomic halogen cations are of considerable interest [1-3] because of their simplicity. They contain only one kind of atom and, contrary to transition metal cluster compounds, the absence of ligands simplifies the bonding aspects. Whereas numerous polyatomic iodine cations are known and I_2^+ [4,5], I_3^+ [6], I_5^+ [7], I_{15}^{3+} [8], and I_4^{2+} [9] salts have been well characterized, much less is known about the lighter halogen polycations.

For bromine, the Br_2^+ cation has been well characterized in the form of its $Sb_3F_{16}^-$ salt [10, 11] and in superacid solutions [5, 12], but for Br_3^+ no structural data and only incomplete vibrational spectra [12-17] had previously been given. Furthermore, some of the vibrational frequencies attributed to Br_3^+ [17] are inconsistent with those observed for isoelectronic $SeBr_2$ [18] and the I_3^+ [1] and Cl_3^+ [19] cations. The only evidence for the existence of a polybromine cation containing more than three bromine atoms was obtained [14] when $Br_3^+[Au(SO_3F)_4]^-$ was reacted with excess Br_2 at 70°C resulting in a solid of the composition $Br_5[Au(SO_3F)_4]$. Raman bands at 304, 295, 267, and 205 cm^{-1} were tentatively attributed [14] to the cation in this compound but are not consistent with our predictions for a centrosymmetric Hal_5^+ cation of C_{2h} symmetry (see below).

For chlorine, the only known polychlorine cation containing salt is $Cl_3^+AsF_6^-$ which is unstable and was characterized by its low-temperature Raman spectrum [19]. The Cl_2^+ ion has been observed only in the gas phase at very low pressures [20, 21]. A claim for the observation of Cl_2^+ by ESR spectroscopy in superacid solutions [22] has subsequently been disputed [2, 19, 23, 24].

In view of the scant information available on the lighter halogen homopolyatomic cations and the accidental isolation of some deeply colored single crystals from a $BrF_2^+AsF_6^-$ sample, we have undertaken a study of the bromine homopolyatomic cations.

Experimental

Materials and Apparatus

Literature methods were used for the syntheses of $BrF_2^+AsF_6^-$ [25] and $O_2^+AsF_6^-$ [26]. The Br_2 and HF were dried by storage over P_2O_5 and BiF_5 [27], respectively. Reactions involving Br_2 were carried out using a flamed out Pyrex-glass vacuum line equipped with grease-free Teflon stopcocks. Anhydrous HF was handled in a stainless steel-Teflon FEP vacuum line [28]. Nonvolatile materials were handled in the dry nitrogen atmosphere of a glove box. Raman spectra were recorded on a Spex Model 1403 spectrophotometer using either the 647.1-nm exciting line of a Kr ion laser or the 514.5-nm line of an Ar ion laser and a previously described [29] device for obtaining the low-temperature spectra. The ^{19}F NMR spectra were recorded at 84.6 MHz on a Varian Model EM 390 spectrometer.

Reaction of $BrF_2^+AsF_6^-$ with Br_2

A flamed out 100 ml Pyrex flask equipped with a Teflon stopcock was loaded in the dry box with $BrF_2^+AsF_6^-$ (3.94 mmol). On the vacuum line, dry Br_2 (13.49 mmol) was added at -196°C and the resulting mixture was kept at 25°C for 2 hr. The flask was cooled to 0°C and volatile products were pumped off at 0°C for 30 min. The chocolate brown solid residue in the flask weighed 2164 mg (weight calculated for 3.94 mmol of $Br_3^+AsF_6^-$ = 1846 mg and 3.94 mmol of $Br_5^+AsF_6^-$ = 2476 mg). The brown solid slowly gave off bromine vapors on standing at room temperature. Pumping on the solid at room temperature for 35 min reduced the weight to 1427 mg. The resulting residue still had some dissociation pressure at ambient temperature as evidenced by the slow evolution of Br_2 vapors above the solid. Low-temperature Raman spectroscopy showed this residue to be mainly $Br_3^+AsF_6^-$ with some $Br_5^+AsF_6^-$ as a by-product.

Reaction of $O_2^+AsF_6^-$ with Br_2

$O_2^+AsF_6^-$ (5.15 mmol) and Br_2 (13.54 mmol) were combined at -196°C in a 100 ml Pyrex flask. The mixture was warmed to 25°C for 2 hr, then cooled back to -196°C. The evolved oxygen (5.14 mmol) was pumped off at -196°C and excess Br_2 was pumped off at 0°C for 10 min. The resulting brown residue (1871 mg, weight calculated for 5.15 mmol of $Br_3^+AsF_6^-$ = 2414 mg) was somewhat inhomogeneous showing smaller patches of material ranging in color from carmine red to greyish-green. Again some Br_2 vapor evolved above the solid on standing at room temperature. Low-temperature Raman spectra of the solid taken from different patches showed mainly $Br_5^+AsF_6^-$ with varying amounts of $Br_3^+AsF_6^-$ as a by-product.

Crystal Structure Determination of $Br_3^+AsF_6^-$

During 20 years of storage of a sample of $BrF_2^+AsF_6^-$ at room temperature in a Teflon tube closed by a stainless steel fitting several single crystals of $Br_3^+AsF_6^-$ had formed. Due to their great difference in color, $BrF_2^+AsF_6^-$ is colorless and $Br_3^+AsF_6^-$ is dark brown, the crystals were easily separated in the dry box. The diffraction data were collected at room temperature, using a Siemens/Nicolet/Syntex $P2_1$ diffractometer with MoKα radiation up to a 2θ limit of 55 deg. 1538 intensity values for an entire reflection sphere were collected and the two equivalent hemispheres merged to give a total of 546 unique reflections. The R factor for averaging was 2.3%. The positions of the As and three Br atoms were obtained by direct methods using the computing package SHELX-86 [30a]. The rest of the atoms were then located from a difference-Fourier map, and the entire structure was anisotropically refined by SHELX-76 [30b] to a final agreement factor of R = 6.08%, using 538 reflections with $I > 3\sigma(I)$. At that point it was realized that the unit cell parameters were virtually identical to those of $[I_3]^+[AsF_6]^-$ [6], and the coordinates were then transformed accordingly, to be consistent with those reported for the $[I_3]^+$ analog. Crystal data and refinement results are summarized in Table 1, the final atomic coordinates and temperature factors are given in Table 2, and the bond distances and angles are given in Table 3.

Results and Discussion

Synthesis of $Br_3^+AsF_6^-$

Single crystals of $Br_3^+AsF_6^-$ were obtained from a sample of $BrF_2^+AsF_6^-$ which had been stored for 20 years at room temperature in a Teflon-stainless steel container. Its formation can be explained by the reduction of a small amount of BrF_2^+ to Br_2 by the container material and a subsequent reaction of $Br_{\overset{2}{\cancel{3}}}$ with BrF_2^+ according to:

$$BrF_2^+AsF_6^- + 2Br_2 \longrightarrow Br_3^+AsF_6^- + 2BrF \tag{1}$$

The BrF is thermally unstable and disproportionates readily [31] to BrF_3 and Br_2, with the BrF_3 most likely being reduced by the container material to additional Br_2, and the Br_2 being consumed according to (1).

To verify reaction (1) and to obtain larger amounts of $Br_3^+AsF_6^-$, a sample of $BrF_2^+AsF_6^-$ was treated at room temperature with an excess of Br_2. The colorless $BrF_2^+AsF_6^-$ was rapidly converted to a dark brown solid. After pumping off the unreacted Br_2 at 0°C, this brown solid consisted of a mixture of $Br_3^+AsF_6^-$ and $Br_5^+AsF_6^-$ (see below). Attempts to convert the $Br_5^+AsF_6^-$ to $Br_3^+AsF_6^-$ by pumping at room temperature was only partially successful and resulted in the loss of both $Br_3^+AsF_6^-$ and $Br_5^+AsF_6^-$. This is not surprising since , at room temperature, $Br_3^+AsF_6^-$ has some dissociation pressure, as evidenced by the build up of Br_2 vapor above the brown solid. This Br_2 vapor can on standing equilibrate with $Br_3^+AsF_6^-$ to reform some $Br_5^+AsF_6^-$ thus explaining the difficulties encountered with preparing and handling samples of pure $Br_3^+AsF_6^-$. The previously reported [13] synthesis of $Br_3^+AsF_6^-$ from BrF_5, Br_2 and AsF_5 is based on the same approach, i.e. conproportionation of a higher bromine fluoride with bromine to BrF and its subsequent reaction with Br_2 and AsF_5 to form $Br_3^+AsF_6^-$ (2-4).

$$BrF_5 + 2Br_2 \rightleftharpoons 5BrF \tag{2}$$

$$5BrF + 5Br_2 + 5AsF_5 \longrightarrow 5Br_3^+AsF_6^- \tag{3}$$

$$BrF_5 + 7Br_2 + 5AsF_5 \longrightarrow 5Br_3^+AsF_6^- \tag{4}$$

In this reaction the formation of $Br_5^+AsF_6^-$ can be suppressed by the use of excess BrF_5 and AsF_5.

We have also repeated the previously reported [13] reaction of $O_2^+AsF_6^-$ with excess Br_2. In this system, O_2 evolution is facile and quantitative, however the formed product appears inhomogenous with varying amounts of $Br_5^+AsF_6^-$ and $Br_3^+AsF_6^-$ being produced.

Crystal Structure of $Br_3^+AsF_6^-$

$Br_3^+AsF_6^-$ is isomorphous with $I_3^+AsF_6^-$ [6]. Both compounds are triclinic with similar unit cells and packing arrangements (see Figure 1). The structures are predominantly ionic containing discrete Hal_3^+ cations and AsF_6^- anions, with some cation-anion interaction (see Figure 2) resulting in a distortion of the AsF_6^- anion from O_h symmetry. As expected, the Br_3^+ cation is symmetric (r_{Br-Br} = 2.270(5) Å) and bent (102.5(2)°). The Br-Br distance in Br_3^+ is similar to that for Br_2 (2.281Å [32]) and resembles in this respect the I_3^+ (2.665(4) Å [6]) and I_2 (2.666Å [32]) couple. The fluorine contacts to Br_3^+ are very similar to those found for I_3^+ in $I_3^+AsF_6^-$ [6], resulting in an approximately planar network of two fluorine bridges to the central and of one fluorine bridge to each terminal bromine atom (see Figure 2). A more detailed discussion of these interactions has previously been given for $I_3^+AsF_6^-$ [6] and, therefore, does not need reiteration.

^{19}F NMR Spectrum of $Br_3^+AsF_6^-$

The ^{19}F NMR spectrum of $Br_3^+AsF_6^-$ in anhydrous HF solution was recorded at room temperature. It consisted of a well resolved quartet of equal intensity (Ø = 65 ppm, upfield from external $CFCl_3$, with $J_{^{75}AsF}$ = 925 Hz and a line width of 100 Hz), in excellent agreement with previous reports for octahedral AsF_6^- [33].

Raman Spectra of $Br_3^+AsF_6^-$, $Cl_3^+AsF_6^-$, and $I_3^+AsF_6^-$

Raman spectra of bromine polyatomic cation salts are very difficult to obtain due to the intense colors of the cations. The Raman spectrum of a randomly oriented single crystal of $Br_3^+AsF_6^-$ at -150°C is shown in Figure 3. The observed frequencies and their assignments are summarized in Table 4. The two bands at 173 and 85 cm^{-1}, respectively, are due to a small amount of Br_5^+ formed during the handling of the crystal and recording of the spectrum and are denoted in Figure 3 by an asterisk. The assignments given in Table 4 are clear cut and do not require further discussion. The fact that the observed AsF_6^- bands deviate from the O_h selection rules, i.e. ν_3 (F_{1u}) becomes Raman active and ν_2 (E_g) is split into its degenerate components, is not surprising in view of the distortion of the AsF_6^- octahedron by fluorine bridging with the Br_3^+ cations. Raman spectra of powdered samples of $Br_3^+AsF_6^-$ were also recorded at 25 and -150°C. They were of lower quality than that of the single crystal material but showed the same main features, i.e. ν_{sym} Br_3^+ at 293 cm^{-1} with a shoulder at 297 for ν_{asym} Br_3^+, δ Br_3^+ at about 120 cm^{-1}, and ν_{sym} AsF_6^- at about 675 cm^{-1}.

Previous literature reports on the vibrational spectra of Br_3^+ suggested for ν_1 (A_1) frequencies of 295 cm^{-1} in $Br_3^+[Pt(SO_3F)_6]^-$ [15], 280 cm^{-1} in $Br_3^+[Au(SO_3F)_4]^-$ [14], 290 cm^{-1} in fluorosulfuric acid solutions [12], for ν_3 (B_1) a frequency of 288 cm^{-1} in $Br_3^+SO_3F^-$ [16], and for ν_2 (A_1) a doublet at 227 and 238 cm^{-1} in an HBr-NO_2 reaction product [17]. Whereas the reported frequencies of the two stretching modes are in fair agreement with our findings for $Br_3^+AsF_6^-$, the previously reported [17] deformation mode frequency is much too high for Br_3^+, as is also obvious from a comparison with the known fundamental vibrations of I_3^+ (see below), Cl_3^+ [19], and isoelectronic $SeBr_2$ [18] which are summarized in Table 5.

The Raman spectra of $Cl_3^+AsF_6^-$ [19] and $I_3^+AsF_6^-$ [6, 34] were also recorded for comparison. The spectrum of $Cl_3^+AsF_6^-$ agreed well with that previously reported [19] with the following exceptions. The unassigned 170 cm^{-1} band was either completely absent or of variable intensity in different samples, and, therefore, does not belong to $Cl_3^+AsF_6^-$. Furthermore, two additional bands at 709 and 686 cm^{-1} were observed in the ν_3 (F_{1u})region of AsF_6^- which resemble those in $Br_3^+AsF_6^-$. In the low frequency region, two lattice vibrations were observed at 132 and 101 cm^{-1}, respectively.

The Raman spectrum of $I_3^+AsF_6^-$ which was prepared from I_2 and AsF_5 in AsF_3 solution [34], was recorded for both the solid state and in anhydrous HF solutions using either 647.1, 514.5, or 488-nm excitation. Due to the intense, dark brown to black color of $I_3^+AsF_6^-$ the quality of the obtainable spectra was poor. With 647.1-nm excitation, the spectra were dominated by a very intense resonance Raman spectrum of I_2^+ [2] which was present in the sample as a minor impurity. In addition to the intense 238 cm^{-1} band of I_2^+ [1, 2], a weak band at 206 cm^{-1} was observed for ν_1 (A_1) of I_3^+. With 488-nm excitation, only a weak band at 208 cm^{-1} was observed. The best spectrum was obtained with 514.5-nm excitation and is shown in Figure 4. It clearly locates ν_1 (A_1) and ν_2 (A_1) of I_3^+ at 205 and 110 cm^{-1}, respectively, in good agreement with the 207 and 114 cm^{-1} values previously reported [1]. However, the previously reported [1] 233 cm^{-1} band for ν_3 (B_1) could not be confirmed. By analogy with Br_3^+ and based on model calculations for the frequency separation of the two stretching modes of an XY_2 group as a function of their bond angle and relative masses [35], ν_3 (B_1) of I_3^+ should be about 5 cm^{-1} higher than ν_1 (A_1). As shown by the insert in Figure 4, the 205 cm^{-1} Raman band of I_3^+ indeed exhibits a pronounced shoulder at 210 cm^{-1} which is assigned to ν_3 (B_1). This reassignment of ν_3 is also supported by our force field calculations (see below). On the low frequency side of the 205cm^{-1} Raman band of I_3^+ another shoulder was observed. A firm assignment cannot be given for this shoulder at the present time, but based on the arguments given in [35] it cannot represent ν_3 (B_1) of I_3^+.

General Valence Force Fields for Cl_3^+, Br_3^+, and I_3^+

General valence force fields were calculated for Cl_3^+, Br_3^+, and I_3^+ using Wilson's GF method [36]. Since the A_1 block (2 frequencies, 3 force constants) is underdetermined, the complete range of possible solutions was computed using Sawodny's method [37]. The resulting force constant ellipses are given in Figure 5. To allow a better comparison, the stretch-bend interaction constants F_{12} and bending constants F_{22} have been normalized for distance.

As can be seen from Figure 5, the values of the stretching force constants F_{11} strongly depend on the choice of F_{12}. In the absence of additional experimental data, assumptions about the values of F_{12} had to be made to select preferred sets of force constants. The method of Thakur $\{$factoring the F_{12} value of the $F_{22} \equiv$ minimum solution [37] by $G_{12}/\sqrt{(G_{11} \cdot G_{22} + G_{12}^2)}$ $\}$ was chosen because it best duplicates the General Valence Force Fields of molecules with similar mass ratios [38]. The internal force constants obtained in this manner for Cl_3^+, Br_3^+, and I_3^+ are summarized in Table 6 and compared to those of the related Hal_2 molecules and Hal_2^+ cations.

As can be seen from Figure 5 and Table 6, the stretching force constants *fr* monotonously increase from Cl_3^+ to I_3^+, in good analogy with those of the Hal_2 molecules and Hal_2^+ cations. The finding that the stretching force constants in Hal_3^+ cations are smaller than those predicted from their bond lengths and the known force constants and bond lengths in the corresponding homonuclear diatomic molecules or ions, is not surprising. From NQR measurements on I_3^+ [39] it is known that in Hal_3^+ cations most of the positive charge resides on the central atom. This results in a significant bond polarity for the Hal_3^+ cations, while the bond polarity in the homonuclear diatomics is zero. Since polar bonding contributes strongly to the bond shortening but not to the stretching force constants, it is not surprising that the stretching force constant of a Hal_3^+ cation should be smaller than that of a Hal_2 molecule or ion possessing the same bond length. A closer inspection of the data of Table 6 reveals that for I_3^+ only our revised assignment for ν_3 results in a plausible value for the stretching force constant *fr*.

The Raman Spectrum of $Br_5^+AsF_6^-$

In the reactions of either $Br_2^+AsF_6^-$ or $O_2^+AsF_6^-$ with an excess of Br_2 (see above) products were obtained which contained in addition to Br_3^+ a second polybromine cation salt. Its Raman spectrum is shown in Figure 6, and the observed frequencies and their assignments are summarized in Table 7. The most likely candidate for this cation is Br_5^+. In the literature, only one brief reference was made [14] to Br_5^+ and Raman bands at 304, 295, 267, and 205 cm^{-1} were tentatively attributed to Br_5^+. Otherwise, the only structural information available for a Hal_5^+ cation is a crystal structure of $I_5^+AsF_6^-$ [7]. The latter study showed that I_5^+ has a centrosymmetric, planar structure of C_{2h} symmetry $[{}_{I}/I\text{-}I\text{-}I/{}^{I}]^+$. It is therefore reasonable to assume an analogous C_{2h} structure for Br_5^+.

A Br_5^+ cation of symmetry C_{2h} possesses nine fundamental vibrations which are classified as $\Gamma = 3A_g + 2A_u + 4B_u$. Of these, the A_g modes are only Raman and the A_u and the B_u modes only infrared active. The following diagram gives an approximate description of these modes.

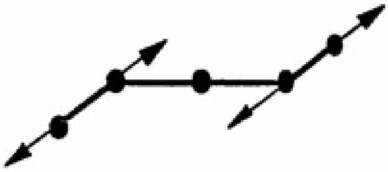

$\nu_1(A_g)$
ν_{sym} terminal

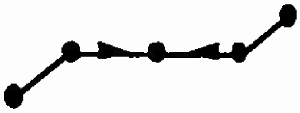

$\nu_2(A_g)$
ν_{sym} central

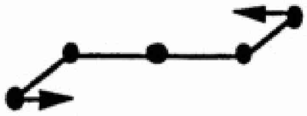

$\nu_3(A_g)$
δ_{sym} in plane

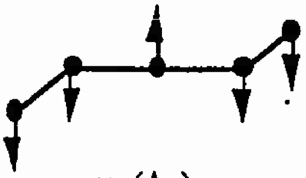

$\nu_4(A_u)$
δ central out
of plane

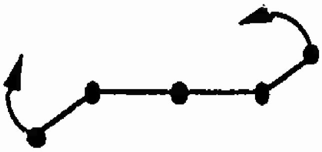

$\nu_5(A_u)$
torsion

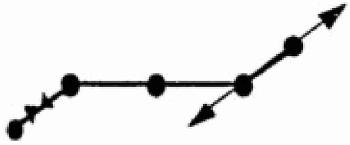

$\nu_6(B_u)$
ν_{as} terminal

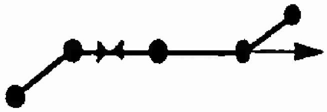

$\nu_7(B_u)$
ν_{as} central

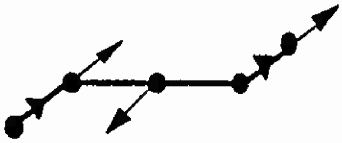

$\nu_8(B_u)$
δ central in
plane

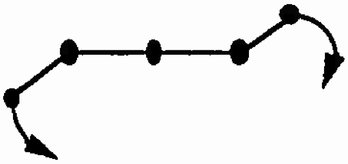

$\nu_9(B_u)$
δ_{as} terminal
in plane

Since in I_5^+ the collinear central I-I bonds (2.895Å) are much longer than the perpendicular terminal ones (2.645Å) [7], the bonding in a Hal_5^+ cation is best described by a semi-ionic, three center-four electron bonding model [40-43], as in the Hal_3^- anions, for the three central halogen atoms and two essentially normal covalent bonds, as in Hal_2 and Hal_3^+, for the perpendicular terminal bonds. Consequently, the frequencies of the three Raman active modes of Br_5^+ can be predicted as follows: ν_1 (A_g) should be similar to that in Br_2 (320 cm^{-1} [2]), ν_2 (A_g) to that of ν_{sym} in Br_3^- (162 cm^{-1} [44]), and ν_3 (A_g) to that of the bending mode in Br_3^+ (124 cm^{-1}, see above).

The observed spectra (Figure 5, Table 7) are in excellent agreement with the above predictions for a Br_5^+ cation of C_{2h} symmetry. Disregarding the weak lines above 300 cm^{-1} which are due to AsF_6^- and the lattice modes which disappear for the HF solution, we are left with three very intense Raman lines at 309, 174, and 84 cm^{-1} in the solid and at 309, 182, and 108 cm^{-1} in the HF solution which in the solution spectrum are all polarized as expected for A_g modes. The frequency differences between the solid state and solution spectra are attributed to solid state and solvation effects. The weak shoulder observed at 190 cm^{-1} for the solid is attributed to the antisymmetric central Br_3 stretching mode ν_7 (B_u), which is activated by solid state effects and occurs for Br_3^- at 193 cm^{-1} [44].

In view of this excellent agreement the observed spectra can be attributed to a Br_5^+ cation of C_{2h} symmetry with bonding conditions similar to those in I_5^+, i.e. a semi-ionic, three center-4 electron bond for the three collinear central bromine atoms and two mainly covalent bonds for the perpendicular terminal bromine atoms. The occurrence of a semi-ionic, three center-four electron bond in Br_5^+ but not in Br_3^+ is readily understood from a simple consideration of the number of valence electrons in each cation. In Br_3^+, all three bromine atoms have an electron octet, whereas in Br_5^+ the central bromine atoms is hypervalent possessing 10 valence electrons which favors the formation of semi-ionic, three center-four electron bonds [43].

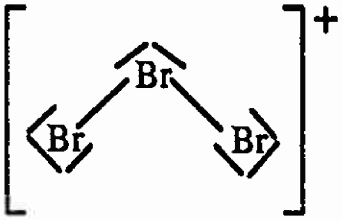

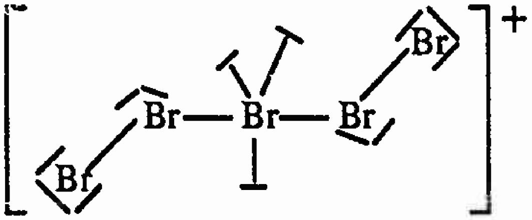

Acknowledgement

One of us (Karl O. Christe) is indebted to Drs. C.J. Schack, W.W. Wilson, and R.D. Wilson for their help, to R. Shroder for the recording of the 514.5-nm Raman spectrum of $I_3^+AsF_6^-$, and to the U.S. Army Research Office for financial support.

References

[1] Gillespie, R. J.; Morton, M. J.; Sowa, J. M.: Adv. Raman Spectrosc., 1 (1972) 539.

[2] Gillespie, R. J.; Passmore, J.: Adv. Inorg. Chem. Radiochem. 17 (1975) 49.

[3] Li, Y.; Wang, X.; Jensen, F.; Houk, K. N.; Olah, G. A.: J. Amer. Chem. Soc., 112 (1990) 3922.

[4] Davis, C. G.; Gillespie, R. J.; Ireland, P. R.; Sowa, J. M.;: Canad. J. Chem. 52 (1974) 2048.

[5] Wilson, W. W., Thompson, R. C.; Aubke, F.: Inorg. Chem. 19 (1980) 1489.

[6] Passmore, J.; Sutherland, G.; White, P. S.: Inorg. Chem. 20 (1981) 2169.

[7] Apblett, A.; Grein, F.; Johnson, J. P.; Passmore, J.; White, P. S.: Inorg. Chem. 25 (1986) 422.

[8] Passmore, J.; Taylor, P.; Whidden, T.; White, P. S.: Canad. J. Chem. 57 (1979) 968.

[9] Gillespie, R. J.; Kapoor, R.; Faggiani, R.; Lock, C. J.; Murchie, M.; Passmore, J.: J. Chem. Soc. Chem. Commun. (1983) 8.

[10] Edwards, A. J.; Jones, G. R.; Sills, R. J. C.: J. Chem. Soc. Chem. Commun., (1968) 1527.

[11] Edwards. A. J.; Jones, G. R.: J. Chem. Soc. A, (1971) 2318.

[12] Gillespie, R. J.; Morton, M. J.: Inorg. Chem., 11, (1972) 586, and J. Chem. Soc. Chem. Commun., (1968), 1565.

[13] Glemser, O.; Smalc, A.: Angew. Chem., Int. Ed. Engl. 8 (1969) 517.

[14] Lee, K.C.; Aubke, F.: Inorg. Chem. 19 (1980) 119.

[15] Lee, K.C.; Aubke, F.: Inorg. Chem. 23 (1984) 2124.

[16] Wilson, W. W.; Winfield, J.; Aubke, F.: J. Fluorine Chem. 7 (1976) 245.

[17] Chen, L. H.; Nour, E. M.; Laane, J. M.: J. Raman Spectrosc., 14 (1983) 232.

[18] Milne, J.: Polyhedron 4 (1985) 65.

[19] Gillespie, R. J.; Morton, M. J.: Inorg. Chem., 9, (1970) 811.

[20] Herzberg, G.: "Molecular Spectra and Molecular Structure," Vol. 1, Van Nostrand-Reinhold, Princeton, NJ, 1960.

[21] "Gmelins Handbuch der Anorganischen Chemie," Chlor, Ergänzungsband, Teil A, p. 183, Verlag Chemie, Weinheim, Germany, 1968.

[22] Olah, G. A.; Comisarow, M. B.: J. Amer. Chem. Soc. 90 (1968) 5033 and 91 (1969) 2172.

[23] Christe, K. O.; Muirhead, J. S.: J. Amer. Chem. Soc. 91 (1969) 7777.

[24] Eachus, R. S.; Sleight, T. P.; Symmons, M. C. R.: Nature (London) 222 (1969) 769.

[25] Christe, K. O.; Schack, C. J. : Inorg. Chem. Soc. 9 (1970) 2296.

[26] Shamir, J.; Binenboym, J.: Inorg. Chim. Acta, 2 (1968) 37.

[27] Christe, K. O.; Wilson, W. W.; Schack, C. J.: J. Fluorine Chem. 11 (1978) 71.

[28] Christe, K. O.; Wilson, R. D.; Schack, C. J.: Inorg. Synth. 24 (1986) 3.

[29] Miller, F. A.; Harney, B. M.: Appl. Spectrosc. 23 (1969) 8.

[30] a) Sheldrix, G. M.; SHELX-86 System of Crystallographic Computational Programs, University of Göttingen, Germany, 1986.

b) Sheldrix, G. M.; SHELX-76 System of Crystallographic Computational Programs, University of Cambridge, England, 1976.

[31] Naumann, D.; "Fluor und Fluorverbindungen," Spezille Anorganische Chemie, Band 2, Steinkopff, Darmstadt, Germany, 1980.

[32] Huber, K. P.; Herzberg, G.; "Molecular Spectra and Molecular Structure," Vol. 4, Van Nostrand-Reinhold, New York, NY, 1979.

[33] Muetterties, E. L.; Phillips, W. D.: J. Amer. Chem. Soc. 81 (1959) 1084. Packer, K. J.; Muetterties, E. L.: Proc. Chem. Soc., London (1964) 147.

[34] Passmore, J.; Taylor, P. J.: Chem. Soc. Dalton Trans. (1976) 804.

[35] Weidlein, J.; Müller, U.; Dehnicke, K.: "Schwingungsspektroskopie," G. Thieme Verlag, Stuttgart, Germany, 1982.

[36] Wilson, E. B.; Decius, J. C.; Cross, P. C.; "Molecular Vibrations. The Theory of Infrared and Raman Vibrational Spectra," Mc Graw Hill Book Co., New York, 1955.

[37] Sawodny, W.: J. Mol. Spectrosc. 30 (1969) 56.

[38] Thakur, S. N.; Rai, S. M.; J. Mol. Structure 5 (1970) 320.

[39] Merryman, D. J.; Corbett, J. D.; Edwards, P. A.: Inorg. Chem. 14 (1975) 428.

[40] Pimentel, G. C.: J. Chem. Phys. 19 (1951) 446.

[41] Hach, R. J.; Rundle, R. E.: J. Amer. Chem. Soc. 73 (1951) 4321.

[42] Rundle, R. E.: J. Amer. Chem. Soc. 85 (1963) 112.

[43] Wiebenga, E. H.; Havinga, E. E.; Boswijk, K. H.: Adv. Inorg. Chem. Radiochem. 3 (1961) 158.

[44] Person, W. B.; Anderson, G. R.; Fordemwalt, J. N.; Stammreich, H.; Forneris, R.: J. Chem. Phys., 35 (1961) 908.

Table 1. Summary of Crystal Data and Refinement Results for $[Br_3]^+[AsF_6]^-$

space group	$P\bar{1}$
a (Å)	7.644(7)
b (Å)	5.641(6)
c (Å)	9.810(9)
α (deg)	99.16(8)
β (deg)	86.61(6)
γ (deg)	100.11(7)
v (Å^3)	411.3(7)
molecules/unit cell	2
formula weight (g)	384.0
absorption coefficient (μ: mm^{-1})	18.6
max. & min. transmission factors (scaled to an average of unity)	0.55 - 1.66
crystal dimensions (mm)	0.64 x 0.34 x 0.33
calculated density (g cm^{-3})	3.47
wavelength (Å) used for data collection	0.71069
sin θ/λ limit (Å^{-1})	0.6497
total number of reflections measured	1538
number of independent reflections	1387
number of reflections used in structural analysis $I > 3\sigma(I)$	538
number of variable parameters	91
final agreement factors	R(F) = 0.0608 R(wF) = 0.0608

Table 2. Final Atomic Coordinates and Temperature Factors for $[Br_3]^+[AsF_6]^-$

Atom	x	y	z	$U_{11}x10^3$	$U_{22}x10^3$	$U_{33}x10^3$	$U_{12}x10^3$	$U_{13}x10^3$	$U_{23}x10^3$
As	0.7857(5)	0.5650(8)	0.7972(4)	46(2)	64(3)	32(2)	19(2)	-3(2)	0(2)
Br1	0.8030(5)	0.8212(8)	0.2097(3)	56(2)	79(3)	30(2)	20(2)	2(2)	5(2)
Br2	0.6162(5)	1.0790(8)	0.1780(4)	58(3)	85(3)	57(3)	20(2)	-10(2)	5(2)
Br3	0.7695(6)	0.8069(9)	0.4394(4)	68(3)	108(4)	32(2)	26(2)	0(2)	3(2)
F1	0.7800(33)	0.7883(45)	0.7066(20)	133(21)	105(20)	32(11)	43(17)	-5(12)	-7(12)
F2	0.8702(32)	0.7820(47)	0.9273(21)	106(18)	102(20)	39(12)	-12(15)	-6(12)	-15(13)
F3	0.9991(34)	0.5559(62)	0.7415(36)	74(18)	172(32)	184(31)	52(19)	52(19)	-12(24)
F4	0.5759(26)	0.5799(60)	0.8601(32)	32(13)	184(30)	169(28)	42(16)	14(15)	59(23)
F5	0.7054(37)	0.3490(52)	0.6663(25)	145(24)	117(24)	71(18)	-23(20)	-37(17)	-38(17)
F6	0.7957(36)	0.3498(56)	0.8913(32)	111(22)	112(24)	147(27)	17(19)	-16(20)	8(21)

Table 3. Bond Distances (Å) and Angles (deg) for $[Br_3]^+[AsF_6]^-$

As — F1		1.660(23)
As — F2		1.693(22)
As — F3		1.696(22)
As — F4		1.695(20)
As — F5		1.686(22)
As — F6		1.652(31)
Br1 — Br2		2.275(5)
Br1 — Br3		2.266(5)

F1 -As -F2	87.4(12)
F1 -As -F3	89.9(15)
F2 -As -F3	86.6(14)
F1 -As -F4	91.0(13)
F2 -As -F4	90.9(15)
F3 -As -F4	177.4(17)
F1 -As -F5	92.4(13)
F2 -As -F5	178.9(13)
F3 -As -F5	92.3(15)
F4 -As -F5	90.2(15)
F1 -As -F6	178.0(14)
F2 -As -F6	90.6(14)
F3 -As -F6	89.6(16)
F4 -As -F6	89.5(14)
F5 -As -F6	89.5(15)
Br2 -Br1 -Br3	102.5(2)

Table 4. Low Temperature Raman Spectrum of a Randomly-Oriented Single Crystal of $Br_3^+AsF_6^-$

obsd. freq. (cm^{-1}) rel. int.	assignments (point group) and approximate made descriptions	
	$Br_3^+(C_2v)$	$AsF_6^-(O_h)$
708(15)		(O_h)
684(4)		$\nu_3(F_{1u})$, as stretch
673(25)		$\nu_1(A_{1g})$, sym in phase stretch
576(9)		$\nu_2(E_g)$, sym out of phase stretch
563(10)		
371(15)		$\nu_5(F_{2g})$, sym bend
297(60)	$\nu_3(B_1)$, asym stretch	
293(100)	$\nu_1(A_1)$, sym stretch	
124(23)	$\nu_2(A_1)$, bend	
69(25)		
39 sh		lattice vibrations
30 sh		

Table 5. Vibrational Frequencies (cm^{-1}) of Br_3^+ Compared to Those of I_3^+, Cl_3^+, and $SeBr_2$

	I_3^+ this work	I_3^+ previous work [1]	Br_3^+ this work	Br_3^+ previous work [12-17]	Cl_3^+ [19]	$SeBr_2$ [18]
$\nu_3(B_1)$	211	233	297	288	508	290
$\nu_1(A_1)$	205	207	293	280-295	489	266
$\nu_2(A_1)$	110	114	124	227/238	225	96

Table 6. Internal Force Constants (mdyn/Å) and Bond Lengths (Å) and Angles (deg) of the Hal_3^+, Hal_2, and Hal_2^+ Series

	Cl_3^+	Cl_2[1]	Cl_2^+[1]	Br_3^+	Br_2[2]	Br_2^+[1]	I_3^+[1]	I_3^+ this work	I_2 [1]	I_2^+[1]
fr	2.607	3.16	4.29	2.063	2.36	3.05	1.923	1.607	1.70	2.12
frr	0.184	–	–	0.192	–	–	0.156	0.097	–	–
$f\alpha$	0.314	--	–	0.216	–	–	0.294	0.273	–	–
$fr\alpha$	0.076	–	–	0.052	–	–	0.070	0.065	–	--
r	[1.98]^a	1.98	1.89	2.268	2.28	2.13	2.665		2.666	2.56
α	[103]^a	–	--	102.7	–	–	101.75		–	–

(a) estimated values

Table 7. Raman Spectra of $Br_5^+AsF_6^-$

obsd. freq. (cm^{-1}) rel. int.		assignments (point group) and approximate made descriptions	
solid -155°C	HF solution 25°C	AsF_6^-(O_h)	Br_5^+(C_{2h})
718(0.5)		$\nu_3(F_{1u})$	
681(0.7)			
670(3.5)	685(4)	$\nu_1(A_{1g})$	
618(0.4)		$\nu_2(E_g)$	
570(0.2)			
563(0.3)			
487(0.2)			
399(0.1)		$\nu_4(F_{1u})$	
366(0.8)		$\nu_5(F_{2g})$	
348(1)			
309(9)	309(20) pol		$\nu_1(A_g)$, sym terminal stretch
190sh			$\nu_7(B_u)$, asym central stretch
174(100)	182(100) pol		$\nu_2(A_g)$, sym central stretch
87(69)	108(68) pol		$\nu_3(A_g)$, sym term. in plane def
66(3)		lattice vibrations	
37(20)			
27(12)			

Diagram Captions

Figure 1. Unit cell packing diagram for $Br_3^+AsF_6^-$, viewed down the b axis.

Figure 2. Br_3^+ cation with closest anion-cation contacts.

Figure 3. Raman spectrum of a single crystal of $Br_3^+AsF_6^-$ recorded at -150°C with random orientation of the crystal. The insert shows the Br_3^+ stretching bands, recorded with tenfold abscissa expansion.

Figure 4. Raman spectrum of an anhydrous HF solution of $I_3^+AsF_6^-$ in a Teflon-FEP tube recorded at 25°C with 514.5-nm excitation. The band shown as an insert was recorded with a smaller slit width of 2 cm^{-1} to resolve the shoulder on the high frequency side.

Figure 5. Range of possible solutions for the A_1 General Valence Force Fields for Cl_3^+, Br_3^+, and I_3^+ (all values in mdyn/Å). The preferred solutions have been marked by vertical lines.

Figure 6. Raman spectrum of $Br_5^+AsF_6^-$. Traces A and B are spectra of the solid recorded at -155°C at two different recorder voltages; trace C is the spectrum of a saturated solution in anhydrous HF at 25°C. Bands marked by an asterisk are due to the Teflon container.

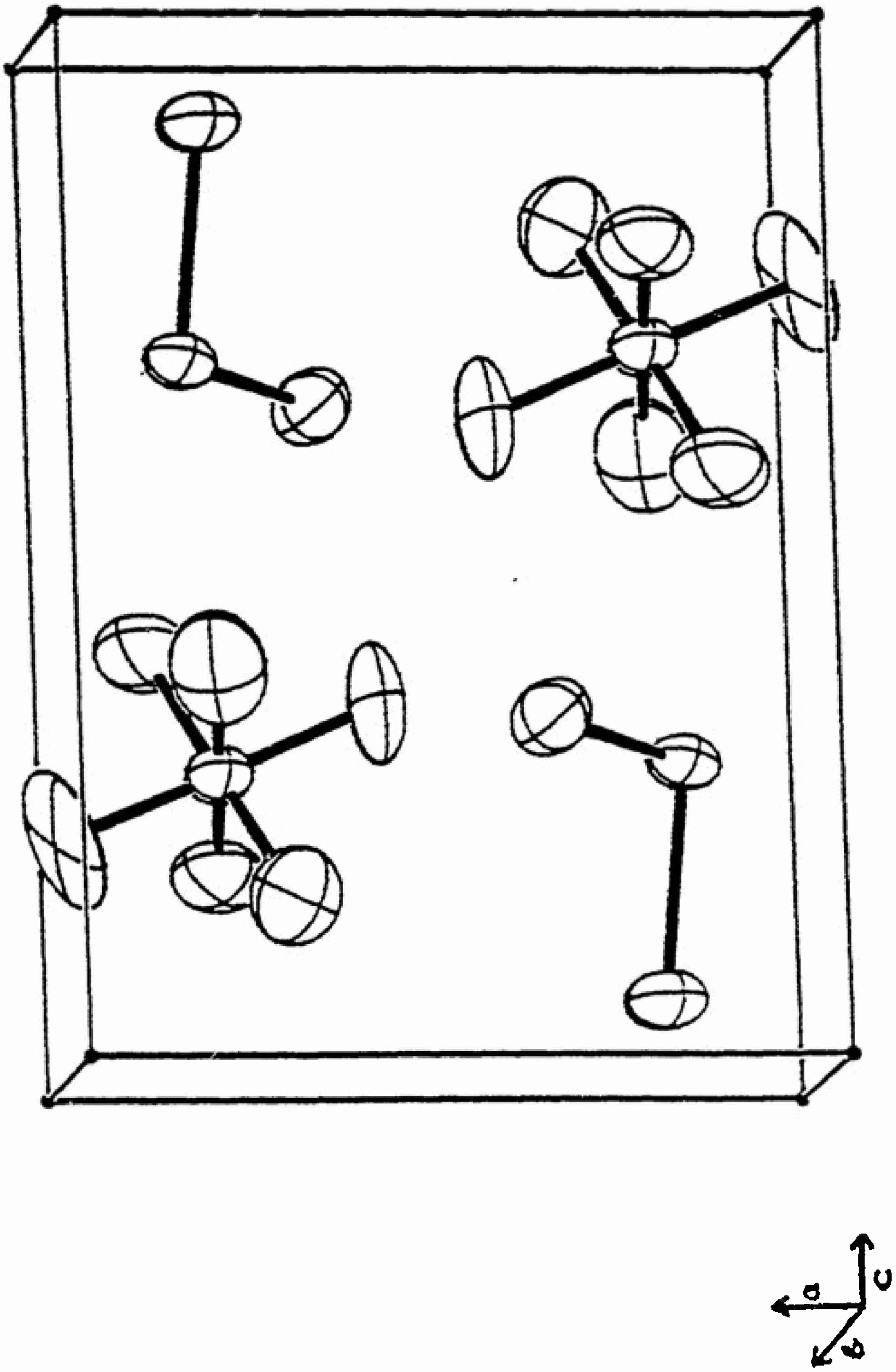
c
a
b

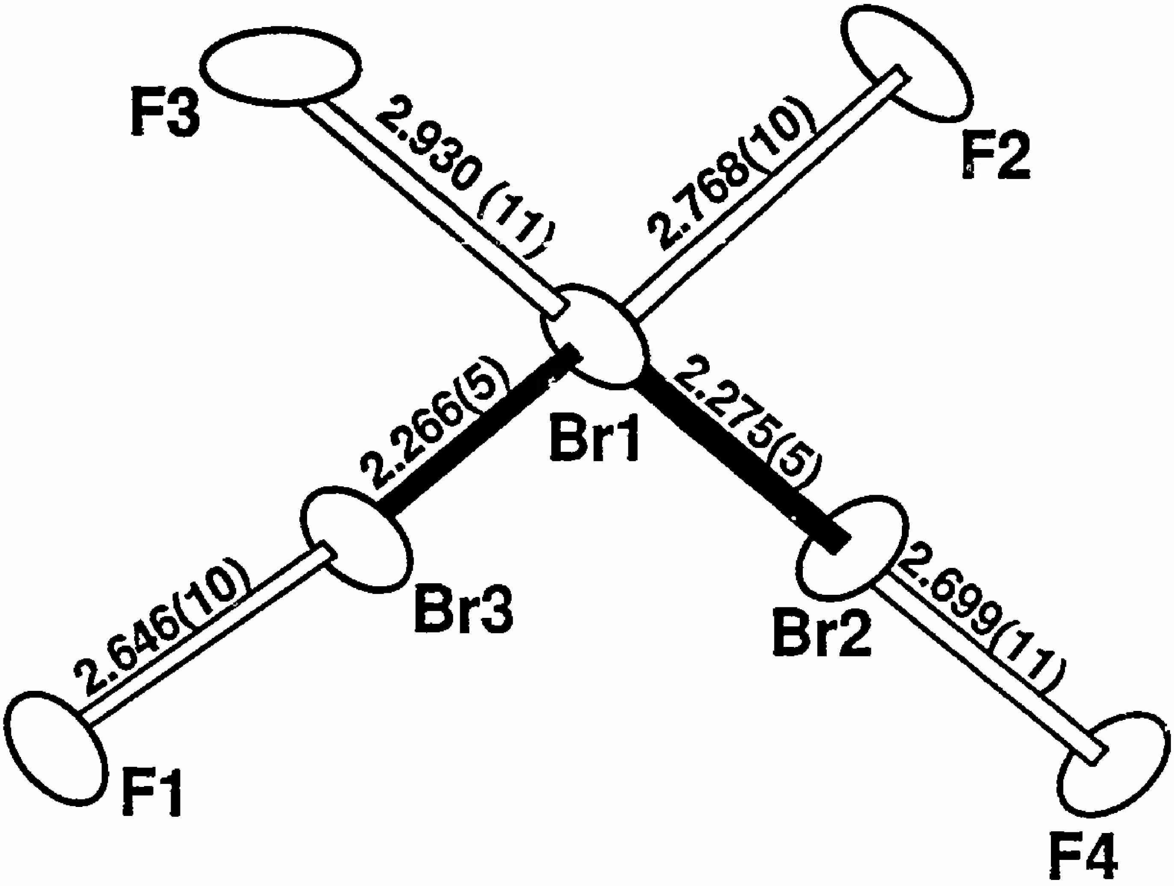
F3
2.930 (11)
2.768(10)
F2
2.266(5)
Br1
2.275(5)
2.646(10)
Br3
Br2
2.699(11)
F1
F4

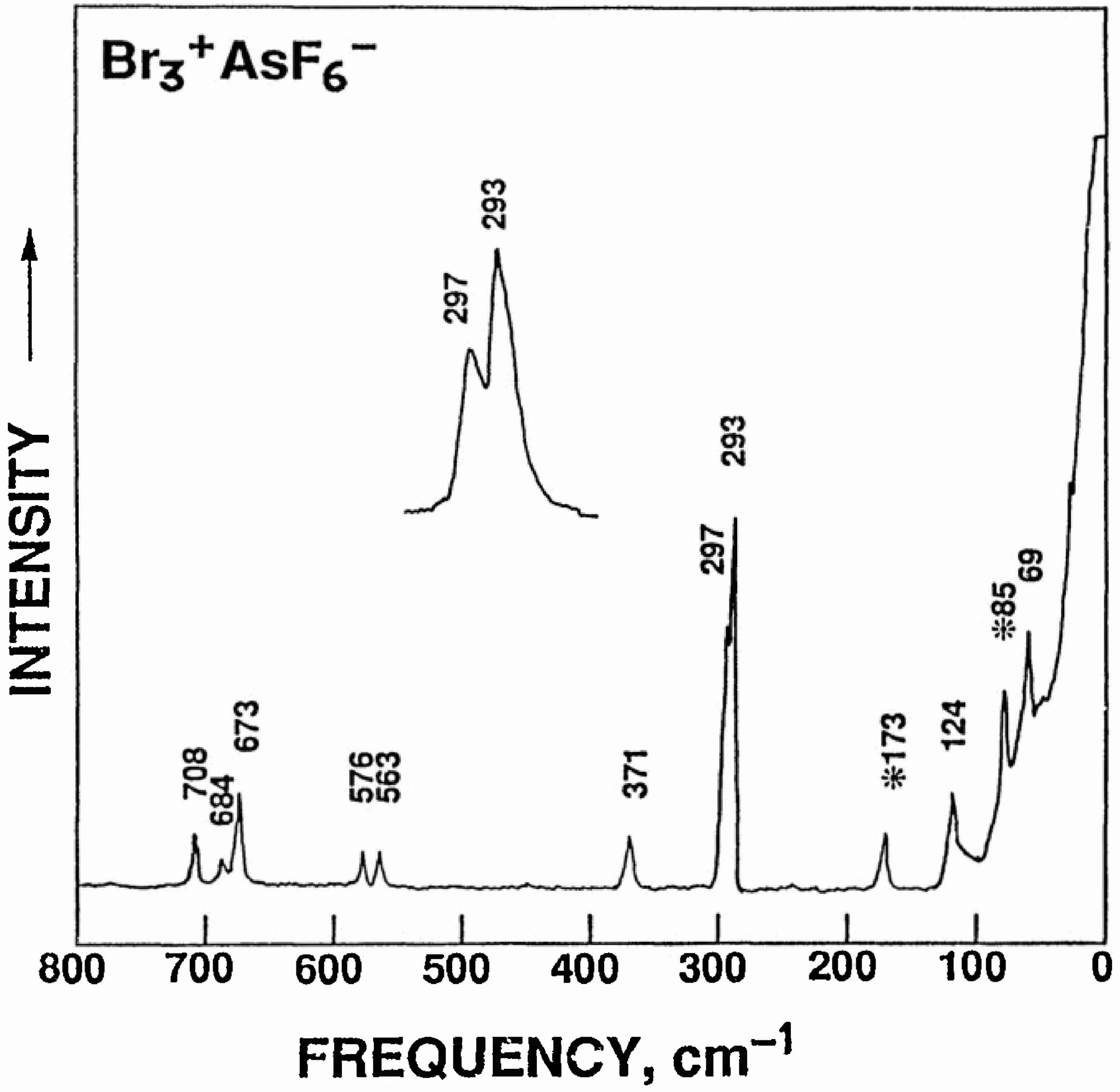
$Br_3^+AsF_6^-$
INTENSITY
297
293
297
293
708
684
673
576
563
371
※173
124
※85
69
800
700
600
500
400
300
200
100
0
FREQUENCY, cm^{-1}

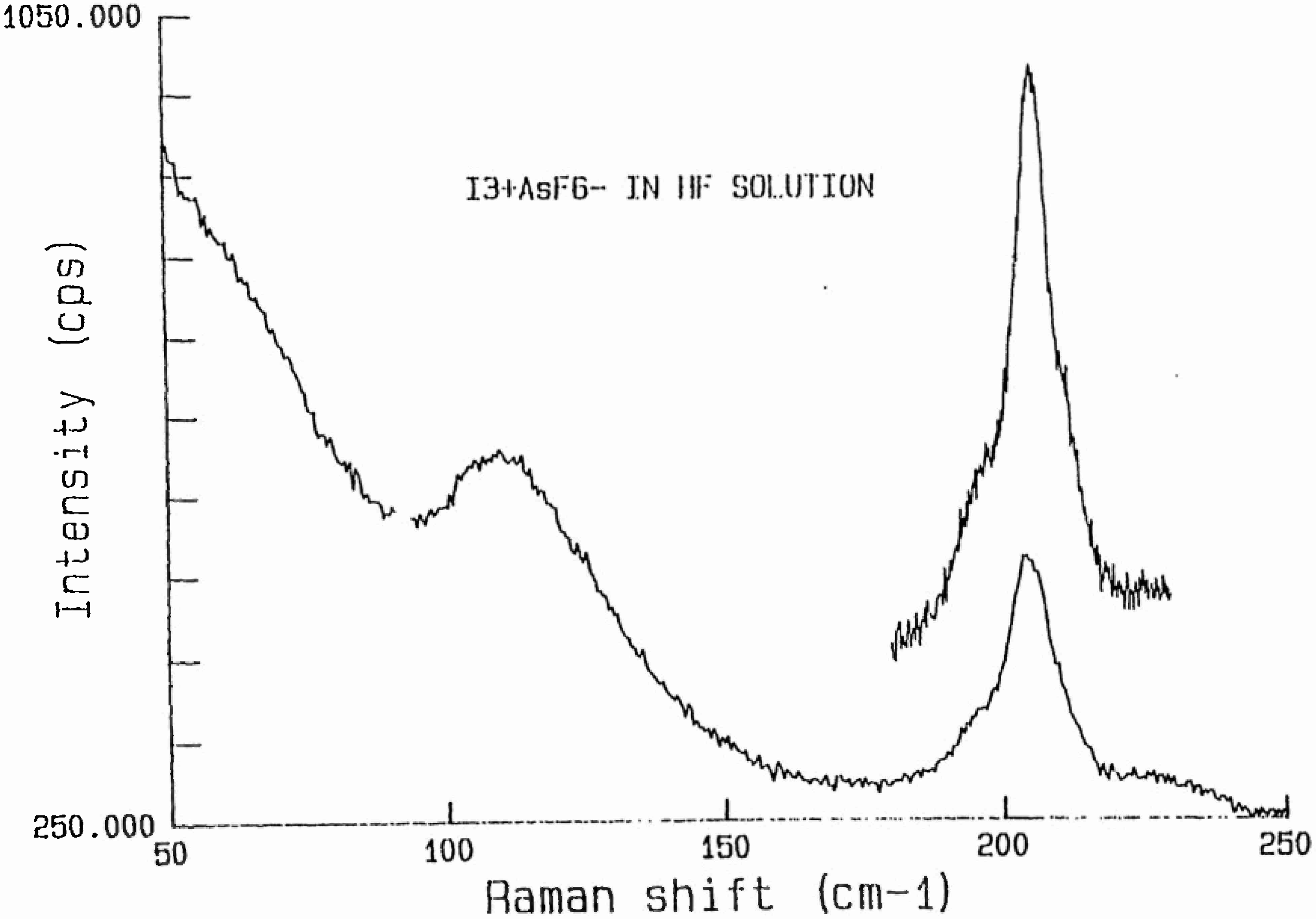
I3+AsF6- IN HF SOLUTION
1050.000
250.000
Intensity (cps)
50
100
150
200
250
Raman shift (cm-1)

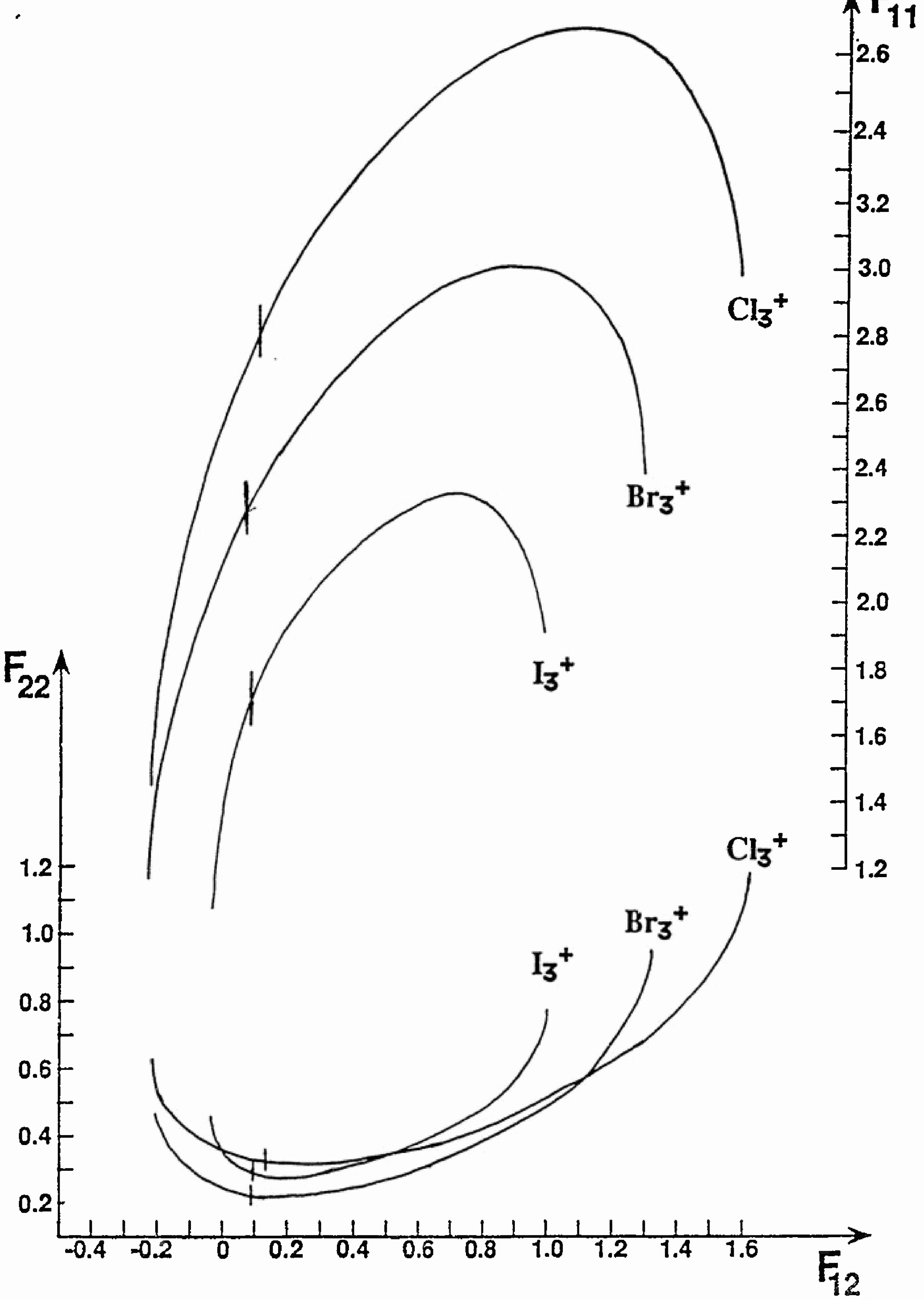
F_{11}
2.6
2.4
3.2
3.0
2.8
2.6
2.4
2.2
2.0
1.8
1.6
1.4
1.2
Cl_3^+
Br_3^+
I_3^+
F_{22}
1.2
1.0
0.8
0.6
0.4
0.2
Cl_3^+
Br_3^+
I_3^+
-0.4
-0.2
0
0.2
0.4
0.6
0.8
1.0
1.2
1.4
1.6
F_{12}

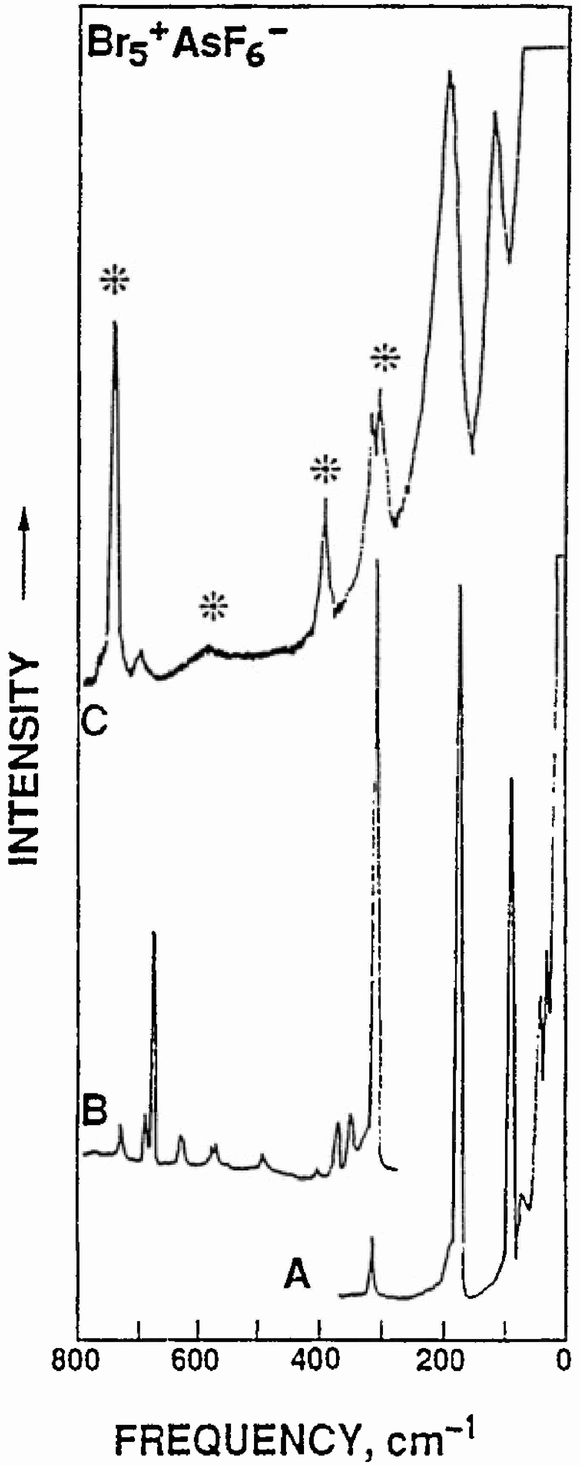
Br5+AsF6−
INTENSITY
C
B
A
800
600
400
200
0
FREQUENCY, cm−1

Controlled Replacement of Fluorine by Oxygen in Fluorides and Oxyfluorides

Karl O. Christe, William W. Wilson, and Carl J. Schack

Rocketdyne Division of Rockwell International Corporation, Canoga Park, California, 91303

I. Introduction

Fluorine-oxygen exchange reactions play an important role in synthetic chemistry. Although numerous methods and reagents have been described for these exchange reactions, the emphasis of these studies has been almost exclusively on the selective replacement of oxygen by fluorine. For example, SF_4 [1] and its derivatives, such as $SF_3N(CH_3)_2$,[2] have been widely used to convert carbonyl groups to CF_2 groups, and inorganic oxides can be transformed into fluorides by reagents such as HF, F_2, or halogen fluorides.[3] However, much less attention has been paid to the opposite reaction, i.e. the conversion of fluorides to oxyfluorides. This is not surprising because generally oxides are more readily preparable than fluorides, and many fluorides undergo facile hydrolysis to the corresponding oxyfluorides and oxides.

For the replacement of fluorine by oxygen, hydrolysis is the most frequently used method. For highly fluorinated compounds of the more electronegative elements, however, these hydrolysis reactions often present significant experimental difficulties, particularly when a controlled and stepwise replacement of fluorine by oxygen is desired. The hydrolysis reactions of these compounds are often violent, as found for XeF_6 [4,5] or ClF_3, [6] and require careful moderation. Thus, SiO_2 combined with a trace of HF can be used for the slow formation of water (1), followed by a continuous regeneration of the HF during the hydrolysis of the fluoride starting material (2). This approach has been demonstrated previously for compounds such as IF_7.[7–10]

$$SiO_2 + 4HF \longrightarrow SiF_4 + 2H_2O \tag{1}$$

$$IF_7 + H_2O \longrightarrow IOF_5 + 2HF \tag{2}$$

Another approach to moderate otherwise violent or uncontrollable hydrolysis reactions involves the use of suitable solvents, such as HF, and of stoichiometric amounts of water, as reported for XeF_6 (3).[5]

$$XeF_6 + H_2O \xrightarrow{HF} XeOF_4 + 2HF \tag{3}$$

In spite of the above improvements in the techniques of hydrolyzing highly reactive fluorides, these reactions remain experimentally challenging and often are dangerous[5] and difficult to scale up

Consequently, alternate reagents which allow the safe, easily controllable, and stepwise replacement of fluorine by oxygen, are highly desirable.

Previously investigated examples for such alternate reagents include SiF_3OSiF_3, SeO_2F_2, POF_3, and several oxides. Most of these alternate reagents exhibit drawbacks. Thus, SiF_3OSiF_3 reacted with XeF_6 (4),

$$XeF_6 + SiF_3OSiF_3 \longrightarrow XeOF_4 + 2SiF_4 \tag{4}$$

but did not work for IF_7, BrF_5, etc.[11] Similarly, the highly toxic SeO_2F_2 was demonstrated only for XeF_6 (5).[12]

$$XeF_6 + SeO_2F_2 \longrightarrow XeOF_4 + SeOF_4 \tag{5}$$

The most versatile of these alternate reagents appears to be POF_3 which reacted with XeF_6 (6),[13] UF_6 (7),[14] ClF_5,[14] and IF_7 (8).[15]

$$XeF_6 + POF_3 \longrightarrow XeOF_4 + PF_5 \tag{6}$$

$$UF_6 + POF_3 \longrightarrow UOF_4 + PF_5 \tag{7}$$

$$IF_7 + POF_3 \longrightarrow IOF_5 + PF_5 \tag{8}$$

Most of the previously reported, oxide based fluorine-oxygen exchange reactions, such as (9),[10] (10),[16] or (11),[17]

$$IF_7 + I_2O_5 \longrightarrow IOF_5 + 2IO_2F \tag{9}$$

$$4ClF_3 + 6NaClO_3 \longrightarrow 6ClO_2F + 6NaF + 2Cl_2 + 3O_2 \tag{10}$$

$$2BrF_5 + CsIO_4 \longrightarrow 2BrOF_3 + CsIO_2F_4 \tag{11}$$

represent useful syntheses for specific compounds, but the exchange reagents have not been studied systematically.

Several years ago, while studying the compatibility of the nitrate and sulfate anions with various halogen fluorides,[18] we surprisingly found that these anions are excellent, general reagents for fluorine-oxygen exchange. Since then, we have systematically investigated the scope of these reactions and present a summary of our results in this review.

II. Reactions of the Nitrate Anion

1. Xenon (VI) Fluoride and Oxyfluorides

Xenon hexafluoride is an ideal test case for the general usefulness of a fluorine-oxygen exchange reagent since it can undergo stepwise fluorine replacement (12). When preparing $XeOF_4$ and XeO_2F_2,

$$XeF_6 \rightarrow XeOF_4 \rightarrow XeO_2F_2 \rightarrow XeO_3 \qquad (12)$$

precise control of the stepwise exchange is of utmost importance because of the shock sensitivity of the potential by-product XeO_3. Other important aspects, besides high yields and ready availability of the exchange reagent, are the ease of product separation and mild reaction conditions to avoid product decomposition.

In our studies[19] it was found that $NaNO_3$ is best suited for the conversion of XeF_6 to $XeOF_4$ (13).

$$XeF_6 + NaNO_3 \xrightarrow[10\ hr]{70°C} XeOF_4 + NaF + NO_2F \qquad (13)$$

The formation of XeO_2F_2 can be suppressed by the use of a moderate excess of XeF_6. The excess of XeF_6 is readily separable from the desired $XeOF_4$ because at the reaction temperature it forms stable $NaXeF_7$ and Na_2XeF_8 salts with the NaF by-product. The only other volatile by-product is NO_2F which is much more volatile than $XeOF_4$ and can be separated easily from the $XeOF_4$ by fractional condensation through traps kept at -78° and -196°C. The yields of $XeOF_4$ are about 80% based on the limiting reagent $NaNO_3$. The use of other alkali metal nitrates is less desirable. In the case of $CsNO_3$ the resulting CsF complexes $XeOF_4$ with formation of $CsXeOF_5$ [20-22] and for $LiNO_3$ the resulting LiF does not complex any unreacted XeF_6 starting material.

For the conversion of $XeOF_4$ to XeO_2F_2, the use of alkali metal nitrates is possible but, due to the relative involatility of XeO_2F_2 and its ease of forming stable $XeO_2F_3^-$ salts, N_2O_5 is the preferred reagent.[23] In the solid state, N_2O_5 has the ionic structure $NO_2^+NO_3^-$ [24,25] and reacts with $XeOF_4$ according to (14).

$$XeOF_4 + NO_2^+NO_3^- \xrightarrow[1.5\ hr]{25°C} XeO_2F_2 + 2NO_2F \qquad (14)$$

In this manner and by the use of an excess of $XeOF_4$, the only product of low volatility is XeO_2F_2, thus allowing for an efficient product separation. Again, the formation of XeO_3 was suppressed by the use of a slight excess of $XeOF_4$ starting material, and the yield of XeO_2F_2 was essentially quantitative. The only minor complication in this XeO_2F_2 synthesis is the formation of an unstable $NO_2^+[XeO_2F_3 \cdot nXeO_2F_2]^-$ type adduct between NO_2F and XeO_2F_2 which requires prolonged pumping on the product at room temperature to ensure complete NO_2F removal from the XeO_2F_2.[23]

Conversion of either XeF_6, $XeOF_4$, or XeO_2F_2 to the highly explosive XeO_3 can be achieved by their reactions with excess N_2O_5.[23] However, no detailed studies were carried out on these systems due to the sensitivity of XeO_3.

2. Chlorine Fluorides and Oxyfluorides

Excess $NaNO_3$ readily reacts with ClF at subambient temperatures to give NaF and $ClONO_2$ (15).[26]

$$ClF + NaNO_3 \rightarrow NaF + ClONO_2 \qquad (15)$$

However, the yield of $ClONO_2$ was only about 75% because of the competing reaction (16)

$$ClF + ClONO_2 \rightarrow Cl_2O + NO_2F \qquad (16)$$

which is favored by an excess of ClF. With a sufficiently large excess of ClF, the overall reaction then becomes (17).

$$2ClF + NaNO_3 \rightarrow Cl_2O + NaF + NO_2F \qquad (17)$$

In addition to the NaF, $ClONO_2$ and NO_2F products, smaller amounts of Cl_2 and ClO_2F were also observed as by-products due to the side reactions (18) and (19) which result in (20) as the net reaction.

$$2ClF + 2Cl_2O \rightarrow 2[FClO] + 2Cl_2 \qquad (18)$$

$$2[FClO] \rightarrow ClF + ClO_2F \qquad (19)$$

$$ClF + 2Cl_2O \rightarrow ClO_2F + 2Cl_2 \qquad (20)$$

Thus, ClF readily undergoes fluorine-oxygen exchange with the NO_3^- anion with the ratio of the major products, $ClONO_2$ and Cl_2O, depending on the stoichiometry of the reactants. Smaller amounts of Cl_2 and ClO_2F formed in this system are due to side reactions.

In the case of ClF_3, the main reaction with the NO_3^- anion is again a facile fluorine-oxygen exchange (21)[26]

$$ClF_3 + NaNO_3 \xrightarrow{25°C} [FClO] + NaF + NO_2F \tag{21}$$

with the thermally unstable FClO either undergoing disproportionation (22) or decomposition (23).

$$2[FClO] \rightarrow ClF + ClO_2F \tag{22}$$

$$2[FClO] \rightarrow 2ClF + O_2 \tag{23}$$

The formation of ClF, ClO_2F, O_2, and NO_2F is favored by the use of an excess of ClF_3. If, however, a large excess of $NaNO_3$ is used, the side reactions (15, 24, 25) are also observed.

$$NO_2F + NaNO_3 \rightarrow N_2O_5 + NaF \tag{24}$$

$$ClO_2F + NaNO_3 \rightarrow ClONO_2 + O_2 + NaF \tag{25}$$

ClF_5 also reacts readily at room temperature with nitrates.[26] Even in the presence of a large excess of ClF_5, the fluorine-oxygen exchange cannot be stopped at the $ClOF_3$ stage but proceeds all the way to ClO_2F (26).

$$ClF_5 + 2MNO_3 \xrightarrow{25°C} ClO_2F + 2NO_2F + 2MF \tag{26}$$

(M = Li, Na, K, Rb, Cs)

This is in marked contrast to BrF_5 and IF_5 (see below) and is due to the extraordinary reactivity of $ClOF_3$ which is much more reactive than ClF_5.[27] Attempts to trap the intermediately formed $ClOF_3$ as $M^+ClOF_4^-$ salts were also unsuccessful indicating that the complexation of $ClOF_3$ with MF is slower than its fluorine-oxygen exchange with the nitrate anion.

When a large excess of nitrate is used in the reaction of ClF_5 with MNO_3 (26), the ClO_2F product can undergo further fluorine-oxygen exchange with NO_3^- as shown in (25). This was confirmed by separate experiments between ClO_2F and either $LiNO_3$ or $NO_2^+NO_3^-$.[26]

Thus, all the chlorine fluorides and oxyfluorides, except for the highly unreactive[27] ClO_3F, undergo rapid fluorine-oxygen exchange with the nitrate anion. Due to the high reactivity of $ClOF_3$ and in contrast to BrF_5 and IF_5, a controlled single step fluorine-oxygen exchange in ClF_5 could not be realized.

3. Bromine Pentafluoride

The reactions of BrF_5 with $M^+NO_3^-$ serve as excellent examples of how the nature of the products can be influenced by the appropriate choices of the M^+ cation and the reaction stoichiometries.[18, 28] With an excess of BrF_5 and M being either Na, K, Rb, or Cs, the correspoonding $M^+BrOF_4^-$ salts can be prepared in 70 - 100% yield under very mild (-30° to 25°C) conditions (27).

$$BrF_5 + MNO_3 \xrightarrow[\text{excess } BrF_5]{-30 \text{ to } 25°C} MBrOF_4 + NO_2F \qquad (27)$$

$$(M = Na, K, Rb, Cs)$$

Since lithium does not form a stable $LiBrOF_4$ salt, the reaction of $LiNO_3$ with excess BrF_5 (28) can be used for a convenient synthesis of free $BrOF_3$.

$$BrF_5 + LiNO_3 \xrightarrow[\text{excess } BrF_5]{0°C} BrOF_3 + LiF + NO_2F \qquad (28)$$

Since $BrOF_3$ is considerably less volatile than BrF_5, the two can be separated readily by fractional condensation or distillation.

While the use of an excess of BrF_5 results in the single step replacement of two fluorines by one oxygen, the application of a 1:3 mole ratio of BrF_5:$LiNO_3$ causes complete fluorine-oxygen exchange with $BrONO_2$ formation (29).[28]

$$BrF_5 + 3LiNO_3 \xrightarrow[\text{excess } LiNO_3]{0°C} BrONO_2 + 3LiF + O_2 + 2NO_2F \qquad (29)$$

If the BrF_5:$LiNO_3$ mole ratio is further changed to 1:5 or greater, N_2O_5 is produced (30)

$$2NO_2F + 2LiNO_3 \rightarrow NO_2^+NO_3^- + 2LiF \qquad (30)$$

which can react with $BrONO_2$ according to (31).[28]

$$NO_2^+NO_3^- + BrONO_2 \rightarrow NO_2^+[Br(ONO_2)_2]^- \qquad (31)$$

4. Iodine Fluorides and Oxyfluorides

The reactions of IF and IF_3 with nitrates were not studied since IF and IF_3 are relatively unstable and easily disproportionate to I_2 and IF_5. With excess IF_5, the alkali metal nitrates undergo a controlled, single step fluorine-oxygen exchange to form the corresponding $MIOF_4$ salts (32).[29]

$$IF_5 + MNO_3 \rightarrow MIOF_4 + NO_2F \qquad (32)$$

$$(M = Li, K, Cs)$$

However, these reactions are more sluggish than the corresponding BrF_5 reactions. As a consequence, the side reaction (33)

$$NO_2F + MNO_3 \rightarrow N_2O_5 + MF \tag{33}$$

becomes faster than (32) resulting in an equal consumption of MNO_3 by (32) and (33). Furthermore, reactions (34) and (35) also become competitive,

$$KF + IF_5 \rightarrow KIF_6 \tag{34}$$

$$CsF + 3IF_5 \rightarrow CsI_3F_{16} \tag{35}$$

and some of the N_2O_5 decomposes to $N_2O_4 + O_2$ under these conditions. Consequently, the $MIOF_4$ salts prepared in this manner, usually contain substantial amounts of IF_6^- and $I_3F_{16}^-$ salts as by-products.

From the reaction of excess IF_7 with either $LiNO_3$ or $NaNO_3$, no IOF_5 is isolated. Instead, IF_5 and O_2 are obtained (36),

$$IF_7 + MNO_3 \xrightarrow{60°C} IF_5 + 1/2\,O_2 + MF + NO_2F \tag{36}$$

indicative of a competing deoxygenation reaction.[29] In the case of $CsNO_3$, the same deoxygenation occurs but the CsF product reacts with IF_5 and IF_7 to give CsI_3F_{16} and $CsIF_8$, respectively. If in (36) an excess of MNO_3 is used, the IF_5 product from (36) can react further with MNO_3 and form $MIOF_4$ salts (32). The fact that the reaction conditions of (36) favor deoxygenation of IOF_5 was experimentally confirmed. It was shown that IOF_5 does not undergo fluorine-oxygen exchange giving IO_2F_3, but loses oxygen giving IF_5 which then undergoes fluorine-oxygen exchange with formation of IOF_4^- salts (32).[29]

The fact that IF_7 readily undergoes fluorine-oxygen exchange either during controlled hydrolysis[7-10] or with POF_3,[15] but not with the NO_3^- anion remains somewhat a puzzle. It has previously been speculated[29] that this lack of fluorine-oxygen exchange in the IF_7-nitrate system might be due to either the instability of an intermediate IOF_6^- anion or the lack of a free valence electron pair on the iodine central atom of IF_7. Since then, however, we have synthesized and characterized stable IOF_6^- salts;[30] thus, the first explanation can be ruled out.

5. Carbonyl Fluoride

The nitrate anion can also exchange carbon bonded fluorine for oxygen. This was demonstrated[31] for carbonyl fluoride, COF_2 (37).

$$COF_2 + MNO_3 \xrightarrow[CsF]{85°C} CO_2 + MF + NO_2F \qquad (37)$$

$$(M = Li, Na)$$

The reactions were carried out in a steel cylinder and, in this manner, essentially quantitative yields of NO_2F are obtainable. Reaction (37) is remarkable because it is a very rare example for the formation of a nitrogen-fluorine bond using a fluorinating agent as mild as COF_2. Furthermore, it is interesting that the heavier alkali metal nitrates, such as $CsNO_3$, do not react under these conditions with COF_2. This was explained[31] by thermochemical calculations which show that for Li and Na the ΔH values are still favorable but become increasingly more positive for the heavier alkali metals. It should be noted that all the ΔH values given in Reference 31 are slightly in error[32] by -11 kcal mol^{-1}, but that the general trend remains the same for the different alkali metals.

6. Mechanism of the Fluorine-Oxygen Exchange Involving Nitrates

Of the nitrate based fluorine-oxygen exchange reactions studied so far, the simplest case is that of MNO_3 and ClF which yields MF and $ClONO_2$ (15).[26] Assuming for the more highly fluorinated starting materials an analogous first reaction step (38),

$$XF_n + MNO_3 \longrightarrow F_{(n-1)}XONO_2 + MF \qquad (38)$$

the formation of an intermediate $F_{(n-1)}XONO_2$ is expected. This intermediate could easily undergo an internal nucleophilic substitution ($S_N i$) reaction,[18] accompanied by NO_2F elimination (39).

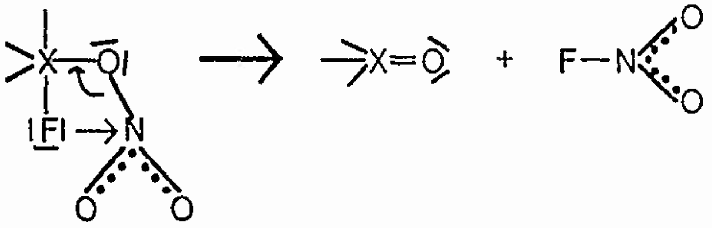

(39)

Such a mechanism could account for the generally observed reaction products, MF, NO_2F, and the corresponding oxyfluoride. If the oxyfluoride end product is amphoteric and can form a stable salt with the cogenerated alkali metal fluoride, then this salt is observed as the final product (40).

$$XOF_{(n-2)} + MF \longrightarrow M^+[XOF_{(n-1)}]^- \qquad (40)$$

If, as for the $ClF + NO_3^-$ reaction (15), the resulting nitrate intermediate no longer contains a fluoride ligand, NO_2F elimination becomes impossible, and the halogen nitrate becomes the final product.

All the nitrate reactions studied so far seem to follow this pattern, except for the IF_7 case where deoxygenation of the expected IOF_5 product occurred (36). Since the IF_7 + MNO_3 reactions require elevated temperatures and conditions under which IOF_5 can undergo deoxygenation,[29] the latter might be a secondary reaction, and the IF_7 + MNO_3 reaction might involve the same primary steps as all the other nitrate reactions.

III. Reactions of the Sulfate Anion

The reactions of the sulfate anion with highly fluorinated compounds of the more electronegative elements resemble those of the nitrate anion. Again, fluorine-oxygen exchange occurs but this exchange generally stops at the SO_3F^- level (41),

$$XF_n + M_2SO_4 \rightarrow XOF_{(n-2)} + MSO_3F + MF \qquad (41)$$

and does not proceed further to the SO_2F_2 stage (42).[33]

$$XF_n + MSO_3F \rightarrow XOF_{(n-2)} + SO_2F_2 + MF \qquad (42)$$

Since MSO_3F is a nonvolatile solid whereas NO_2F is a volatile gas, the use of M_2SO_4 may be more convenient than that of MNO_3 if the desired product is volatile but either complexes with NO_2F or is difficult to separate from it. Compared to the nitrate anion, the sulfate anion is less reactive and requires longer reaction times and or higher temperatures. Consequently, the reactions of the sulfate anion were not studied as extensively as those of the nitrate anion and were limited to the following examples.

1. Bromine Pentafluoride

At room temperature Cs_2SO_4 readily undergoes fluorine-oxygen exchange with BrF_5 (43).[33]

$$BrF_5 + Cs_2SO_4 \xrightarrow[\text{1 day}]{25°C} CsBrOF_4 + CsSO_3F \qquad (43)$$

Even with an 80 fold excess of BrF_5, the fluorine-oxygen exchange did not proceed past the $CsSO_3F$ stage. Attempts were made to use this reaction for the synthesis of free $BrOF_3$ by the replacement of Cs_2SO_4 with Li_2SO_4 since lithium does not form a stable $BrOF_4^-$ salt. Under conditions (0°C, 1 day) which worked well for $LiNO_3$ (28), no reaction was observed for Li_2SO_4. This shows that the SO_4^{2-} anion is less reactive than NO_3^-.

2. Iodine Fluorides

Reaction temperatures in excess of 70°C were required to initiate a slow reaction between IF_7 and Li_2SO_4. Even at this temperature, the conversion of the Li_2SO_4 was only about 6 - 7%. As in the case of NO_3^-, deoxygenation of the IOF_5 occurred and IF_5 and O_2 were the observed products (44).[34]

$$IF_7 + Li_2SO_4 \xrightarrow{70°C} IF_5 + 0.5\,O_2 + LiSO_3F + LiF \qquad (44)$$

Attempts to convert IOF_5 with Li_2SO_4 to IO_2F_3 at 75° were, as in the case of NO_3^-, also unsuccessful.[34]

3. Xenon Fluorides

At room temperature, excess XeF_6 reacts with Li_2SO_4 to give the expected $XeOF_4$ in high yield (45).[34]

$$XeF_6 + Li_2SO_4 \xrightarrow{25°C} XeOF_4 + LiSO_3F + LiF \qquad (45)$$

The $XeOF_4$ can be reacted further with Li_2SO_4 to give XeO_2F_2 in modest yield (46).[34]

$$XeOF_4 + Li_2SO_4 \xrightarrow{25°C} XeO_2F_2 + LiSO_3F + LiF \qquad (46)$$

As in the case of NO_3^-, care must be taken to use excess $XeOF_4$ to avoid the formation of explosive XeO_3.

IV. Summary

Oxoanions, such as NO_3^- or SO_4^{2-}, are effective, readily available, nontoxic, and low cost reagents for controlled, stepwise fluorine-oxygen exchange in highly fluorinated compounds of the more electronegative elements. Product separations can be faciliated greatly by appropriate choices of the anion, the countercations and the mole ratios of the reagents. The reactions appear to be quite general, controllable, safe, and scalable.

Acknowledgements

The authors are indebted to Mr. R.D.Wilson for help and to the Army Research Office, the Air Force Astronautics Laboratory, and the Office of Naval Research for financial support of this work.

References

1. Burmakov, A. I., Kunshenko, B. V., Alekseeva, L. A., and Yagupolskii, L. M., in New Fluorinating Agents in Organic Synthesis (L. German and S. Zemskov, Eds.), Springer Verlag, Berlin (1989), pp. 197-253.
2. Hudlicky, M., in Organic Reactions, John Wiley and Sons, Inc., New York (1988), pp.513-637.
3. Many examples for these types of reactions can be found in Vol. 3 and 4 of Inorganic Reactions and Methods (J. J. Zuckerman and A. P. Hagen, Eds.), V.C.H. Publishers, Inc., New York (1989).
4. Chernik, C. L., Claassen, H. H., Malm, J. G., and Plurien, P. L., in Noble-Gas Compounds (H. H. Hyman, Ed.), University of Chicago Press (1963), p. 106.
5. Schumacher, G. A. and Schrobilgen, G. J., Inorg. Chem., (1984), 23, 2923.
6. Bougon, R., Carles, M., and Aubert, J., C. R. Acad. Sci., Ser. C, (1967), 265, 179.
7. Gillespie, R. J. and Quail, J. W., Proc. Chem. Soc., (1963), 278.
8. Schack, C. J., Pilipovich, D., Cohz, S. N., and Sheehan, D. F., J. Phys. Chem., (1968), 72, 4697.
9. Alexakos, L. G., Cornwell, C. D., and Pierce, S. B., Proc. Chem. Soc., (1963), 341.
10. Bartlett, N. and Levchuck, L. E., Proc. Chem. Soc., (1963), 342.
11. Jacob, E., Z. Naturforsch., (1980), 35 b, 1095.
12. Seppelt, K. and Rupp, H. H., Z. Anorg. Allg. Chem., (1974), 409, 331.
13. Nielsen, J. B., Kinkead, S. A., and Eller, P. G., Inorg. Chem., (1990), 29, 3621.
14. Kinkead, S. A. and Nielsen, J. B., paper 47 presented at the ACS Ninth Winter Fluorine Conference, St. Petersburg, FL (February, 1989).
15. Schack, C. J. and Christe, K. O., J. Fluorine Chem., (1990), 49, 167.
16. Christe, K. O., Wilson, R. D., and Schack, C. J., Inorg. Nucl. Chem. Lett., (1975) 11, 161.
17. Christe, K. O., Wilson, R. D., and Schack, C. J., Inorg. Nucl. Chem. Lett., (1981) 20, 2104.
18. Wilson, W. W. and Christe, K. O., Inorg. Chem., (1987) 26, 916.

19. Christe, K. O. and Wilson, W. W., Inorg. Chem., (1988) 27, 1296.

20. Selig, H., Inorg. Chem., (1966), 5, 183.

21. Waldman, M. C. and Selig, H., J. Inorg. Nucl. Chem., (1973), 35, 2173.

22. Schrobilgen, G. J., Martin-Rovet, D., Charpin, P., and Lance, M., J.C.S. Chem. Comm., (1980), 894.

23. Christe, K. O. and Wilson, W. W., Inorg. Chem., (1988) 27, 3763.

24. Grison, E., Eriks, K., and De Vries, J. L., Acta Crystallogr., (1950), 3, 290.

25. Wilson, W. W. and Christe, K. O., Inorg. Chem., (1987) 26, 1631.

26. Christe, K. O., Wilson, W. W., and Wilson, R. D., Inorg. Chem., (1989) 28, 675.

27. Christe, K. O. and Schack, C. J., Adv. Inorg. Chem. Radiochem., (1976) 18, 319.

28. Wilson, W. W. and Christe, K. O., Inorg. Chem., (1987) 26, 1573.

29. Christe, K. O., Wilson, W. W., and Wilson, R. D., Inorg. Chem., (1989) 28, 904.

30. Christe, K. O., Wilson, W. W., Schobilgen, G. J., Mercier, H., and Sanders, J., to be published.

31. Schack, C. J. and Christe, K. O., Inorg. Chem., (1988) 27, 4771.

32. The authors are grateful to Dr. W. Jolly for bringing the error to their attention.

33. Christe, K. O., Wilson, W. W., and Schack, C. J., J. Fluorine Chem., (1989) 43, 125.

34. Wilson, W. W. and Christe, K. O., unpublished results.

High-Coordination Number Fluoro- and Oxofluoro-Anions; IF_6O^-, TeF_7^-, IF_8^- and TeF_8^{2-}

Karl O. Christe,*[a] Jeremy C.P. Sanders,[b] Gary J. Schrobilgen*[b] and William W. Wilson[a]

Rocketdyne, a Division of Rockwell International Corporation, Canoga Park, California 91303, U.S.A.;[a] the Department of Chemistry, McMaster University, Hamilton, Ontario L8S 4M1, Canada[b]

Summary- The hypervalent, highly coordinated, high-oxidation state anions IF_6O^-, TeF_7^-, IF_8^- and TeF_8^{2-} have been synthesized in anhydrous CH_3CN using anhydrous $N(CH_3)_4^+F^-$ as the fluoride ion source; the anions have been characterized by NMR spectroscopy and vibrational spectroscopy and represent examples of seven- and eight-coordinate species having symmetries C_{5v} (IF_6O^-), D_{5h} (TeF_7^-) and D_{4d} (IF_8^-, TeF_8^{2-}).

The study of fluoro-anions having coordination numbers higher than six and, in particular, those involving free valence electron pairs, have recently received considerable attention.[1-6] To a large extent, these studies have been greatly facilitated by the development of a synthesis of anhydrous $N(CH_3)_4^+F^-$ [7] and the realization that this salt is an excellent reagent for the preparation high-oxidation state complex fluoro- or oxofluoro-anions. Furthermore, the high solubilities of these $N(CH_3)_4^+$ salts in solvents such as CH_3CN or CHF_3 permit the gathering of valuable structural information through NMR and vibrational studies and the growing of single crystals suitable for X-ray structure determinations.

Our recent success with the preparation of the XeF_5^- anion,[4] the first known example of a pentagonal planar AX_5E_2 (where E stands for a free valence electron pair) species, prompted us to study some closely related iodine and tellurium compounds. Furthermore, there are relatively few examples of main-group species which allow the applicability of the valence shell electron pair repulsion (VSEPR) rules to coordination numbers exceeding six to be tested.[5] In this note, we report on the syntheses and structures of the novel IF_6O^- anion and on the $N(CH_3)_4^+$ salts of TeF_7^-, TeF_8^{2-} and IF_8^-.

The salt, $N(CH_3)_4^+IF_6O^-$, was prepared according to equation (1)

$$N(CH_3)_4^+F^- + IF_5O \xrightarrow[-31\ ^\circ C]{CH_3CN} N(CH_3)_4^+IF_6O^- \qquad (1)$$

by the reaction of anhydrous $N(CH_3)_4^+F^-$ with a threefold excess of IF_5O in dry CH_3CN at -31 °C for 30 min. The solvent and unreacted IF_5O were pumped off at -31 °C leaving behind $N(CH_3)_4^+IF_6O^-$ as a colorless crystalline solid in quantitative yield. According to DSC and pyrolysis data, the compound starts to decompose at about 137 °C with formation of CF_4, COF_2 and IF_4O^- as the major products.

The ^{19}F NMR spectrum of $N(CH_3)_4^+IF_6O^-$ in CH_3CN solution recorded at -40 °C (Figure 1) is consistent with the structure predicted by the VSEPR rules, consisting of a pentagonal bipyramidal structure of C_{5v} symmetry (Structure I) in which the oxygen atom occupies an axial position. The spectrum consists of a doublet at 166.0 ppm, assigned to the equatorial fluorines, and a 1:5:10:10:5:1 sextet at 111.1 ppm, assigned to the axial fluorine trans to oxygen. Both resonances are broadened by partially quadrupole-collapsed spin coupling to ^{127}I ($I = 5/2$). The fluorine-fluorine scalar coupling, $^{2}J(^{19}F_a-F_e)$ = 205 Hz, is very similar in magnitude to those for IF_5O (271 - 280 Hz)[9] and cis-$IO_2F_4^-$ (204 Hz in CH_3CN).[10]

The vibrational spectra of IF_6O^- are also in excellent agreement with symmetry C_{5v}. The assignments were made by comparison with the related IF_7 molecule (see Table 1) and XeF_5^- anion.[4]

The reactions between TeF_6 and alkali metal fluorides have been reported previously, although definitive characterization of the products was never achieved.[11,12] The reactions of TeF_6 with CsF and RbF suspended in C_6F_6 resulted in products approaching the limiting compositions $CsF \cdot TeF_6$ and $2RbF \cdot TeF_6$, respectively.[12] Vibrational studies on these materials were tentatively interpreted as indicating D_{5h} and D_{4d} structures for TeF_7^- and TeF_8^{2-}, respectively. However, since both compounds decomposed in solution, a fuller characterization of their nature was precluded.

The preparation of $N(CH_3)_4^+TeF_7^-$ was similar to that for the IF_6O^- salt except that only a 5% excess of TeF_6 was allowed to react with $N(CH_3)_4^+F^-$ according to equation (2). The solvent and an excess of TeF_6 were pumped off at room temperature leaving a white solid in quantitative yield.

$$N(CH_3)_4^+F^- \quad + \quad TeF_6 \quad \xrightarrow[-40\ °C]{CH_3CN} \quad N(CH_3)_4^+TeF_7^- \qquad (2)$$

The room temperature ^{125}Te NMR spectrum of $N(CH_3)_4^+TeF_7^-$ in CH_3CN consists of a 1:7:21:35:35:21:7:1 octet centered at 327.4 ppm (Figure 2). The octet fine structure arises from the one-bond spin-spin coupling between the central ^{125}Te and the ^{19}F ligands [$^1J(^{125}Te-^{19}F)$ = 2876 Hz] and is in accord with a TeF_7^- anion structure in which all seven fluorines are rendered equivalent on the NMR time scale by a facile intramolecular exchange process. The ^{19}F NMR spectrum is also consistent with the TeF_7^- anion undergoing a fluxional process in solution, and consists of a single environment (16.1 ppm) and natural abundance satellite spectra arising from $^1J(^{123}Te-^{19}F)$ = 2385 Hz and $^1J(^{125}Te-^{19}F)$ = 2876 Hz. Under high resolution at an external field strength of 11.744 T, the central line displays the isotopic shift pattern arising from the natural abundance spinless tellurium isotopes corresponding to the fluorines of the ^{130}Te, ^{128}Te, ^{126}Te, ^{124}Te and ^{122}Te isotopomers, with each isotopomer shifted successively to higher frequency of $^{130}TeF_7^-$ by 0.004 ppm. Earlier NMR studies have shown that the isoelectronic IF_7 molecule also undergoes rapid intramolecular exchange and gives rise to a single fluorine environment in the room temperature ^{19}F NMR spectrum with partially quadrupole-collapsed fine structure arising from $^1J(^{127}I-^{19}F)$.[13]

The vibrational spectra of TeF_7^- have been assigned by analogy with those of the isoelectronic IF_7 molecule (Table 1) and are in agreement with a pentagonal bipyramidal structure of D_{5h} symmetry (Structure II). In general, the TeF_7^- frequencies are shifted to lower frequencies relative to those of IF_7, in accordance with the formal negative charge of TeF_7^-.

The syntheses of $Cs^+IF_8^-$,[14] $NO^+IF_8^-$ [14,15] and $NO_2^+IF_8^-$ [15] have previously been reported, and the ionic nature of these salts was established by the observation of the vibrational bands characteristic for NO^+ and NO_2^+.[14,15] Although partial Raman[14] and infrared spectra[15] had been reported for IF_8^-, no conclusions could be drawn from these data about the exact structure of this interesting octacoordinated anion. To allow a better characterization of the IF_8^- anion, we have prepared the new $N(CH_3)_4^+IF_8^-$ salt and its isoelectronic tellurium analog, TeF_8^{2-}, by the reaction of $N(CH_3)_4^+F^-$ with excess IF_7 and a stoichiometric amount of $N(CH_3)_4^+TeF_7^-$, respectively.

$$N(CH_3)_4^+F^- + IF_7 \xrightarrow[-31\ ^\circ C]{CH_3CN} N(CH_3)_4^+IF_8^- \qquad (3)$$

$$N(CH_3)_4^+F^- + N(CH_3)_4^+TeF_7^- \xrightarrow[0\ ^\circ C]{CH_3CN} [N(CH_3)_4^+]_2TeF_8^{2-}\downarrow \qquad (4)$$

For reaction (3) the solvent and unreacted IF_7 were pumped off at -22 °C and 0 °C, respectively, leaving behind colorless $N(CH_3)_4^+IF_8^-$ in quantitative yield. In the case of reaction (4), $[N(CH_3)_4^+]_2TeF_8^{2-}$ was isolated in admixture with ca. 20 - 30 % $N(CH_3)_4^+TeF_7^-$. The $[N(CH_3)_4^+]_2TeF_8^{2-}$ salt has a strong tendency to dissociate in CH_3CN, thus far preventing the preparation of a sample containing only the TeF_8^{2-} anion. At room temperature, the TeF_8^{2-} anion is highly dissociated into TeF_7^- and F^-, resulting in rapid solvent attack by F^- [16] and formation of HF_2^- anion. In the presence of a five-fold excess of $N(CH_3)_4^+F^-$ at -5 °C, where the rate of F^- attack on the solvent is slow, only TeF_7^- and F^- were observed in the ^{19}F NMR spectrum, but owing to the insolubility of $[N(CH_3)_4^+]_2TeF_8^{2-}$, no resonance attributable to TeF_8^{2-} anion could be observed. The $N(CH_3)_4^+IF_8^-$ salt is a crystalline solid which, according to DSC data, is stable up to about 110 °C where it undergoes exothermic decomposition.

The IF_8^- and TeF_8^{2-} anions possess eight fluorine ligands and no free central atom valence electron pair. Their structures could therefore be a cube of symmetry O_h, which is unlikely owing to steric interactions,[8] a dodecahedron of symmetry D_{2d} or a square antiprism of symmetry D_{4d} (Structures III and IV).[17-20] Distinction among these three possibilities was made by vibrational spectroscopy. The dodecahedral structure is expected to give rise to two polarized stretching modes and four deformation modes (two polarized; two depolarized) exclusively in the Raman. The infrared bands are mutually nonexclusive and comprise four stretching modes and five deformation modes which are all depolarized in the Raman. All Raman and infrared bands observed for IF_8^- and TeF_8^{2-} are mutually exclusive, thereby eliminating D_{2d} symmetry. For the cubic O_h structure, two stretching modes are expected (one polarized; the other depolarized) and two depolarized deformation modes in the Raman, as well as one stretching and one deformation mode in the infrared. All these modes should be mutually exclusive.[18] For the square antiprismatic D_{4d} structure, one polarized and two depolarized stretching modes are expected as well as one polarized and three depolarized deformation modes in the Raman. In the infrared, two stretching and three deformation modes are expected, which again should be mutually exclusive.[17,19,20] Although the full number of fundamentals for D_{4d} was not observed (see Table 2), probably because of either low relative intensities or accidental coincidences, the observation of a polarized Raman deformation band at 462 cm^{-1} and of at least two infrared active deformation modes at 410 and 314 cm^{-1}, respectively, eliminate the alternative O_h symmetry and establish the square antiprismatic D_{4d} structure for IF_8^-. It was not possible to obtain polarization data on TeF_8^{2-} owing to the insolubility of the salt and its tendency to dissociate in CH_3CN. However, the vibrational spectra of TeF_8^{2-} can be assigned by their close analogy to those of IF_8^- (Table 2) and it may be concluded that TeF_8^{2-} also possesses a square antiprismatic structure.

X-ray crystal structure determinations on these and other closely related anions are underway both in our laboratories and in an independent effort by Prof. K. Seppelt and coworkers at the Freie Universität, Berlin.

Acknowledgements. The authors thank U.S. Air Force Astronautics Laboratory, Edwards AFB, California (K.O.C. and G.J.S.), the U.S. Army Research Office (K.O.C.) and the Natural Sciences and Engineering Research Council of Canada (G.J.S.) for financial support; and Prof. K. Seppelt for bringing his X-ray structural studies to our attention.

References

1. W.W. Wilson and K.O. Christe, Inorg. Chem., 1989, 28, 4172.
2. K.O. Christe and W.W. Wilson, Inorg. Chem., 1989, 28, 3275.
3. K.O. Christe, W.W. Wilson, R.V. Chirakal, J.C.P. Sanders and G.J. Schrobilgen, Inorg. Chem., 1990, 29, 3506.
4. K.O. Christe, E.C. Curtis, D.A. Dixon, H.P. Mercier, J.C.P. Sanders and G.J. Schrobilgen, J. Am. Chem. Soc., in press.
5. A.R. Mahjoub, A. Hoser, J. Fuchs and K. Seppelt, Angew. Chem. Int. Ed.

Engl., 1989, 28, 1526.

6. A.R. Mahjoub, B. Nuber and K. Seppelt, private communication.

7. K.O. Christe, W.W. Wilson, R.D. Wilson, R. Bau, J. Feng, J. Am. Chem. Soc., 1990, 112, 7619.

8. R.J. Gillespie and I. Hargittai, "The VSEPR Model of Molecular Geometry," Allyn and Bacon, Boston, 1991.

9. R.J. Gillespie and J.W. Quail, Proc. Chem. Soc., 1963, 278; M. Brownstein, R.J. Gillespie and J.P. Krasznai, Can. J. Chem., 1978, 56, 2253.

10. K.O. Christe, R.D. Wilson and C.J. Schack, Inorg. Chem., 1981, 20, 2104.

11. E.L. Muetterties, J. Am. Chem. Soc., 1957, 79, 1004.

12. H. Selig, S. Sarig and S. Abramowitz, Inorg. Chem., 1974, 13, 1508.

13. R.J. Gillespie and J.W. Quail, Can. J. Chem., 1964, 42, 2671; E.L. Muetterties and K.J. Packer, J. Am. Chem. Soc., 1964, 86, 293.

14. C.J. Adams, Inorg. Nucl. Chem. Lett. 1974, 10, 831.

15. F. Seel and M.J. Pimpl, J. Fluorine Chem. 1977, 10, 413.

16. K.O. Christe and William W. Wilson, J. Fluorine Chem. 1990, 47, 117.

17. A. Beuter, W. Kuhlmann and A. Sawodny, J. Fluorine Chem. 1975, 6, 367.

18. C.W.F.T. Pistorius, Bull. Soc. Chim. Belg. 1959, 68, 630.

19. H.L. Schläfer and H.F. Wasgestian, Theoret. Chim. Acta, 1963, 1, 369.

20. K.O. Hartman and F.A. Miller, Spectrochim. Acta, Part A, 1968, 24A, 669.

Figure Captions

Figure 1. The ^{19}F NMR spectrum of $N(CH_3)_4^+IF_6O^-$ recorded at 471.599 MHz in CH_3CN solvent at -40 °C.

Figure 2. The ^{125}Te NMR spectrum of $N(CH_3)_4^+TeF_7^-$ recorded at 157.792 MHz in CH_3CN solvent at 30 °C.

Table 1. Vibrational Frequencies (cm^{-1}) and Tentative Assignments for IF_6O^-, IF_7 and TeF_7^-

		IF_6O^- (C_{5v})[a]			IF_7 (D_{5h})[b]	TeF_7^- (D_{5h})[a]
A_1	ν_1 ν I=O	873 (vs, IR; 5.3, R (p))				
	ν_2 ν IF ax	649 (s, IR; 8.8 R (p))	A_1'	ν_1 ν sym MF_2 ax	675 (2.0, R (p))	597 (2.6, R)
	ν_3 ν sym IF_5	584 (10, R (p))		ν_2 ν sym MF_5	629 (10, R (p))	640 (10, R)
			A_2''	ν_3 ν asym MF_2 ax	746 (s, IR)	695 (vs, IR)
	ν_4 δ umbrella IF_5	359 (s, IR)		ν_4 δ umbrella MF_5	363 (s, IR)	332 (s, IR)
E_1	ν_5 ν asym IF_5	585 (vs, IR)	E_1'	ν_5 ν asym MF_5	672 (vs, IR)	625 (vs, IR)
	ν_6 δ wag I=O	457 (4.9, R)		ν_6 δ scissoring MF_2 ax	425 (vs, IR)	384 (vs, IR)
	ν_7 δ wag IF ax	405 (vs, IR)				
	ν_8 δ asym IF_5 in plane	260 (s, IR; 0.2, R)		ν_7 δ asym MF_5 in plane	257 (w, IR)	c
			E_1''	ν_8 δ wag MF_2 ax	308 (0.6, R)	299 (0.6, R)
E_2	ν_9 ν asym IF_5	530 (0.4, R)	E_2'	ν_9 ν asym MF_5	509 (0.9, R)	458 (1.6, R)
	ν_{10} δ scissoring IF_5 in plane	341 (6.2, R)		ν_{10} δ scissoring MF_5 in plane	342 (0.6, R)	326 (0.7, R)
	ν_{11} δ pucker IF_5	d	E_2''	ν_{11} δ pucker MF_5	d	d

a Spectra recorded for the $N(CH_3)_4^+$ salts at 25 °C.

b Frequencies are taken from H.H. Eysel and K. Seppelt, J. Chem. Phys., 1972, 56, 5081. A number of modes have been reassigned so that they are consistent with the corresponding assignments for XeF_5^- (ref. (4)), which have been confirmed by a force constant analysis and theoretical calculations

c Mode not observed.

d Inactive in both the infrared and Raman spectra.

Table 2. Vibrational Frequencies (cm^{-1}) and Assignments for IF_8^- in $N(CH_3)_4^+IF_8^-$ in Point Group D_{4d}

Raman				Infrared (solid 25 °C)		Assignment in D_{4d}
IF_8^-			TeF_8^{2-}	IF_8^-	TeF_8^{2-}	
solid		CH_3CN sol'n				
25 °C	-142 °C					
660 (0+)	660 (0+)					ν_{12} (E_3)
				590 vs, br	558 vs	ν_4 (B_2)
						ν_6 (E_1)
587 (10)	595 (10) 588 (6.5)	590 (10) p	582 (10)			ν_1 (A_1)
550 (0.3)	550 (0.5)	550 (0+) dp	490 (0.2), br			ν_9 (E_2)
463 (1.8)	463 (1.9)	462 (0.5) p	408 (1.9)			ν_2 (A_1)
				410 s	375 vs	ν_5 (B_2)
						ν_8 (E_1)
411 (0.7)	419 (0.9) 410 (1.4)	410 sh[a]	388 (1.8)			ν_{10} (E_2)
	380 (0+)[b]		325 (0.3)			ν_{13} (E_3)
				314 m	265 w	ν_7 (E_1)

[a] Shoulder on strong CH_3CN solvent band.

[b] This band could possibly be due to the $N(CH_3)_4^+$ cation.

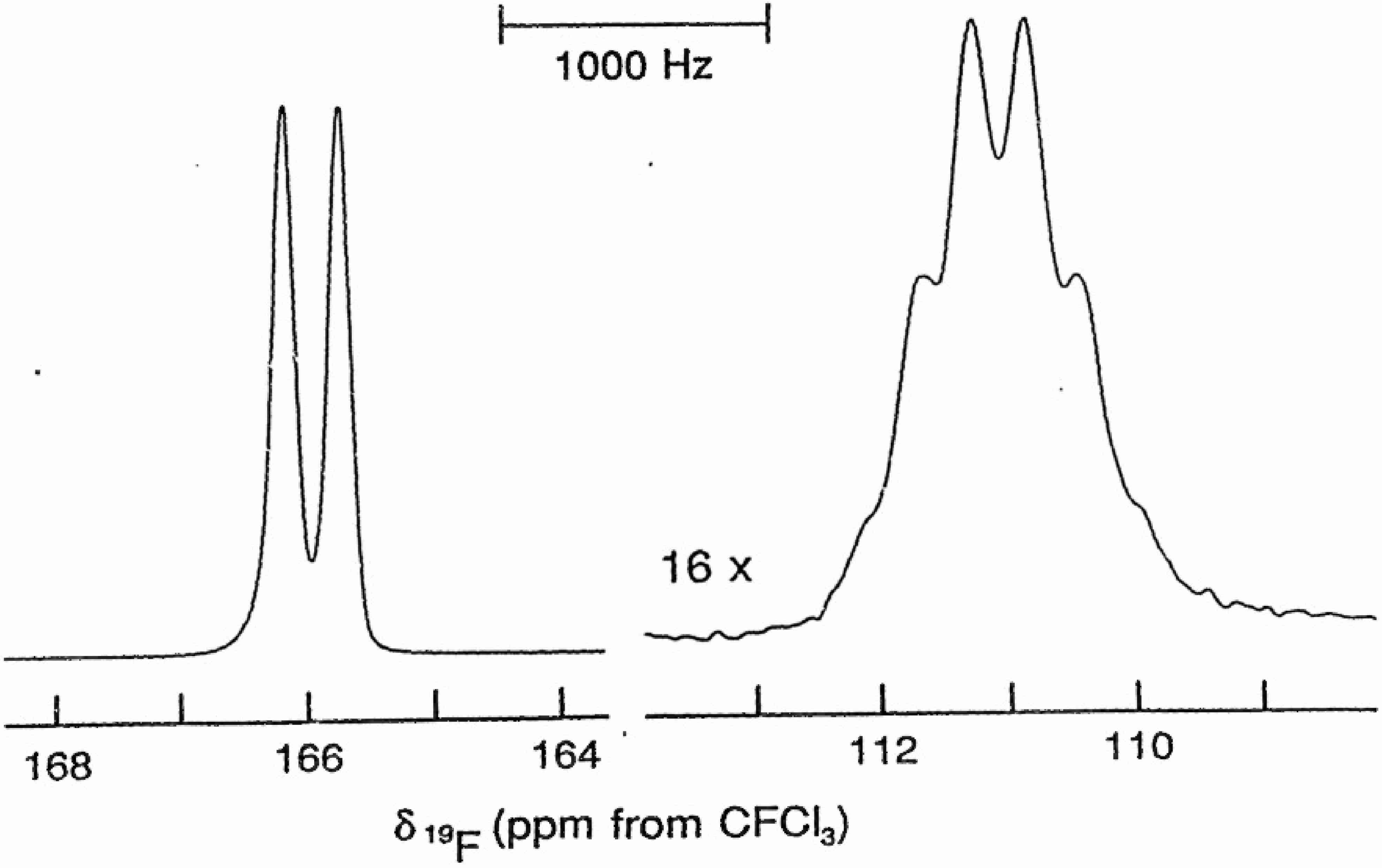
1000 Hz
16 x
168
166
164
112
110
δ 19F (ppm from CFCl3)

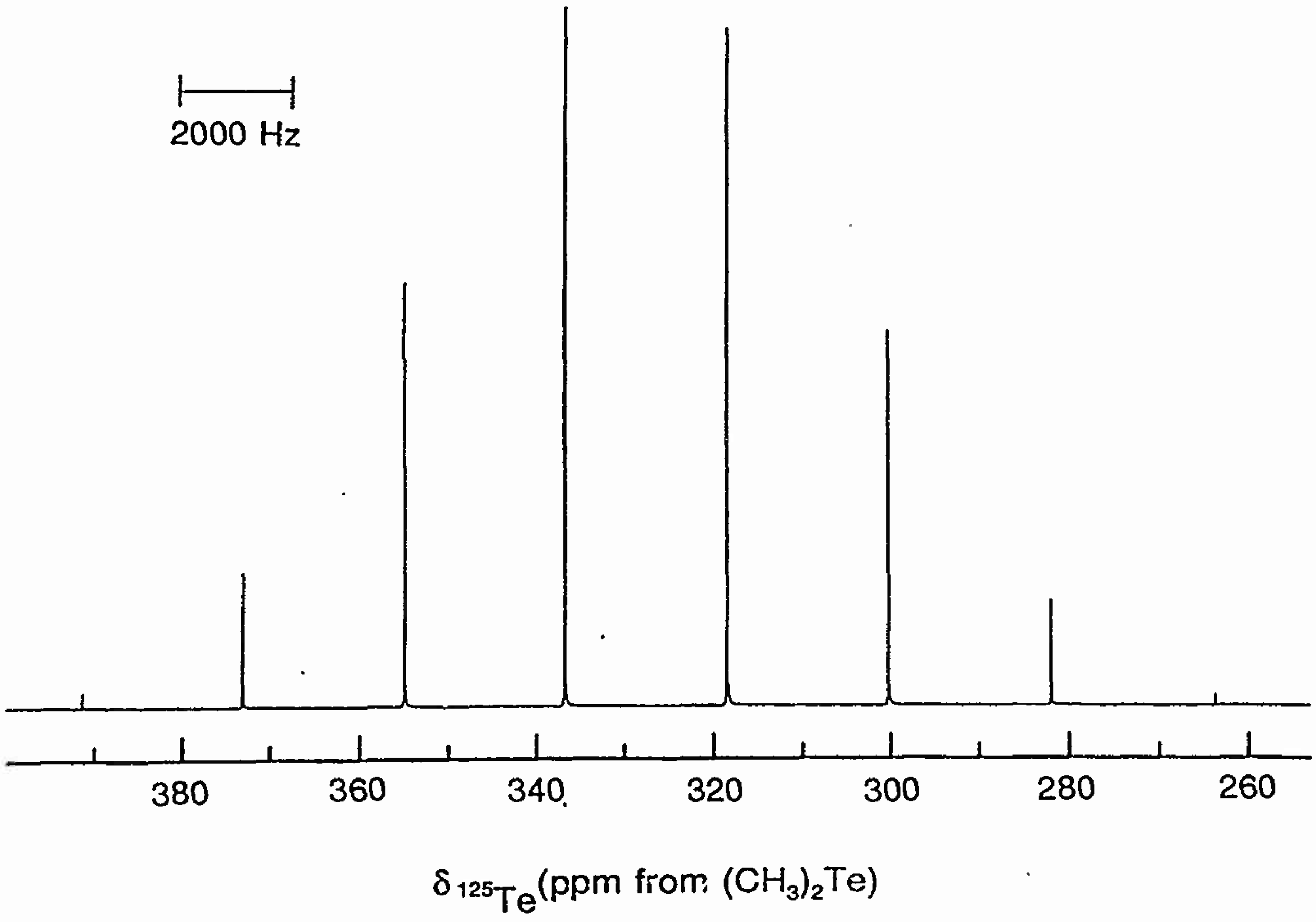
2000 Hz
380
360
340
320
300
280
260
δ 125Te(ppm from (CH3)2Te)

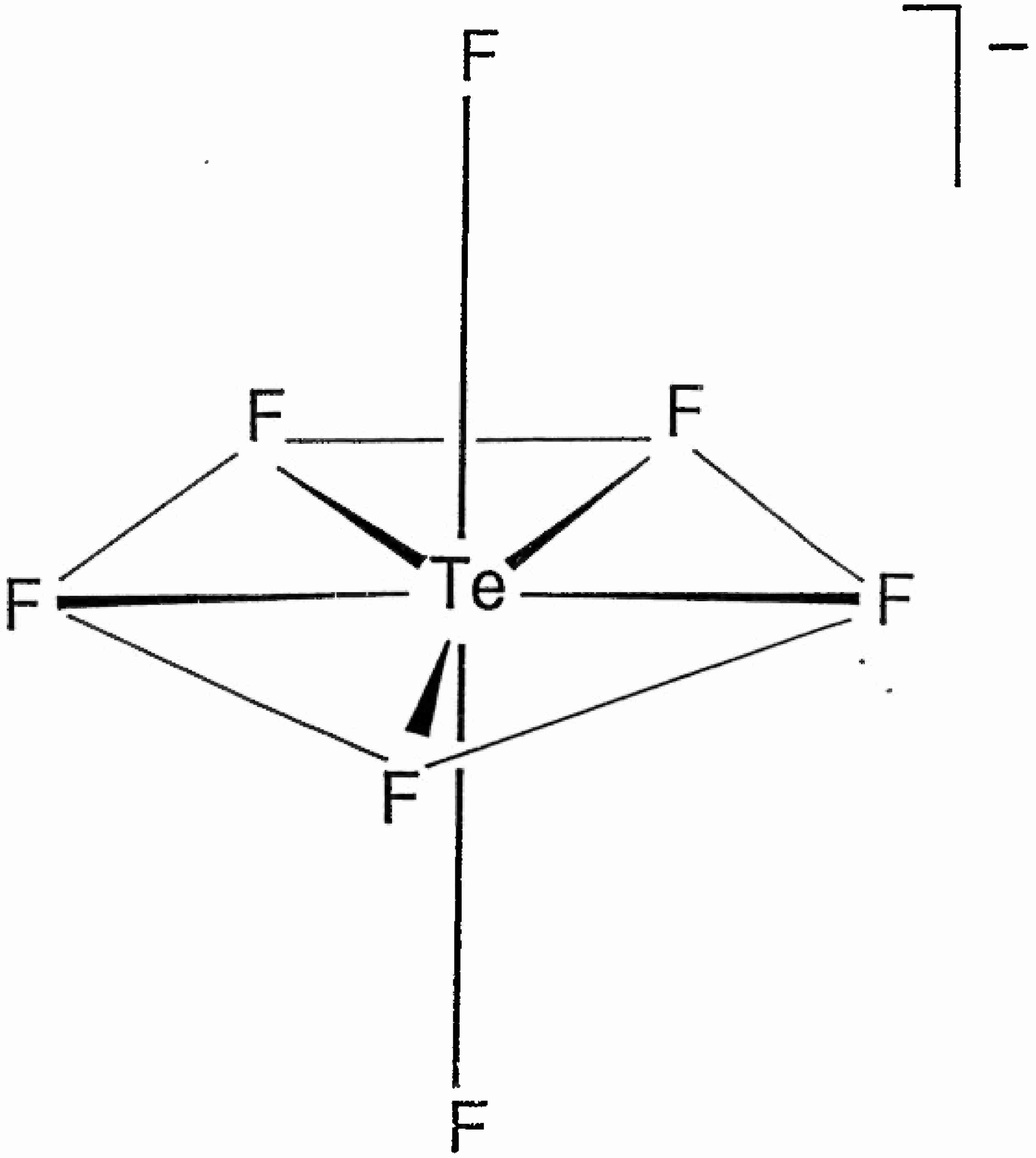
F
−
F
F
F
Te
F
F
F

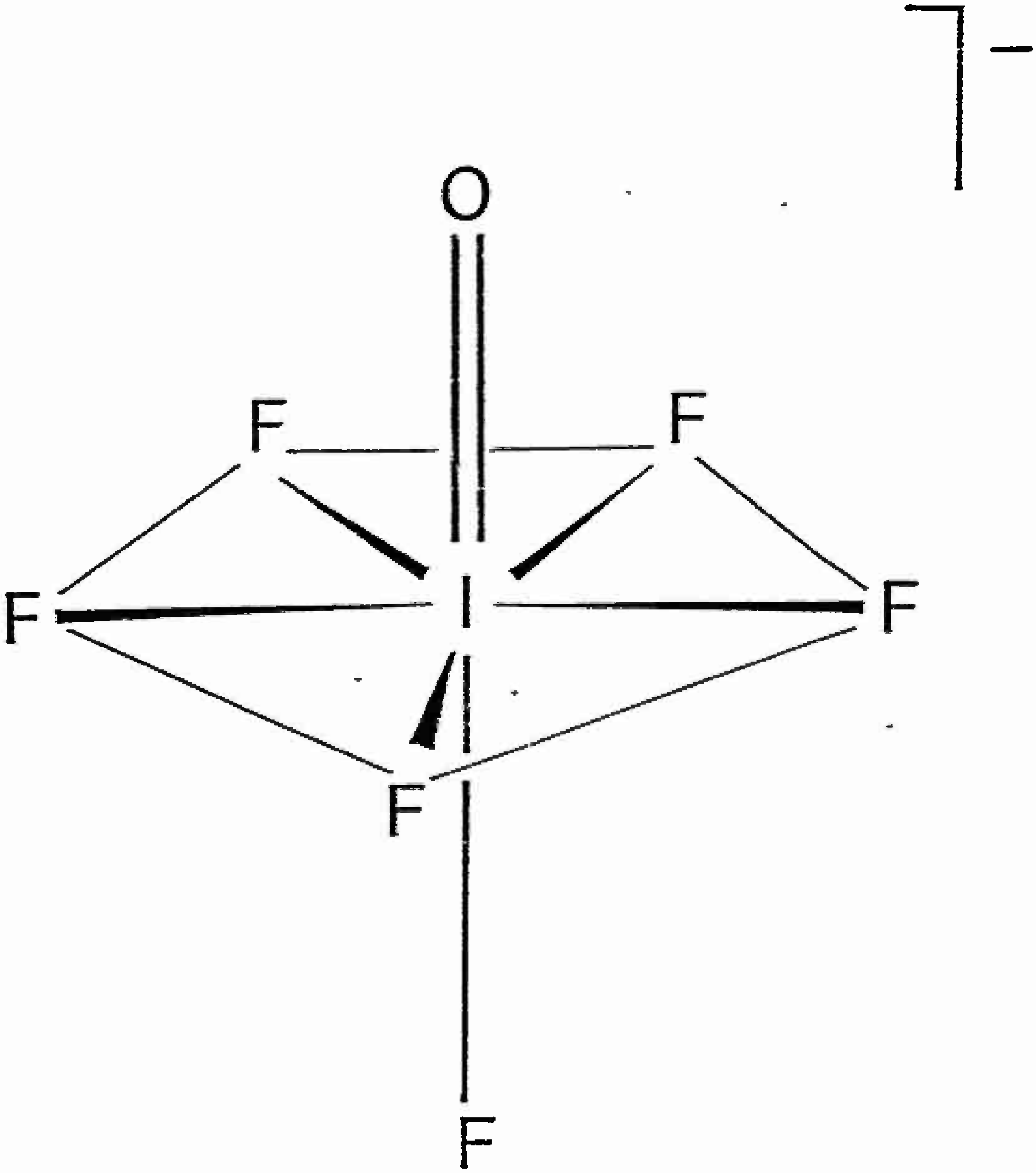

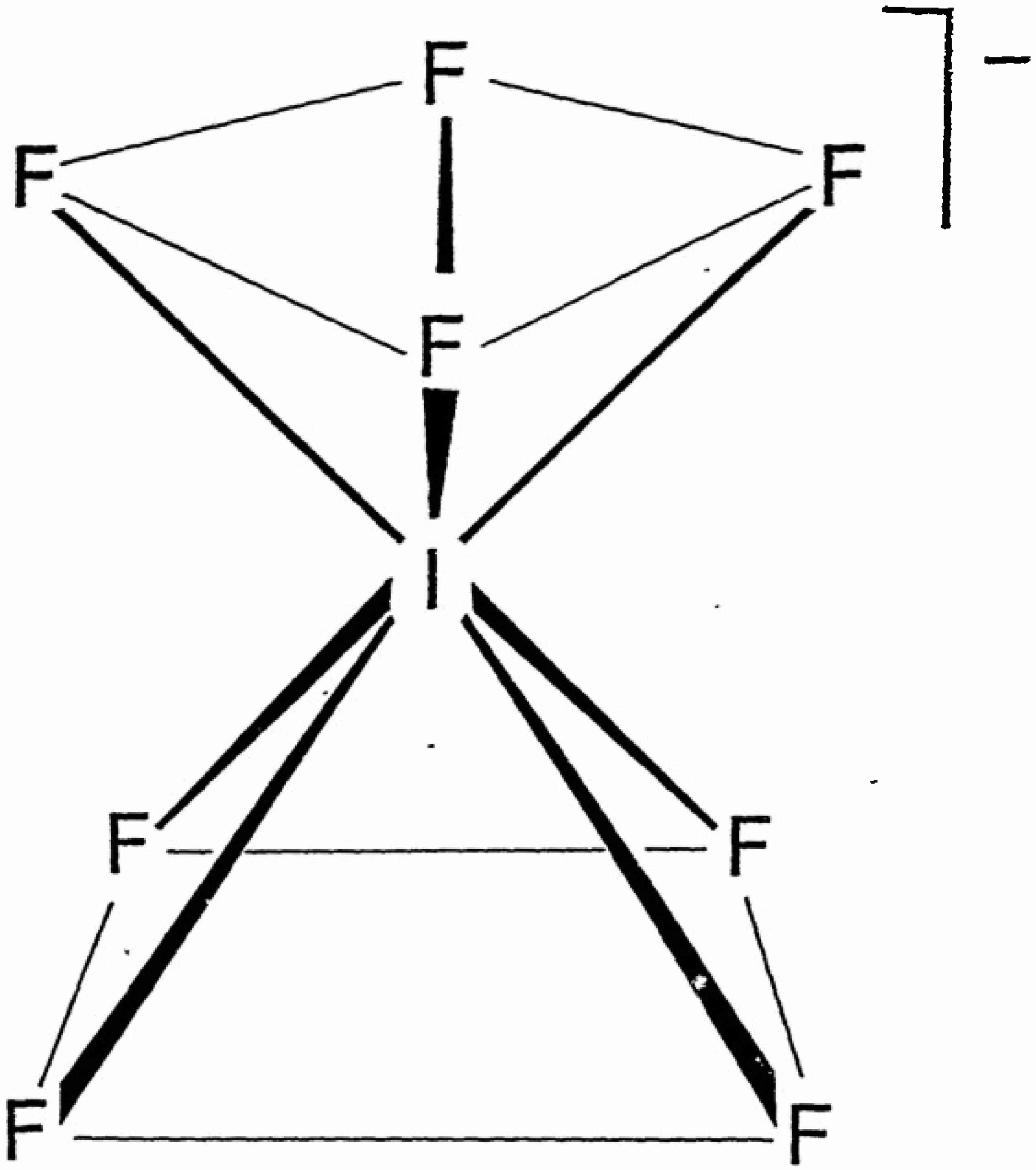
F
F
F
F
I
F
F
F
F
−

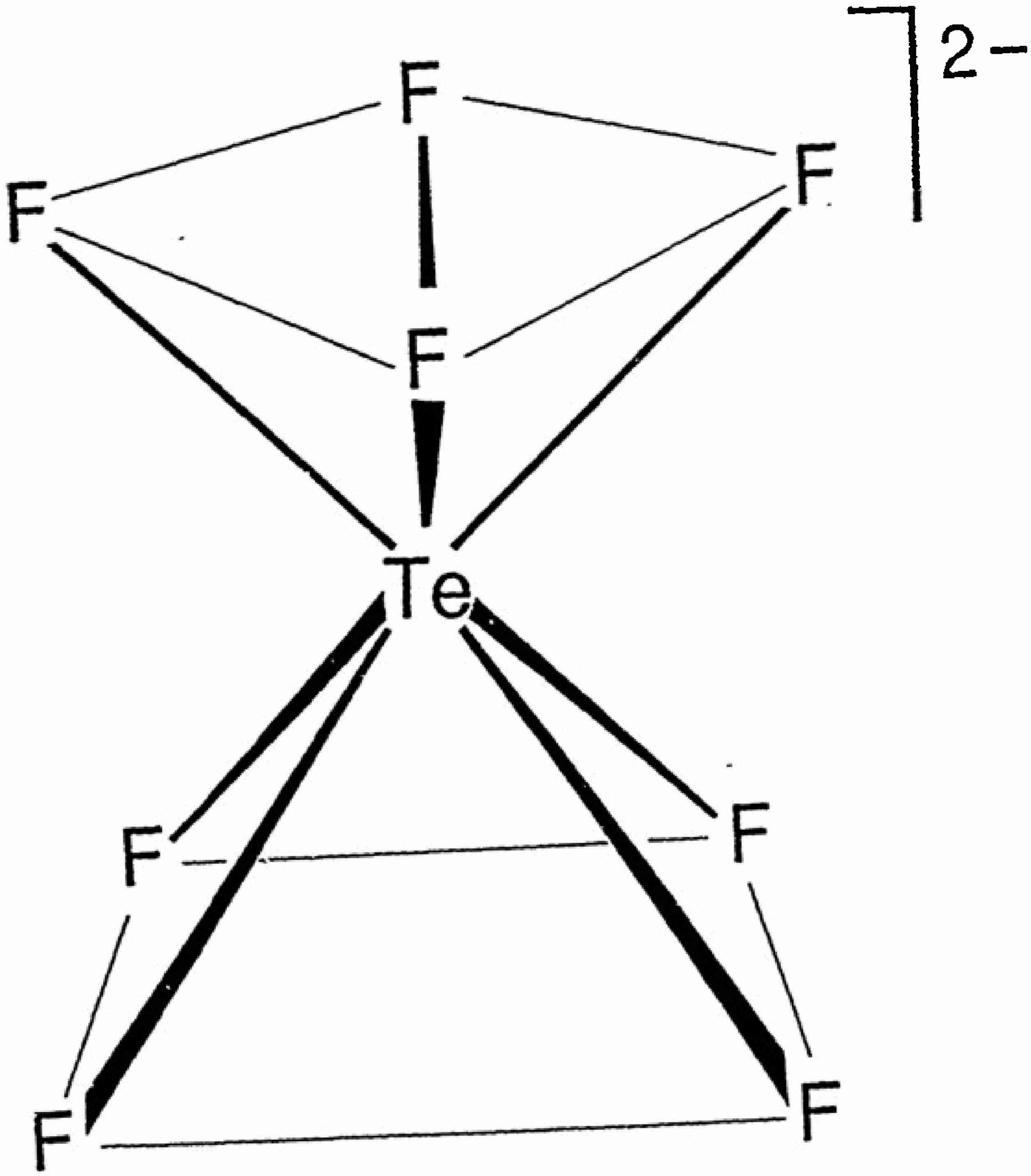
2-
F
F
F
F
Te
F
F
F
F

APPENDIX R

A Quantitative Scale for the Oxidizing Strength of Oxidative Fluorinators

Karl O. Christe*[†] and David A. Dixon*[††]

Contributions from Rocketdyne, A Division of Rockwell International Corporation,
Canoga Park, California, 91303,
and
The Central Research and Development Department, E.I. du Pont de Nemours and Company, Inc.,
Experimental Station, Wilmington, Delaware, 19880

ABSTRACT

A quantitative scale for the oxidizing strength of oxidative fluorinators has been developed for the first time. This scale is based on relative F^+ detachment energies which were obtained by local density functional calculations and is anchored to its F^+ zero point by an experimental value for KrF^+. The oxidizing strength of 27 oxidizers was determined in this manner. The results were analyzed and shown to be consistent with previous qualitative experiments. The heats of formation of these oxidizers were also determined from their F^+ detachment energy values.

[†] Rocketdyne

[††] du Pont

INTRODUCTION

The synthesis of fluorine containing strong oxidizers generally requires powerful fluorinating agents. In this context, the question as to which agent is most powerful and which agent can oxidize a given substrate frequently arises. The ranking of these fluorinating agents according to their strength is very difficult. Direct electrochemical measurements of their oxidation potentials are not possible because the latter generally exceed the decomposition voltages of the available solvents. Therefore, no oxidizer strength scales exist at the present time, and the only data available are isolated observations[1-4] that some compounds can oxidize certain substrates while others cannot. Frequently, however, a lack of reaction is due to the choice of unfavorable reaction conditions or high activation energies and not necessarily to an insufficient oxidation potential, a thermodynamic measure.

Strong oxidizers can be separated into two main classes. The first one consists of one electron oxidizers such as PtF_6 or UF_6, and the second one of oxidative fluorinators such as KrF^+, ClF_6^+ or N_2F^+. The case of one electron oxidizers has previously been analyzed by Bartlett and is best exemplified by his classic example of the reaction of PtF_6 with O_2 (1).[5]

$$O_2 + PtF_6 \rightarrow O_2^+PtF_6^- \qquad (1)$$

The reaction enthalpy, ΔH°, of (1) can be derived from the Born-Haber cycle given by Figure 1 where IP, EA, and U_L stand for the first ionization potential of O_2, the electron affinity of PtF_6, and the lattice

$$\begin{tikzcd}
O_{2(g)} \arrow[d, "IP"] & + & PtF_{6(g)} \arrow[d, "EA"] \arrow[r, "\Delta H^\circ"] & O_2^+PtF_6^-{}_{(s)} \\
O_2^+{}_{(g)} & + & PtF_6^-{}_{(g)} \arrow[ur, "U_L"'] &
\end{tikzcd}$$

Figure 1. Born-Haber Cycle for a Typical One-Electron Oxidation Reaction

energy of solid $O_2^+PtF_6^-$, respectively. Neglecting entropy changes, $\Delta H°$ must be negative for the reaction to occur spontaneously. Since the ionization potentials of the substrates are usually known and the lattice energies of the solid products can be estimated quite accurately, the occurrence or lack of spontaneous reaction with different substrates was used[4] to place upper and lower limits on the electron affinity of the oxidizing species. This method allows one to estimate rough electron affinity values which in turn can be taken as a measure for the oxidizing power of these one-electron oxidizers. Since these electron transfer reactions do not involve significant activation energies, the "go - no go" reaction approach works rather well.

The case of oxidative fluorinators, such as KrF^+or N_2F^+, is more complex and has not been analyzed previously. The oxidizer strengths of these species is not a simple function of the electron affinity or ionization potential of the atom or molecule to which the formal "F^+" unit is attached. This was exemplified by a recent qualitative study[1] which showed that N_2F^+ (IP_{N_2} = 360.6 kcal mol^{-1})[6] is a weaker oxidative fluorinator than KrF^+ (IP_{Kr} = 324.2 kcal mol^{-1}).[6] Therefore, we have undertaken efforts to analyze this case and to define, if possible, a quantitative oxidizer strength scale.

RESULTS AND DISCUSSION

Born-Haber Cycles for Oxidative Fluorination Reactions

The case of oxidative fluorination reactions is more complex than that of one-electron oxidations. In addition to the transfer of a positive charge, an existing bond must be broken and a new one must be formed. Furthermore, the bond breaking can require a substantial activation energy and, therefore, complicates experiments aimed at the determination of relative oxidizer strengths based on the observation or lack of observation of a reaction.

Consider the reaction between N_2F^+ and Xe in HF solution[1] as a typical example of an oxidative fluorination reaction. Assuming that the solvation energies of N_2F^+ and Xe are about the same as those of

XeF^+ and N_2, this reaction can be expressed by equation (2). Figure 2 shows two Born-Haber cycles, (2a) and (2b), which can be used to describe reaction (2).

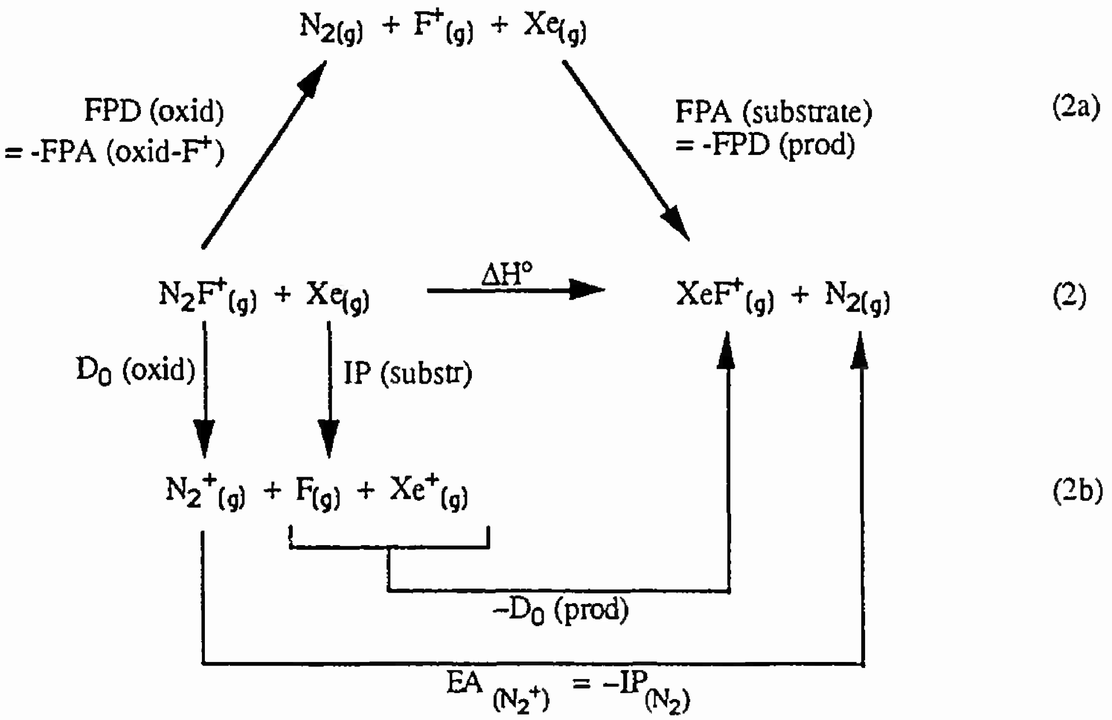

Figure 2. Two Born-Haber Cycles Which can be Used for the Description of a Typical Oxidative Fluorination Reaction

As in the case of the one-electron oxidations, ΔH° must be negative for a spontaneous reaction and, for the cycles (2a) and (2b), is given by (3a) and (3b), respectively.

$$\Delta H^\circ = \text{FPA (subst)} - \text{FPA (oxid-F}^+\text{)} \qquad (3a)$$

$$\Delta H^\circ = \text{I (substr)} - \text{I (oxid-F}^+\text{)} + D_0 \text{ (oxid)} - D_0 \text{ (prod)} \qquad (3b)$$

where FPA = F^+ affinity, FPD = F^+ detachment energy, IP = first adiabatic ionization potential, D_0 = bond dissociation energy, and EA = electron affinity. At the present time, neither cycle (2a) nor (2b) seemed useful for the determination of reliable ΔH° values since the F^+ affinities and bond dissociation energies are generally unknown.

Calculations

If one considers reaction (2) as the transfer of F^+ from one compound to another, it is very similar to the transfer of a proton from one base to another (reaction 4).

$$N_2H^+_{(g)} + Xe_{(g)} \longrightarrow XeH^+_{(g)} + N_{2(g)} \qquad (4)$$

Such proton transfer reactions can be calculated quite accurately by molecular orbital methods for both relative values and for absolute values.[7] The agreement with experiment for proton transfer processes is usually excellent if one employs good geometries and if adequate basis sets with some consideration of the correlation energy are included in the calculations.

Such a theoretical model could also be employed for the calculation of relative FPA's. However, most of the compounds under consideration as strong oxidants contain atoms predominantly from the right hand side of the periodic table and, contrary to H^+, F^+ has a significant number of electrons. Thus, some method is needed which, even for describing the geometries, includes correlation effects. Since there are a significant number of compounds, all of which need to have their geometries optimized, one also requires a computationally efficient method. Rather than using traditional Hartree-Fock methods (scaling as N^4 with N = number of basis functions) including correlation corrections (scaling as N^m, $m \geq 5$), we chose the local density functional (LDF) method (scaling as N^3).[8]

The LDF method is based on the Hohenberg-Kohn theorem[9] which states that the total energy E_t is a functional of the charge density ρ as follows:

$$E_t[\rho] = T[\rho] + U[\rho] + E_{XC}[\rho] \qquad (5)$$

where T is the kinetic energy of the non-interacting electrons of density ρ, U is the classical Coulomb electrostatic energy and E_{XC} includes all of the manybody contributions to the energy. The first two terms can be evaluated using straight-forward techniques. The most important contributions to E_{XC} are the exchange energy and the correlation energy and it is in the final term where the local density approximation is introduced. A good approximation for the final term is derived from the exchange-correlation energy of the uniform electron gas with the assumption that the charge density varies slowly on the scale of exchange and correlation effects. The form of the exchange-correlation energy employed in our calculations is that of von Barth and Hedin.[10]

The calculations were done with the program DMol[10] on a CRAY-YMP computer system. DMol employs numerical functions for the atomic basis sets. These atomic basis sets are exact spherical solutions to the density functional equations. All of the calculations were done with a double numerical basis-set augmented by d ($l = 2$) polarization functions. Because exact numerical solutions are employed, this basis set is of higher quality than a normal molecular orbital basis set of the same size. Furthermore, basis set superposition errors should be minimized because of the quality of the basis set.

The various integrals required for the solution of equation (5) need to be evaluated on a grid due to our use of numerical basis functions.[12] The number of radial points is given by

$$N_R = 1.2 \cdot 14\,(Z + 2)^{1/3} \tag{6}$$

where Z is the atomic number and the maximum distance for any function is 12 a.u. The angular integration points N_0 are generated at the NR radial points to form shells around each nucleus with N_0 ranging from 14 to 302 depending on the density. Fitting functions for the spherical harmonics were all done with an angular momentum number $\ell' = \ell + 1 = 3$.

Geometries were optimized by using analytic gradient methods.[13, 14] Because numerical methods are used, the error in atomic coordinates determined by the optimization are on the order of 0.001 Å which gives bond lengths and angles with errors at least an order of magnitude smaller than the differences between calculated and experimental values. The spin state of each structure is a singlet except for those of O_2 and F^+ which are triplets.

Oxidizer Strength Scale

Although a knowledge of the relative FPA's allows the prediction of whether a certain reaction is thermodynamically feasible and which oxidizer is stronger with respect to another one, it provides only a relative oxidizer strength scale. To obtain an absolute scale, one must identify the thermodynamic property governing the oxidizer strength, define a zero point for the scale, and then anchor the relative oxidizer strength values derived from the LDF calculations to the chosen zero point by an experimentally known number since LDF theory overestimates absolute binding energies.

According to the Born-Haber cycle (2a) and equation (3a) the reaction enthalpy ΔH° equals the difference between the F^+ affinities of the substrate and of the oxidizer minus F^+. Hence, F^+ affinities are a useful criterion for an oxidizer strength scale. Since the F^+ affinity (FPA) of a substrate equals the negative value of the F^+ detachment energy (FPD) of the corresponding product, equation (3a) can be rewritten as (7),

$$\Delta H^\circ = \text{FPD (oxid)} - \text{FPD (prod)} \qquad (7)$$

and an oxidative fluorination reaction can be considered as the formal transfer of an F^+ cation from an oxidizer to a substrate. Since the F^+ detachment energy for F^+ itself obviously is zero, F^+ is the ideal zero point for an oxidizer strength scale based on F^+ detachment energies. On this scale, then, increasing FPD values signify decreasing oxidizer strength.

The third objective, i.e. the anchoring of the relative FPD values to the F^+ zero point, was accomplished by calculating the F^+ affinity of Kr from experimental data. From the known heat of formation of KrF_2, the appearance potential of KrF^+ from KrF_2, and the first adiabatic ionization potential of Kr, the bond energy and heat of formation of gaseous KrF^+ have been estimated[15] to be 37 and 303.1 kcal mol^{-1}, respectively, as shown by the right half of (8).

$$\begin{array}{lccccc} & \text{Kr} + \text{F}^+ & \xrightarrow{\text{FPA} = -118.9} & \text{KrF}^+ & \xleftarrow{D_{\text{KrF}^+} = -37} & \text{Kr}^+ + \text{F} \\ \Delta H_f^\circ & 0 \quad 422.0 & & 303.1 & & 324.2 \quad 18.9 \text{ kcal mol}^{-1} \end{array} \qquad (8)$$

From the known heats of formation of gaseous KrF^+ and F^+,[6] the F^+ affinity of Kr can then be estimated as -118.9 kcal mol^{-1}, as shown by the left half of (8). The combination of this experimentally derived value with the F^+ affinity differences obtained by our LDF calculations permits the construction of the absolute oxidizer strength scale given in Table 1.

The quality of the values in Table 1 was crosschecked for XeF^+. Using the previously published experimental data,[15] the FPD of XeF^+ was estimated (9) as 170.0 kcal mol^{-1}, in good agreement with our computed value of 167.8 kcal mol^{-1} given in Table 1.

$$\begin{array}{llllll} & \mathrm{Xe} + \mathrm{F}^+ & \xrightarrow{\mathrm{FPA} = -170.0} & \mathrm{XeF}^+ & \xleftarrow{D_{\mathrm{XeF}^+} = -48} & \mathrm{Xe}^+ + \mathrm{F} \\ \Delta Hf^\circ & 0 \quad 422.0 & & 252.0 & & 281.1 \quad 18.9\ \mathrm{kcal\ mol^{-1}} \end{array} \qquad (9)$$

An additional crosscheck was made for the yet unknown ArF^+ cation for which recent ab initio calculations[16] have yielded an Ar–F bond energy value of 49 ± 3 kcal mol^{-1}. Using this value, the F^+ affinity of Ar can be estimated as -87.4 kcal mol^{-1} (10) which is in excellent agreement with our FPD value of 87.3 kcal mol^{-1} from Table 1.

$$\begin{array}{llllll} & \mathrm{Ar} + \mathrm{F}^+ & \xrightarrow{\mathrm{FPA} = -87.4} & \mathrm{ArF}^+ & \xleftarrow{D_{\mathrm{ArF}^+} = -49} & \mathrm{Ar}^+ + \mathrm{F} \\ \Delta Hf^\circ & 0 \quad 422.0 & & 334.6 & & 364.7 \quad 18.9\ \mathrm{kcal\ mol^{-1}} \end{array} \qquad (10)$$

Heats of Formation of the Oxidizers

The knowledge of the F^+ detachment energies of the oxidizers (see Table 1) also provides a convenient source for their heats of formation ΔHf°. The latter are given by equation (11),

$$\Delta Hf^\circ_{(XF^+g)} = \Delta Hf^\circ_{(Xg)} + \Delta Hf^\circ_{(F^+g)} - FPD_{(XF^+g)} \qquad (11)$$

where $\Delta Hf^\circ_{(F^+g)}$ equals 422.0 kcal mol^{-1}; $\Delta Hf^\circ_{(Xg)}$, the heat of formation of the parent molecule, is usually known, and the FPD values are taken from Table 1. The resulting $\Delta Hf^\circ_{(XF^+g)}$ values have been included in Table 1. Only few experimental estimates are available for these formation enthalpies. For example, the value of 204 kcal mol^{-1} previously reported[17] for $\Delta Hf^{o}_{(NF_4^+g)}$ is in good agreement with our value of 207 kcal mol^{-1} given in Table 1.

Characteristics of the Oxidizer Strength Scale

The following comments can be made about the data given in Table 1.

(i) F^+ detachment energies are a good measure for the oxidizing power of an oxidative fluorinator. The oxidizing power of a compound decreases with an increase in its F^+ detachment energy.

(ii) A negative value for the F^+ detachment energy of an XF^+ species signifies a species that is unstable with respect to decomposition to ground state $X(^1S)$ and F^+ (^3P).

The negative F^+ detachment energy values for NeF^+ and HeF^+, listed in parentheses in Table 1 are due to the fact that for all of our calculations the following spin states were used (12).

$$XeF^+(^1\Sigma^+) \xrightarrow{FPD} X(^1S) + F^+(^3P) \qquad (12)$$

Whereas for XeF^+, KrF^+ and ArF^+ a $^1\Sigma^+$ state is the ground state, NeF^+ and HeF^+ have an $x^3\pi$ ground state. Their $^1\Sigma^+$ states are excited states which lie 30.3 and 23.8 kcal mol^{-1}, respectively, about their ground states.[16] If for NeF^+ and HcF^+ the FPD's are computed for their $x^3\pi$ ground states (13),

$$XF^+(x^3\pi) \longrightarrow X(^1S) + F^+(^3P) \qquad (13)$$

slightly positive values of about 3.6 and 1.4 kcal mol^{-1}, respectively, are obtained. This was shown by recent high level ab initio calculations[16, 18] which suggest that in their ground states these cations are only weakly bound.

(iii) Except for NeF^+ and HeF^+, the F^+ detachment energies listed in Table 1 do not represent the X-F bond dissociation energies, D_0. Since usually the first ionization potential of X is lower than that of the F atom (422 kcal mol^{-1}),[6] the lowest energy bond dissociation process becomes the one which yields X^+ and F atoms (14).

$$XF^+(^1\Sigma^+) \xrightarrow{D_0} X^+(^2P) + F(^2P) \qquad (14)$$

(iv) The previous reached[2] conclusion that KrF^+ is the strongest presently known oxidative fluorinator was confirmed.

(v) For the halogen fluoride cations, XF_n^+, the oxidative fluorinator strength increases with increasing n and decreasing atomic weight of X. The only exception to this rule is BrF_6^+ which, by analogy to the known BrO_4^- -ClO_4^- case,[19] is a slightly stronger oxidative fluorinator than ClF_6^+.

(vi) For the presently known xenon fluoride cations, the influence of the xenon oxidation state on the oxidizer strength is rather small and, somewhat surprisingly, XeF_3^+ ranks slightly above XeF_5^+ and XeF^+. The oxidative fluorinator strength of the yet unknown XeF_7^+ cation is considerably higher than those of the remaining XeF_n^+ cations and rivals that of KrF^+. The latter fact also explains the failure of our previous attempts to prepare XeF_7^+ from KrF^+ and XeF_6.

(vii) The oxidative fluorination reactions can be considered as a formal transfer of F^+ from the oxidizer to a substrate and involve the breaking of an existing and the formation of a new bond. Even when proceeding through a probable intermediate activated complex, as shown by equation (15) for the $Xe + N_2F^+$ reaction,

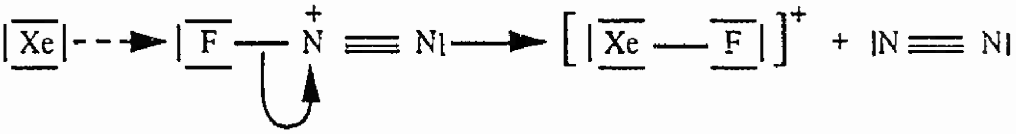

$$|\overline{\underline{Xe}}| \dashrightarrow |\overline{\underline{F}} - \overset{+}{N} \equiv N| \longrightarrow [|\overline{\underline{Xe}} - \overline{\underline{F}}|]^+ + |N \equiv N| \qquad (15)$$

such a reaction could either require a substantial activation energy, or, in cases such as NF_4^+,[20] could be sterically hindered. Hence, it is not surprising that some of the reactions, deemed possible form the rankings in Table 1, have so far experimentally not been observed. Of the previously observed oxidative fluorination reactions,[1-3, 21-28] none violates the rankings given in Table 1, thus supporting our results. The only somewhat ambiguous case is a previous report[28] which indicated that $ClF_2^+AsF_6^-$ oxidized Xe to $Xe_2F_3^+$. However, this reaction was carried out in the absence of a solvent at a temperature where the unstable $Cl_2F^+AsF_6^-$ decomposes. Furthermore, the product was $Xe_2F_3^+$ and not XeF^+ which may have an FPD value which is significantly different from that of XeF^+. Therefore, the mechanism and nature of the products of this reaction should be studied under more carefully controlled conditions and the FPD of $Xe_2F_3^+$ must be calculated, before any conclusions can be drawn for this special case.

(viii) Among the yet unknown oxidizers which are listed in Table 1 and rank in oxidizing power below KrF^+, are XeF_5O^+ and ClF_4O^+. Previous attempts to oxidatively fluorinate XeF_4O [25, 26, 29] or ClF_3O [30] have always resulted in oxidation of the oxygen ligand, i.e. O_2 evolution, instead of XeF_5O^+ or ClF_4O^+ formation, respectively. These results indicate that in the case of high oxidation state oxyfluorides, the oxygen ligand might become easier to oxidize than the central atom thus foiling attempts aimed at their oxidative fluorination.

CONCLUSION

A quantitative oxidizer strength scale is now available for the first time. It is expected to significantly contribute to our understanding of oxidizer chemistry and to the future syntheses of novel and known oxidative fluorinators. It also stresses the importance of employing high activation energy sources such as discharges or plasmas to generate intermediate F^+ cations if novel oxidizers are desired which are more powerful than KrF^+.

ACKNOWLEDGEMENT

The work at Rocketdyne was financially supported by both the U.S. Army Research Office and the Air Force Phillips Laboratories. K. Dobbs (du Pont) is thanked for performing some of the calculations.

REFERENCES

1. Christe, K .O.; Wilson, R. D.; Wilson, W. W.; Bau, R.; Sukumar, S.; Dixon, D. A., *J. Amer. Chem. Soc.*, in press.

2. Christe, K. O.; Wilson, W. W.; Wilson, R. D., *Inorg. Chem.*, 1984, 23, 2058.

3. Sokolov, V. B.; Dobrychevskii, Yu. V.; Prusakov, V. N.; Ryzhkov, A. V.; Koroshev, S. S., *Dokl. Akad. Nauk SSSR*, 1976, 229, 641.

4. Bartlett, N., *Angew. Chem. Internat. Edit.*, 1968, 7, 433.

5. Barlett, N.; Lohmann, D. H., *Proc. Chem. Soc.*, 1962, 277 and *J. Chem. Soc.*, 1962, 5253.

6. Wagman, D. D.; Evans, W. H.; Parker, V. B.; Schuman, R. H.; Halow, I.; Bailey, S. M.: Churney, K. L.; Nuttall, R. L. *J. Phys. Chem.*, Ref. Data 1982, Vol. 11, Suppl. 2.

7. Dixon, D. A.; Lias, S.G. in "Molecular Structures and Energies, Vol. 2," Liebman, J. F. and Greenberg, A. Eds. VCH Publishers: Deerfield Beach, Fl., 1987, Chapt. 7, p. 269.

8. (a) Parr, R. G.; Yang W.; "Density Functional Theory of Atoms and Molecules," Oxford University Press, New York, 1989.
   (b) Salahub, D. R. in "Ab Initio Methods in Quantum Chemistry - II" Lawlwy, K.P. Ed. J. Wiley and Sons, New York, 1987.
   (c) Wimmer, E.; Freeman, A. J.; Fu, C. L.; Cao, P. L; Chou, S. H; Delley, B., in "Supercomputer Research in Chemistry and Chemical Engineering," Jensen, and K. F. Truhlar, D. G., Eds.; ACS Symposium Series, *Amer. Chem Soc.*, Washington, D. C., 1987, p. 49.
   (d) Jones, R. O.; Gunnarsson, O. *Rev. Mod. Phys.*, 1989, 61, 689.
   (e) Dixon, D. A.; Andzelm, J.; Fitzgerald, G.; Wimmer, E.; Delley, B., "Science and Engineering on Supercomputers," Pitcher, E. J. Ed., *Computational Mechanics Publications*: Southampton, England, 1990, p. 285.
   (f) Dixon D. A.; Andzelm J.; Fitzgerald, G.; Wimmer, E; Jasien, P., in "Density Functional Methods in Chemistry," Labanowski, J. K.and Andzelm. J. Eds. , Springer-Verlag: New York, 1991, Chapt. 3, p. 33.

9. Hohenberg, P; Kohn, W., *Phys. Rev. B*, 1964, 136, 184.

10. von Barth, U.; Hedin, L., *Phys. C*, 1972, 5, 1629.

11. Delley, B. *J. Chem. Phys.* 1990, 92, 508. Dmol is available commercially from BIOSYM Technologies, San Diego, CA.

12. This grid can be obtained by using the FINE parameter in DMol.

13. For a discussion of Hartree-Fock methods, see (a) Komornicki, A, Ishida, K.; Morokuma, K, Ditchfield, R; Conrad, M. *Chem. Phys. Let.*, 1977, 45, 595. (b) Pulay, P. in "Applications of Electronic Structure Theory," Schaefer, H.F. III, Ed.; Plenum Press: New York, 1977, p. 153. (c) Jorgenson, P.; Simons, J. Eds. "Geometrical Derivatives of Energy Surfaces and Molecular Properties," NATO ASI Series C. Vol. 166, D. Reidel: Dordrecht 1986, p. 207.

14. (a) Delley, B., in "Density Functional Methods in Chemistry," Labanowski, J.K.and Andzelm. J.W., Eds. Springer-Verlag: New York, 1991, Chapt. 11, p. 101.
   (b) Fournier, R; Andzelm, J.; Salahub, D.R., *J. Chem. Phys.*, 1989, 90, 6371.
   (c) Versluis, L.; Ziegler, T., *J. Chem. Phys.*, 1988, 88, 3322.

15. Bartlett, N; Sladky, F. in "Compreh. Inorg. Chem. Vol. 1, p. 213-330, Pergamon Press, Oxford, 1973. The appearance potentials are due to J. Berkowitz, unpublished work.

16. Frenking, G; Koch, W.; Deakyne, C. A.; Liebman, J. F.; Bartlett, N., *J. Amer. Chem. Soc.*, 1989, 111, 31.

17. Goetschel, C. J.; Campanile, V. A.; Curtis, R. M.; Loos, K. R.; Wagner, D. C.; Wilson, J. N., *Inorg. Chem.*, 1972, 11, 1696.

18. (a) Frenking, G.; Koch, W.; Cremer, D.; Gauss, J.; Liebman, J. F., *J. Phys. Chem.*, 1989, 93, 3397, 3410.
(b) Deakyne, C. A.; Liebman, J. F.; Frenking, G.; Koch, W. ibid., 1990, 94, 2306.

19. Greenwood, N. N.; Earnshaw, A. in "Chemistry of the Elements," Pergamon Press, Oxford, 1984, p. 1020.

20. Christe, K. O.; Wilson, W. W.; Schrobilgen, C. J.; Chirakal, R. V.; Olah, G. A., *Inorg. Chem.* 1988, 27, 789.

21. Gillespie, R. J.; Schrobilgen, G. J., *J. Chem. Soc.*, 1974, 13, 1230.

22. Artyukhov, A. A.; Khoroshev, S. S., *Koord. Khim.*, 1977, 3, 1478.

23. Christe, K. O.; Wilson, W. W.; Curtis, E. C., *Inorg. Chem.* 1983, 22, 3056.

24. Stein, L., *Chemistry*, 1974, 47, 15.

25. McKee, D. E.; Adams, C. J.; Zalkin, A.; Bartlett, N., *J. Chem. Soc., Chem. Commun.*, 1973, 26.

26. Holloway, J. H.; Schrobilgen, G. J., *J. Chem. Soc., Chem. Commun.*, 1975, 623.

27. Meinert, H.; Gross, U., *Z. Chem.*, 1968, 8, 345.

28. Christe, K. O.; Wilson, R. D., *Inorg. Nucl. Chem. Letters*, 1973, 9, 845.

29. Christe, K. O.; Wilson, R. D., *J. Fluorine Chem.*, 1976, 7, 356.

30. Christe, K. O.; Wilson, W.W.; Wilson, R. D., unpublished results.

Table 1. Absolute Oxidizer Strength Scale and Formation Enthalpies for Oxidative Fluorinators

Oxidative Fluorinator[a]	F$^+$ Detachment Energy (kcal mol^{-1})[b]	Formation Enthalpy[c] (kcal mol^{-1})	
XF$^+$	FPD (XF$_g$$^+$)	ΔHf°(XF$^+$ g)	ref for ΔHf°(X)
(F$^+$)	0	422.0	(6)
(HeF$^+$) (x$^3\pi$)	1.4	420.6	(6)
($^1\Sigma^+$)	(-13.2)	(435.2)	(6)
(NeF$^+$) (x$^3\pi$)	3.6	418.4	(6)
($^1\Sigma^+$)	(-16.6)	(438.6)	(6)
(F$_3$$^+$)	63.0	359.0	(6)
(ArF$^+$)	87.3	334.7	(6)
KrF$^+$	118.9	303.1	(6)
(XeF$_7$$^+$)	119.7	219.2	(15)
(OF$_3$$^+$)	125.2	302.7	(6)
(O$_2$F$^+$)[f]	136.8	285.2	(6)
(ClF$_4$O$^+$)	138.6	248.0	(d)
N$_2$F$^+$	142.3	279.7	(6)
(XeF$_5$O$^+$)	142.8	273.2	(e)
BrF$_6$$^+$	143.8	175.7	(6)
ClF$_6$$^+$	150.3	212.5	(d)
XeF$_3$$^+$	155.4	240.7	(15)
ClF$_4$$^+$	161.7	221.3	(6)
XeF$_5$$^+$	161.9	197.6	(6)
ClF$_2$O$_2$$^+$	164.0	225.4	(d)
XeF$^+$	167.8	254.2	(6)
ClF$_2$$^+$	170.1	238.9	(6)
BrF$_4$$^+$	177.0	184.0	(6)
IF$_6$$^+$	178.0	37.4	(6)
Cl$_2$F$^+$	182.1	239.9	(6)
NF$_4$$^+$	183.1	207.5	(6)
BrF$_2$$^+$	185.4	214.2	(6)
IF$_4$$^+$	215.1	90.9	(15)
IF$_2$$^+$	216.5	182.7	(6)

(a) The cations listed in parentheses have so far not been isolated in the form of stable salts.

(b) All FPD values were computed for XF$^+$ and X being singlet ground states and F$^+$ being a triplet ground state, except for HeF$^+$ and NeF$^+$ which have triplet ground states (see text) and O$_2$F$^+$ (see footnote f).

(c) calculated by equation (7) using ΔHf°(X) values from ref. 6, 15, c, and d.

(d) Barberi, P.; Carre, J.; Rigny, P. *J. Fluor. Chem.*, 1976, 7, 511.

(e) Gunn, S. R., *J. Amer. Chem. Soc.*, 1965, 87, 2290.

(f) Calculated for the singlet state of O$_2$F$^+$ going to the triplet state of O$_2$.

United States Patent [19]
Schack et al.

[11] **Patent Number: 4,675,088**
[45] **Date of Patent: Jun. 23, 1987**

[54] SYNTHESIS OF R_fOTEF_5

[75] Inventors: **Carl J. Schack**, Chatsworth; **Karl O. Christe**, Calabasas, both of Calif.

[73] Assignee: **The United States of America as represented by the Secretary of the** Air Force, Washington, D.C.

[21] Appl. No.: **824,822**

[22] Filed: **Jan. 31, 1986**

[51] Int. Cl.⁴ **B01J 19/12; C07C 165/00; C01B 7/24**

[52] U.S. Cl. **204/157.94**; 204/158.11; 204/158.12; 260/550; 423/466; 423/508; 570/123; 570/137

[58] **Field of Search** 260/550; 568/604, 683, 568/684; 423/466, 508; 570/123, 137; 204/157.94, 158.11, 158.12

[56] **References Cited**

U.S. PATENT DOCUMENTS

4,462,975	7/1984	Schack et al.	423/473
4,508,662	4/1985	Schack et al.	260/550
4,578,225	3/1986	Schack et al.	260/550

OTHER PUBLICATIONS

C. Schack et al, J. of Fluorine Chemistry, vol. 26(1), pp. 19-28 (1984); vol. 27(1), pp. 53-60 (1984); vol. 24(4), pp. 467-476 (1984).

D. Naumann, W. Habel, P. Reinelt, E. Renk, "Ligandenaustauschreaktionen an Perfluororganohalogen-Verbindungen" Forschungsberichte des Landes Nordrhein-Westfalen, Nr. 3115, (1982).

Primary Examiner—Mary E. Ceperley
Attorney, Agent, or Firm—Charles E. Bricker; Donald J. Singer

[57] **ABSTRACT**

Pentafluorotellurium hypohalites are reacted with fluorocarbon iodides to form intermediate adducts which are thereafter decomposed to form fluorocarbons containing the TeF_5O— group.

12 Claims, No Drawings

SYNTHESIS OF R_fOTEF_5

STATEMENT OF GOVERMENT INTEREST

The invention described herein may be manufactured and used by or for the Government of the United States for all governmental purposes without the payment of any royalty.

BACKGROUND OF THE INVENTION

This invention relates to a method for synthesizing fluorocarbon fluids containing an oxypentafluorotellurium group (—$OTeF_5$).

The TeF_5O— group is inherently dense and when incorporated into fluorocarbon fluids it provides enhanced density to those materials. Additionally, the ether-like oxygen link furnishes molecular flexibility, lessening of steric hindrances, and retention of fluid properties.

Fluorocarbon fluids containing the —$OTeF_5$ group find particular utility as agents for a wide variety of applications requiring high density fluids. They are especially useful as flotation agents for gyroscopes, compasses and like instruments which must be dampened to minimize excessive vibration and oscillation problems.

In our U.S. Pat. No. 4,508,662, issued Apr. 2, 1985 to C. J. Schack and K. O. Christe, we disclose the reaction of pentafluorotellurium hypochlorite with olefinic reactants to form fluorocarbon adducts containing the —$OTeF_5$ group. In our pending U.S. patent application Ser. No. 617,456, filed May 29, 1984, we disclose the reaction of xenon bis-pentafluorotellurium oxide with olefinic reactants to form fluorocarbon adducts containing multiple —$OTeF_5$ groups.

It is an object of the present invention to provide a novel process for forming fluorocarbon adducts containing the —$OTeF_5$ group.

Other objects and advantages of the present invention will become apparent upon consideration of the following detailed description.

SUMMARY OF THE INVENTION

In accordance with the present invention there is provided a novel process for producing fluorocarbon compounds containing the —$OTeF_5$ group which comprises the steps of reacting a fluorocarbon iodide containing 1 to 5 carbon atoms with a pentafluorotellurium hypohalite to form an intermediate adduct, and decomposing the intermediate to provide the desired compounds.

The reactions for synthesizing the desired fluorocarbon fluids in accordance with the invention are illustrated by the following equations:

$$2TeF_5OX + R_fI \rightarrow R_fI(OTeF_5)_2 + X_2 \qquad (I)$$

$$2R_fI(OTeF_5)_2 \rightarrow R_fOTeF_5 + R_fI + I(OTeF_5)_3 \qquad (II)$$

wherein X is —Cl or —F and R_f is a fluorinated hydrocarbon group of the general formula —$C_mF_nY_p$ wherein Y is —H, —F, —Cl or —Br and wherein m is an integer between 1 and 5, p is an integer having a value of about 2m/3 (rounded to the next higher or lower value) and n is an integer having a value of 2m+1−p. Examples of suitable fluorocarbon iodides include CF_3I, HCF_2CF_2I, CF_3CF_2I, $ClCF_2CF_2I$, $BrCF_2CF_2I$, $HCF_2CF_2CF_2I$, CH_3CHFCF_2I, $ClCF_2CF_2CF_2I$, $CF_3CFBrCF_2I$, C_4F_9I, C_4HF_8I, C_4ClF_8I, C_4BrF_8I and cyclo-C_5F_9I.

The pentafluoroetellurium hypohalites can be prepared following the procedures given in U.S. Pat. No. 4,508,662. The fluorocarbon iodides are commercially available from, for example, PCR, Inc., Gainesville, FL, and Columbia Organics, Camden, S.C.

The reaction (I) between the pentafluorotellurium hypohalite and fluorocarbon iodide is initiated at subambient temperatures. The hypohalite reactant and the fluorinated hydrocarbon reactant are cocondensed at subambient temperature and allowed to gradually warm toward ambient temperature. The progress of the reaction may be monitored by removing and measuring the evolved halogen gas or other products volatile at the reduced temperature.

Decomposition of the adduct formed by the reaction I is accomplished by heating the adduct or by exposure to UV radiation or a combination thereof.

The conditions of reaction (I) and decomposition (II) will vary depending upon the reactants employed. In the case of the methyl adduct, the reaction (I) is carried out at or below about −78° C. for about 10 to 100 hours. In the case of the C_2 to C_5 reactants, the reaction (I) mixture is cocondensed at a temperature sufficiently low to ensure condensation of both reactants. Liquid nitrogen may be employed for this step. The reactor containing the condensed reactants is then closed and thereafter allowed to slowly warm to, for example, about −78° C. in a liquid nitrogen —CO_2 slush bath. The reaction mixture may be held at −78° C. for 0.1 to 10 hours, then warmed slowly to ambient temperature. Except for the methyl adduct, the reaction mixture is maintained at ambient temperature for about 10 to 60 hours and then the resulting reaction products are separated by removing the volatile material. Decomposition of the methyl adduct is accomplished by warming the material above −78° C.

The final product R_fOTeF_5 is obtained by decomposition of the above adducts. Decomposition of the ethyl and higher alkyl adducts is accomplished by heating the $R_fI(OTeF_5)_2$ material to at least about 100° C., preferably about 115°-120° C. for about 1 to 10 hours. Alternatively, the $R_fI(OTeF_5)_2$ material can be photolytically decomposed using UV radiation of sufficient intensity to accomplish the desired decomposition in a reasonable time.

In the examples which follow, volatile materials were manipulated in a stainless steel vacuum line equipped with Teflon FEP U-traps, 316 stainless steel bellows-seal valves, and a Heise Bourdon tube-type gauge. The synthetic reactions employed here were usually conducted in stainless steel cylinders. Infrared spectra were recorded on a Perkin Elmer Model 283 spectrophotometer using cells equipped with AgBr windows. Raman spectra were recorded at ambient temperature on a Cary Model 83 spectrophotometer with the use of the 488 Å exciting line of an Ar ion laser. To avoid decomposition, the Raman spectrum of the yellow solid, $I(OTeF_5)_3$, was recorded at −140° C. on a Spex Model 1403 spectrophotometer using the 6471 Å exciting line of a Kr ion laser and a premonochromator for the elimination of plasma lines. Sealed quartz tubes, 3 mm OD, or Pyrex mp capillaries were used as sample containers. ^{19}F nmr spectra were recorded at 84.6 MHz on a Varian Model EM390 spectrometer with internal $CFCl_3$ as a standard with negative chemical shifts being upfield from $CFCl_3$.

The following examples illustrates the invention:

EXAMPLE

$2TeF_5OCl + R_fI \rightarrow R_fI(OTeF_5)_2$, General Procedure

A tared cylinder was cooled to −196° C. and measured quantities of R_fI and TeF_5OCl were successively condensed in. The closed cylinder was placed in a dewar containing a liquid N2-dry ice slush and this was allowed to warm slowly from −196° to −78° C. in a dry ice chest. Monitoring the progress of the reaction at −78° C. was accomplished by removing and measuring the evolved Cl_2 or other products volatile at −78° C. After a period at −78° C. the reaction mixtures were warmed slowly to ambient temperature to complete the oxidative addition reaction. For CF_3I the resulting adduct was unstable and decomposed above −78° C. to give CF_3OTeF_5 (trapped at −126° C. on fractionation) and other products. For the other fluorocarbon iodides, after removal of all volatile materials at room temperature, there remained in the cylinders the colorless addition compounds of compositions, $R_fI(OTeF_5)_2$. These were low melting solids, $C_2F_5I(OTeF_5)_2$, 30°-31° C. and n-$C_3F_7I(OTeF_5)_2$, 49°-51° C., i-$C_3F_7I(OTeF_5)_2$, 16°-17° C.

Synthesis data are given in Table I, below:

TABLE I

Synthesis of $R_fI(OTeF_5)_2$

R_fI (mmol)	TeF_5OCl (mmol)	Temp Max °C.	Time (days)	Product	Yield, %[a]
CF_3I (0.91)	1.85	−78	4	$CF_3I(OTeF_5)_2$	~80
C_2F_5I (1.10)	2.58	+25	3	$C_2F_5I(OTeF_5)_2$	95
n-C_3F_7I (2.56)	5.62	+25	2	n-$C_3F_7I(OTeF_5)_2$	94
i-C_3F_7I (2.16)	4.73	+25	2	i-$C_3F_7I(OTeF_5)_2$	97

[a] Yield based on the limiting reagent

GENERAL PROCEDURE

$2R_fI(OTeF_5)_2 \rightarrow R_fOTeF_5 + R_fI + I(OTeF_5)_3$

In the dry box a tared cylinder was loaded with a weighed amount of the $R_fI(OTeF_5)_2$ compound. The cylinder was then evacuated, closed and placed in an oven at 115°-120° C. for several hours. After recooling to ambient temperature, the contents of the reactor were separated by fractional condensation, measured and identified by their infrared and ^{19}F nmr spectra. In addition to the R_fOTeF_5 product generally obtained (see text), the significant volatile products were R_fI and some R_fF. Lesser amounts of the TeF_6 and TeF_5OTeF_5 were sometimes encountered. Left behind in the cylinder was crude $I(OTeF_5)_3$ identified by infrared and Raman spectroscopy and usually present in 80-90% yield based on the disproportionation reaction shown. For the photolytic decomposition of $R_fI(OTeF_5)_2$, Pyrex reactors were loaded in the dry box, evacuated, and irradiated with a Hanovia 100 W Utility lamp. Along with $I(OTeF_5)_3$ the photolysis products included variable amounts of the coupling product R_fR_f, isomers of C_6F_{14}, and C_3F_7I.

TABLE IIa

Thermal Decomposition of $R_fI(OTeF_5)_2$

Adduct	Temp. max °C.	Time (hours)	Product	Yield %[a]
$CF_3I(OTeF_5)_2$	25	2	CF_3OTeF_5	17
$C_2F_5I(OTeF_5)_2$	115	21	$C_2F_5OTeF_5$	78
n-$C_3F_7I(OTeF_5)_2$	115	26	n-$C_3F_7OTeF_5$	30
i-$C_3F_7I(OTeF_5)_2$	120	10	(note [b])	—

TABLE IIb

UV Decomposition of $R_fI(OTeF_5)_2$

Adduct	Temp °C.	Time (hours)	Product	Yield %[a]
n-$C_3F_7I(OTeF_5)_2$	25	18	n-$C_3F_7OTeF_5$	77
i-$C_3F_7I(OTeF_5)_2$	25	16	(note [b])	—

[a] Yield based on the stoichiometry of reaction II

[b] no R_fOTeF_5

Identification of the products of the process of this invention as based on spectroscopic properties. Data for $C_2F_5OTeF_5$ and n-$C_3F_7OTeF_5$ were consistent with the literature data for these compounds.

The ^{19}F NMR spectrum of CF_3OTeF_5 was that expected for an AB_4 spin system (TeF_5O— possesses one apical and four equatorial fluorines) and an alkyl fluorocarbon. Observed NMR parameters were [ppm(multiplicity)]; where b-broad, d-doublet, t-triplet, and qi-quintet. For $F^ATe_4{}^BOCF_3{}^X$: A-50.2, B-44.3 (B_4), X-51.6 (qi); $J_{AB}=190$, $J_{BX}=4.4$. Infrared bands noted were, cm^{-1} (intensity): 1263(s), 1233(s), 1192(s), 743(s), 710(m), and 324(s).

Various modifications and alterations may be made in the present invention without departing from the spirit thereof or the scope of the appended claims.

We claim:

1. A high density TeF_5O— substituted, fluorocarbon having the formula

$$YCF_2OTeF_5$$

wherein Y is —H, —F, —Cl or —Br.

2. The compound of claim 1 wherein Y is —F.

3. A process for synthesizing a TeF_5O— substituted fluorocarbon having the formula

$$R_fOTeF_5$$

which comprises the steps of:

(a) cocondensing a primary fluorocarbon iodide having the formula R_fI and a pentafluorotellurium hypohalite having the formula TeF_5OX wherein X is —Cl or —F at a subambient temperature;

(b) allowing the resulting mixture of reactants to warm toward the ambient temperature whereby said reactants react to form an intermediate product having the formula $R_fI(OTeF_5)_2$;

(c) applying energy to decompose said intermediate; and

(d) recovering said TeF_5O— substituted fluorocarbon;

wherein R_f— is a fluorinated hydrocarbon group of the general formula —$C_mF_nY_p$, wherein Y is —H, —F, —Cl or —Br, m is an integer having a value of 1 to 5, p is an integer having a value of about 2m/3 rounded to the next lower or higher number and n is an integer having a value of 2m+1−p.

4. The process of claim 3, wherein said fluorocarbon iodide is trifluoromethyl iodide and said hypohalite is selected from the group consisting of pentafluorotellurium hypofluorite and pentafluorotellurium hypochlorite.

5. The process of claim 4 wherein said reacting step is carried out at a temperature between co-condensation temperature of said iodide and said hypohalite reactants and about −78° C. for about 10 to 100 hours and wherein said decomposing step is carried out by warming the material above −78° C.

6. The process of claim 3 wherein said hypohalite is pentafluorotellurium hypochlorite.

7. The process of claim 6 wherein said fluorocarbon iodide is pentafluoroethyl iodide.

8. The process of claim 6 wherein said fluorocarbon iodide is heptafluoro-n-propyl iodide.

9. The process of claim 3 wherein said fluorocarbon iodide has between 2 and 5 carbon atoms and wherein said reacting step is carried out at a temperature between about −78° C. and ambient temperature for about 0.1 to 10 hours and thereafter at ambient temperature for about 10 to 60 hours.

10. The process of claim 9 wherein said decomposing step is carried out by heating said intermediate product to at least about 100° C. for about 1 to 10 hours.

11. The process of claim 10 wherein said intermediate is heated to about 115°-120° C.

12. The process of claim 9 wherein said decomposing step is carried out photolytically.

* * * * *

APPENDIX T

United States Patent [19]
Christe

[11] **Patent Number:** **4,695,296**
[45] **Date of Patent:** **Sep. 22, 1987**

---

[54] **METHOD FOR THE SELECTIVE SEPARATION OF GASES**

[75] Inventor: **Karl O. Christe**, Calabasas, Calif.

[73] Assignee: **Rockwell International Corporation**, El Segundo, Calif.

[21] Appl. No.: **739,806**

[22] Filed: **May 31, 1985**

[51] **Int. Cl.⁴** **B01D 53/04**

[52] **U.S. Cl.** **55/68; 55/75; 502/60**

[58] **Field of Search** 55/68, 75; 502/36, 60, 502/85

[56] References Cited

U.S. PATENT DOCUMENTS

3,061,654	10/1962	Gensheimer et al.	55/75 X
3,078,637	2/1963	Milton	55/75 X
3,078,638	2/1963	Milton	55/75 X
3,078,639	2/1963	Milton	55/75 X
3,266,221	8/1966	Avery	55/75 X
3,305,656	2/1967	Devins	55/75 X
3,594,331	7/1971	Elliott, Jr.	502/60
3,630,965	12/1971	Voorhies, Jr. et al.	502/60 X
3,644,220	2/1972	Kearby	502/60 X
3,699,056	10/1972	Takase et al.	502/60
3,751,878	8/1973	Collins	55/68 X
3,839,539	10/1974	Elliott, Jr.	502/60 X
3,885,927	5/1975	Sherman et al.	55/75 X
4,249,915	2/1981	Sircar et al.	55/75 X
4,297,335	10/1981	Lok et al.	502/60 X
4,356,156	10/1982	Dyer et al.	502/60 X
4,472,178	9/1984	Kumar et al.	55/75 X

Primary Examiner—Robert Spitzer
Attorney, Agent, or Firm—H. Fredrick Hamann; Harry B. Field; Clark E. DeLarvin

[57] **ABSTRACT**

A method for the selective removal of an oxide of carbon from a gas stream containing the same and a halogen which comprises contacting such a gas stream with a water-free, prehalogenated molecular sieve having a pore size of at least 4 angstroms whereby the oxide of carbon is selectively retained by the sieve without retention of the halogen.

10 Claims, No Drawings

METHOD FOR THE SELECTIVE SEPARATION OF GASES

BACKGROUND OF THE INVENTION

1. Field of the Invention

The present invention broadly relates to a method for the selective removal of an oxide of carbon from a gas stream containing the same and an elemental halogen. In accordance with a particularly preferred embodiment, the invention provides a method for the selective removal of CO_2 from a gas stream containing the same and fluorine, which stream is obtained from a high-power, pulsed, chemical DF laser.

2. Description of the Prior Art

It is well known that carbon dioxide is readily removable from substantially inert gas streams by various methods. For example, the removal of carbon dioxide from a gas stream by reaction with a base is well known, as is the use of a molecular sieve for effecting such separation. Methods also have been suggested for the separation of weak acids such as H_2S from gas streams containing the same and CO_2 by utilizing an absorbent which preferentially removes the H_2S along with only a minor amount of CO_2.

The removal of carbon dioxide from a gas stream containing the same and a halogen presents a very difficult problem. More particularly, the halogens, and fluorine in particular, are the more reactive elements known whereas CO_2 is relatively inert. To the best of the inventor's knowledge, no expedient method for the selective removal of CO_2 from a fluorine-containing gas exists, though the need for such a method does exist for use in conjunction with a pulsed chemical deuterium fluoride (DF) laser.

In a pulsed DF laser, molecular fluorine is dissociated by a suitable energy source such as flash photolysis or an electron beam into atomic fluorine as exemplified by the following equation:

$$F_2 \xrightarrow{\Delta E} 2F$$

The atomic fluorine (F) then is reacted with deuterium to produce the lasing species, vibrationally excited DF^* which lases at a wavelength of about 3.8 μm, as exemplified by the following equation:

$$\dot{F}+D_2\rightarrow DF^*+\dot{D}$$

Typically, the gas utilized in a pulsed DF laser comprises about 95% helium as a diluent and the balance will include a four-fold excess of F_2 over D_2. To maintain a high efficiency and minimize the inventory of stored gas required for operation of the laser it is necessary to remove the ground state deuterium fluoride formed during lasing. Removal of the DF is accomplished in a suitable scrubber, typically one containing activated sodium fluoride. The remaining helium diluent and the unused fluorine are recycled to the laser.

A particular advantage of a DF laser is its dual wavelength capability. Specifically, it has been found that excited DF can efficiently transfer its energy to CO_2 which can lase at a wavelength of 10.6 μm. Thus, the laser can be operated either on the DF or the CO_2 lines. An important requirement for dual wavelength operation, however, is the ability to switch from one mode to the other without sacrificing the advantages gained by the gas recirculation. Since switching from CO_2 lasing to DF lasing requires removal of the CO_2, an effective method for the selective removal of CO_2 from the fluorine-containing gas stream is essential.

SUMMARY OF THE INVENTION

The present invention provides a means for the selective removal of an oxide carbon from a gas stream containing the same and an elemental halogen. Broadly, the present invention comprises passing such a gas stream through a pretreated molecular sieve whereby the oxide of carbon is selectively retained by the sieve and the halogen along with the other constitutents of the gas stream pass therethrough. The molecular sieve must be pretreated and have a pore size of at least four angstroms (Å). The pretreatment comprises rendering the molecular sieve substantially inert towards the halogen by (1) removal of all free water from the sieve and (2) by halogenation of the sieve until it is completely stable (inert) towards the halogen. It has been found that such a treatment changes the chemical properties of the molecular sieve and results in a sieve which will selectively remove oxides of carbon from a gas stream containing the same and a halogen. The selection of the specific molecular sieve is not critical but it will generally comprise a zeolite or, as they are often referred to, an aluminosilicate.

It is a particular advantage of the present invention that it provides a method for the selective removal of carbon dioxide from a gas stream containing the same and a highly reactive halogen such as fluorine. Thus, the present invention is particularly suited for the treatment of a gas from a dual mode DF laser which is to be switched back from CO_2 to deuterium fluoride lasing.

It is therefore an object of the invention to provide a method for the selective removal of CO_2 from a fluorine-containing gas stream.

A broader object of the invention is to provide a method for the selective removal of an oxide of carbon from a gas stream containing same and at least one elemental halogen.

Another object of the invention is for the selective removal of CO_2 from a gas stream containing the same and fluorine which is devoid of complexity, relatively light in weight, and thus suitable for use in space applications.

A more specific object of the invention is to provide a process which will remove CO_2 but will not remove either fluorine or helium from a recirculating gas obtained from a dual wavelength, pulsed, chemical deuterium fluoride laser.

These and other objects, advantages and novel features of the present invention will be more readily apparent from the following detailed description.

DESCRIPTION OF A PREFERRED EMBODIMENT

In accordance with the present invention, a gas stream containing an oxide of carbon and a halogen is passed through a pretreated molecular sieve having a pore size of at least about 4 angstroms whereby the oxide of carbon is selectively removed and retained in the sieve. The molecular sieves utilizable in accordance with the present invention may be characterized as zeolites which are crystaline aluminosilicates of group 1-A and group 2-A elements and may be represented by the general formula

$$M_{x/n}[(AlO_2)_X(SiO_2)_Y]$$

where n is the valence of the cation M, X and Y are the total number of tetrahedra per unit cell, and Y/X typically may have a value of from 1 to about 100 and preferably of from 1 to about 5. Typical aluminosilicates suitable for use in accordance with the present invention, are commercially available molecular sieves such as Linde's A or X types. The chemical composition of these materials is similar, the only variations are the ratio of AlO_2 to SiO_2 and the specific cations M. For example, the Linde types 4A, 5A and 13X may be represented, respectively, by the formulae

$$Na_{12}[(AlO_2)_{12}(SiO_2)_{12}],$$

$$Ca_{4.5}Na_3[(AlO_2)_{12}(SiO_2)_{12}]$$

and

$$Na_{86}[(AlO_2)_{86}(SiO_2)_{106}]$$

The key aspect of the present invention is the manner in which the molecular sieve (aluminosilicate) is treated. An aluminosilicate having a pore size of at least about 4 angstroms is first dried, preferably in a dynamic vacuum maintained at a temperature within a range of from about 200° to 300° C. to remove any free water therefrom. Thereafter, the aluminosilicate is slowly halogenated with an elemental halogen (such as fluorine) at a lower temperature, typically ambient. The reaction is exothermic and must be accomplished slowly to avoid subjecting the aluminosilicate to an excessive temperature. Generally, the halogenation of the aluminosilicate will be repeated until the aluminosilicate reaches a saturation level ie., will absorb no more halogen. This is readily determinable since the aluminosilicate will maintain a constant weight and no additional halogen will be taken up. The aluminosilicate so treated can then be used for the selective adsorption of an oxide of carbon, such as CO_2, from a gas mixture containing the same and the selected halogen.

The subject invention is particularly suitable for use in conjunction with a pulsed, dual wavelength, chemical deuterium fluoride laser which utilizes a recirculation gas system. The recirculation gas system will include both a DF scrubber (a high surface area body of a material, such as NaF, for removal of DF) and the CO_2 scrubber of the present invention arranged in series in the recirculation gas system flow loop. While the CO_2 removal method of the present invention will also be capable of removing some of the DF, generally a sodium fluoride based scrubber is much more efficient and will provide the desired low levels of ground state DF in the lasing gas which is essential for high power yields in a chemical DF laser.

To minimize the pressure drop or flow resistance in such a recirculation gas system, the materials utilized for removal of DF and CO_2 will preferably be in the form of a bed of granules or pellets confined in a housing. The precise size of granules or pellets, size of housing, depth of the bed and the like will be a function of, among other things, the flow rate of the recirculating gas and the quantity of DF and CO_2 to be removed.

The general nature of the invention having been set forth, the following example is presented as a specific illustration thereof. It will be understood that the invention is not to be limited in this specific example of a preferred embodiment but rather is susceptible to various modifications as will be apparent to one of ordinary skill in the art to which this invention pertains.

EXAMPLE

A 16.37 gram quantity of a commercially available molecular sieve (Linde type 4A) pellets was obtained and activated by heating to 300° C. under a dynamic vacuum to remove any water therefrom. The pellets were then placed into an alumina tube which was equipped with a valve and connected to a stainless steel vacuum source. The alumina tube was evacuated and the pellets contained within the tube repeatedly exposed to gaseous fluorine at substantially ambient temperature until the pressure of fluorine above the pellets remained constant over several hours and the pellets had attained a constant weight.

The alumina tube was then evacuated and about 1.3 millimoles of a gas mixture having a composition (mole %) He 52.0, CO_2 41.7, F_2 3.8, and HF 2.5 was introduced into the alumina tube containing the treated pellets. The gas was subsequently withdrawn and it was determined that the pellets had adsorbed 0.51 millimoles of gas and the pellets had increased in weight by 22 milligrams which corresponded to a molecular weight of the absorbed species of 43.1 (based on $CO_2=44$). Thus, this demonstrated that substantially quantitative adsorption of the CO_2 by the pellets was obtained (within the limits of the accuracy of the measurements taken). This essentially quantitative adsorption was further confirmed by an infrared spectrum of the residual gases which was recorded at 100 torr pressure. The spectrum did not show any detectable amount of CO_2.

As will be apparent to those skilled in the art, numerous modifications and variations of the present invention are possible in light of the above teaching. It is to be understood therefore, that within the scope of the appended claims, the invention may be practiced other than as specifically described herein.

What is claimed is:

1. A method for the selective removal of an oxide of carbon from a gas stream containing the same and an elemental halogen comprising: bringing the gas stream to be treated into contact with a water-free, molecular sieve which has been prehalogenated with elemental halogen whereby the oxide of carbon is selectively retained in the molecular sieve.

2. The method of claim 1 wherein the halogen is fluorine and the molecular sieve is prefluorinated.

3. The method of claim 1 wherein the oxide of carbon is CO_2.

4. The method of claim 1 wherein said oxide of carbon is CO_2 and said halogen is fluorine.

5. The method of claim 4 wherein said gas stream is the lasing medium of a dual wavelength, pulsed chemical DF laser.

6. The method of claim 5 wherein said gas stream consists essentially of a major amount of helium and a minor amount of CO_2 and fluorine.

7. The method of claim 1 wherein the molecular sieve is an aluminosilicate.

8. The method of claim 6 wherein said aluminosilicate has the composition $Na_{12}[(AlO_2)_{12}(SiO_2)_{12}]$.

9. A method for the selective removal of CO_2 from a gas stream containing the same and fluorine comprising passing the gas stream through a bed of pellets consisting of an aluminosilicate having a pore size of at least about 4 angstroms which has been prefluorinated with elemental fluorine.

10. The method of claim 9 wherein said gas stream is the lasing medium of a dual wavelength pulsed chemical DF laser and comprises a major amount of helium, and said aluminosilicate has the composition $Na_{12}[(AlO_2)_{12}(SiO_2)_{12}]$

* * * * *

APPENDIX U

United States Patent [19]

Christe

[11] **Patent Number: 4,711,680**

[45] **Date of Patent: Dec. 8, 1987**

---

[54] PURE FLUORINE GAS GENERATOR

[75] Inventor: Karl O. Christe, Calabasas, Calif.

[73] Assignee: Rockwell International Corporation, El Segundo, Calif.

[21] Appl. No.: 497,287

[22] Filed: May 23, 1983

[51] Int. Cl.^{4} D03D 23/00; C01B 7/20

[52] U.S. Cl. 149/109.4; 149/119; 423/464; 423/500; 423/504

[58] Field of Search 149/109.4, 119; 423/464, 500, 504

[56] References Cited

U.S. PATENT DOCUMENTS

2,996,353	8/1961	Deyrup	423/464
3,337,295	8/1967	White et al.	423/464
3,709,748	1/1973	Roberto	149/119
3,843,546	10/1974	Sobolev et al.	423/464
3,963,542	6/1976	Pilipovich	149/193
3,980,509	9/1976	Lubowitz et al.	149/119
3,989,808	11/1976	Asprey	423/504
4,001,136	1/1977	Channell et al.	149/119
4,108,965	4/1978	Christe	149/119
4,172,884	10/1979	Christe et al.	423/[illegible]
4,284,617	8/1981	Bowen et al.	423/504
4,292,287	9/1981	Orlett et al.	423/500
4,374,112	2/1983	Christe et al.	149/119
4,379,128	4/1983	Hähn et al.	423/464
4,410,377	10/1983	Christe et al.	149/119
4,421,727	12/1983	Wilson et al.	149/119
4,446,920	5/1984	Woytek et al.	149/119
4,543,242	9/1985	Aramaki et al.	423/406

Primary Examiner—Edward A. Miller

Attorney, Agent, or Firm—H. Fredrick Hamann; Harry B. Field; David C. Faulkner

[57] ABSTRACT

A solid grain pure fluorine gas generator which comprises the in-situ generation of a thermodynamically unstable transition metal fluoride from its stable anion by a displacement reaction with a stronger Lewis acid, followed by the spontaneous irreversible decomposition of said unstable transition metal fluoride to a stable lower fluoride and elemental fluorine of superatmospheric pressure.

21 Claims, No Drawings

PURE FLUORINE GAS GENERATOR

BACKGROUND OF THE INVENTION

1. Field of the Invention

This invention relates to high-power pulsed chemical HF or DF lasers (PCL) and, more specifically, to solid grain pure fluorine gas generators therefor.

2. Description of the Prior Art

In a PCL, molecular fluorine is dissociated by an energy source, such as flash photolysis or an electron beam, into atomic fluorine

$$F_2 \xrightarrow{\Delta E} 2\dot{F}$$

which then reacts with either H_2 or D_2 to produce the lasing species vibrationally excited HF^* or DF^*.

$$\dot{F} + D_2 \longrightarrow DF^* + \dot{D}$$

Since elemental fluorine has a low boiling point of −188° C., it is usually stored either as a liquid at cryogenic temperatures or as a gas under high pressure. Both storage modes present great safety hazards and logistics problems, and therefore are unacceptable for military and space applications. In view of these problems solid grain fluorine gas generators are highly desirable. Such systems are composed of storable solids which are capable of generating gaseous fluorine on demand. Depending on the nature of the chemical laser, additional constraints are imposed on these generators. For example, a PCL is best operated in a gas recirculation mode at atmospheric pressure using He as a diluent and a fourfold excess of fluorine with respect to H_2 or D_2. Such a PCL requires a pure fluorine gas generator because any gaseous by-products would build up in the recirculating gas with an increase in the number of cycles, and because other fluorine sources, such as NF_3, are not efficiently dissociated by flashlamps, and their reaction rates with D_2 are too slow.

All the solid grain fluorine gas generators developed up to this point are for continuous wave single pass HF-DF lasers and are based on the thermal decomposition of NF_4^+ salts, as described in U.S. Pat. Nos. 3,963,542 and 4,172,884. These generators produce about equimolar amounts of F_2 and NF_3, and therefore cannot be used in a PCL, particularly when operated in a gas recirculation mode. Several systems capable of generating pure fluorine have previously been reported, but have either been refuted or exhibit serious drawbacks, as shown by the following examples: (i) The report by Brauner (J. Chem. Soc., 65 (1894) 393) that pyrolysis of K_3PbF_7 yields F_2 was refuted by Ruff (Z. anorg. allgem. Chem., 98 (1916) 27,38); and (ii) the thermal decompositions of CoF_3 (NSWC Report WOL TR 77-23) and $K_2NiF_6.KF$ (J. Fluorine Chem., 7 (1976) 359) require impractically high temperatures and are based on equilibrium reactions which at lower temperatures result in a reformation of the starting materials under fluorine uptake. Consequently, none of these systems are useful for PCL applications which require a solid grain gas generator fulfilling the following conditions: generation of pure fluorine to avoid buildup of gases which deactivated the laser; (2) generation of F_2 at high pressure to minimize the size of the gas accumulator and to permit feeding of an atmospheric pressure laser; (3) generation of F_2 at moderate temperatures to avoid metal fires in the generator and fluorine losses to the hardware, to minimize the energy requirements for the generator, and to obtain a fast generator response time; and (4) the F_2 generating reaction must be irreversible to eliminate the need for either continuous heating of the generator or complex hardware allowing rapid removal of the F_2 while the generator is hot.

SUMMARY OF THE INVENTION

Accordingly, there is provided by the present invention a system which overcomes all the drawbacks of the prior art while meeting all of the above requirements for a solid grain pure fluorine gas generator for a PCL. This system is based on the fact that certain high oxidation state transition metal fluorides are thermodynamically unstable and decompose even at room temperature by an irreversible reaction to a lower fluoride and elemental fluorine, as shown by the following generalized equation where M stands for a typical transition metal and the oxidation state of M is assumed to be +IV

$$MF_4 \rightarrow MF_2 + F_2$$

Although free MF_4 is usually not known and does not exist as a stable molecule, the +IV oxidation state of M can be stabilized by anion formation, i.e. in the form of MF_6^{2-}. Thus, a stable A_2MF_6 salt, where A is a typical alkali metal such as potassium or an alkaline earth metal, can be prepared by a high temperature fluorination of a stoichiometric mixture of AF and MF_2 according to:

$$2AF + MF_2 + F_2 \xrightarrow{T} A_2MF_6$$

If the A_2MF_6 prepared in this manner is then subjected to a displacement reaction with a Lewis acid Y which is stronger than MF_4, the following displacement reaction can be carried out which results in the in-situ formation of MF_4:

$$A_2MF_6 + 2Y \rightarrow 2AYF + [MF_4]$$

Since free MF_4 is thermodynamically unstable, it spontaneously decomposes to MF_2 and F_2 in an irreversible reaction which permits the generation of high pressure fluorine without the possibility of a back reaction:

$$[MF_4] \rightarrow MF_2 + F_2$$

Since it was found that A_2MF_6 can be premixed with Y and forms stable mixtures until the melting point or onset of sublimation of Y is approached, the temperature of the above displacement reaction can be controlled by a judicious choice of Y.

OBJECTS OF THE INVENTION

Therefore, it is an object of the invention to provide a solid grain fluorine gas generator producing pure fluorine.

Another object is to provide a fluorine generator which is based on an irreversible reaction and therefore can provide F_2 of superatomospheric pressure.

A further object of the invention is a generator producing superatmospheric F_2 at moderate temperatures thereby avoiding material compatibility problems, minimizing energy requirements, and providing rapid and controllable fluorine evolution.

Other objects, advantages and novel features of the present invention will become apparent from the following detailed description.

DESCRIPTION OF THE PREFERRED EMBODIMENT

According to the present invention, pure fluorine gas at superatompsheric pressure can be generated at moderate temperatures from a solid grain comprising a mixture of a stable salt of a high oxidation state transition metal fluoride anion with a strong Lewis acid. The selected transition metal must possess the ability to form stable complex fluoro anions in oxidation states which are unstable for the free transition metal fluoride parent molecule. When through a displacement reaction the anion is converted to the free parent molecule, the high oxidation state of the anion is destabilized and the unstable free parent molecule undergoes spontaneous decomposition to a lower oxidation state fluoride and elemental fluorine. Since the amount of fluorine evolution depends, in part, on the difference between the highest stable oxidation state of the complex fluoro anion and that of the free parent molecule, the transition metal is chosen in such a way to maximize this difference. Furthermore, the transition metal should be as light as possible for a maximum fluorine yield, and should also be rather inexpensive. Consequently, the preferred transition metals of this invention are those of the first transition metal period of the periodic system, particularly Mn, Fe, Co, Ni, and Cu. Thus, Ni and Cu are known to form stable complex fluoro anions in the +IV oxidation state, i.e. NiF_6^{2-} and CuF_6^{2-}, whereas the highest stable oxidation state parent molecules are NiF_2 and CuF_2, respectively. The overall reaction can then be described by the following equation

$$A_2MF_6+2Y \rightarrow 2AYF+MF_2+F_2$$

where M stands for the transition metal. Obviously, this invention is not limited to hexafluoro anions. For example, tetrafluoro anions such as CuF_4^- or AgF_4^- are well known and can undergo the following analogous reaction:

$$AMF_4+Y \rightarrow AYF+MF_2+0.5F_2$$

For A any cation capable of forming stable MF_6^{2-} or MF_4^- salts can be used. Typical examples are alkali metals (Li^+ to Cs^+) and alkaline earth metal cations (Mg^{2+} to Ba^{2+}). From overall F_2 yield considerations, multiple charged light cations are preferred.

The following selection criteria apply to the Lewis acid Y. It should be a stable nonvolatile solid at room temperature and be compatible with the transition metal fluoride salt. It also must be a stronger Lewis acid than the transition metal fluoride which is to be displaced from its salt, and it should melt or sublime at a moderately higher temperature, in the range of about 50° to about 300° C., to minimize the energy required to effect the displacement reaction. Again, a low molecular weight and an ability to form multiple charged anions are desirable for Y to achieve a maximum F_2 yield. Typical examples for suitable Lewis acids are BiF_5, NbF_5, or TiF_4. However, combinations of several Lewis acids might also be used to tailor their melting point to the desired range by taking advantage of eutectics. Similarly, polyanion salts, such as alkali metal polybifluorides, could be used to convert Lewis acids which in their free state are volatile at ambient temperature, into stable and usable solids.

The general nature of the invention having been set forth, the following examples are presented as specific illustrations thereof. It will be understood that the invention is not limited to these examples, but is susceptible to various modifications that will be recognized by one of ordinary skill in the art.

All reactions were carried out in a well passivated (with 2 atm of F_2 at 200° C.) stainless steel apparatus comprising of a 30 ml Hoke cylinder equipped with a cross fitting and a feed-through for a thermocouple well which almost touched the bottom of the cylinder. A pressure transducer (Validyne DP-15) and a Hoke valve leading to a stainless steel vacuum line were connected to the two remaining sides of the cross. Weighed amounts of the transition metal fluoride salt and the Lewis acid were thoroughly mixed in the dry nitrogen atmosphere of a glove box and loaded into the apparatus. The apparatus was then connected to the vacuum line, evacuated, and leak checked. The bottom of the cylinder was rapidly heated by the hot air stream from a heat gun, and the pressure evolution and inside temperature of the reactor were followed on a strip chart recorder. The evolved fluorine was measured by standard PVT methods and analysed for its purity by reacting it with mercury. The material balance was further crosschecked by weighing the reactor before the reaction and after removal of the evolved fluorine.

EXAMPLE 1

A mixture of K_2NiF_6 (0.369 g) and BiF_5 (1.372 g) was rapidly heated, as described above. When the inside temperature reached about 60° C., rapid fluorine evolution started, resulting in a maximum pressure of 990 torr at a reactor temperature of 170° C. The purity of the evolved fluorine (1.1 mmol) was shown by mercury analysis to be in excess of 99%.

EXAMPLE 2

A mixture of Cs_2CuF_6 (0.89 g) and BiF_5 (1.20 g) was rapidly heated, as described in Example 1. Again, pure fluorine (0.9 mmol) was evolved, resulting in a maximum pressure of 836 torr.

EXAMPLE 3

A mixture of Cs_2MnF_6 (2.115 g) and BiF_5 (4.515 g) was rapidly heated, as described in Example 1. Again, pure fluorine (1.0 mmol) was evolved, resulting in a maximum pressure of 929 torr.

EXAMPLE 4

A mixture of K_2NiF_6 (1.584 g) and TiF_4 (0.774 g) was rapidly heated, as described in Example 1. Again, pure fluorine (0.87 mmol) was evolved in the temperature range 65° to 170° C., resulting in a maximum pressure of 810 torr.

EXAMPLE 5

A mixture of K_2NiF_6 (0.486 g), TiF_4 (0.240 g) and BiF_5 (0.590 g) was rapidly heated, as described in Example 1. Again, pure fluorine (0.88 mmol) was evolved in the temperature range 60° to 180° C., resulting in a maximum pressure of 820 torr.

Obviously, numerous modifications and variations of the present invention are possible in light of the above teaching. It is therefore to be understood that within the scope of the appended claims the invention may be practiced otherwise than as described herein.

What is claimed and desired to be secured by Letters Patent of the United States is:

1. A solid grain pure fluorine gas generator, comprising:

a stable salt containing an anion derived from a thermodynamically unstable high-oxidation state transition metal fluoride; and

at least one Lewis acid which is stronger than said transition metal fluoride and stably solid at ambient temperatures, but which melts or sublimes at temperatures moderately above ambient.

2. The gas generator of claim 1 where the cation of said stable salt containing an anion derived from a thermodynamically unstable high-oxidation state transition metal fluoride is selected from the group consisting of alkali metals and alkaline earth metals.

3. The gas generator of claim 2 wherein said cation is an alkali metal.

4. The gas generator of claim 3 wherein said alkali metal is selected from the group consisting of potassium and cesium.

5. The gas generator of claim 2 wherein said cation is an alkaline earth metal.

6. The gas generator of claim 1 wherein the transition metal of said transition metal fluorine is selected from the group of manganese, iron, cobalt, nickel, and copper.

7. The gas generator of claim 6 wherein said transition metal is manganese.

8. The gas generator of claim 6 wherein said transition metal is copper.

9. The gas generator of claim 6 wherein said transition metal is nickel.

10. The gas generator of claim 1 wherein said anion is a doubly charged hexafluoride anion.

11. The gas generator of claim 10 wherein said anion is NiF_6^{2-}.

12. The gas generator of claim 10 wherein said anion is CuF_6^{2-}.

13. The gas generator of claim 10 wherein said anion is MnF_6^{2-}.

14. The gas generator of claim 1 wherein said anion is a tetrafluoro anion.

15. The gas generator of claim 14 wherein said tetrafluoro anion is CuF_4^-.

16. The gas generator of claim 14 wherein said tetrafluoro anion is AgF_4^-.

17. The gas generator of claim 1 wherein said Lewis acid is BiF_5.

18. The gas generator of claim 1 wherein said Lewis acid is TiF_4.

19. The gas generator of claim 1 wherein said Lewis acid is NbF_5.

20. The gas generator of claim 1 wherein said Lewis acid is a mixture of BiF_5 and TiF_4.

21. A method of generating pure fluorine, comprising the steps of:

mixing a stable salt containing an anion derived from a thermodynamically unstable high-oxidation state transition metal fluoride with a Lewis acid, wherein said Lewis acid is stronger than said transition metal fluoride and melts or sublimes at temperatures moderately above ambient;

causing the temperature of said mixture to reach the melting or sublimation temperature of said Lewis acid;

reacting said melting or subliming Lewis acid with said stable salt containing an anion derived from a thermodynamically unstable high-oxidation state transition metal fluoride to generate a thermodynamically unstable high-oxidation state transition metal fluoride which decomposes into a lower oxidation state fluoride and pure fluorine.

* * * * *

APPENDIX V

United States Patent [19]

Christe

[11] **Patent Number:** **4,903,479**

[45] **Date of Patent:** **Feb. 27, 1990**

[54] **RADIATION AUGMENTED ENERGY STORAGE SYSTEM**

[75] Inventor: **Karl O. Christe**, Calabasas, Calif.

[73] Assignee: **Rockwell International Corporation**, El Segundo, Calif.

[21] Appl. No.: **169,701**

[22] Filed: **Mar. 18, 1988**

[51] **Int. Cl.⁴** **F02K 9/42**

[52] **U.S. Cl.** **60/203.1; 60/214; 60/257; 60/39.461**

[58] **Field of Search** 60/257, 39.461, 205, 60/211, 214, 203.1, 204

[56] **References Cited**

U.S. PATENT DOCUMENTS

3,071,924	1/1963	Carr	60/39.461
4,182,663	1/1980	Vaseen	204/157.3
4,214,439	7/1980	Browning et al.	60/39.463
4,548,033	10/1985	Cann	60/203.1

OTHER PUBLICATIONS

Barrere et al. *Rocket Propulsion* Elsevier Publishing Co. New York; 1960, p. 643.

"Radiation Augmented Propulsion Feasibility", S. C. Hurlock et al, Final Report, AFRPL TR-85-068, Dec. 1985.

"Ozone", M. Horvath, et al, Topics in Inorganic and General Chemistry, Monograph 20, Elsevier, Amsterdam, 1985, pp. 196–201.

"Raketentreibstoff", A. Dadieu et al, Springer Verlag, Wien-New York, 1968, pp. 367–368.

Primary Examiner—Louis J. Casaregola
Attorney, Agent, or Firm—H. Fredrick Hamann; Harry B. Field; David C. Faulkner

[57] **ABSTRACT**

This invention relates to an improved method of storing solar radiation energy in a spacecraft and using it with high efficiency for space propulsion.

2 Claims, 1 Drawing Sheet

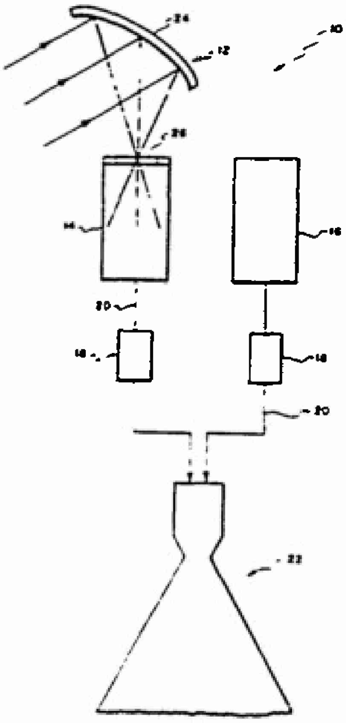

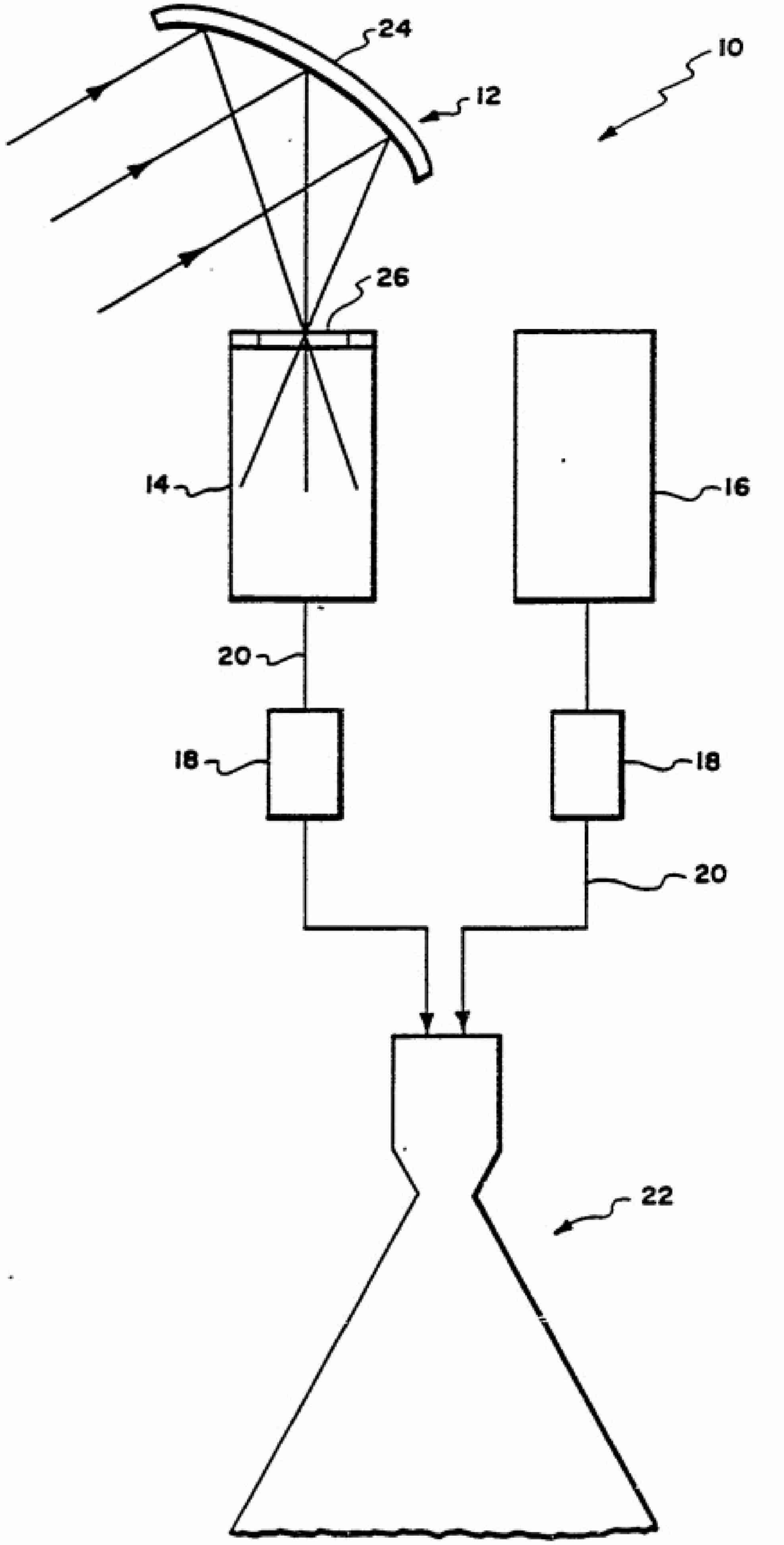
24
10
12
26
14
16
20
18
18
20
22

RADIATION AUGMENTED ENERGY STORAGE SYSTEM

BACKGROUND OF THE INVENTION

1. Field of the Invention

The present invention relates to an improved method of storing solar radiation energy in spacecrafts and utilizing it in a highly efficient manner for space propulsion or attitude control thrusters.

2. Prior Art

In outer space, solar radiation is a free source of energy and is widely used for the generation of electricity. Its usefulness for rocket propulsion applications, however, is curtailed because of the following drawbacks: (1) the relatively high cost of solar cells; (2) the relatively low efficiency of these cells, typically in the 10-20% range; (3) the requirement of heavy battery systems for accumulating and storing the electric energy thus generated; and (4) the low efficiency of converting the electric energy into readily available propulsion energy.

A chemical scheme, i.e. the photolysis of chlorine molecules to chlorine atoms has been proposed for the conversion of the solar energy into chemical energy ("Radiation Augmented Propulsion Feasibility", S. C. Hurlock et al, Final Report, AFRPL TR-85-068, Dec. 1985.) However, such a system is impractical in view of the great difficulty of storing chlorine free radicals at a useful pressure without their instant recombination to molecular chlorine and the very low performance of chlorine as an oxidizer in a rocket propulsion system.

OBJECTS OF THE INVENTION

It is therefore an object of this invention to provide an improved radiation augmented energy storage system which efficiently uses solar energy for rocket propulsion purposes.

Another object is to provide easy storage of the energy without the need for battery systems.

Another object is to efficiently recover stored energy for rocket propulsion purposes.

Yet another object is to utilize the same rocket engines and hardware which are being used for the basic propulsion systems, thus eliminating or minimizing the need for any extra, highly specialized hardware.

A further object is to provide a propellant system which is compatible, mixable and interchangeable with the basic liquid oxygen-hydrogen bipropellant system used as the main propellants but provides increased performance.

Other objects, features, and many of the attendant advantages of this invention will become readily appreciated by reference to the following detailed description.

SUMMARY OF THE INVENTION

Accordingly, the present invention provides a method of efficiently storing radiation energy in space and converting it into propulsion energy which comprises the following steps:

(1) photolytically converting oxygen to ozone,

(2) stabilizing the ozone in a solvent,

(3) either extracting a portion of the ozone from the solvent, or, if the solvent is liquid oxygen, using the resulting solution as such, and

(4) combusting either the extracted ozone or the ozone-oxygen mixture with hydrogen in a thruster.

DETAILED DESCRIPTION OF THE INVENTION

In the method of the present invention, oxygen is photolytically converted to ozone. The production of ozone from O_2 by photochemical methods is well known, and has been reviewed, for example, in the book "Ozone", M. Horvath, L. Bilitzky, and J. Huttner, Topics in Inorganic and General Chemistry, Monograph 20, Elsevier, Amsterdam, 1985, pages 196-201. Quantum yields of about 2 are readily achieved. In a typical ozone production process, gaseous O_2 is photolyzed and the O_3 is removed from the resulting O_2-O_3 mixture by freezing it out at liquid oxygen temperature (see "Raketentreibstoffe", A. Dadieu, R. Damm, and E. W. Schmidt. Springer Verlag, Wien-N.Y., 1968, pages 367-368).

Since pure liquid ozone is difficult to handle in a safe manner and can detonate, it is advantageous to store the ozone in a suitable solvent. The resulting ozone solutions can then be handled safely. Suitable solvents are either liquid oxygen or fluorocarbons, such as CF_4, CF_3Cl, $CHClF_2$, $CF_2Cl—CFCl_2$, etc. Of these solvents, liquid oxygen is of particular advantage because the preferred propellant combination used for space propulsion is liquid oxygen and hydrogen. Since ozone has a higher energy content than oxygen, the performance of the O_2/H_2 propellant system can be increased significantly by the use of O_2 which contains ozone. The performance calculations given in the following Table clearly demonstrate the benefits obtainable by substituting oxygen by ozone. As can be seen, the specific impulse of the O_3/H_2 system exceeds that of the O_2/H_2 system by 54 seconds and even that of the F_2/H_2 system by 21 seconds.

TABLE

Optimized Specific Impulse for Different Oxidizer - Hydrogen Propellant Combinations

System	R*	Ivac 1000 — ϵ = 40	Tc** °K
Cl/H_2	9.695	332.3	2952
F_2/H_2	8.709	491.0	4203
O_2/H_2	3.968	457.7	3137
O_3/H_2	3.921	512.1	3366

*Mole ratio of oxidizer to fuel

**Flame temperature

The use of liquid oxygen as a solvent for the ozone offers the additional advantage that the ozone does not have to be recovered and separated from the solvent, but can be used directly as a solution.

Whereas the use of liquid O_2 enriched with ozone offers distinct advantages for the main propulsion engines, the small attitude control thrusters use only relatively small amounts of propellants at a given time. Therefore, these attitude control thrusters can advantageously be operated with pure ozone as the oxidizer. For this application, the photolytically produced ozone is dissolved in a relatively nonvolatile fluorocarbon in a storage cylinder. When needed, it is withdrawn as a gas from the cylinder and combusted with hydrogen in a thruster, such as disclosed in U.S. Pat. No. 4,548,033, incorporated herein by reference. Since the fluorocarbon storage medium used is nonvolatile, it is not consumed and is required in only small amounts. Furthermore, these attitude control thrusters are being fired only intermittently. Therefore, the bulk of the oxidizer can be stored as liquid O_2, with only as much O_2 being photolytically converted to O_3 as needed at a given time.

As shown in the FIGURE, a conversion/storage and utilization assembly 10 consists of a solar energy focusing unit 12, propellant storage tanks 14 and 16, pumps 18, conduits 20, and a thrust chamber 22 for converting propellants into energy.

The solar energy focusing unit 12 is aligned and integrally connected by a truss support (not shown) so that sunlight, as indicated by the arrows, is reflected and focused by a reflective parabolic mirror 24, through a light transmitting aperture 26 integrally associated with propellant storage tank 14. As sunlight enters tank 14, a photolytic reaction occurs with liquid oxygen contained therein converting a portion of the oxygen into ozone.

When impulse power is to be produced by the utilization assembly 10, pumps 18 are activated, by controlled means known in the art, causing the flow of an ozone and oxygen mixture from tank 14 and a fuel such as liquid hydrogen from tank 16. These fluids are transported by conduits 20 into the assembly thrust chamber 22 where they are converted into energy.

As can be seen from the above description, the present invention offers numerous advantages over the state of the art. Among these advantages are:

(1) the radiation energy is directly deposited in the oxidizer used for the main propulsion system, thus eliminating inefficient energy conversion processes and the need for heavy energy storage systems, such as batteries;

(2) the amount of additional hardware required is minimized because the same propellants and thrusters are shared with the basic O_2/H_2 propulsion system; and

(3) the O_3/H_2 system offers a very substantial increase in performance, even higher than that of the F_2/H_2 system.

The foregoing detailed description is provided by way of illustration and intended only to be limited by the scope of the following appended claims.

What is claimed and desired to be secured by Letters Patent of the United States is:

1. A method of converting radiation energy into chemical energy to produce a high-performance propellant, said method comprising:

(a) Photolytically converting oxygen to ozone;

(b) storing and stabilizing the ozone in liquid oxygen to form an ozone/liquid oxygen solution; and

(c) combusting the ozone/liquid oxygen solution with hydrogen.

2. The method of claim 1 wherein the solution of ozone in liquid oxygen is an oxidizer.

* * * * *